THE PRODUCTION, CHARACTERISATION AND APPLICATIONS OF POLYCLONAL AND MONOCLONAL ANTIBODIES TO WARFARIN

A thesis submitted for the degree of Ph.D.

by

Brian Fitzpatrick B.Sc. (Hons)

January 2001

Based on research carried out at

School of Biotechnology,

Dublin City University,

Dublin 9,

Ireland.

Under the supervision of Professor Richard O'Kennedy

Declaration:

I hereby certify that this material, which I now submit for assessment on the programme of study leading to the award of Doctor of Philosophy, is entirely my own work, and has not been taken from the work of others, save and to the extent that such work is cited and acknowledged within the text of my work.

Signed Sheila Hopkins

Date: 14/2/01

Acknowledgements

Sincere thanks to Prof. Richard O' Kennedy for his constant support and guidance over the past few years, and especially his patience over the last few months! In particular, for sharing his wealth of experience and knowledge throughout my studies.

Thanks to all my friends at DCU and elsewhere (far too many to mention), for all those unforgettable, and sometimes better forgotten nights out! More importantly I thank them for their unreserved friendship and support over the years. In particular, I dedicate this thesis to my parents for everything they have done for me, without whom this would never have been possible. To my brother for his 'continual harassment', at least now I can say to him it's finished! Finally, I reserve special thanks for Mairead, for her patience, companionship and helping me to keep things in perspective over the last two years.

Table of Contents:

Chapter 1 : Introduction

List of Figures:

List of Tables:

Abbreviations

4'-AW	4'-aminowarfarin
4'-AW-BSA	4'-azowarfarin-BSA
4'-AW-DST-BSA	4'-aminowarfarin-disuccinimidyl tartrate-BSA
χ^2	Chi squared (i.e. averaged squared residual per data point)
BIA	biomolecular interaction analysis
BSA	bovine serum albumin
bsAb	bispecific antibody
CDR	complementarity determining regions of antibody
CM	carboxymethylated
conc (c)	concentration
DNA	deoxyribonucleic acid
DST	disuccinimidyl tartrate
EDC	N-ethyl-N'-(dimethylaminopropyl) carbodiimide
EDTA	ethylenediaminetetra-acetic acid
ELISA	enzyme-linked immunosorbent assay
Fab	binding region of antibody above the hinge region
Fc	constant region of antibody molecule
FCS	foetal calf serum
FIA	flow injection analysis
Fv	variable binding region of antibody
HAT	Hypoxanthine aminopterin thymidine
HT	Hypoxanthine thymidine
HBS	Hepes buffered saline
HPLC	High Performance Liquid Chromatography
HSA	Human serum albumin
IgG	immunoglobulin class G
IgA	immunoglobulin class A
IgD	immunoglobulin class D
IgE	immunoglobulin class E
IgM	immunoglobulin class M
IR	infra-red
Ka	association affinity constant
ka	association rate constant
Kd	dissociation affinity constant
kd	dissociation rate constant

kobs	observed rate constant
Lm	mass transport rate of analyte in bulk
Ln	natural logarithm
Log	logarithmic
Lr	Onsager coefficient of reaction flux
mAb	monoclonal antibody
max	maximum
MTL	mass transport limitation
MW	molecular weight
n	refractive index
NEAA	non-essential amino acids
NHS	N-hydroxysuccinimide
nm	nanometre
NMR	nuclear magnetic resonance
PAGE	Polyacrylamide gel electrophoresis
PBS	phosphate buffer saline
PBMC	peripheral blood monocytes
PDA	photodiode array
PEG	polyethylene glycol
pH	log of the hydrogen ion concentration
R	regression coefficient
Req	equilibrium binding response
RI	refractive index
Rmax	maximum binding response
scFv	single chain Fv antibody derivative
SE	standard error
SEC	Size Exclusion Chromatography
SDS	sodium dodecyl sulphate
SPR	surface plasmon resonance
TE	transverse electric
TIR	total internal reflection
TLC	thin layer chromatography
TM	transverse magnetic
UV	ultraviolet
VH	variable region of heavy chain
VL	variable region of light chain
X	immobilised ligand

Units

µg	microgram
(k)Da	(kilo) Daltons
µl	microlitre
µM	micromoles
°C	degrees Celcius
AU	arbitrary units
cm	centimetres
g	grams
h	hours
K	degrees Kelvin
kg	kilogram
l	litre
m	metre
M	molar
mg	miligram
min	minute
ml	millilitre
mm	millimetres
nM	nanomolar
mol	molar
pg	picograms
rpm	revolutions per minute
RU	response units
sec, s	seconds
v/v	volume per unit volume
w/v	weight per unit volume

Publications & Presentations:

Fitzpatrick, B. and O' Kennedy, R. 'The development and validation of a biosensor assay for the detection of warfarin in biological fluids'. (submitted).

Fitzpatrick, B. and O' Kennedy, R. 'The use of a novel biosensor assay for the determination of warfarin plasma concentrations in clinical samples'. (In preparation).

J. Quinn, P. Patel, **B. Fitzpatrick**, B. Manning, P. Dillon, S. Daly, R. O'Kennedy, M. Alcocer, H. Lee, M. Morgan and K. Lang. 'The use of regenerable, affinity ligand-based surfaces for immunosensor applications'. (1999). *Biosensors and Bioelectronics, 1999, 14: 587-95.*

Fitzpatrick, B. and R. O' Kennedy, 'The development of a Surface Plasmon Resonance based immunoassay for the detection of warfarin in biological matrices' oral presentation at Inaugural Analytical Science Network Initiative, University College Cork, September 1997.

Cooke D., **Fitzpatrick B.**, O'Kennedy R., McCormack T. & Egan D. (1997) "Coumarins – Multifaceted molecules with many analytical and other applications" In: *Coumarins: Biology, Applications and Mode of Action,* (Eds: R O'Kennedy & R.D. Thornes), John Wiley & Sons, Chichester, pp 303-332.

Abstract

The research presented in this thesis describes the production and applications of polyclonal and monoclonal antibodies to warfarin, an anticoagulant used in the management of a variety of thromboembolic disorders.

4'-nitrowarfarin was initially reduced in the presence of zinc and dilute acetic acid to 4'-aminowarfarin, which was characterised by a combination of infra-red spectral and nuclear magnetic resonance studies. 4'-aminowarfarin was then used for the production of a variety of drug-protein conjugates, incorporating different carrier molecules and coupling chemistries. They were subsequently characterised by a combination of SDS-PAGE, UV-spectral studies and size-exclusion high performance liquid chromatography (HPLC) with UV (280 nm) and photodiode array (200-400 nm) detection. The drug-protein conjugates were then used for the production, purification and characterisation of both mouse monoclonal and rabbit polyclonal antibodies to warfarin.

Rabbit polyclonal antibodies were initially produced and used in the development of a competitive ELISA for warfarin and also for the development of a BIACORE-based inhibition immunoassay. A panel of murine monoclonal antibodies to warfarin was also generated by somatic cell fusion procedures, using the spleens of mice, following *in vivo* immunisation with a variety of warfarin-protein conjugates. Positive clones were selected and cloned by limiting dilution. Antibody concentration determinations of purified antibody fractions and 'spent' hybridomas were made using a well-based ELISA technique and a biosensor assay. Affinity determinations of the selected monoclonal antibody preparations to warfarin and structurally related analogues were then determined using a well-based ELISA technique and also using several different assay formats using 'real-time' biomolecular interaction analysis.

The affinity-purified antibody preparations were then used in the development of a BIACORE-based inhibition immunoassay for warfarin in biological matrices. The stability of various immobilised ligands was initially determined and working concentration ranges were determined for each antibody preparation. A selected monoclonal antibody (i.e. 3-2-19) was then used for the determination of warfarin in plasma ultrafiltrate, which reflects the free active concentration of the drug in plasma. The samples assayed by BIACORE inhibition immunoassay were also analysed by HPLC for the purposes of validating the developed immunoassay technique. The technique was then used for the determination of the degree of protein-binding of warfarin in patient plasma samples, following determination of the total warfarin plasma concentration by HPLC.

Chapter 1

Introduction

1.1. History/Background:

The emergence of warfarin as a drug of therapeutic potential can be attributed to the fine work of Karl Paul Link and his team at the University of Wisconsin during the late 1930's and early 1940's [Link, 1943-44, -45, -59]. In the early 1920's cattle were found to be bleeding to death on the plains of North Dakota and Alberta, Canada. Many perceived this to be due to a new type of haemorrhagic septicaemia. The pioneering investigators, two veterinarians, Schofield in Canada and Roderick in North Dakota, concluded that the disease was in fact due to improperly cured hay from *Melilotus alba* or the *M. officinalis* family.

Both Schofield and Roderick soon recognised that withdrawal of the spoiled hay, or transfusion of fresh blood from normal cattle could control the onset of the 'disease'. In 1931, Roderick observed that the disease occurred in two phases: an initial prolongation of the prothrombin time (up to week 2) followed by spontaneous haemorrhage (weeks 3 to 5). Using Howell's prothrombin precipitation technique, Roderick demonstrated that solutions of 'prothrombin' from 'affected' cattle were unable to coagulate unlike those prepared from normal cattle and concluded that the delayed/complete removal of the clotting power of the blood was in fact due to a prothrombin deficiency.

In 1933 work began in the laboratory of K.P. Link to isolate the offending agent. The first step was the development of a reproducible and sensitive prothrombin assay to assess the anticoagulant potency of the test hay samples received. This resulted in the development of a bioassay using dilute plasma (12.5%) that facilitated the more sensitive detection of smaller changes in prothrombin activity for measuring the 'potency' of test hays (Campbell *et al.*, 1948). Initial extraction, isolation and identification of the anticoagulant agent proved difficult. This led to the development of an elaborate extraction scheme whereby the anticoagulant was eventually crystallised by Campbell in 1939 (Campbell *et al.*, 1948) and identified by Heubner as 3,3'-methylenebis-4-hydroxycoumarin or Dicoumarol. The biological synthesis of dicoumarol occurs during the spoilage of cured hay, whereby, coumarin is oxidised to 4-hydroxycoumarin which, when coupled with formaldehyde, leads to the production of dicoumarol (Figure 1.1).

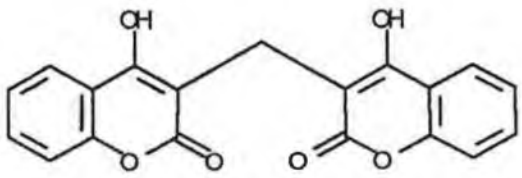

Figure 1.1: Structure of Dicoumarol (3,3'-methylenebis-4-hydroxycoumarin)

Over 100 analogues of the parent 4-hydroxycoumarin compound, were synthesized and tested for anticoagulant potency using Campbell's bioassay (Stahmann *et al.* 1944). The work of Stahmann concluded that the minimal structural requirements for anticoagulant activity were an intact 4-hydroxycoumarin residue with the 3-position substituted by a carbon residue or H-atom, whilst maximum anticoagulant activity requires 4-hydroxycoumarin with the 3-position containing a keto group in a 1,5-spatial relationship with respect to the 4-hydroxycoumarin group. Warfarin (3-(α-acetonylbenzyl)-4-hydroxycoumarin) was subsequently synthesized by Ikawa in 1944 (Ikawa *et al.*, 1944), with the name warfarin arising out of a combination of the letters from Wisconsin Area Research Foundation and coumarin.

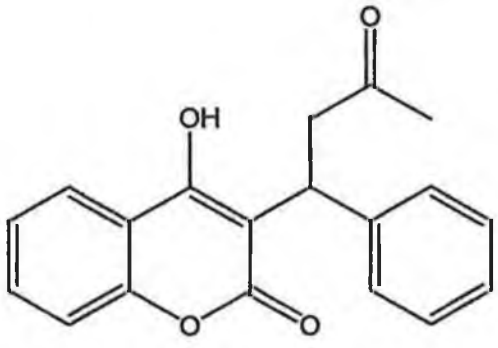

Figure 1.2: Structure of Warfarin (3-(α-acetonylbenzyl)-4-hydroxycoumarin)

Dicoumarol was originally used as a rat poison. However, it's activity was not sufficiently potent for adequate rodent control, primarily due to the large vitamin K intake by rodents from grains and cereals. Warfarin was subsequently used to a much greater effect and became the market leader in rodent control. The clinical potential of the drug was not fully realised until the ingestion of the drug in the form of rat poison by an army inductee who was subsequently admitted to hospital, with what had previously been described as the symptoms of 'sweet clover

disease'. The incident acted as a catalyst and reignited interest in the coumarin anticoagulants which had been dismissed a decade previously (Link, 1943-44). Two clinicians Shapiro (1953) and Clatanoff (1954) observed from their studies on warfarin that it possessed greater potency and bioavailability (irrespective of the route of administration) than any of the other oral anticoagulants tested, and pioneered it's use in the clinical setting.

Today, warfarin is the most widely prescribed oral anticoagulant (Hirsh *et al.* 1995) for the treatment of a variety of clinical conditions including atrial fibrillation, acute myocardial infarction and has shown recent promise as a HIV-1 inhibitor (section 1.9.1.) The chemical structures of several structural analogues of warfarin that are clinically widely used, are shown in Figure 1.3.

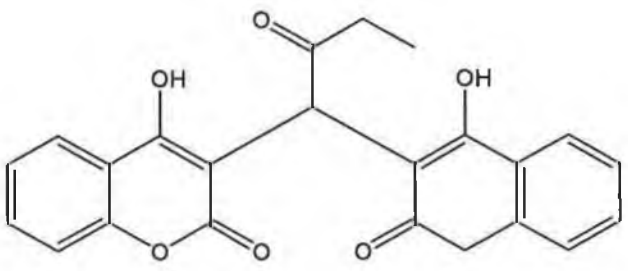

Ethylbiscoumate

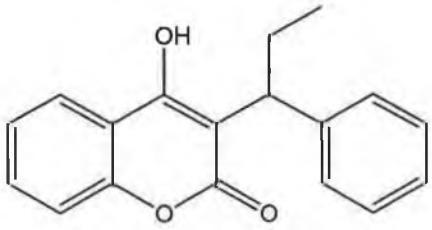

Phenprocoumon

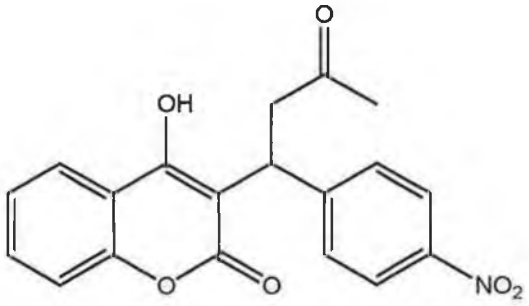

Acenocoumarin

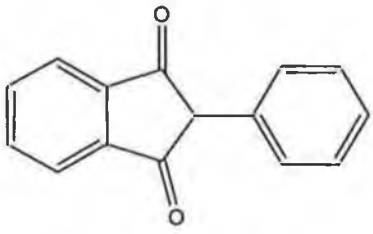

Phenindione

Figure 1.3: *Chemical structure of Oral Anticoagulants*

1.2. Mechanism of Action of Warfarin:

One of the most important biological functions of vitamin K is the post-translational modification of precursor proteins to form clotting factors, which involves the γ-carboxylation of glutamic acid residues (GLU) to γ-carboxyglutamic acid (GLA) residues in the presence of vitamin K and molecular oxygen (section 1.2.3. and Figure 1.4). In conjunction with this carboxylation reaction, an epoxidation reaction occurs, converting the active form of vitamin K to vitamin K 2,3-epoxide, which is in turn converted back to the quinone form by vitamin K_1 epoxide reductase to complete the vitamin K cycle (Suttie, 1993). Consequently, any interference with the normal functioning of the vitamin K cycle will impair the production of active clotting factors.

1.2.1. Vitamin K cycle:

Dietary intake and microbiological synthesis in the gut meets the vitamin K requirement of mammals, and phylloquinone is the most active source to meet the vitamin K requirements in humans. O'Reilly (1976) outlined the major factors necessary to prevent vitamin K deficiency as: (a) normal dietary intake of the vitamin (b) the presence of bile in the intestine (c) a normal absorptive surface in the liver and (d) a normal liver.

The direct link between vitamin K and blood coagulation was first established by Heinrik Dam whilst studying the dietary effects of chickens fed a 'lipid-free' diet. Dam (1929) discovered that the blood of chickens maintained on such a diet was devoid of clotting activity. However, when cereals were replaced back into the diet, the coagulation status of the chickens returned to normal. Vitamin K (phylloquinone, 2-methyl-3-phythyl-1,4-naphtoquinone) was identified as the agent necessary to cure the clotting defect in the chickens. The haemorrhagic condition was initially believed to be solely due to the depletion of the concentration of prothrombin (factor II). However, it was later discovered that the levels of factors VII, IX and X were also depleted and these proteins subsequently became known as the Vitamin K-dependent clotting factors (Suttie, 1993). A unique feature of the vitamin K-dependent proteins is the γ-carboxyglutamyl residues (Gla) formed during post-translational modification of these proteins (section 1.2.3. and Figure 1.4).

1.2.2. Isolation and Identification of 'Abnormal' Prothrombins:

The possibility that two distinct forms of prothrombin may exist was first stated by Hemker *et al.* (1963) whilst studying patients undergoing oral anticoagulant therapy. The presence of a protein,

which was antigenically similar to native prothrombin, but lacking its biological activity was first demonstrated by Ganrot and Nilehn (1968) and Josso *et al.* (1968). It was subsequently demonstrated that the two forms of prothrombin could be separated in the presence but not the absence of calcium ions (Stenflo, 1970). Stenflo and Ganrot (1972) then purified the 'abnormal' prothrombin to homogeneity using a combination of gel filtration and polyacrylamide gel electrophoresis, and found that the levels of the 'abnormal' prothrombin were elevated following dicoumarol treatment whilst normal prothrombin levels were found to be decreased. The amino acid and carbohydrate composition of the two forms of prothrombin were found to be indistinguishable, whilst the electrophoretic mobility of the abnormal prothrombin was found not to vary with the concentration of calcium ions in the buffer. The 'abnormal' form of the clotting factors formed during anticoagulation therapy subsequently became known as PIVKA's (Proteins Induced by Vitamin K Antagonism).

The specific difference between the two forms of prothrombin was identified to be due to the presence of additional carboxyl molecules of glutamic acid residues in the prothrombin molecule (Nelsestuen *et al.*, 1974; Stenflo *et al.*, 1974). It is the γ-carboxyglutamyl residues (Gla) situated in the amino terminal of vitamin K-dependent proteins, which confer the unique metal-binding properties of this class of calcium-binding proteins. Upon occupancy of these metal-binding sites, the vitamin K-dependent proteins undergo a conformational change that allows the proteins to interact with the phospholipid bilayers or cell membranes. The inability of abnormal prothrombins to bind to phospholipid bilayers results in these 'acarboxy' proteins exhibiting a slower activation of the coagulation cascade and the observed anticoagulation effect manifested as a prolonged prothrombin times.

1.2.3. Vitamin K-dependent carboxylase:

The enzyme responsible for the post-translational modification of the glutamic acid residues (GLU) on precursor clotting factors to γ-carboxyglutamyl residues (GLA), necessary for the clotting ability of clotting factors is the vitamin K-dependent carboxylase (Berkner, 2000). The carboxylation reaction requires molecular oxygen, carbon dioxide and vitamin K as a cofactor. The hydroquinone form of vitamin K (vitamin KH_2) is reduced to the epoxide form of the vitamin (vitamin K 2,3-epoxide) in conjunction with the carboxylation reaction. Vitamin K 2,3-epoxide is then recycled to the quinone form of the vitamin by a vitamin K-epoxide reductase. Elevated levels of the epoxide form of the vitamin can be found in the plasma of orally anticoagulated

patients (Nakamura *et al.*, 1994). The quinone form of the vitamin is subsequently reduced back to the hydroquinone form of the vitamin by a vitamin K reductase as shown in Figure 1.4. to complete the vitamin K cycle.

Oral anticoagulants exert their anticoagulant effect by inhibiting the cyclic inter-conversion of vitamin K, by inhibition of the epoxide- and vitamin K-reductases leading to a depletion of the hydroquinone (i.e. active) form of the vitamin. By inhibiting this regeneration of the epoxide form of the vitamin back to the hydroquinone form, partially carboxylated forms of the vitamin K-dependent clotting factors of varying Gla content are secreted; and pools of these partially carboxylated forms of prothrombin have been isolated and studied (Malhortra *et al.*, 1981; 1991). A decrease in the number of Gla residues on the prothrombin molecule from 10 to 9 was found to result in a 30% decrease in coagulant activity, whilst a decrease to below 6 Gla residues reduces the coagulant activity by almost 95%.

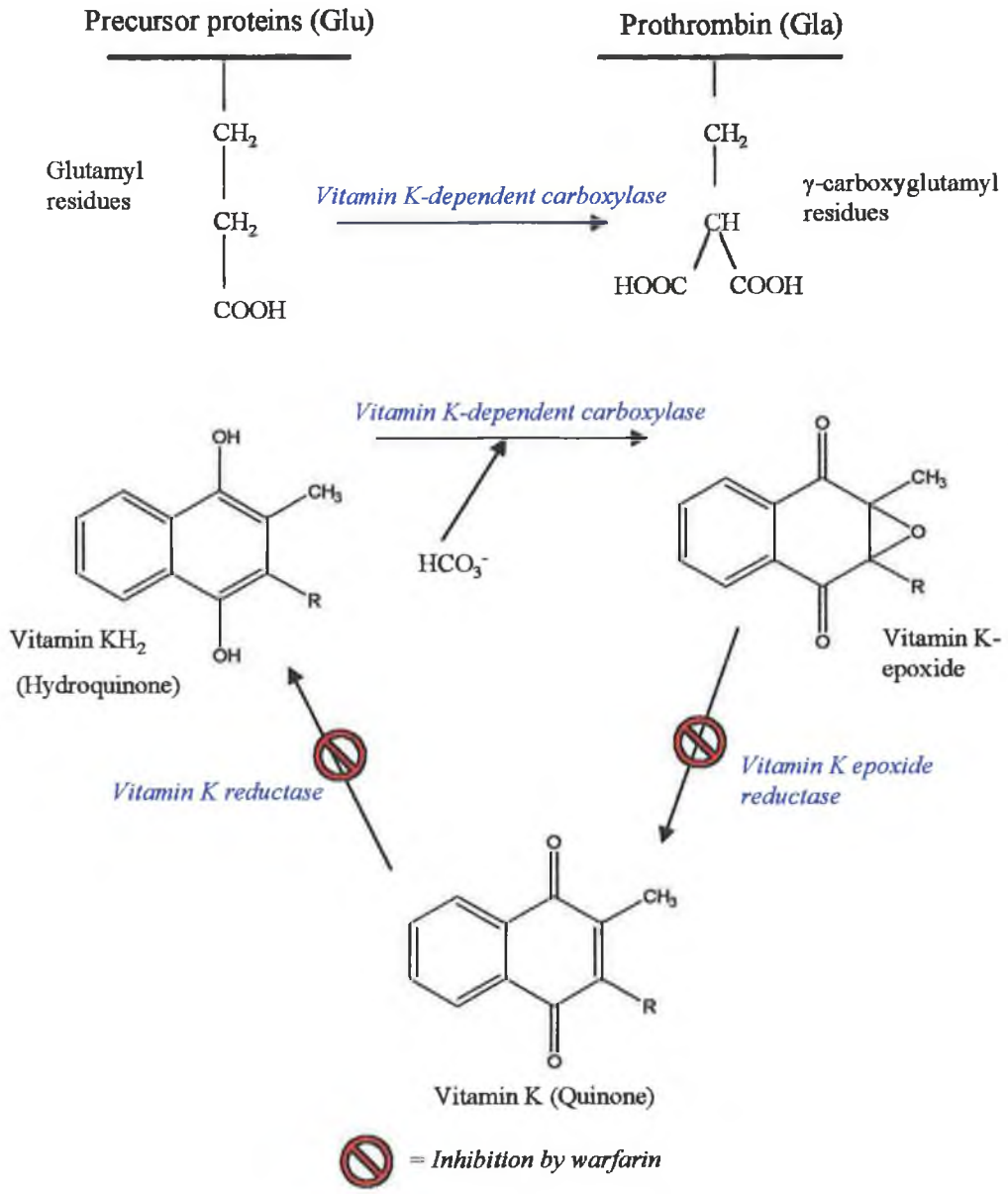

Figure 1.4: *Conversion of glutamic acid residues (Glu) on precursor proteins to γ -carboxyglutamic acid residues (Gla) necessary for the production of active clotting factors. The reaction is catalysed by a vitamin K-dependent carboxylase and in tandem with this reaction the hydroquinone form of vitamin K is oxidised to a 2,3-epoxide form of the vitamin. The epoxide is then reduced to the quinone form by a vitamin K epoxide reductase, which is then regenerated to the hydroquinone form by vitamin K reductase. Oral anticoagulants inhibit the cyclic regeneration of vitamin K producing only partially carboxylated clotting factors with little/no clotting ability.*

1.3. Pharmacokinetics of Warfarin

Warfarin exists as a racemic mixture of two optical isomers: *(R)*- and *(S)*- warfarin, whose potencies and pharmacokinetics have been extensively reviewed (Lewis & Trager, 1970; Hermans & Thijssen, 1993; King *et al.*, 1995). Warfarin enantiomers exhibit stereoselectivity and regioselectivity in their metabolism by human cytochromes P450 (Kaminsky & Zhang, 1997).

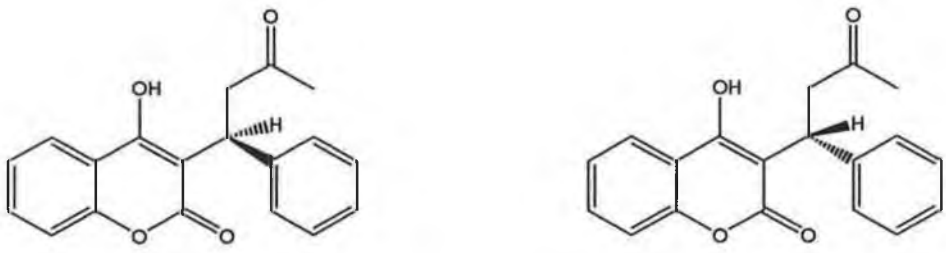

(R)-Warfarin *(S)*-Warfarin

Figure 1.5: *Optical enantiomers of warfarin.*

1.3.1.Absorption

Following oral administration warfarin is almost completely absorbed from the gastrointestinal tract (Hirsh *et al.*, 1995), with peak plasma concentrations being reached 60-90 minutes following administration (King *et al.*, 1995). No identifiable differences between the absorption profiles of the two enantiomers have been identified.

1.3.2. Distribution & Protein Binding

Following absorption the drug is highly protein bound (>99%), leaving only a small portion of free active drug circulating in the plasma (section 4.1.4.). The binding of warfarin and it's analogues to human serum albumin have been extensively studied (Ferrer *et al.* 1998; Bertucci *et al.*, 1999; Dockal *et al.*, 1999). Human serum albumin is composed of three structurally similar globular domains, HSA I, HSA II and HSA III. Dockal *et al.* (1999) have recently probed the ligand-binding specificities of HSA much more selectively using three cloned recombinant domains of HSA. The affinity of HSA to warfarin was then studied using the technique of induced circular dichroism. The primary warfarin-binding site was found to be located on domain II with a secondary binding site was found on domain I. Bertucci *et al.* (1999)

demonstrated that the (S)-enantiomer has a higher affinity for HSA using competitive displacement studies on a chiral stationary matrix to which HSA was anchored. This high degree of protein binding predisposes warfarin to a range of possible drug interactions, which can have a dramatic effect on the degree of anticoagulation achieved (section 1.8).

1.4. Warfarin metabolism:

The metabolism of warfarin in human shows great inter-individual variability (O'Reilly *et al.*,1963; Lewis & Trager, 1970; Lewis *et al.*, 1973). The mean half-life of warfarin is 36-42 hours and is independent of dose. Warfarin is essentially catalysed by a series of Cytochrome P450 enzymes to a series of hydroxylated metabolites (Kaminsky & Zhang, 1997), and a series of carbonyl reductases in the endoplasmic reticulum and cytosol reduce the carbonyl side chain to yield diastereomeric alcohols (Herman & Thijssen, 1989) (Figure 1.6).

The (S)- isomer has approximately 5 times the anticoagulant potency (Vanscoy and Coax , 1995) of the (R)- isomer. The hydroxywarfarins exhibit no anticoagulant potency, whilst the warfarin alcohols have a significantly reduced anticoagulant potency relative to the parent molecule (Lewis *et al.*, 1973).

The plasma half-life and extent of protein binding of other oral anticoagulants are listed in Table 1.1 (Kelly & O'Malley, 1979; Palereti & Legnani, 1996).

Table 1.1 Extent of Plasma protein Binding and Plasma Half-Life:

Oral Anticoagulant	Plasma Half-life ($t_{1/2}$) (hrs)	Protein Binding (%)
R-Warfarin	35-58	99
S-Warfarin	24-33	99
R-Acenocoumarol	8-10	99
S-Acenocoumarol	0.5-1.0	99
Phenprocoumon	72-120	99
Dicoumarol*	24-96	99
Ethylbiscoumate*	2-5	90

* Both dicoumarol and ethylbiscoumate have two coumarin ring structures (*Figure 1.1. and 1.3*) and a dose-dependent half-life which increases with increasing dose.

Early studies involving warfarin metabolism identified the hydroxywarfarins, namely 6- and 7-hydroxywarfarin, and the warfarin diastereomeric alcohols, as the primary metabolites of warfarin (Lewis & Trager, 1970). Pohl *et al.* (1976) demonstrated the stereochemical aspects of warfarin metabolism using rat liver microsomes and found that the formation of 7-hydroxywarfarin was selective for the (R)- enantiomer, which was also metabolised more rapidly than the (S)- isomer.

Recent studies using human microsomes and recombinant P450's have probed the regio- and stereoselectivity of warfarin much more extensively (Rettie *et al.* 1992; Zhang *et al.*, 1995). Zhang *et al.* (1995) probed the (R)- warfarin metabolism using two isozymes namely CYP4501A1 and CYP4501A2, and found that (R)- warfarin 6-hydroxylation rates could be used as markers of hepatic P4501A2, whilst 6-hydroxylation/8-hydroxylation rates could be used as markers for P4501A1. These particular isozymes have been shown to be of particular importance because of their ability to bioactivate chemical carcinogens.

Rettie *et al.* (1992) demonstrated that a CYP4502C9 is responsible for ultimately terminating the anticoagulant activity of the more potent (S)- enantiomer, through the stereoselective metabolism of (S)- warfarin to 7-hydroxy and 6-hydroxywarfarin metabolites in the ratio of 3.5:1, respectively.

Two of the human cytochromes involved in the metabolism of warfarin exhibit polymorphisms, i.e. CYP2C9 and CYP1A1. Mutations in CYP2C9 results in three allelic variants CYP2C9*1, CYP2C9*2 and CYP2C9*3. A case study by Steward *et al.* (1997) describes a patient showing extreme sensitivity to warfarin at low doses and further analysis showed that the patient was homozygous for CYP2C9*3. Patient plasma analysis showed that plasma (S-)/(R-) ratios were eight times that of the normal patient group. The authors concluded that expression of allelic variant of CYP2C9*3 resulted in the diminished clearance of (S-) warfarin and a subsequent increased therapeutic response. A similar study Takahashi *et al.* (1998) examined 86 patients on warfarin for genetic polymorphisms of CYP2C9 and it was found that patients who were heterozygous for the CYP2C9 mutation had reduced metabolism of (S-) warfarin but not the (R-) warfarin enantiomer. The authors postulated that genetic polymorphisms of CYP2C9 may possibly account for the wide range of variability in therapeutic patient dosing, as a result of the reduced *in vivo* metabolism of the more potent (S)-enantiomer.

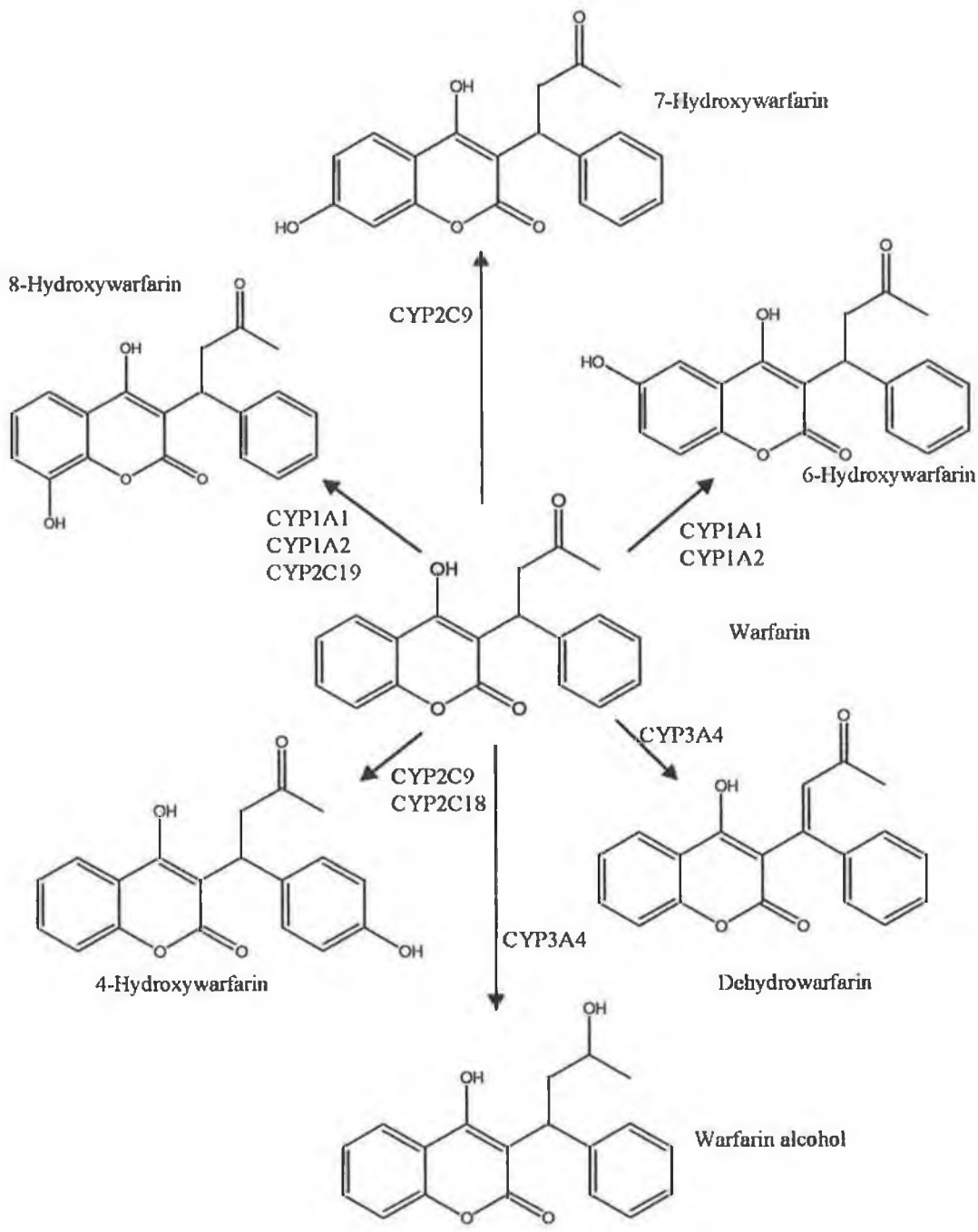

Figure 1.6. Main metabolic pathways of warfarin in humans

1.5. Excretion

Elimination of warfarin is primarily related to changes in the degree of drug protein binding, which alters the plasma concentration of circulating free drug available for metabolism. The major metabolites of warfarin 6- and 7-hydroxywarfarin and the two diasteromeric warfarin alcohols are eliminated in the urine with less than 2 % of the administered dose excreted as warfarin, although the rate of elimination shows high inter-individual variability with plasma half lives ranging from 20-60 hours (Lewis and Trager, 1970; Palareti and Legnani, 1996).

1.6. Microbial Models of Mammalian metabolism

The metabolism of warfarin has been extensively studied in mammalian systems and consequently provides an excellent model for the study of microbial systems to monitor warfarin metabolism. Microbial models of drug metabolism may be defined as: 'the use of micro-organisms (bacteria, fungi and yeasts) to facilitate the study of the metabolism of a variety of drugs in mammalian systems' (Davis, 1988). The use of microbial models to study the metabolism of drugs was first proposed by Smith & Rosazza (1974) following a study of microbiological hydroxylations of a variety of aromatic substances. The majority of Phase I biotransformations (oxidations, dehydrogenations, reductions, hydrolyses) have been observed in microorganisms.

The use of such microbial systems offers considerable advantages over traditional *in-vivo* and *in-vitro* studies making them attractive options for a number of reasons including:

(a) Facile manipulation of experimental parameters to facilitate the production of a particular metabolite e.g. Increased aeration to increase the production of oxidative metabolites.

(b) Preparative-scale metabolite production: allows for the facile scale-up of bio-transformation products thereby allowing structure elucidation. As reactions are enzyme-mediated they can be used for preferential product stereoselectivity as chemical reagents can frequently yield complex reaction mixture products.

(c) Single vs. multiple pathways: as outlined above experimental parameters can be tailored to produce a particular metabolite simplifying isolation and purification procedures.

(d) Reduced experimental costs: microbial biotransformations are comparatively inexpensive.

(e) Lessen animal demand: becoming of greater importance with the growing ethical and legal demands to reduce animal usage.

Davis and co-workers (1986, -87, -88) have extensively studied the microbial metabolism of warfarin. The bacterium *Nocardia corallina* (ATCC 19070) was shown to exhibit complete substrate and product stereoselectivity with racemic warfarin being reduced to (S)-warfarin-(S)-alcohol with no reduction of (R)-warfarin (Davis *et al.*, 1982)(Figure 1.7). *Arthrobacter* species (ATCC 19140) exhibited stereoselectivity in the (S)-reduction of racemic warfarin to (R)-(S)-warfarin-(S)-alcohol (Davis and Rizzo, 1982).

Aspergillus niger has been shown to metabolise warfarin to α-diketone metabolites (Rizzo and Davis, 1988), whilst *Cunnighamella bainieri* was found to produce 4-hydroxywarfarin as the primary metabolite (Rizzo & Davis, 1986). *Catharanthus roseus* metabolised racemic warfarin to 6-hydroxywarfarin and diastereomeric warfarin alcohols (Hamada *et al.*, 1993), with the fungus *Beauveria bassiana* (IMI 12939) producing 4-hydroxywarfarin, α-diketone and two ring cleaved warfarin metabolites, previously unreported (Griffiths *et al.*, 1992). *Cunninghamella elegans* (ATCC 36112) was found to produce several of the phenolic metabolites of warfarin including 4-, 6-, 7- and 8-hydroxywarfarin whilst also suggesting production of a previously unreported phenolic metabolite, namely: 3-hydroxywarfarin (Wong & Davis, 1987). A list of some of the micro-organisms studied to date and the major metabolites produced are given in Table 1.2.

Table 1.2: Metabolites of warfarin produced by microbial systems *in vitro*:

Micro-organism	***Authors***	***Metabolites produced***
Cunnighamella elegans	Wong & Davis (1991, 1989)	6-, 7-, 8-, 4- and 3-hydroxywarfarins, diastereomeric alcohols, warfarin diketone and aliphatic hydroxywarfarins
Aspergillus niger	Rizzo & Davis (1988)	α-diketone metabolites
Nocardia corallina	Davis & Rizzo (1982)	(S)-warfarin-(S)-alcohol
Arthrobacter species	Davis & Rizzo (1982)	S-reduction of racemic warfarin to (R)-(S)-warfarin-S-alcohol
Beauveria bassiana	Griffiths *et al.* (1992)	4-hydroxywarfarin, α-diketone and two ring cleaved warfarin metabolites
Catharanthus roseus	Hamada *et al.* (1993)	6-Hydroxywarfarin and the warfarin alcohols

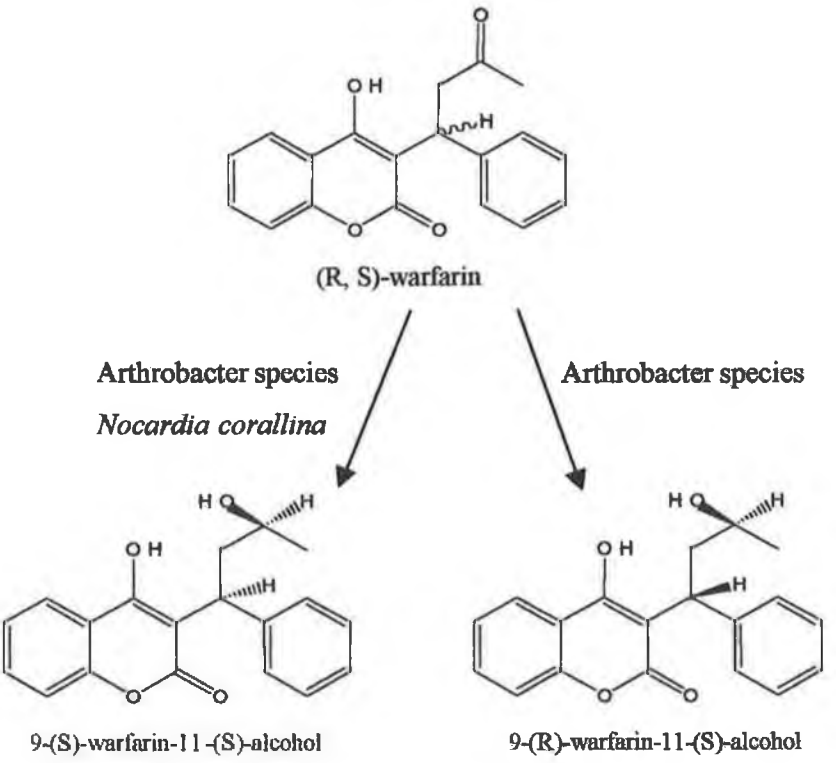

Figure 1.7: *Reduction of R, S-warfarin to S-warfarin-S-alcohol by Arthrobacter species and Nocardia corallina and to R-warfarin-S-alcohol by Arthrobacter species.*

1.7. Warfarin Resistance:

Resistance to warfarin has been defined as: "the inability of Oral Anticoagulant Therapy (OAT) to bring the Prothrombin Time (PT) down to adequate levels of anticoagulation when administered at a dose near or equivalent to the normally recommended doses" (LeFrere *et al.*, 1987). Occurrences of warfarin resistance in the literature are somewhat rare, consisting primarily of case reports.

For the purposes of this review, it may be simpler to describe warfarin resistance as hereditary resistance (HR), or acquired resistance (AR), as outlined by the proposed classification system outlined below in Figure 1.8:

Proposed Warfarin Resistance Classification Scheme

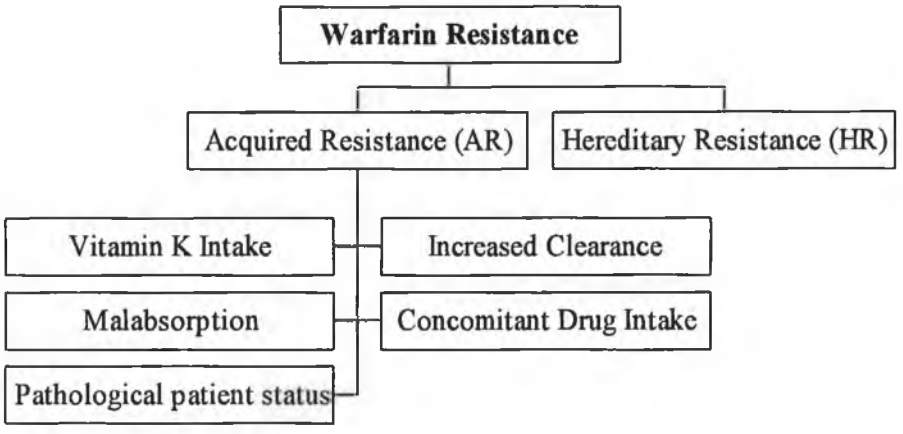

Figure 1.8: *Proposed Warfarin resistance classification scheme, outlining the major classifications of warfarin resistance namely, acquired (AR) and hereditary (HR) resistance. HR is believed to be caused by an abnormal receptor with an increased affinity for vitamin K and a reduced affinity for the coumarins, whilst there are many mechanisms that can be used to describe the various modes of acquired resistance.*

1.7.1. Hereditary Resistance:

The cases of definitive resistance in the literature are rare, as only four definitive cases of hereditary resistance have been confirmed by similar studies of family members (O' Reilly 1964, -70; Alving *et al.*, 1985; Warrier *et al.*, 1986). Hereditary resistance is believed to be caused by an abnormal receptor with an increased affinity for vitamin K and a reduced affinity for the

coumarins. Cases of this nature were first described over 30 years ago with the inability of patient to attain the desired degree of anticoagulation even with greater than 20 times the normal therapeutic concentration (O' Reilly, 1964). The patient's twin brother's response to warfarin was also documented to be similar to that of the patient. Other family members were also tested and it was postulated then (O' Reilly, 1964), that HR is an autosomal dominant characteristic. Warrier *et al.* (1986) reported the case of a 12 year old black girl who required greater than 10 times the average daily dose to achieve adequate levels of anticoagulation, familial follow-up studies showed that the girls mother was also found to have a similar resistance to warfarin therapy. The resistance was not absolute and could be overcome with large doses of the drug, suggesting an altered affinity of the enzyme or hepatic receptor for warfarin.

Other cases of warfarin resistance in the literature have been documented as HR (Keuh *et al.*, 1982; Holt *et al.*,1983; Diab *et al.*, 1994), although as no other family members were tested for this resistance, hereditary resistance cannot be confirmed; although such studies were not possible in all cases (Keuh *et al.*, 1982).

1.7.2. Acquired Resistance:

Several cases of acquired resistance (AR) to warfarin have been reported in the literature (De Wolff and Cate, 1979; Lutomski *et al.*, 1987; MacLaren *et al.*, 1997) and some of the mechanisms which have been implicated in cases of AR are shown in Figure 1.8.

Several cases of warfarin resistance associated with *intra-venous* lipid administration have also been documented (Lutomski *et al.*, 1987; MacLaren *et al.*, 1997), and the use of heparin therapy has been recommended for those receiving lipid emulsions in such cases. The precise mechanism of this particular interaction is not fully understood and has been suggested to be due to enhanced binding of warfarin to albumin, or a result of enhanced clotting factor production.

The literature contains one report of warfarin resistance in a patient due to malabsorption (Talstad *et al.*, 1994). The case study reveals a patient who after two years of satisfactory anticoagulation therapy with warfarin experienced selective malabsorption of warfarin and it's congeners. The dosage required after two years of warfarin therapy was 5 times the initial prescribed dosage. Non-compliance, concomitant drug intake or gastro-intestinal disease could not be used to explain the malabsorption. Enhanced clearance of warfarin has also been reported

(Hallak *et al.*, 1993) and found to be due to an intrinsically high oral clearance of the more active (S)- isomer. Familial studies were also carried out to rule out the possibility of HR, with one of the patient's sisters demonstrating a similar metabolic profile.

Accidental ingestion of exogenous vitamin K from liquid oral supplements (O' Reilly, 1971; Lee and Schwartz, 1981) or from leafy green vegetables particularly rich in vitamin K such as kale and broccoli (Walker, 1984) has also led to thrombotic events. Several instances where patients have demonstrated signs of acquired resistance to warfarin have also been reported (Lee *et al.*, 1981). However, many of these have been attributed to patients ingesting a diet rich in leafy green vegetables as part of a weight reducing diet, the net result being the increased exogenous intake of vitamin K undermining the previous adequate levels of anticoagulation.

Chu *et al.* (1996) recently described the first reported naturally occurring mutation in the propeptide sequence of Factor IX that directly affects the carboxylation by γ-glutamyl carboxylase. A patient whose PT was in the desired therapeutic range was admitted to hospital with bleeding complications. It was subsequently found that the patients Factor IX activity was <1% on warfarin therapy, but returned to normal levels when warfarin therapy was terminated. A mutation predicting a substitution of an Ala- residue to a Thr-residue at position 10 in the pro-peptide region of Factor IX was found. Ala-residues at position 10 in vitamin K-dependent proteins are highly conserved and, therefore, likely to be important in the binding of the carboxylase for γ-carboxylation. This in turn results in a reduced affinity of the carboxylase for the Factor IX precursor and demonstrates a previously unreported mechanism of warfarin 'sensitivity'.

In an attempt to aid the physician in the diagnosis of patients with an abnormal response to warfarin, Bentley *et al.* (1986) produced a dosage-algorithm from a study of well-controlled patients. The study provides the physician with two algorithms that can help the physician identify the causes of the abnormal warfarin response and dose accordingly.

1.8. Drug Interactions:

Warfarin is currently the most widely prescribed oral anticoagulant in the United States and potential interactions with a variety of other drugs have been examined with several excellent reviews published to date (Serlin and Breckenridge, 1983; Buckley and Dawson, 1992; Freedman

and Olatidoye, 1994; Wells *et al*, 1994; Chan, 1995; Harder and Thurmann, 1996). Concomitant drug therapy with warfarin can have a profound impact on the level of anticoagulant effect achieved, potentiating the anticoagulant effect through several mechanisms such as protein binding displacement leads to a hypothrombinaemic effect, which can lead to serious bleeding complications. The coumarin anticoagulants possess three distinguishing characteristics that render them susceptible to potentiating/inhibiting drug interactions:

(a) A narrow therapeutic range

(b) Highly plasma/protein bound

(c) Metabolised by cytochrome P450.

The interactions with warfarin can be broadly described as occurring by either pharmacodynamic or pharmacokinetic mechanisms (Serlin & Breckenridge, 1983; Harder and Thurmann, 1996) aswell as some interactions best characterised as idiopathic in nature (Freedman and Olatidoye, 1994). The pharmacokinetic interactions result in alterations in the circulating drug concentration by means of a change in the degree of plasma protein binding, increased metabolism, reduced absorption or increased plasma excretion. Pharmacodynamic interactions generally speaking have no effect on the circulating concentration of drug, but they can have a synergistic action resulting in increased anticoagulation through various mechanisms: for example, with NSAIDs (Non-Steroidal Anti-Inflammatory Drugs).

The interaction of cholestyramine with warfarin has been reported to reduce the oral bioavailability of warfarin with a reduction in the prothrombin time (PT) of approximately 25%. Cholestyramine binds warfarin in the intestinal tract which interrupts the enterohepatic recirculation of warfarin, by decreasing reabsorption it will increase its elimination rate and increased excretion of unchanged warfarin into the stool (O' Reilly, 1987). The effect of plasma protein binding displacement by several classes of drugs has also been documented (Buckley and Dawson, 1992; Harder and Thurmann, 1996). O'Reilly (1987) has suggested that the effects of plasma protein displacement of warfarin from its protein binding sites are overstated, as the resultant increase in free plasma warfarin concentration following protein displacement causes a transient increase in the degree of anticoagulation. The drug however, is then redistributed throughout the body and the rate of metabolism increases until the plasma concentration returns to pre-steady state levels (Koch-Weser and Sellers, 1971).

The majority of pharmacokinetic interactions with warfarin are caused by a change in the metabolism of warfarin either by an increase in enzyme induction (e.g. with rifampicin) which

leads to an increase in the rate of metabolism of warfarin, decreasing it's plasma half-life, thereby reducing the anticoagulant effect; or else enzyme inhibition (e.g. cimetidine) whereby the plasma half-life is extended, augmenting the anticoagulant effect.

The stereoselective nature of warfarin metabolism can also result in the preferential metabolism of a particular isomer. For example, sulfinpyrazole causes inhibition of the catalytic activity of P4502C9, the isozyme which is primarily responsible for the metabolism of the more potent (S)-isomer to it's inactive metabolites, namely (S)-6- and (S)-7-hydroxywarfarin in the ratio's of 3.5:1, respectively (He *et al.*, 1995). The effect of sulfinpyrazole is biphasic, which means that an initial potentiation is followed by inhibition of the anticoagulant effect (Wells *et al.*, 1994). He *et al.* (1995) concluded from their *in vitro* studies using human liver microsomes, which showed a reduced inhibitory effect *in vitro* rather than *in vivo*, that the drug interaction may be due to a circulating sulphide metabolite of sulfinpyrazole, rather than sulfinpyrazole itself, and suggested that the cause of many other drug-drug interaction may be as a result of the effects of a circulating metabolite rather than the parent drug.

Warfarin drug interactions with the NSAIDs (Non-Steroidal Anti-Inflammatory Drugs) have also been extensively reviewed (Pullar and Capell, 1983; Chan, 1995) and Chan has described the mechanisms and significance of the as occurring by means of three possible mechanisms:

1. Direct Hypoprothrombinemic effect of aspirin, which inhibits the clotting factor synthesis of factors VII, IX and X.
2. Pharmacokinetic mechanisms: Displacement of warfarin from plasma albumin by NSAIDs and inhibition of metabolism of (S-)-warfarin by phenylbutazone.
3. Pharmacodynamic interactions through a direct effect on platelet function thereby prolonging clotting time.

Chan (1995) suggests that the combined use of NSAIDs and warfarin be generally discouraged because of the increased risk of warfarin-associated bleeding episodes. It is suggested that if NSAIDs are required by patients already receiving warfarin therapy, that they should be introduced slowly over the first week or two of therapy, and the PT monitored closely. Similarly, the PT should be monitored when the administration of the NSAIDs is stopped because of the possibility of potential loss of anticoagulant control (Hirsh *et al.*, 1995).

The major pharmacodynamic interactions that may occur with warfarin include interactions :

- Drugs affecting availability of Vitamin K: antibiotics that affect the cyclic inter-conversion of the vitamin K cycle such as the cephalosporins also augment the anticoagulant effect by producing vitamin K deficiency from 'bowel sterilization' (O'Reilly, 1976; Bechtold *et al.*,1984).
- Drugs affecting haemostasis: NSAIDs such as aspirin, as noted previously, augment the anticoagulant effect through their inhibitory effect on platelets.
- Certain pathological disease states: Hepatic dysfunction impairs the normal synthesis of clotting factors, and liver disease alone results in a prolongation of the prothrombin time. Hypermetabolic states, such as hyperthyroidism, augment the anticoagulant effect of warfarin through two possible mechanisms - increased catabolism of clotting factors or that D-thyroxine increases the affinity of warfarin for it's receptor site in the liver and thus decreases the rate of clotting factor synthesis (Demirkan *et al.*, 2000). The decreased response of oral anticoagulants in hypothyroid states is suggested to be due to the reduced catabolism of clotting factors.

Freedman and Olatidoye (1994) have described those interactions with warfarin whose mechanism is not fully understood as being idiopathic in nature. The use of dietary vitamin E supplements is currently increasing because of the growing evidence that they may be useful in preventing atherosclerosis and coronary heart disease (Rimm *et al.*, 1993), and consequently the number of patients taking these supplements is increasing. The levels of the four vitamin K-dependent clotting factors were found to be depleted in a patient ingesting vitamin E supplements and on warfarin therapy (Corrigan *et al.*, 1981). The patient had multiple haemorrhagic complications, and the authors postulated a link between the vitamin E supplement and vitamin K. However, a study by Kim & White (1996) using high dose vitamin E supplements with a small patient group whose PT were stable on warfarin therapy concluded that the likelihood of an interaction between warfarin and vitamin E was minimal and that the supplements could be used safely.

1.9. Uses & Applications:

Warfarin is primarily used in the treatment of a variety of thromboembolic disorders, including atrial fibrillation, deep vein thrombosis and threatened stroke. The intensity of the anticoagulant treatment as measured by the INR is adjusted according to the severity of the thromboembolic

condition. Guidelines as to the correct levels of anticoagulation have been recommended based on the results of several well-designed clinical trials (Hirsh *et al.*, 1995; Sebastien and Tresch, 2000)(Table 1.4). A brief description of several alternative applications of warfarin are described below.

1.9.1. HIV-1 inhibitor:

The urgent requirement for suitable therapeutic agents to arrest the development of the AIDS epidemic has led to the identification of a wide variety of potential agents. The variety of therapeutic agents developed to date, have primarily been peptidomimetic HIV-1 inhibitors whose poor oral bioavailability and rapid excretion has limited their therapeutic potential. A point mutation in the HIV-1 genome was shown to result in non-infectious virions, illustrating the therapeutic potential of HIV-protease inhibitors as targets for AIDS therapy (Kohl *et al.*, 1988).

Warfarin has shown promising results as a potent HIV inhibitor *in vitro* (Bourinbaiar *et al.*, 1993 (a, b); Tummino *et al.*, 1994; Thaisrivongs *et al.*, 1994 -96). Tummino *et al.* (1994) studied 13 analogues of warfarin and found that 9 of the analogues studied show significant inhibitory activity of HIV-1 protease. Results demonstrated that substitution of the benzopyran-2-one ring at the 6-, 7- and 8-positions greatly modulates the inhibitory activity, with 7-,8-dimethylwarfarin being the most potent inhibitor (Ki= 1.9μM). The inhibitory activity was shown not to be greatly affected by substitution of the phenyl substituent of the 3-oxo-butyl group.

Bourinbaiar *et al.* (1993(a)) evaluated the effects of several coumarin compounds on HIV infectivity and replication. In separate experiments conducted, the presence of the coumarin-based compounds at the time of inoculation using free HIV virus showed reduced levels of infectivity. Similar experiments where MOLT-4 lymphocytes were co-cultured in the presence of HIV-1 infected ACH-2 lymphocytes in the presence of coumarin compounds also demonstrated reduced levels of HIV-1 infectivity. These results suggest that the coumarin molecules tested had inhibitory effect on both the incidence of the cell-free and cell-cell mediated HIV-infection, respectively. The effects of 7-hydroxy-, 4-hydroxycoumarin and warfarin were then tested on chronically infected ACH-2 lymphocytes, and all of the compounds tested exhibited an antiviral effect. The incorporation of ^{3}H-leucine was determined to assess whether the inhibitory effects of the coumarins, was due to growth suppression of the cells. The growth pattern of the cells showed a reduction in the RT activity, suggesting the anti-viral effect of coumarins is unrelated to the suppression of cell proliferation. The cellular viability of the drug-treated cells was also

comparable to that of control cells. The results suggest that the HIV-1 specificity of the coumarins is greater than that of RT-selective nucleoside inhibitors such as AZT which are ineffective in inhibiting the cell-cell transmission of HIV-1. The coumarins have the additional advantage of being able to inhibit viral production without being cytostatic, (Bourinbaiar *et al.*, 1993(b)) a property of few anti-viral drugs.

Studies by Thaisrivongs *et al.* (1994, -96) using a fluorescent-based screening assay of over 5000 compounds revealed phenprocoumon (substitution of 3-oxobutyl group of warfarin with ethyl substituent) as a potent HIV-1 protease inhibitor and demonstrated that it had improved inhibitory activity (Ki=1μM) compared to warfarin. The crystal structure of phenprocoumon/HIV-1 protease complex was studied at 2.5 A° resolution and revealed that the two oxygen atoms of the lactone moiety were positioned within hydrogen bonding distance of the two amides of the enzyme. This relationship between the hydrogen bonding and the enzyme formed the basis for the design of more potent non-peptidomimetic HIV protease inhibitors (U-96988, Ki=38nM) which entered phase I clinical trials. Subsequent studies identified a family of sulfonamide-containing 5,6-dihydro-4-hydroxy-2-pyrones, one of which was shown to be effective against a panel of AZT-resistant HIV-1 clinical isolates in PBMC (Thaisrivongs *et al.*, 1996). Clinical trials of Tipranavir a potent orally bioavailable HIV-1 protease analogue of the 5,6-dihydro-4-hydroxy-2-pyrones sulfonamide class (Ki= 8pM) is currently underway (Thaisrivongs and Strohbach, 1999).

1.9.2. Antimetastatic properties:

Warfarin has also demonstrated potential as an anti-metastatic agent in several clinical trials and animal models conducted (Zacharski *et al.* 1981, Amirkhosravi & Francis 1995). Warfarin has shown particularily promising results in the treatment of SCCL (Small Cell Carcinoma Lung) a tumour cell type that is characterised by a coagulation associated pathway (Zacharski *et al.*, 1984). Zacharski *et al.* (1981) found that the median survival rates of warfarin-treated patients was increased to 50 weeks compared to 24 weeks for the control group. The study also found that the warfarin-treated group showed a significant time to increased progression of disease. An independent study by Chahinian *et al.* (1989) to evaluate the combined effects of warfarin and chemotherapy in SCCL showed that the complete and partial response rates were similarly significantly elevated by approximately 7% overall in the warfarin-treated group.

Warfarin has also been used in the treatment of a variety of other illnesses including IgA nephropathy, which occurs as a general defect in the clearance of immune complexes, and IgA complexes which are poorly solubilised by the complement system deposit in the kidneys (Nolin and Courteau, 1999). Intraglomerular coagulation has been associated with the glomerular injury in IgA nephritis, as the mesangial cells swell and multiply within the glomerulus causing thrombosis. The use of a combined triple therapy of dipyridamole (an anti-platelet agent), cyclophosphamide and warfarin was found to be particularly effective in preventing the progression of the disease (Woo *et al.*, 1996).

1.10. Warfarin: Contraindications:

1.10.1 Pregnancy:

Oral anticoagulants are used during pregnancy to prevent venous thromboembolism in high-risk patients (Ginsberg and Hirsh, 1995). Warfarin can cross the placental barrier and may cause damage to the foetus *in utero*, and have been associated with a condition known as Foetal Warfarin Syndrome (FWS). There is also an increased risk of foetal mortality and stillbirth with the use of warfarin during pregnancy. The use of warfarin during the first 6 weeks of pregnancy may be safe (Ginsberg and Hirsh, 1995) however the risk of warfarin embryopathy is increased if taken during weeks 6-12 of the first trimester (Hall *et al.*, 1980). In a study of 418 pregnancies in which oral anticoagulants were used (Hall *et al.*, 1980) one sixth resulted in abnormal liveborn infants and one sixth in abortion or stillbirth with the remaining two thirds of births apparently normal. The majority of embryopathies with warfarin therapy were noted to occur when warfarin is taken during the first trimester of pregnancy, and nasal hypoplasia is the most common occurrence which results in a flattened upturned appearance of the nose, whilst in severe cases the nose appears depressed into the face (Hall *et al.*, 1980). Hall *et al.*, (1980) found that in all cases of embryopathy warfarin was administered between weeks 6 and 9 of gestation. The authors also concluded that there does not seem to be a critical time period for CNS associated abnormalities, however the majority occur during the second and third trimester. The CNS abnormalities were found to be due more debilitating than those of embryopathy, with a significant incidence of mental retardation (30%). Other CNS abnormalities associated with warfarin administration during pregnancy include Dandy-Walker syndrome (Kaplan, 1985) and blindness (Hall *et al.*, 1980). A study by Gartner *et al.* (1993) on the use of various coumarin derivatives and the associated teratogenic risk during pregnancy found that eye anomalies appear to occur only with warfarin therapy and the incidence of CNS-malformations was greater with phenprocoumon therapy. A recent study by Chan *et al.* (2000) of women with mechanical prosthetic valves

requiring oral anticoagulant therapy during pregnancy found that the incidence of foetal embryopathy is higher in women maintained on warfarin therapy throughout the full pregnancy. In a second group of women, where warfarin was substituted with heparin therapy between weeks six and twelve there was an increased risk of thromboembolic complications.

1.10.2. Overdose/ Reversal of effect:

Bleeding is the most common complication of warfarin therapy and the risk of patient haemorrhage increases with increasing intensity of oral anticoagulant treatment. Excessive anticoagulation with warfarin can be controlled with discontinuation of drug treatment, replacement with fresh frozen plasma or tissue factor concentrates, or with administration of vitamin K1 (Baglin, 1998). There are very few guidelines as to the adequate dose level of vitamin K required to achieve the desired degree of anticoagulation, although recommendations as to possible doses have been made (Vanscoy and Coax, 1995; Taylor *et al.*, 1999). When the anticoagulant effect of warfarin needs to be reduced, decreasing the administered dose should be the first consideration. If more immediate effects are required, vitamin K can be administered orally or slowly *intra-venously*, although the administration of vitamin K *intra-venously* has been associated with anaphlyaxis. In a recent study of patients whose PT's were outside the therapeutic range (over-anticoagulated) Brigden *et al.* (1998) found that alcoholism and liver disease were more prevalent in the over-anticoagulated group compared to the control group and that non-compliance and drug-interactions were also identified in 20% of reported cases. Reduction of the anticoagulant dose of the over-anticoagulated patients has been reported to be as safe and effective as vitamin K treatment in many cases (Glover and Morrill, 1995; Brigden *et al.*, 1998).

There have also been several reported cases of attempted overdosage using warfarin and its congeners (Swigar *et al.*, 1990; Kriz-Kozak and Lammle, 1999, Figure 4.23). Kruse and Carlson (1992) report the case of attempted suicide with brofadicoum overdosage in a 25-year old male. Brofadicoum a structural analogue of warfarin, was initially developed to overcome the increased prevalence of rodents resistant to warfarin ingestion, and has a toxic potency 200 times that of warfarin and a half-life almost 60 times longer. The patient was initially treated with fresh plasma and oral vitamin K and released. However, the patient subsequently returned some 15 weeks later following further ingestion of brofadicoum and died from a brain haemorrhage.

1.10.3. Necrosis:

Warfarin-induced skin necrosis is a rare complication associated with warfarin or other coumarin derivatives with a prevalence of 0.01-1.0% (Sallah *et al.*, 1998; Chan *et al.*, 2000). It usually occurs within the first 10 days of therapy, although there have been cases of reported late-onset necrosis (Essex *et al.*, 1998). Warfarin-induced skin necrosis is often associated with initial high loading doses of the drug. The precise mechanism of the induced necrosis is still unclear, although it is believed to result from a transient imbalance in the anticoagulant-procoagulant system, leading to decrease in the anticoagulant protein C during warfarin therapy. Approximately one-third of patients who have skin necrosis have been found to be protein C deficient. Protein C is a vitamin K-dependent protein that in conjunction with protein S, inactivates activated factors V and VIII, down-regulating coagulation. The plasma half-life of protein C is approximately 6-8 hours, so following warfarin ingestion a hypercoaguable state may exist as a result of the rapid fall in protein C activity, relative to the procoagulant factors II and X which have considerably longer half-lives. Protein C-deficient persons show a more dramatic fall in protein C concentrations making them even more predisposed to thromboembolic episodes (Zimbelman *et al.*, 2000). Occasionally the necrosis can be severe enough to warrant amputation of the affected areas or even result in mortality (Jillella and Lutcher, 1996). Miura *et al.* (1996) found that it generally occurs in obese women over 50 years of age who have been treated for thrombophlebitis or pulmonary embolism and seems more prevalent in areas where there is an increased subcutaneous fat content. The recommended alternative is to resume warfarin therapy with an initial low loading dose of the drug, as the use of heparin has been associated with osteoporosis (Hirsh *et al.*, 1995)

1.10.4. Fracture risk

Warfarin has also been associated with an increased incidence of fracture risk (Booth and Myer, 2000). The putative effect of vitamin K on bone is thought to be mediated by its role as a cofactor for the carboxylation of certain glutamic acid residues to γ-carboxyglutamic acid residues (Gla) in vitamin K-dependent proteins. Several vitamin K-dependent proteins have been identified in the skeleton such as osteocalcin and matrix Gla protein (MGP). Caraballo *et al.* (1999) reported an increased incidence of fracture in those patients undergoing oral anticoagulant therapy. The incidence of fracture risk was also shown to be positively correlated with the intensity of anticoagulant treatment, suggesting an adverse effect of warfarin on the axial skeleton

in humans, although the authors concluded that the incidence of risk of fracture does not imply an overall increase in the likelihood of osteoporosis.

1.11. Monitoring Anticoagulant Therapy:

The anticoagulant effect of warfarin can be measured using a variety of indices, the most commonly used method being the Prothrombin test (PT time).

1.11.1. Prothrombin Time (PT)

The PT is sensitive to changes in the concentrations of factors II, VII and X. During the first few days of warfarin therapy; the PT primarily reflects the decrease in plasma concentration of factor VII which has the shortest half-life, and, subsequently the depression of levels of factors II and X. The time taken for all of the coagulation factors to reach new steady-state levels varies from 2-7 days, depending on the half-life of the various clotting factors. If an immediate anticoagulant effect is required heparin is usually overlapped with warfarin therapy for the first 4-5 days of treatment.

Table 1.3: Half-life of Vitamin-K dependent clotting factors.

Clotting Factor	Half-Life (hours)
Factor II (Prothrombin)	72-96
Factor VII	4-6
Factor IX	20
Factor X	48-70

The PT is performed by mixing citrated plasma with calcium and a tissue thromboplastin reagent that contains the tissue extract and phospholipid necessary to activate the coagulation cascade. There can be considerable variation in the degree of 'responsiveness' of the commercially available thromboplastins depending on the tissue (lung, brain or placenta) and species (rabbit vs. human) of origin. The degree of 'responsiveness' of a particular thromboplastin reflects its ability to activate Factor X by Factor VII as the level of each decreases (Hirsh, 1995). Consequently there could be considerable variation in the PT's reported by different laboratories depending on the thromboplastin reagent used making inter-laboratory comparison of PT's very difficult indeed.

In an attempt to try and standardise the varying responsiveness of the various thromboplastins used the INR (International Normalised Ratio) system was introduced by the World Health Organization in 1977. A batch of human brain thromboplastin was designated as the first standard reference batch of thromboplastin against which all other preparations could be referenced (Poller, 1987). The following algorithm was developed to allow for proper standardisation when reporting PT's.

$$PTR = \frac{Patient\ Plasma\ PT}{Control\ Plasma\ PT}$$

$$INR = PTR^{ISI}$$

PTR: Prothrombin Time ratio = Ratio of Prothrombin time of patient plasma to that of control plasma.

ISI: International Sensitivity Index

The ISI, International Sensitivity Index, measures the responsiveness of various thromboplastins relative to international reference standards. The lower the ISI the more responsive the thromboplastin used.

Despite the potential benefits and concensus on the use of the INR system several problems also exist with its use (Hirsh *et al.*, 1995). The first problem is that of the use of insensitive thromboplastins (ISI≥2.5) resulting in erroneous INR's as the calculated PTR is raised to the power of the ISI (Vanscoy and Coax, 1995). Therefore, the use of thromboplastins with ISI's close to 1.0 is suggested. Similarly, manufacturers assigning an incorrect ISI to a specific batch of thromboplastin can have an erroneous effect on the recorded PT.

Furie *et al.* (1984) suggested that measurement of the native prothrombin antigen is more predictive of bleeding and thromboembolic complications in patients treated with warfarin. Furie *et al.* (1990) found in a randomised trial, using the traditional PT and the prothrombin antigen concentration assay, that there was a significant decrease in the number of complications with the native prothrombin antigen group than the PT measured anticoagulated group. Overall there was an 85% decrease in the complication rate with the prothrombin antigen-measured group, suggesting possible clinical benefit for its measurement. Despite the reduced incidence of bleeding episodes associated with the prothrombin antigen assays determined by Furie *et al.*

(1990), the PT remains the most commonly employed technique clinically, primarily as a result of the rapidity of analysis that is feasible.

The intensity of anticoagulation required will also vary considerably depending on the thromboembolic condition, and recommended INR ranges have been made by the American College of Chest Physicians (ACCP) and are outlined below in Table 1.4 (Beckey *et al.*, 1999). The current trend towards less intense anticoagulation aims to reduce both the frequency and risks of bleeding episodes and the need for frequent monitoring. The key, however, is the balance between effect and side-effect (Lodwick, 1999).

Table 1.4. Recommended International Normalised Ratios (INRs) for various thromboembolic conditions

Indication	Recommended INR
Deep Vein Thrombosis (DVT)	2.0-3.0
Mechanical heart valves	2.5-3.5
Prevention of recurrent MI after initial MI	3.0-4.5
Prevention of systemic embolism in atrial fibrillation	2.0-3.0

MI=Myocardial infarction

The frequency of bleeding episodes associated with warfarin therapy is related to the degree of anticoagulant therapy. Gitter *et al.* (1995) found that the incidence of bleeding episodes was greatest during the first month of therapy (1.6%), and decreased to approximately 1/3 of that rate during the first 3 months. The study also found that a malignant condition was most strongly associated with bleeding episodes.

Determining the optimal dose of warfarin for any patient is a highly individualised matter as there is great inter-patient variability in the PT response to warfarin (Lutomski *et al.*, 1995). Dosing is generally begun with an initial loading dose of warfarin (5-10 mg) and the INR is monitored carefully during the first weeks of therapy until the desired INR range has been reached. Sun and Chang (1995) developed an elaborate computer software program incorporating warfarin pharmacokinetics and pharmacodynamics in an attempt to improve the accuracy in evaluating steady-state dosages during initialisation of warfarin therapy required. The study showed that

current physician-determined-doses required a greater number of INR measurements and the statistical frequency of patient underdosing was greater compared to the computer-modelled dosage values. The study suggested possible merits for the use of computer modelling with respect to predicting steady-state dosage requirements in the clinical setting coupled with proper clinical evaluation. Oates *et al.* (1998) recently described a method for initiating warfarin therapy in elderly out-patients using a decision tree and dosage algorithm which included factors such as alcohol intake, concomitant medication, age, sex, weight and liver failure. The dosage scheme developed which involved predicting the maintenance dose following 2 weeks of 2mg warfarin requiring for only weekly INR determinations to be made. Only the sex of the patient had a significant enough effect to be included in the dosage prediction algorithm.

The influence of patient age as a discriminant in warfarin dosage requirements has also been examined and studies have shown that a significant correlation exists between the two. Gurwitz *et al.* (1992) found that for each decade past 50 years of age mean warfarin requirements decreased by approximately 1mg. This increased sensitivity to warfarin in the elderly has also been postulated to be due to decreased clearance of warfarin with age (Mungall, 1992). Warfarin 'sensitivity' has also been described in the elderly where the increased effect of warfarin has been suggested to be due to an increased affinity for warfarin rather than vitamin K (Shepherd *et al.*, 1977; Vanscoy and MacAuley, 1991)

Gender differences have also been associated with increased sensitivity to warfarin. A study by Hara *et al.* (1994) examined gender differences in the anticoagulant effect of warfarin in rats. The study found in male and female rats both fed warfarin from 2 weeks of age that the PT was prolonged to the same degree at 4 weeks but that the effect was reduced with ageing and at 14 weeks no anticoagulant effect was observed in the female rats. Ovariectomized rats showed a similar prolongation of the coagulation time comparable to the male rats which was subsequently reduced by the addition of 17-β-estradiol. Male rats treated with 17-β-estradiol also showed a prolongation of prothrombin time and it was concluded that the gender difference observed in the anticoagulant effect of warfarin in rats may be due to the estradiol levels in plasma as the plasma levels of warfarin remained unchanged.

1.12. Warfarin -The 'Rebound Phenomena':

The expression 'rebound-phenomena' is used to describe a hypercoagulable state that exists following withdrawal of warfarin treatment. Cessation of warfarin therapy commonly results in the low-grade activation of the coagulation system, although the degree of activation is transient in most cases. However, higher levels of activation have been observed for certain individuals predisposing them to an increased incidence of thrombotic complications (Palareti and Legnani, 1996).

The first reported effects of recurrent thromboembolism in patients following cessation of oral anticoagulation treatment upon warfarin withdrawal was reported by Cosgriff & Stuart (1953). It was suggested that a state of 'hypercoagulability of the blood' existed in these patients and coined the term 'rebound phenomenon' to describe the condition. The development of newer more sensitive techniques capable of detecting markers of blood hypercoagulability has allowed for the detection of lower levels of different markers of hypercoagulability (e.g. activated factor VII, prothrombin fragments).

Two hypothesis have been used to explain the nature of the increased levels of blood coagulation and thrombin generation following withdrawal of oral anticoagulant therapy (Palareti and Legnani, 1996). The first explanation is that increased levels of blood coagulation have been observed in patients with venous or arterial thrombotic disease, independent of the occurrence of the thrombotic episodes (Bauer *et al.*, 1985; Merlini *et al.*, 1994). The reduced prothrombin levels during warfarin therapy balance the levels of increased coagulation, and when anticoagulant therapy is withdrawn the activation of coagulation is no longer 'counterbalanced' by the oral anticoagulant effect. This 'catching up' effect of the procoagulant factors was first described by Wright (1960) and later by Hirsh (1982).

The second explanation describes how an actual 'rebound phenomena' may actually occur following cessation of warfarin therapy. The levels of Factor VII (triggers blood activation and has a role in thrombotic events) and Factor IX showed recovery times of *circa.* 2 days (Schofield *et al.*, 1987), whilst the activated form of factor VIIa were shown to reach significantly higher levels when anticoagulant therapy is stopped compared to pretreatment levels. Conversely, the return to normal levels of the anticoagulant proteins C and S was slower creating an imbalance between pro- and anticoagulant factors which may lead to activation of blood coagulation (Palareti and Legnani, 1996). It has been shown that the degree of hypercoagulability is more

marked when discontinuation of warfarin is immediate rather than gradual. When anticoagulants are phased out gradually, the differences between the procoagulant and anticoagulant proteins are less marked reducing the likelihood of blood activation and the possibility of the 'rebound phenomenon'.

1.13 Aims of thesis:

Current methodologies for the detection of warfarin require extensive sample pre-treatment and derivatisation for the measurement of the unbound fraction of warfarin in plasma and are unsuitable for the routine analysis. The aim of this thesis was to develop a panel of antibodies to warfarin, which it was envisaged would be used in the development of a rapid, sensitive BIACORE inhibition immunoassay suitable for the analysis of warfarin in biological fluids.

Chapter 3 describes the derivatisation of 4'-nitrowarfarin to 4'-aminowarfarin which following characterisation, was used in the production of drug-protein conjugates. The drug-protein conjugates were then used for the production of polyclonal antibodies to warfarin in rabbits. The affinity-purified polyclonal antibodies were then used in the development of a competitive ELISA for warfarin.

Chapter 4 describes the development and validation of a BIACORE-based inhibition immunoassay for the detection of the free fraction of warfarin in plasma ultrafiltrate. Several assay formats were investigated and the use of directly immobilised drug surfaces were shown to possess the optimal stability and ligand binding characteristics for the routine analysis of biological samples. The assay system developed was subsequently validated against an existing validated HPLC technique for the analysis of warfarin, and showed excellent correlation with approximately 10-fold lower limits of detection. The validated assay was then used for the determination of the unbound fraction of warfarin in patient samples and used to calculate the degree of plasma protein-binding.

Chapter 5 describes the production and characterisation of a panel of monoclonal antibodies to warfarin following somatic cell fusion procedures. Detailed affinity analysis of selected monoclonal antibodies was then carried out using a well-based ELISA technique and also by BIACORE analysis. Both techniques produced equivalent thermodynamic data and the relative merits of each procedure are discussed.

Chapter 2

Materials & Methods

2.1. Equipment

Table 2.1 *Equipment model used and suppliers.*

Class	Model	Source
BIACORE™	BIACORE™ 1000, BIACORE™ 3000	BIACORE AB
Centrifuges	Heraeus Christ Labofuge 6000	Heraeus Instruments Inc.
	Biofuge A Microcentrifuge	Heraeus Instruments Inc.
	Sorvall refrigerated centrifuge	Du Pont Instruments
CO_2 Tissue culture incubator	EG 115 IR	Heraeus Instruments Inc./Jouan
HPLC Apparatus	System Beckman Gold	Beckman Gold
	Varian Star 9030 pump, 9012 UV detector, Fluorescence detector, AI-200 autosampler	J.V.A. Analytical Ltd.
Microscope	Nikon Diaphot inverted microscope	Micron Optical Co. Ltd.
pH meter	3015 pH meter	Jenway Ltd.
NMR Spectrometer	400MHz AC400 NMR spectrometer	Brucker Ltd.
IR Spectrophotometer	Nicolet	The Nicolet Instrument Corp.
Protein Electrophoresis Apparatus	Atto dual minislab system AE-6450	Atto Corp.
Rocker Platform	Stuart Platform Shaker STR6	Lennox
HPLC column C18	Supleco Discovery™	Supelco
	Biosep SEC-4000	Phenomenex
Spectrophotometers	U.V.-160A Spectrophotometer	Shimadzu Corp.
	Titertek Multiscan plate reader	Medical Supply Company
Sonicator & Waterbath	RM6 Lauda waterbath	A.G.B. Scientific Ltd.
Laminar Flow Unit	Holten 2448K laminar air flow unit	Holten Laminar A/S
Blood Tube Rotator	SB1 Blood tube rotator	Medical Supply Company
Evaporation Unit	Pierce Evaporation Unit	Pierce
Millipore Filtration Apparatus	Millipore Filtration Device	A.G.B. Scientific Ltd.
Ultrafiltration Cell	Stirred Cell 8400	Amicon Inc.

Full Addresses:

AGB: Dublin Industrial Estate, Dublin 11, Ireland.

Amicon Inc.: Beverly, Massachusetts 01915, U.S.A.

Atto Corp.: 2-3 Hongo 7-Chrome, Bunkyo-Kui, Tokyo 113, Japan.

BIACORE AB: St. Albans, Hertfordshire AL13AW, England.

Brucker Ltd.: Banner Lane, Coventry CV4 9GH, England.

Du Pont Instruments: Instrument Products Division, Newtown, Connecticut 06470, U.S.A.

Heraeus Instruments Inc.: 111-a Corporate Boulevard, South Plainfield, New Jersey 07080, U.S.A.

Holten Laminar A/S: Gydevang 17, DK 3450 Allerod, Denmark.

Jenway Ltd.: Gransmore Green, Felsted Dunmow, Essex, CM6 3LB, England.

Jouan: Zone Industrialle de Brais, Saint Nazaire, France.

J.V.A. Analytical Ltd.: Long Mile Rd., Dublin 12, Ireland.

Lennox: P.O Box 212A, John F. Kennedy Dr., Naas Rd., Dublin 12, Ireland.

Medical Supply Company: Damastown, Mulhuddart, Dublin 15, Ireland.

Nicolet Instrument Corp.: 5225-1 Verona Rd., Madison, WI 53711, U.S.A.

Nikon Corporation: 2-3 Marunouchi 3-chome, Chiyoda-ku, Tokyo, Japan.

Pharmacia Biosensor: St. Albans, Hertfordshire AL1 3AW, England.

Phenomenex: Melville House, Queens Avenue, Hurdsfield Ind.Est., Macclesfield, Cheshire SK10 2BN, England.

Pierce: 3747 North Meridian Road, PO box 117, Rockford, IL 61105, U.S.A.

Shimadzu Corp.: 1 Nishinokyo-Kuwabaracho, Nakagyo-ku, Kyoto 604, Japan.

Supelco: Supelco Park, Bellefonte, PA 16823-0048, U.S.A.

2.2.1. Consumable items

Table 2.2 *Consumables used and suppliers*

Class	Item	Source
Hardware	CM5 Chips	Pharmacia Biosensor
	TLC plates	Riedel de Haen
	HPLC vials	J.V.A. Analytical Ltd.
	0.2 μm filters	A.G.B. Scientific Ltd.
	Eppendorf tubes, sterile universal containers and gilson tips	Sarstedt Ltd.
	Nunc Maxisorp plates	Nunc
	Tissue Culture plastic-ware	Corning Costar
	Nanosep™ Ultrafiltration membranes	Amicon Inc.

Full Addresses:

Amicon Inc.: Beverley, Massachusetts 01915, U.S.A.

Corning Costar: High Wycombe, Buckinghamshire HP13 6EQ, England.

Nunc: P.O. Box 280-Kamstrup DK, Roskilde, Denmark.

Riedel de Haen: Wunstorfer Straβe, D-3106, Seelze 1, Hanover, Germany.

Sarstedt Ltd.: Sinnottstown Lane, Drinagh, Co. Wexford.

2.2.2. Reagents and Chemicals

All chemicals were reagent grade and were purchased through **Sigma Chemical Co**. (Poole, Dorset, England) except as noted below.

Table 2.3 *Reagents & Chemicals used and suppliers:*

Class	Chemical	Supplier
Chemicals	Acencoumarin (Sintrom®)	Ciba-Geigy
	Deuterated dimethyl sulphoxide (DMSO)	Aldrich Chemical Co.
Biochemistry	Alkaline phosphatase-labelled antibodies	Southern Biotechnology Ltd.
	Phosphate buffered Saline tablets	Oxoid Ltd.
Tissue culture	Briclone	N.C.T.C.C.
	Dulbecco's modification of Eagles medium	Gibco BRL
	Fetal calf serum	Gibco BRL
	HEPES	Gibco BRL
	Hybridoma SFM™	Gibco BRL
	L-glutamine	Gibco BRL
	Non-essential amino acids	Gibco BRL
	Phosphate-buffered saline tablets	Oxoid
	Sodium pyruvate	Gibco BRL

Aldrich Chemical Co.: Old Brickyard, New Rd., Gillingham, Dorset SP8 4JL, England.
Ciba-Geigy: CH-4002 Basle, Swizerland.
Gibco BRL: Trident House, Renfrew Rd., Paisley PA4 9RF, Scotland.
N.C.T.C.C.: National Cell and Tissue Culture Centre, Glasnevin, Dublin 9, Ireland.
Oxoid: Basingstoke, Hampshire, England.
Southern Biotechnology: 160A Oxmoor Boulevard, Birmingham, Alabama 35209, U.S.A.

2.3. Standard solutions:

Phosphate Buffered Saline (PBS-1):

One tablet was dissolved per 100 mls of distilled water according to the manufacturer's instructions. When dissolved, the tablets prepare Dulbecco's A PBS which contains 10 mM phosphate buffer and 0.14 M NaCl, pH 7.2-7.4 (referred to in text as PBS-1).

Phosphate Buffered Saline 2 (PBS-2):

PBS-1 was prepared as described above, with 0.3 M NaCl added (referred to in text as PBS-2).

Wash Buffer:

PBS-1 containing 0.05% Tween-20 (v/v).

Diluent Buffer:

PBS-1 containing 0.05% (v/v) Tween-20 and 5% (v/v) FCS.

Hepes Buffered Saline (HBS):

Hepes buffered saline (BIACORE running buffer) containing 50 mM NaCl, 10 mM HEPES, 3.4 mM EDTA and 0.05% (v/v) Tween-20 was prepared by dissolving 8.76 g of NaCl, 2.56 g of HEPES, 1.27 g of E.D.T.A. and 500 µl of Tween 20 in 800ml of distilled water. The pH of the solution was then adjusted to pH 7.4 by the addition of 2M NaOH. The final volume was then made up to 1,000 ml in a volumetric flask. The solution was filtered through 0.2 µm filter and degassed prior to use.

SDS-PAGE (Sodium Dodecyl Sulphate-PolyAcrylamide Gel Electrophoresis) solutions:

Protein Electrophoresis

Polyacrylamide Gel Electrophoresis (PAGE)

Polyacrylamide gel electrophoresis (PAGE) was carried out using the discontinuous system, in the presence of sodium dodecyl sulphate (SDS), as described by Laemmli (1970). 8% (w/v) resolving and 4% (w/v) stacking gels were normally used and prepared from the following stock solutions as outlined in Table 2.4.

Stock Solutions:

(A) 30% (w/v) acrylamide containing 0.8% (w/v) bis-acrylamide.

(B) 1.5 M Tris-HCl, pH 8.8, containing 0.4% (w/v) SDS.

(C) 0.5 M Tris-HCl, pH 6.8, containing 0.4% (w/v) SDS.

(D) 10% (w/v) ammonium persulphate.

Solution	*Resolving Gel*	*Stacking Gel*
Acrylamide (A)	3.3. ml	0.83 ml
Distilled Water	4.17 ml	2.9 ml
Resolving Gel Buffer (B)	2.5 ml	-------
Stacking Gel Buffer (C)	-------	1.25 ml
Ammonium Persulphate (D)	100 µl	25 µl
TEMED	10 µl	5 µl

Table 2.4. The quantities of stock solutions required for the preparation of resolving and stacking gel used for polyacrylamide gel electrophoresis.

Samples were dissolved in solubilisation buffer (0.06 M Tris-HCl, pH 6.8, 2% (w/v) SDS, 25% (v/v) glycerol, 0.014 M 2-mercaptoethanol, 0.1% (w/v) bromophenol blue) and boiled for 8 mins before loading onto the gel. The gel was electrophoresed in electrode buffer, pH 8.3, containing Tris (0.025 M), glycine (0.192 M) and 0.1% (w/v) SDS, at 15 mA (stacking) and 25 mA (resolving) using an ATTO vertical mini electrophoresis system until the blue dye reached the bottom of the gel.

Staining of gels with Coomassie Brilliant Blue:

Gels were stained with Coomassie staining solution for visualisation of protein bands. Gels were stained for 1 hour in 0.2% (w/v) Coomassie Brilliant Blue in methanol:acetic acid:distilled water (3:1:6). Gels were destained overnight in methanol:acetic acid:distilled water (3:1:6).

Coomassie Blue Stain Solution

Coomassie Blue R-250	1.250 g
Methanol	227 ml
dH_2O	227 ml
Glacial acetic acid	46 ml

The components were dissolved, mixed thoroughly, filtered through Whatman paper grade number 1, and stored at room temperature (R.T.) in a dark bottle.

Destain Solution

Methanol	150 ml
Glacial acetic acid	50 ml
dH_2O	300 ml

The above components were mixed, thoroughly, and stored at R.T.

Electrophoresis Buffer

Tris.HCl	03.00 g
Glycine	14.40 g
SDS	01.00 g

The components were dissolved in 1L of dH_2O, and stored at R.T.

Sample Buffer

1M Tris.HCl (pH 6.8)	0.60 ml
50% (v/v) Glycerol	5.00 ml
10% (w/v) SDS	2.00 ml
2-ME (2-Mercaptoethanol)	0.50 ml
1% (w/v) Bromophenol blue	0.90 ml

The components were thoroughly mixed together, and stored at -20°C.

Acrylamide Stock Solution (A)

Acrylamide	29.20 g
Bisacrylamide	00.80 g

The components were dissolved in 100ml dH_20, and stored in the dark at 4°C.

4X Resolving Gel Buffer (B)

2M Tris-HCl (pH 8.8)	75.0 ml
10% (w/v) SDS	04.0 ml
dH_20	21.0 ml

The components were thoroughly mixed together, and stored at 4°C.

4X Stacking gel Buffer (C)

1M Tris.Cl (pH 6.8)	50.0 ml
10% (w/v) SDS	04.0 ml
dH_2O	46.0 ml

The components were thoroughly mixed together, and stored at 4°C.

Ammonium Persulphate Solution (D)

Ammonium persulphate	0.10 g
dH_2O	1.00 ml

The components were mixed thoroughly and stored at R.T.

Electrophoresis buffer

Tris	03.10 g
Glycine	14.40 g
Methanol	200.0 ml

The components were dissolved in 1,000 ml of dH_2O, and stored at R.T.

2.4. Chemical derivatisation and purification of 4'-aminowarfarin:

2.4.1. Production of 4'-aminowarfarin (3-(α-acetonyl-p-aminobenzyl)-4-hydroxycoumarin:

2.00 g of acenocoumarin (4'-nitrowarfarin) were added to a flask containing 3.00 g of zinc granules and 50 ml of 30% (v/v) acetic acid solution. The reaction was allowed to proceed at room temperature with constant stirring and followed by TLC (Thin Layer Chromatography) as described in section 2.4.2. Allowing the chemical reduction of the nitro- group proceed for too long, also resulted in the partial reduction of the ketone groups on the parent acenocoumarin molecule. Consequently, the reaction was stopped before reaching completion. Filtering the reaction mixture through Whatman filter paper (grade number 1) quenched the reaction mixture. This served two purposes, firstly to remove the reaction catalyst and unwanted zinc granules, and secondly, to remove the nitro- containing starting material, acenocoumarin, which is only partially soluble, compared to 4'-aminowarfarin in dilute acid solutions. The filtered acidic reaction mixture was then quickly back-extracted into ethyl acetate. The ethyl acetate extract was then dried for 20 minutes over anhydrous magnesium sulphate in a round-bottomed flask with constant stirring. The resulting solution was then filtered and vacuum dried under rotary evaporation.

2.4.2. TLC Analysis of 4'-aminowarfarin:

TLC analysis of the reaction mixture was performed by removing a portion of the reaction mixture with the aid of a glass Pasteur pipette into an eppendorf tube. This solution was then extracted into ethyl acetate after vortexing for 2 minutes on a vortex apparatus. The ethyl acetate extract was then spotted onto a TLC plate and placed in a tank containing a solution of methanol:chlorofrom (2:98, v/v) as mobile phase. The TLC plate was developed and viewed under a UV lamp. When the reaction had proceeded sufficiently far enough, the reaction was quenched as per section 2.4.1.

2.4.3. Silica column chromatography of 4'-aminowarfarin:

The mobile phase (methanol:chloroform, 2:98)(v/v) was mixed with silica grade 40 to form a slurry, which was then added to a 20 cm glass column. The mobile phase was then recycled through the column several times with the aid of a peristaltic pump, to ensure adequate packing of the column, and allowed to elute until it just covered the top of the silica column. The partially purified reaction mixture, containing the putative reaction product (i.e. 4'-

aminowarfarin) and trace impurities of the starting material 4'-nitrowarfarin, was resuspended in the minimum volume of column mobile phase, and carefully applied to the top of the packed silica column bed. The reaction mixture was then drawn evenly onto the silica column, and the glass bulb reservoir refilled with column mobile phase and reconnected to the peristaltic pump. 5 ml fractions of the column eluant were collected in test-tubes and analysed for character and purity by TLC analysis under UV light (section 2.4.2). The fractions corresponding to the 4'-aminowarfarin sample were then pooled and rotary evaporated under vacuum.

2.4.4. Analysis of 4'-aminowarfarin by Infra-Red spectroscopy:

20 mg of 4'-aminowarfarin were mixed with potassium bromide (KBr), and the mixture was crushed using a mortar and pestle to produce a very fine powdered suspension. The powdered suspension was then compressed using a disc press. The resulting disc was then placed in the slot of Nicolet® spectrometer that had been previously blanked with a potassium bromide disc. The spectra were analysed and peak identification was made by comparison to reference spectra.

2.4.5. Analysis of 4'-aminowarfarin by Nuclear Magnetic Resonance spectroscopy:

20 mg of 4'-aminowarfarin were dissolved in deuterated dimethyl sulfoxide (DMSO). This solution was then filtered through glass wool into a NMR tube. This sample was then analysed using a 400MHz Brucker® NMR spectrometer. The resulting proton NMR spectra were then integrated using dedicated Brucker® software that allowed for proton integration and identification.

2.5. Production of drug-protein conjugates:

4'-aminowarfarin-protein conjugates were produced and characterised as described in section 2.5.1.-2.6.3. for use as immunogens and subsequent screening procedures, in the production of monoclonal and polyclonal antibodies to warfarin.

2.5.1. Diazotisation of primary amine:

The acidified nitrite solution provides the source for the nitrosonium ion (I) which electrophilically replaces the hydrogen in the primary amino group to form the N-nitroso derivative (II). This has a tautomeric structure, the hydroxydiazo form (III) yielding the diazonium ion (IV) under acidic conditions.

An outline of the reaction mechanism involved in the diazotisation of the primary amine to allow for subsequent coupling is given below:

$$ArNH_2 + 2H^+ + 2HCl \rightarrow ArN{\equiv}N^+Cl^- + NaCl + H_2O$$

Reaction scheme:

$2NO_2^- + 2H^+ \rightarrow 2HNO_2 \Leftrightarrow O{=}N{-}O{-}N{=}O + H_2O$

$O{=}N{-}O{-}N{=}O \Leftrightarrow O{=}N^+ + {}^-O{-}N{=}O$ (I)

Nitrosonium ion

$ArNH_2 + {}^+N{=}O \xrightarrow{-H^+} ArNH{-}N{=}O$ (II)

N-Nitrosoderivative

$ArNH{-}N{=}O \Leftrightarrow ArN{=}N{-}OH$ (III)

Hydroxydiazoform

$ArN{=}N{-}OH + H^+ \Leftrightarrow ArN{\equiv}N^+ + H_2O$ (IV)

Acidic conditions — Diazonium ion

2.5.2. Drug conjugate preparation:

The drug-protein conjugates were produced according to the method of Satoh *et al.* (1982). A 0.014 mM solution of sodium nitrite was prepared by dissolving 9.7 mg in 10 ml of water. 350 mg of 4'-aminowarfarin were then dissolved in 50mls of a solution containing 0.1 M

HCl and 7 mM potassium bromide. The sodium nitrite solution was added dropwise to the solution containing 4'-aminowarfarin, and maintained with continuous stirring on an ice-bath for 1 hour. This solution was then added dropwise to a 5% (w/v) solution of BSA (Bovine Serum Albumin), the pH was maintained between 9.0-9.5 with the simultaneous addition of 0.1 M NaOH. This solution was then stirred overnight at 4°C. The resulting dark brown solution was then dialysed against several changes of PBS-1, and lyophilised prior to further studies.

For the production of KLH (Keyhole Limpet Haemocyanin) conjugates, the protein solution was made up in PBS-1 containing 0.9 M NaCl, to allow for solubilisation of KLH. 100 mg of 4'-aminowarfarin were activated as per section 2.5.1. and added to 40 mg of KLH, and the reaction followed as described above. The resulting drug-protein solution was dialysed against several changes of PBS-1 with 1.0 M NaCl added. The resulting dark brown solution was lyophilised for further studies.

2.5.3. Production of conjugates utilising DST crosslinkers:

Sulfo-DST (DisulfoSuccinimidyl tartrate) is a water-insoluble, homo-bifunctional N-Hydroxysuccinimide ester. Primary amines are principal targets for NHS esters. Accessible α-amine groups present on the N-termini of peptides and proteins react with NHS-esters.

20 mg of BSA were dissolved in 2 ml of PBS-1 and 90 mg of 4'-aminowarfarin in a 1% (v/v) DMSO solution were added to the protein solution. The crosslinker that was prepared just prior to use in PBS-1 to a final concentration of 5 mM, was then added to the protein and drug mixture. The reaction mixture was incubated on ice for 2 hours. The reaction was then quenched for 15 minutes by the addition of a 1 M Tris-HCl buffer, pH 7.5, and incubated for a further 15 minutes.

2.6. Characterisation of drug-protein conjugates:

All drug-protein conjugates were characterised by a combination of SDS-PAGE, UV and HPLC-photodiode array (PDA) scans.

2.6.1. HPLC-PDA and HPLC-UV analysis of drug-protein conjugates and affinity-purified antibody:

The Beckman system Gold™ HPLC system was attached to a PDA or UV detector. Samples were separated using a Biosep SEC-4000 (Phenomenex) column with a particle diameter of 10μm. The mobile phase consisted of PBS-1, which had been previously filtered and degassed. The flow rate was set to 1.0 ml/min. HPLC-PDA scans were produced and recorded from 200-400 nm. From the resulting spectra and plot overlays of the PDA-scans obtained for the drug-protein conjugates and protein solutions, a peak at approximately 310nm (λ_{max} warfarin =308 nm) can be seen that corresponds to the drug portion of the conjugate. Size exclusion chromatography of drug-protein conjugates, affinity-purified antibody fractions and standards of known molecular weight was also carried out using the experimental conditions described above, except that UV detection at 280 nm was used instead of PDA detection. From the constructed calibration curve of log (molecular weight) versus time, it was possible to estimate the molecular weight of the drug-protein conjugates and purified antibody fractions.

2.6.2. SDS-PAGE analysis of drug-protein conjugates:

SDS-PAGE gels were run according to the conditions described in section 2.3. Drug-protein conjugates and 'control'-protein (i.e. protein solutions which underwent the same chemical procedure except the drug was omitted from the coupling step) were prepared in solubilisation buffer and placed in adjacent wells in the gel using a Hamilton syringe. Proteins used in all characterisation procedures were subjected to the same experimental procedures as those for the proteins used in the coupling reactions.

2.6.3. Ultraviolet spectroscopy:

The lyophilised drug-protein conjugates were prepared in PBS-1, and their UV spectra analysed from 200-400 nm. UV spectra of similar concentrations of 'control' protein were also prepared and recorded. The UV spectrum of the 4'-aminowarfarin drug molecule was also recorded over a similar wavelength range. Direct comparison of the three spectra gave putative confirmation of the conjugation of 4'-aminowarfarin to the protein molecules, to form the conjugates of interest.

2.7. Production of immunoaffinity matrices:

Immunoaffinity matrices were prepared by the chemical coupling of 4'-azowarfarin-BSA to sepharose-4B and Triazine 4XL. The immunoaffinity matrices were then used for the affinity-purification of polyclonal antibodies to warfarin from ammonium sulphate precipitated rabbit immunoglobulin fractions.

2.7.1. Preparation of 4'-azowarfarin-BSA sepharose column:

4'-azowarfarin-BSA was coupled to CNBr-Sepharose 4B according to the manufacturer's instructions. 6 g of CNBr-Sepharose 4B was weighed out and swollen in 100 mM HCl for 1 hour, giving approximately 20 ml of wet gel. The gel was then sucked dry on a Buchner funnel with a filter of pore size 0.2 μm, and washed twice with 250 ml of PBS-1. 200 mg of 4'-azowarfarin-BSA was then dissolved in coupling buffer (0.1 M $NaHCO_3$, pH 8.3, with 0.5 M NaCl).

The coupling solution was then added dropwise to the gel, under gentle rotation, and the mixture rotated overnight at 4°C. The reaction mixture/ gel was then washed successively with 200 ml each of, 0.1 M sodium bicarbonate pH 8.5, PBS-1, and PBS-1 containing 1.0 M NaCl. The excess active amine groups were then blocked, by mixing the gel with 40 ml of 1.0 M ethanolamine for 2 hours under gentle rotation. The gel was then washed with 0.1 M acetate buffer, pH 4.0, containing 0.5 M NaCl and with coupling buffer, and stored in PBS-1 with azide (0.02%, v/v) at 4°C.

2.7.2. Preparation of a 4'-azowarfarin-BSA Triazine column:

Triazine activated agarose 4XL is a unique activated adsorbent for highly efficient immobilisation of proteins and other ligands. Coupling occurs primarily through surface lysine and histidine residues on the ligand to yield neutral linkages that exhibit good stability across the pH range.

Using a Buchner funnel, the gel was allowed to drain through a 0.2 μm filter, the storage preservative discarded, and the gel washed with at least 20 volumes of distilled water and allowed to drain under gravity. The Triazine 4XL gel was then washed with at least 10 volumes of coupling buffer (50 mM acetate buffer, pH 5.0 containing 0.5 M NaCl) and allowed to drain under gravity, and placed into a universal container suitable for mixing. A 10 mg/ml solution of 4'-azowarfarin-BSA was then made up in 50 mM acetate buffer, pH 5.0, sodium chloride was then added to bring final concentration to 0.5 M NaCl. The gel was then added to an equal volume of protein solution with gentle mixing at 4°C for 2 hours.

The gel was then washed with 10 volumes of coupling buffer, and the gel resuspended in 2 M imidazole, pH 5.0, and mixed for 2hrs at room temperature to block residual active groups. The gel was then washed with 5 volumes of ultrapure (UP) water and 5 volumes of 20% (v/v) ethanol, coupling buffer, PBS-1 containing 1.0 M NaCl and stored in PBS-1 with azide (0.02%, v/v) until required.

2.8. Animal experiments:

2.8.1. Licensing

All procedures involving the use of animals were approved and licensed by the Department of Health, and every precaution was taken to ensure the minimum distress to the animals.

2.8.2.1. Immunisation protocol for mice for the production of monoclonal antibodies to warfarin.

Balb/C mice of age 5-10 weeks old were used for the production of monoclonal antibodies to warfarin, using the immunisation schedule described below:

Day 1: A 2 mg/ml solution of 4'-azowarfarin-thyroglobulin/Keyhole Limpet Haemocyanin (KLH) or 4'-aminowarfarin-DST-thyroglobulin (DiSuccinimidyl Tartrate) was prepared in PBS-1 and mixed with an equal volume of Freund's Complete Adjuvant (FCA). This solution was then vortexed to form an emulsion, and 300 µl of the emulsion used to immunise mice by intraperitoneal (i.p.) injection.

Day 21: Mice were re-immunised intraperitoneally with a similar dose of the immunogen above in Freund's Incomplete Adjuvant (FICA).

Day 28: Mice were bled from the tail vein, and the specific antibody titre determined.

Post-Day 28: Mice were boosted intraperitoneally with a similar mix of conjugate and FICA as per day 21.

Post-Day 28: The above immunisation and blood sampling sequence was continued until a satisfactory antibody titre was recorded. Once the antibody titre was sufficiently high, the mouse was immunised intravenously (i.v.)(250 µl))(3-4 days prior to sacrifice) with the respective conjugate in PBS-1.

The mouse was then sacrificed by cervical dislocation, the spleen removed and used for subsequent monoclonal antibody fusion procedures.

2.8.2.2. Immunisation protocol for the production of rabbit polyclonal antibodies to warfarin:

New Zealand White Rabbits > six months old were used for the production of polyclonal antiserum to warfarin, using the immunisation schedule described below:

Day 1: A 2 mg/ml solution of 4'-azowarfarin-thyroglobulin/Keyhole Limpet Haemocyanin (KLH) was prepared in PBS-1 and mixed with an equal

volume of Freund's Complete Adjuvant (FCA). The rabbit was then immunized at various sites by intradermal injection with an emulsion (1 ml) consisting of a 1 mg/ml solution of the immunogen (4'-azowarfarin-thyroglobulin/Keyhole Limpet Haemocyanin (KLH)) mixed 1:1 with Freund's Complete Adjuvant (FCA).

Day 21: A 1ml-blood sample from the ear vein (primary bleed) was removed, and the specific antibody titre determined.

Day 31: The rabbit was re-immunised as before using Freund's incomplete adjuvant.

Day 41: A 1 ml blood sample was obtained as before (secondary bleed), and the specific antibody titre determined (section 2.11.1).

***Antiserum recovery*:**

The above cycle of blood sampling/titration and re-immunisation was carried out at 10-day intervals until the antibody titre was seen to plateau. At this stage the animal was sacrificed, and the blood recovered by cardiac puncture.

2.8.3. Preparation of rabbit serum:

The harvested rabbit serum was allowed to clot at room temperature for 2 hours and refrigerated overnight at 4°C. The serum was then centrifuged at 4,000 r.p.m. for 30 minutes. The supernatant was removed and stored at –20°C until required.

2.8.4. Monoclonal antibody production by ascitic growth:

Ascitic fluid (also called ascites) is an intra-peritoneal fluid extracted from mice that have developed a peritoneal tumour. For antibody production, the tumour is induced by injecting hybridoma cells into the peritoneal cavity of mice of the same genetic background as the hybridoma.

Balb/C mice of the same genetic background as the hybridomas were given an intra-peritoneal injection of 0.5 ml of pristane (2,6,10,14-tetramethylpentadecane). This solution acts as an immuno-adjuvostimulant /irritant to the mice, which respond by secreting nutrients and recruiting monocytes and lymphoid cells into the peritoneum, thus creating a rich environment for hybridoma growth. 7-10 days later, 2-3 $x10^7$ hybridoma cells were injected intra-peritoneally. Tumour growth was evident after 1-2 weeks and the mice were sacrificed. The ascitic fluid was drained under sterile conditions by insertion of a needle into the peritoneal cavity. The harvested cells were then cultured as described in section 2.10.4.

2.9. Antibody purification:

2.9.1. Purification of polyclonal rabbit serum:

2.9.1.1. Ammonium sulphate precipitation:

The ammonium sulphate precipitation of rabbit serum was carried out according to the method of Hudson & Hay (1980). 10ml of rabbit serum were diluted 1:2 with PBS-1 and the required volume of saturated ammonium sulphate was added to bring the final concentration to 45% (v/v). This mixture was then stirred at room temperature for 30 minutes, and the resulting precipitate centrifuged at 3,000 r.p.m. for 20 minutes. The precipitate was then resuspended in a volume of PBS-1, equal to that of the original volume of serum. Saturated ammonium sulphate was then added to bring the final concentration to 40% (v/v) and the mixture centrifuged at 3,000 r.p.m. for 20 minutes. The pelleted precipitate was then resuspended, in a volume equal to one-third of the original volume of serum. The resuspended precipitate was then dialysed overnight against PBS-2 with 0.02% (w/v) sodium azide at 4°C.

2.9.1.2. Affinity purification of polyclonal anti-warfarin antibodies:

A 10 ml 4'-azowarfarin-BSA sepharose-4B column was equilibrated with running buffer (PBS-2 containing Tween 0.05% (v/v)). The dialysed ammonium sulphate rabbit immunoglobulin fraction was applied to the immunoaffinity column, collected and passed through the column twice more to ensure saturation of the column. The column was then washed with two column volumes of wash buffer. 0.1 M glycine-HCl (pH 2.5) was then added to the column and fractions collected in 1ml eppendorf tubes containing 150 µl 1.0 M Tris–HCl, pH 8.5. The Tris-HCl buffer immediately neutralized the acidic immunoglobulin fractions eluted from the column, thus preserving the immunological activity of the eluted antibody fractions. The absorbance of each fraction was measured, at 280 nm, and the fractions containing immunoglobulin were pooled and dialyzed against PBS-2 at 4°C.

2.9.2. Monoclonal antibody purification:

2.9.2.1. Concentration of tissue culture supernatant:

200 ml of spent supernatant from the relevant hybridoma cell line was collected over a period of time as described in section 2.10.4. Sodium azide was added to a final

concentration of 0.02% (w/v) to the supernatants, which were then stored at 4°C until required.

The supernatant was concentrated 10-fold to a final volume of 20 ml, using a stirred ultrafiltration cell with a 76 mm diaflo ultrafilter membrane, with a molecular weight cut-off of 100,000 daltons, and the concentrate stored at 4°C until required.

2.9.2.2. Protein G/A affinity purification of murine and goat anti-mouse immunoglobulin:

1ml of a suspension of immobilised protein G (immobilised on Sepharose 4B) (stored in PBS-1 containing 20% (v/v) ethanol) was equilibrated in a column with 20ml of PBS-1. 10 ml of concentrated hybridoma supernatant, or, 2 ml of goat serum containing anti-mouse immunoglobulin was passed through the column, the eluate collected and passed through the column a second time. 25 ml of wash buffer was passed through the column and, subsequently, the retained protein was eluted with 0.1 M glycine-HCl buffer (pH 2.5). 850 µl fractions of eluate were collected in eppendorf tubes containing 150 µl of Tris-HCl (pH 8.5). The absorbance of each fraction was measured, at 280 nm. Those fractions containing significant protein were pooled, dialysed against PBS-2 and stored at –20°C until required for further use.

2.10. Mammalian Cell Culture:

All mammalian cell cultures were cultured aseptically and grown in a humidified 5% CO_2 atmosphere, at 37°C.

2.10.1. Preparation of mammalian cell culture media:

All cell lines were grown in DMEM (Dulbecco's modification of Eagle's medium) supplemented with 10% (v/v) foetal calf serum (FCS), 2 mM L-glutamine, and 25 μg/ml gentamycin (referred to as DMEM).

For somatic cell fusion procedures, three additional media preparations were prepared. DMEM lacking foetal calf serum was prepared for use during somatic cell fusion procedures. Additionally, HAT (Hypoxanthine, Aminopterin and Thymidine) medium was prepared, which consisted of DMEM supplemented with 1 mM sodium pyruvate, non-essential amino acids (NEAA; 1%, v/v), 100 μM hypoxanthine, 400 nM aminopterin, and 16 μM thymidine (referred to as HAT medium). This particular culture medium allowed for the selective growth of hybridoma cells post-fusion in the presence of Sp2/0 cells, which are unable to proliferate in HAT medium because they lack the requisite enzyme systems (section 5.1.1.). DMEM supplemented with 1 mM sodium pyruvate, non-essential amino acids (1%, v/v), 100 μM hypoxanthine and 16 μM thymidine was also prepared (referred to as HT medium).

2.10.2. Recovery of frozen cells:

Cells were recovered from liquid nitrogen by rapidly thawing at 37°C, and transferring to a sterile universal containing DMEM. The cells were then centrifuged at 2,000 r.p.m. for 10 minutes, resuspended in fresh culture medium, transferred to a tissue culture flask and incubated at 37°C in a humidified 5% CO_2 incubator. Prior to incubation, a 100 μl sample of the resuspended pellet was tested for cell viability using Trypan blue (section 2.10.3.). Only cells with > 90% viability on recovery from frozen stocks were further cultured.

2.10.3. Cell counts and Viability testing:

All cell counts were made using an improved Neubauer Counting Chamber. Viable cell counts were obtained by mixing 100 μl of cell suspension with 20 μl of a commercial isotonic Trypan blue solution (Sigma, 0.25% (w/v)). The viable cell count was carried out within 5 min. of the addition of Trypan blue. A sample of this mixture was then used to perform the cell and viability count. Viable cells excluded the dye and remained white,

while dead cells were stained blue. Cells were visualised under phase contrast on an inverted microscope at 40 X magnification. All cells were pelleted by centrifugation, and all centrifugations were at 2,000 r.p.m. for 5 minutes unless otherwise stated.

2.10.4. Growth of suspension cell lines:

The Sp2/0 (ATCC CRL 1581) cell line was cultured in DMEM. The cells were subcultured, using a split ratio of 1:4, at approximately 70% confluency. For subculturing, the cells were flushed off the surface of the flask using a Pasteur pipette, collected and centrifuged at 2,000 r.p.m. The pellet was then resuspended in 4 ml of fresh culture medium. 1 ml of the resuspended pellet was then transferred to T-75 flasks containing 14 ml of fresh DMEM.

2.10.5. Storage of cell lines:

Cells were harvested from the surface of a confluent T-75 flask by flushing the surface of the flask with a Pasteur pipette, and pelleted by centrifugation at 2,000 r.p.m. Pellets were resuspended in 4 ml of a 10% (v/v) solution of DMSO (Dimethyl sulphoxide) in FCS, and aliquoted into 4 cryovials. A freezing-tray was used to gradually cool the cells, over a 2.5 hr. period, in the vapour-phase of liquid nitrogen. They were then immersed in the liquid-phase for long-term storage.

2.10.6. Mycoplasma screening:

Cell lines were screened for mycoplasma contamination in conjunction with the National Cell and Tissue Culture Centre, Dublin City University.

2.10.6.1. Cell culture of NRK cells:

Adherent NRK (normal rat kidney) cells were cultured in DMEM. When cells had reached 70% confluency, the medium was poured off, and the flask rinsed three times with 10ml of sterile PBS. 3ml of trypsinising solution (Gibco 0.025% (v/v) and 0.02% EDTA (v/v)) was added to the flask, which was replaced back in the incubator until all of the cells had detached. 5 ml of fresh DMEM was then added to this cell suspension, which was then centrifuged at 2,000 r.p.m. and the pellet resuspended in the required volume of fresh DMEM.

2.10.6.2. Screening for mycoplasma contamination:

NRK cells were cultured for at least 3 passages prior to mycoplasma screening in antibiotic-free medium. Hoechst stain was used for visualisation of the mycoplasma. Mouse myeloma cell lines used for somatic cell fusion procedures, and various hybridoma cell lines were

grown in antibiotic-free media for 2 weeks prior to screening for mycoplasma, to ensure any intracellular antibiotic was removed. Cells were then seeded at a low density and allowed to proliferate for 3 days to 70% confluence, the conditioned medium was then removed and stored for subsequent screening at –20°C.

NRK (Normal Rat Kidney) cells were prepared to a final cell density of 2 x 10^3 cells/ml in a modified version of DMEM containing 5% FCS (v/v) and 1% L-glutamine (v/v), and 1 ml of cell suspension was then added onto sterile coverslips in petri-dishes. The cells were then incubated at 37°C overnight. The following day, 0.5 ml of conditioned medium was removed from the test samples and added to the NRK cells growing on the coverslips. The petri-dishes were then incubated for a further 3-4 days at 37°C.

The medium from each petri-dish was then removed and the coverslips were washed twice with sterile PBS, and once with PBS/Carnoy's fixative (cold). 2 ml of Carnoy's fixative (glacial acetic acid: methanol, 1:3, v/v) was then added to each coverslip and allowed to fix for 10 minutes. The samples were then allowed to air-dry overnight.

2ml of the DNA-intercalating dye Hoechst 33258 (working stock 50 ng/ml) was then added to each sample. The samples were then allowed to stain for 10 minutes in low-light. After 10 minutes, the stain was very carefully removed and each coverslip washed with 3 x 2 ml of sterile distilled water. The washed coverslips were then mounted onto slides, and with the aid of a drop of mounting medium observed under the microscope using the 100 X objective lens using a fluorescent microscope. Uncontaminated cells show strong fluorescence in the nuclei only, whereas mycoplasma contaminated cells are detected by cytoplasmic staining of the mycoplasmic DNA.

2.10.7. Hybridoma production and isolation:

2.10.7.1. Somatic cell fusion:

Sp2/O cells were grown for at least two weeks, prior to fusion. Cells were not grown above 50% confluency, and were subcultured at a split ratio of 1:2 the day before fusion. On the day of fusion, the medium was poured off the Sp2/0 cells, and fresh DMEM lacking FCS was added. Cells were resuspended and counted. The cells were stored on ice until required.

Splenocytes, from an immunised mouse were harvested, resuspended in DMEM lacking FCS, and counted. The splenocytes and Sp2/O cells were mixed to give a cell ratio of 10

splenocytes per Sp2/0 cell. This cell mixture was pelleted by centrifugation at 1,250 r.p.m. and washed 4 times with 5 ml of DMEM lacking FCS.

All of the supernatant, from the final wash, was removed, except for 50-100 µl (simply pouring of the supernatant sufficed). The cells were resuspended by tapping the outside of the centrifuge tube with a finger until all of the cell pellet could be observed to be in solution. The cell suspension was placed in an ice-water bath, and 1.5 ml of 50% (v/v) PEG (polyethylene glycol, molecular weight 1540 Da) which had been previously cooled to 4°C was added to the cell suspension, over a 1 minute period, with constant mixing. Mixing was maintained for another 1.5 minutes. The centrifuge tube was removed from the ice-water bath, and enclosed in the palm of the hand. 20 ml of pre-warmed (37°C) DMEM lacking FCS was then added at a constant rate with the aid of a Gilson pipette over a 5 minute interval with continual, slow, swirling of the centrifuge tube. The resulting suspension was placed at 37°C in a water bath for 15-20 minutes. The suspension was centrifuged, at 1,000 r.p.m. for 10 minutes, and the cells resuspended at a cell density of $1.2x10^6$ cells/ml, in HAT medium supplemented with 5% (v/v) Briclone. The suspension was plated, in 96 well plates, at 0.1 ml per well, and incubated for 7 days. On day 7, 50 µl of fresh HAT medium supplemented with 5% (v/v) Briclone was added to each well. On day 8, 50 µl of spent medium was removed and fresh medium was added. Wells were then fed as required.

2.10.7.2. Screening for specific monoclonal antibody production:

70 µl of 'spent' hybridoma supernatant was removed from the masterplate wells, and replaced with fresh DMEM supplemented with 5% (v/v) Briclone. The 'spent' hybridoma medium was then screened for specific anti-warfarin antibody production by conventional ELISA as described in section 2.11.1. Positive wells from the initial screening were then transferred to 48-well plates, and subsequently to 6-well plates for cloning.

2.10.7.3. Cloning of anti-warfarin specific hybridomas:

Cells from wells, which tested positive in the ELISA, were expanded in HAT medium, from 96-well plates, to 48-well plates and finally to 6-well plates. Cells were cloned, by limiting dilution, when they had reached 50% confluency. Briefly, cells were resuspended, and diluted to 100 cells/ml in HT supplemented with 5% (v/v) Briclone. The cell suspension was plated, then, at 100 µl/well in 96-well plates. After 7 days, 50 µl of fresh HT containing 5% (v/v) Briclone was added, and on day 8 half the medium was changed. Wells were fed as required. Screening for positive wells proceeded, using an ELISA as per section 2.11.5, using neat medium from the well, as the test sample. Selected hybridoma supernatants were

then screened at this stage using a variety of drug-protein conjugates employing different coupling chemistries and in a competitive assay format as described in section 2.11.5. Only cells that demonstrated inhibition in the competitive assay format were expanded further. Positive wells were expanded, as already described, and recloned twice at 10 cells/well, and once at 1 cell/well. The second time, cells were cloned in DMEM containing 10% (v/v) FCS, NEAA (1%, v/v), and 1 mM sodium pyruvate rather than in HT medium. Positive wells at this stage were considered, to be monoclonal.

2.11. Solid phase immunoassays:

2.11.1. ELISAs for titration of antibody levels in serum samples/hybridoma supernatants:

100 µl of a solution of 50 µg/ml 4'-azowarfarin-BSA prepared in PBS-1, was added to all of the wells of a Nunc maxisorp plate, and incubated at room temperature overnight. Wells were washed with 5 x 200 µl of wash buffer, and 100 µl of a 5% (v/v) solution of FCS in PBS-1 was added to each well, and incubated for 90 minutes at 37^{0}C. This was to 'block' any remaining adsorption sites on the plastic surface.

Wells were then washed out with 5 x 200 µl of wash buffer. 100 µl of test sample (i.e. the appropriate dilution of rabbit/mouse serum sample or hybridoma supernatant) was added to the wells of the plate. Samples were diluted in PBS-1 containing 0.05% (v/v) Tween-20 and 5% (v/v) FCS, and for the determination of antibody titres in mouse and rabbit serum, serial doubling dilutions were started at a dilution of 1/200. Hybridoma supernatants were normally screened neat for specific antibody. Samples were incubated for 90 minutes at 37°C.

Wells were washed with 5 x 200 µl of wash buffer, 100 µl of secondary antibody (alkaline phosphatase conjugated to a goat anti-mouse antibody or a goat anti-rabbit antibody), diluted as required in diluent buffer, was added to each well and incubated for 90 minutes at 37°C.

Wells were washed with 5 x 200 µl of wash buffer, and 100 µl of substrate was added per well. The substrate used was para-nitrophenyl phosphate (pNPP) provided in tablet form, and dissolved in the required volume of dH_2O immediately before use, according to the manufacturers instructions. Substrate was left to develop in the dark at room temperature, or overnight at 4°C. Absorbance readings were read at 405 nm using a Titertek plate reader.

2.11.2. Isotyping of monoclonal antibodies:

ELISA plates were coated and blocked as described in section 2.11.1. 100 µl of culture supernatant from positive hybridomas, following cloning by limiting dilution, was then added to each well of the coated plate. Alkaline-phosphatase labeled goat anti-mouse immunoglobulin subtypes were then added to the wells and the ELISA developed as described in section 2.11.1. Wells giving positive results defined the monoclonal antibody isotype.

2.11.3. Determination of antibody working dilution:

ELISA plates were coated and blocked as described in section 2.11.1. Serial dilutions of purified monoclonal and affinity-purified rabbit polyclonal antibody were then prepared in diluent buffer, starting dilutions at 1/1000. Ten serial dilutions were then prepared by doubling dilution in diluent buffer. 100 µl of test sample was then added to the wells of the plate in triplicate, and incubated at 37°C for 90 minutes.

Wells were then washed with 5 x 200 µl of wash buffer, and 100µl of the appropriate secondary antibody (i.e. alkaline phosphatase conjugated to a goat anti-rabbit or anti-mouse isotype specific antibody) prepared in diluent buffer was added to each well, and the plate incubated at 37°C for 90 minutes. Wells were then washed with 5 x 200 µl of wash buffer and 100 µl of substrate (pNPP) was added per well. The plate was developed at room temperature in the dark or overnight at 4°C. Absorbance was measured using a Titertek plate reader at 405 nm. The optimal dilution of purified antibody (i.e. rabbit polyclonal/mouse monoclonal) was determined in this manner as the dilution taken from the mid-point of the linear portion of the sigmoidal curve obtained.

2.11.4. Determination of optimal conjugate loading density:

4'-azowarfarin-BSA was prepared in PBS-1 at various concentrations, namely 100, 50, 25, 10, and 5 µg/ml. A 100 µg/ml solution of BSA control was also prepared in PBS-1 as a control. 100µl of the respective conjugate concentration was used to coat two rows of a Nunc Maxisorp immunoplates overnight at room temperature. The ELISA was developed as per section 2.11.3. The optimal conjugate loading density was defined as that coating density that gave the widest linear working range over the greatest range of antibody dilutions used.

2.11.5. Competitive ELISA

Nunc Maxisorp plates were coated and blocked as described in section 2.11.1. Serial dilutions of warfarin ranging in concentration from 0.03-5,000 ng/ml were prepared in diluent buffer lacking FCS (5%, v/v). 50 µl of each drug concentration was then added to the wells of a coated microtitre plate, and 50 µl of purified antibody at 2 x working dilution was added to the wells of the plate. The plate was then developed as described in section 2.11.1. Absorbance values were then measured at 405 nm using a Titertek plate reader. Absorbance values at each antigen concentration were then divided by the absorbance measured in the presence of zero antigen to give normalised absorbance readings (see

Appendix 1A). A plot of the normalised absorbance reading versus antigen concentration (ng/ml) was used to construct the calibration curve.

2.11.6. Affinity analysis using ELISA:

The method of Friguet *et al.* (1985) was employed (section 5.2.6.1). Briefly, the day before the ELISA analysis, a series of antibody-antigen mixtures were prepared in eppendorf tubes and placed on a rocking platform at room temperature overnight, and allowed to reach equilibrium. These solutions each contained a constant but unknown concentration of antibody. This concentration was nominally referred to as "1". The antibody:antigen solutions each contained a constant concentration of antibody, and varying but known concentrations of antigen ([A]). Additionally, serial doubling dilutions of antibody were prepared from that antibody dilution given the nominal antibody concentration of "1". These dilutions were used to construct a standard curve of nominal antibody concentration versus absorbance at 405 nm. The following morning, the nominal concentration of free antibody in each solution was determined by ELISA, as per section 2.11.1. Absorbance readings at 405nm values were related to nominal concentration values, by reference to the constructed standard curve of nominal antibody concentration versus absorbance at 405 nm.

The fraction of total antibody, bound by antigen (v), was calculated for each antigen concentration. The slope of a plot of 1/v versus 1/[A] (Klotz plot) defined the dissociation constant for the interaction.

2.11.7. Determination of mouse immunoglobulin concentrations by affinity-capture ELISA

Goat anti-mouse immunoglobulin which had been previously affinity-purified according to section 2.9.2.2. was diluted to a final concentration of 10 μg/ml in PBS-1, and 100 μl added to the wells of an ELISA plate and allowed to coat overnight at room temperature. The plate was then blocked as described in section 2.11.1. Dilutions of mouse IgG of known concentration ranging from 3.90-1000 ng/ml were prepared in diluent buffer. Dilutions of affinity-purified antibody and hybridoma supernatant ranging from 1/2000 to 1/16,000 and 1/1,000 to 1/4,000, respectively, were also prepared in diluent buffer. 100 μl of the solutions containing mouse IgG of known concentration, and the dilutions of both hybridoma supernatant and affinity-purified antibody were added to the wells of the ELISA plate in triplicate. The ELISA was developed as described in section 2.11.1 using a goat anti-mouse alkaline phosphatase-labelled secondary antibody. A calibration curve of absorbance at 405 nm versus mouse IgG concentration allowed for the determination of the mouse IgG concentration in the affinity-purified and hybridoma supernatants.

2.12. BIACORE Studies:

2.12.1. Preconcentration studies:

The BIACORE™ with CM5 chips, was used for all 'real-time' analyses. For a detailed description of the theory and practice of this instrument, the reader is referred to Jönnson *et al.* (1991). For preconcentration studies, 4'-azowarfarin-BSA was dissolved at a concentration of 50 μg/ml in 10 mM sodium acetate buffer, at a range of pH values between 3.8-5.5. These were passed, sequentially, over an underivatised chip surface, and that pH giving the greatest mass (measured in terms of response units (RU)) pre-concentrated at the surface of the chip, was used for subsequent warfarin-BSA immobilisation procedures.

2.12.2.1. Immobilisation of drug-protein conjugates:

The chip surface was activated, by passing 35 μl of a solution containing 0.05 M NHS and 0.2 M EDC in ultra-pure (UP) H_2O, over the chip surface at a flow rate of 5 μl/min. 35 μl of a solution of 4'-azowarfarin-BSA in 10 mM acetate buffer, pH 4.8, was passed over the surface at a flow rate of 5 μl/min. Unreacted NHS groups were 'capped' (section 4.2.2.), by passing 35 μl of a 1 M ethanolamine (pH 8.5) solution over the surface at a flow rate of 5 μl/min.

2.12.2.2. Direct immobilisation of drug onto chip surface:

Direct immobilisation of drug directly onto the chip surface, was performed manually outside the BIACORE instrument. The chip was first allowed to equilibrate to room temperature. 40 μl of HBS buffer (section 2.4.) was added to the sensor chip well and left for 5minutes, this served to prime the chip surface. This solution was then removed using lint-free adsorbent paper, taking great care to ensure that paper did not touch the dextran matrix. Equal volumes of 0.4 M EDC and 0.1 M NHS were then mixed, and 40 μl of the resulting solution, containing 0.05 M NHS and 0.2 M EDC in UPH_2O, was added to the chip well and left for 15 minutes. The EDC/NHS was then removed using adsorbent paper. 4'-aminowarfarin, at a concentration of 50 μg/ml in 10m M sodium acetate buffer, pH 5.5, was then added to the chip well and allowed to react for 20 minutes. The chip was then blocked by adding 40 μl of a 1.0 M ethanolamine (pH 8.5) solution to the chip well and left for 20 minutes. The chip was then extensively washed with distilled water and dried under nitrogen. The chip could then be stored in HBS or in a desiccator for later use.

2.12.3. Regeneration studies:

To assess the stability of the immobilised drug-protein conjugates or directly immobilised drug surfaces, a known concentration of antibody was passed over the chip surface and the surface regenerated with mild acid/base solution (10-25 mM HCl was usually sufficient to dissociate the complex). This cycle of binding and regeneration was usually completed for greater than 100 cycles, and the binding signal measured to assess the stability and suitability of the immobilised surface for assay purposes.

2.12.4. Non-specific binding studies:

Purified monoclonal and polyclonal antibody solutions, and hybridoma supernatants at the requisite dilution were passed over an immobilised BSA surface and the dextran matrix itself. Non-specific binding to either dextran or immobilised BSA surface was 'titered' out by the addition of either molecule to the antibody solution.

2.12.5. Universal standard curve:

4'-aminowarfarin was immobilised on a sensor chip as described in section 2.12.2.2. Serial dilutions of antibody supernatant and purified antibody were passed over the surface under conditions of mass transfer limitation (MTL) at 10 µl/min for 4 minutes (section 5.1.11.2 and 5.2.4.2.) The rate of antibody binding (dR/dT) was calculated from the slope of the binding curve and plotted against the logarithm of the reciprocal of the antibody dilution factor used. From the curve and algorithm, the concentration of antibody [nM] in both solutions was calculated.

2.12.6. Competitive/Inhibition assays:

Warfarin was prepared at a series of concentrations ranging from 0.03-5,000 ng/ml by serial dilution, using Hepes Buffered Saline (HBS) as diluent. Antibody was then mixed with the various antigen concentrations using the BIACORE autosampler. The antibody:antigen mixture was allowed to equilibrate for a specified time interval (normally 5-10 minutes). The equilibrium mixtures were then passed sequentially, in random order, over the chip surface at 10 µl/min for 4 minutes, and the chip surface regenerated between cycles by pulses of the appropriate regeneration solution for each antibody type (section 4.2.3.1.). The amount of bound antibody following injection of the antibody:antigen mix was measured in terms of response units (R). The respective responses (R), were then divided by the response measured for the antibody:antigen mixture containing zero antigen (R_0), to give normalised binding responses (R/R_0)(Appendix 1A). A plot of antigen concentration ng/ml versus

normalised binding responses (R/R_0) could then be used to construct the calibration plot using BIAevaluation 3.1 software.

2.12.7. Solution affinity analysis using BIAcore:

4'-azowarfarin-BSA (13,000 RU) was immobilised using the conventional EDC/NHS coupling chemistry. Serial dilutions of Protein G-purified anti-warfarin monoclonal antibodies of known concentration were passed over the immobilised surface, and a calibration curve was constructed of mass bound measured in terms of response units, versus antibody concentration (nM). A known concentration of antibody was then incubated with varying concentrations of warfarin (nM), and allowed to reach equilibrium overnight. The equilibrium samples were then sequentially passed over the immobilised surface and the binding response calculated. The response values measured were used to calculate the amount of 'free antibody' in the equilibrium mixtures, from the constructed calibration curve. A graph was then constructed of drug concentration (nM) versus 'free antibody concentration' (nM), and using the solution phase interaction models in BIAevaluation 3.1 software, the overall affinity constant could be determined.

2.12.8. Steady state affinity analysis using BIAcore

4'-azowarfarin-BSA (~1200 RU) and BSA (~1500 RU) were immobilised on separate flow cell surfaces of a sensor chip. Serial dilutions of purified monoclonal antibodies to warfarin of known concentration, were then sequentially passed over the chip surfaces using 'on-line' reference curve subtraction. A graph was then constructed of the equilibrium binding response (Req) measured versus antibody concentration (nM). Using the steady-state interaction model in BIAevaluation 3.1 software, the affinity constant could then be calculated for the interaction.

2.13 HPLC studies:

2.13.1. Preparation of plasma ultrafiltrate:

50 ml of blank plasma obtained from Sigma, was placed in an Amicon concentration device containing a 1 kDa molecular weight cut-off membrane. The plasma ultrafiltrate was collected under positive pressure and stored at –20°C until required for further analysis.

2.13.2. Extraction of warfarin from plasma samples:

1.0 ml of patient plasma was placed in blood tubes and 50 µl of internal standard, *p*-chlorowarfarin, was added to a final concentration of 500 ng/ml. 1.0 ml of 1.0 M sulphuric acid was then added to the plasma samples, which were then placed on a blood-tube rotator for 30 minutes. 5 mls of ethyl acetate were then added to the plasma acid extracts, and placed back on the blood tube rotator for a further 60 minutes. The samples were then centrifuged at 3,500 r.p.m., and 4.5mls of the organic layer removed and placed in evaporating tubes under nitrogen at 35°C. The samples were then reconstituted in 200 µl of mobile phase as described in section 2.13.4. prior to injection onto the HPLC system. Drug concentrations were measured using the HPLC method described in section 2.13.4.

2.13.3. Preparation of patient plasma ultrafiltrate:

Patient samples were placed in Nanosep™ ultrafiltration devices that contain a 1 kDa molecular weight membrane cut-off filter. The samples were centrifuged at 8,000 r.p.m. on a microcentrifuge for 30 minutes. Following ultracentrifugation, the plasma ultrafiltrate was collected and analysed by HPLC and BIACORE immunoassay as described in section 2.13.4. and 2.12.6., respectively.

2.13.4. HPLC detection of warfarin in plasma ultrafiltrate and plasma:

Mobile phase for HPLC analysis of warfarin in plasma ultrafiltrate and plasma, was prepared by mixing 570 ml of acetonitrile, with 426 ml of water and 4 ml of glacial acetic acid together in a volumetric flask. The mobile phase was then filtered through a 0.2 µm filter, and placed in a sonicator for 20 minutes. HPLC measurements were performed using a Varian Star HPLC system comprising 9012-pump, 9050-UV detector, AI-200 autosampler and Varian Star software version 5.1. The chromatographic separation was achieved on a Supelco Discovery™ C-18 column, of dimensions 150 x 4.6 mm, and a particle diameter of 5 µm, using a flow rate of 1.0 ml/min. UV detection of the column effluent was recorded at 308 nm (the absorbance maxima of warfarin in the particular mobile phase).

2.13.5. Fluorescent post-column HPLC detection of warfarin in patient plasma samples:

Mobile phase was prepared as described 2.13.4. Plasma samples for analysis were prepared as described in section 2.13.2. A post-column reaction coil was then used to mix the column effluent, with the post-column reagent, 12% (v/v) triethanolamine at a flow rate of 0.3 ml/min. Fluorescent detection was performed at excitation and emission wavelengths, of 310 and 370 nm, respectively.

Chapter 3

Production and Applications of Polyclonal Antibodies to Warfarin

3.1. Introduction:

The mammalian immune system has evolved a diverse range of powerful mechanisms to identify foreign cells, viruses and macromolecules and eliminate them from the body. The mechanisms by which the body's immune system performs this 'natural surveillance' can be broadly divided into two categories: non-adaptive and adaptive immunity.

Non-adaptive immunity is a cell-mediated non-specific response to foreign cells and includes such internal systems as phagocytosis by macrophages and cell lysis by natural killer (NK) cells. The body has also developed external barriers such as skin and mucous membranes that prove effective against environmental agents. Similarly, chemical influences such as pH and secreted fatty acids also provide effective barriers against invading micro-organisms.

The adaptive immune response can be further divided into the humoral and cell-mediated immune response. In contrast to non-adaptive immunity, the effectiveness of the adaptive immune response improves with re-exposure to the foreign molecule, and the agent to which the acquired immune response is induced is commonly referred to as the immunogen. Immunogenicity can be defined as the ability of a foreign molecule to elicit an immune response, whilst the term antigenicity refers to the ability of a particular molecule to be bound by antibody, and the antibody-bound molecule is consequently referred to as the antigen. There are three main types of lymphocytes that mediate the acquired immune response: B-cells, cytotoxic T cells (T_C) and helper T-cells (T_H). T-cells recognise antigen only when it is associated with a membrane component of the major histocompatability complex (MHC), resulting in the differentiation of T-cells into memory and effector cells. T_H cells recognise antigen in conjunction with MHC II proteins and are responsible for the release of cytokines that play a crucial role in the amplification of the immune response. T_H cells are made up of two distinct populations namely: T_H1 and T_H2 that differ in terms of their cytokine secretion characteristics. T_H1 cells are primarily responsible for the activation of cytotoxic T-cells (IL-2, IFN-γ), whilst T_H2 cells are responsible for the activation of B-cells (IL-4, IL-5). T_C cells bind to MHC I molecules peptide-bound molecules generating cytotoxic T-lymphocytes that are responsible for the destruction of the target cell by apoptosis, or causing the release of cytotoxic substances (e.g. perforins) which cause membrane permeability leading to target-cell death. The humoral immune system is mediated by B-cells in conjunction with T-helper cells, and it is the complex interactions between these three particular cell types that mediates the humoral and cellular immune system.

The lymphatic system describes the organs that are responsible for lymphocyte maturation, differentiation and proliferation. The lymphoid organs can be further divided into primary and secondary lymphoid organs that are responsible for the maturation and proliferation of T and B-lymphocytes and the proliferation of antigen-driven differentiation, respectively. The primary lymphoid organs are the thymus gland and the bone marrow, which are responsible for the antigen-independent differentiation of progenitor cells from the bone marrow into T lymphocytes, and the development of antibody-producing B-cells, respectively. The majority of T-cell maturation takes place during foetal development, which involves the maturation into various classes of T-cells capable of binding to various epitopes or antigenic determinants via a specific cell-surface receptor on the T-cell (T-cell receptor, TCR).

The secondary lymphoid organs comprise the spleen, lymph nodes and a variety of other secondary systems including the mucosa-associated lymphoid tissues (MALT) and tonsils. It is in these particular organs where antigen-driven differentiation takes place.

3.1.2. The Humoral Immune response:

To elicit an immune response the particular antigen must possess three particular characteristics, namely: a high molecular weight, a degree of 'foreignness' to the host, and a degree of chemical complexity. With regard to molecular weight it is usually only macromolecules with a molecular weight of greater than 6 kDa that are capable of invoking an immune response. Small molecular weight compounds such as drug molecules are incapable of stimulating an immune response themselves, however, following conjugation to larger molecular weight carriers; the small molecular weight haptens can become immunogenic. The antigen must also possess a degree of chemical complexity, as large macromolecules with repeating units are seldom immunogenic. Finally, the immune system must also recognise the antigen as foreign (i.e. 'non-self') and be able to respond immunologically.

The first exposure of an individual to an immunogen is generally referred to as the primary immune response. It is the culmination of a series of events following this primary immune response that 'primes' the immune system for subsequent exposure to the particular antigen. Following exposure to antigen, which may have been as a direct result of an immunisation procedure or a result of injury, macrophages and other cells of the reticuloendothelial system (RES) engulf the foreign antigen and as all of these cells process antigen in the same non-specific fashion they are collectively termed – antigen presenting cells (APC). The use of adjuvants (e.g. Freund's Complete Adjuvant), altering the form of the antigen and using various immunisation sites are effective ways of increasing the immunogenicity of a

particular antigen. Generally speaking particulate insoluble antigens are the best immunogens. Adjuvants function in two ways: they firstly protect the antigen by trapping it in a local deposit, and secondly, they attract macrophages and increase the local rate of phagocytosis.

Following phagocytosis, the antigen is presented on the surface of the antigen-presenting cells (APC) in conjunction with MHC (Major Histocompatability Complex) Class II. T_H cells then bind with the MHC class II-antigen complex via their T cell receptors, which resemble antibody molecules in many respects. The T-cell receptor is a heterodimer comprised of α- and β-chains that are comprised of variable and constant regions, which form the binding site. The binding of the T_H cell to the APC triggers a series of events resulting in T-cell proliferation and differentiation and the release of interleukin-1 (IL-1). The activated T_H cells are responsible for the release of IL-2 that plays a key role in B-cell proliferation. In a similar fashion, antigens are also processed by B-cells, although the uptake is specific for each particular antigen. The antibody-antigen complex is internalised and the antigen processed and expressed on the surface with class II protein which provides a source of complex for binding to the T_H cells that are specific for the antigen-protein complex (Figure 3.1).

For the generation of a strong immune response the interaction between B and T-cells is of crucial importance in regulating antibody production, and leading to B-cell production and the production of antigen-specific antibody. The processing of antigen by B-cells followed by T-cell recognition of the displayed fragment, leads to B-cell stimulation by T_H cells. The failure to form such complexes is why haptens (e.g. small molecules such as drug compounds) are unable to invoke the necessary binding between the T-cell receptors and class II determinants, and why the use of carrier molecules (e.g. thyroglobulin) must be employed. The binding of the T_H to B-cells, causes the B-cells to synthesise a receptor for interleukin-4 (IL-4) which is synthesised by activated T_H cells, and in turn leads to the production of IL-5 by B-cells which results in differentiation of B-cells into memory and plasma cells. Plasma cells are responsible for the secretion of large amounts of specific antibody and are terminally differentiated with a lifespan of approximately 3-4 days. B memory cells do not secrete antibody but remain in the body for long periods with their specific antibody cell-surface receptor primed for future exposure to the antigen.

The process of B-cell differentiation is accompanied by somatic mutation of the amino acid sequences of the variable heavy and light chains, producing antibodies with differing affinities for the antigen in the germinal centres of the spleen and lymph nodes which contain follicular dendritic cells that retain the antigen on their surface for presentation to B-cells.

The higher affinity B-cells are preferentially selected for proliferation as their cell-surface antibody is capable of binding the antigen more efficiently, in a process known as affinity maturation. B-cells with low-affinity towards the particular antigen are selected against by apoptosis, ensuring the proliferation of only the higher affinity variants. Class-switching also occurs during the differentiation process, whereby the B-cells expressing the IgM/D cell surface antibody may switch to synthesis of IgG, IgA or IgE molecules. Consequently, upon re-exposure to the antigen the immune response evokes a much more potent response involving the memory B-cells that are of higher affinity and predominantly of the IgG class.

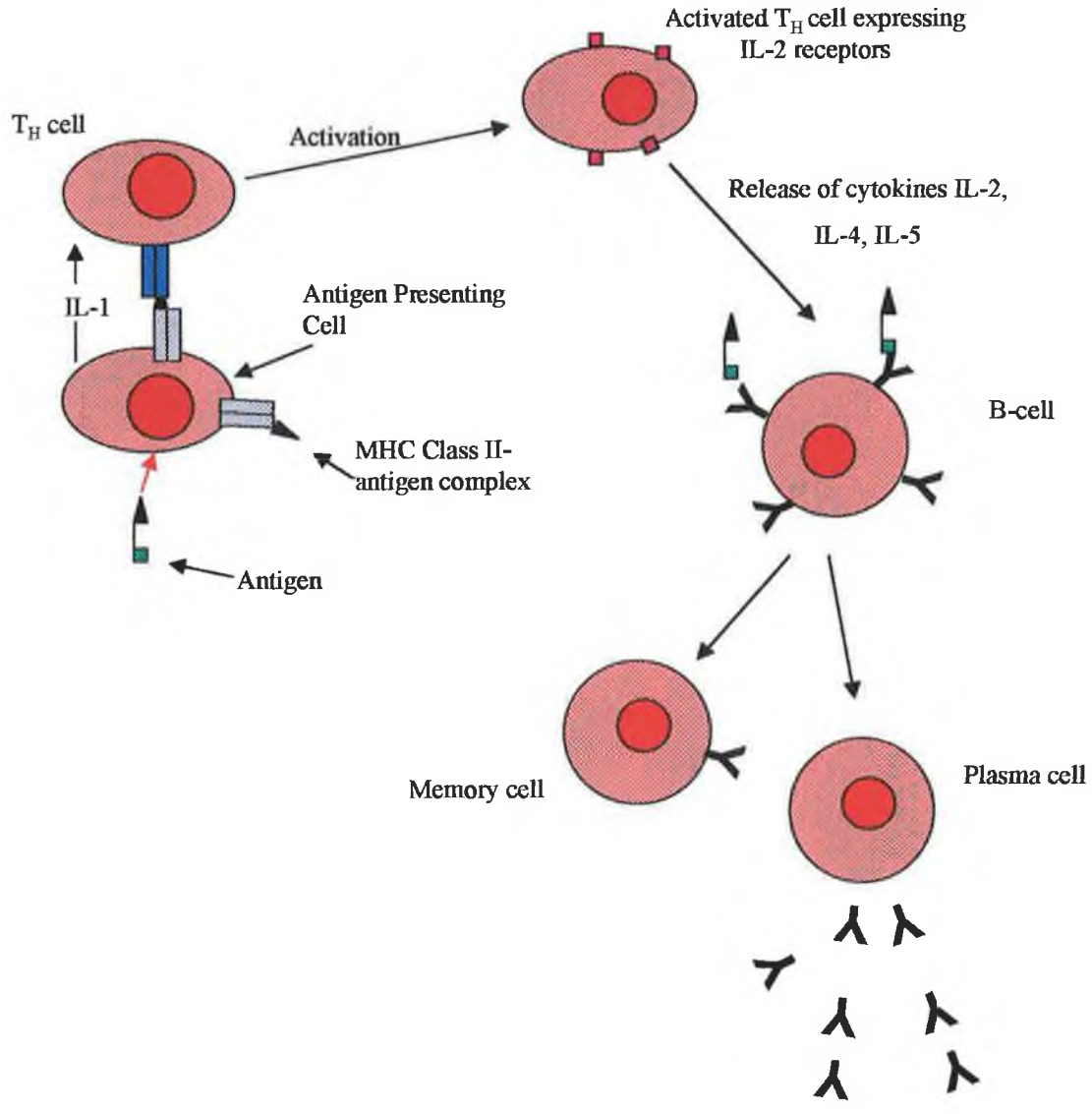

Figure 3.1: *The interaction between an antigen presenting T-cell and B-cell leading to T- and B-cell activation in a primary response. Antigen is initially phagocytosed by antigen presenting cells (APC) and presented on the surface as MHC class II-antigen complex. T_H cells bind to this complex through their T-cell receptor, triggering T-cell proliferation and differentiation. For the generation of a strong humoral immune requires the interaction of T_H cells and B-cells. B cells can also bind and process antigen, and recognition of the displayed fragment by T_H cells leads to the B-cell stimulation, proliferation and differentiation into memory and plasma cells capable of producing large quantities of antibody following affinity maturation in the germinal centers.*

3.1.3. Antibody Structure:

Antibodies are glycoproteins of the immunoglobulin supergene family (Steward, 1985), which share a variety of key structural and functional features. Analysis of the structure of antibodies began in earnest in 1959, following the discovery by Porter that immunoglobulins could be separated into various parts following digestion with papain, namely into two Fab portions and one Fc portion (Figure 3.2). Edelman then discovered that digestion with mercaptoethanol further reduced the γ-globulin into four chains: two identical sets of molecules, designated heavy (≈53 kDa) and light (≈22 kDa) chains because of their differing molecular weights.

One light chain associates with the amino terminal of one heavy chain to form an antigen-binding domain (Fab). Interchain disulphide bonds hold the heavy and light chains together with various intrachain bonds in various antibody chains. Five main classes of antibody (isotypes) have been resolved that differ in the structure of their heavy chains (Table 3.1). The basic four-chain model holds for all antibody isotypes with specific heavy chains for each class, γ for IgG, μ for IgM, δ for IgD, α for IgA and ε for IgE. The light chains have also been serologically divided into κ and λ chains, although these are similar in each isotype class. Each antibody isotype has been further divided into sub-classes (e.g. IgG_1, IgG_{2a}, etc.). It is the variation in the heavy chain sequences that accounts for the variation in effector function elicited by the various proteins at differing stages during the immune response. The intrachain disulphide bonds within the antibody molecule are responsible for the formation of loops within the chains, resulting in the formation of globular domains of approximately 100 amino acid residues in length. The structure of the domains of each antibody chain has been designated by a letter signifying their position on the antibody molecule. The V_H and V_L exhibit the greatest degree of variability in amino acid sequence, whilst the constant regions (i.e. C_L, C_H1, C_H2 etc.) are much more constant in terms of amino acid sequence (Figure 3.2).

The hinge region is a short amino acid sequence situated between the C_H1 and C_H2 regions of the immunoglobulin heavy chains (with the exception of IgM and IgE) and is composed primarily of proline and cysteine residues. The hinge region permits flexibility of between 60-180° of the two Fab arms of the antibody molecule, allowing the Fab arms to open and close to accommodate antigen binding.

The variable region of an antibody is responsible for the antigen recognition, specificity and affinity and is comprised of approximately 110 amino acid residues. Variability within the V region is a highly organised process within specific regions of the variable region, known as

the hypervariable regions, forming a region complementary in structure to the antigen epitope and these are so called the complementarity-determining regions (CDRs). The CDR region can be further sub-divided into three different regions (i.e. CDR1, CDR2 and CDR3) of about 10 amino acid residues in length between which lies more conserved sequences known as the framework residues. When the heavy and light chains are formed the variable (V) region is formed, the CDR sequences are exposed, forming a cleft that serves as the antigen-binding pocket. It is the precise amino acid sequence, shape and positioning of this cleft or pocket as result of the combination of the six CDR sequences which form hypervariable loops that confers the particular antibody specificity.

Table 3.1: *Functions and Structural Features of Antibody Isotypes*

Characteristic	IgG	IgM	IgD	IgA	IgE
Molecular Weight	150 kDa	950 kDa	175 kDa	165 kDa (monomeric) 390 kDa (secretory)	190 kDa
Heavy chain	γ	μ	δ	α	ε
Valency	2	5/10	2	4	2
Concentration in serum	8-16 mg/ml	0.5-2 mg/ml	40 μg/ml	1-4 mg/ml	0.4 μg/ml
Function	Secondary response	Primary response	Poorly understood, it is a surface component of many B-cells	Major Ig component of external secretions (e.g. saliva, sweat, tears)	Protection against parasites and involved in allergic reactions

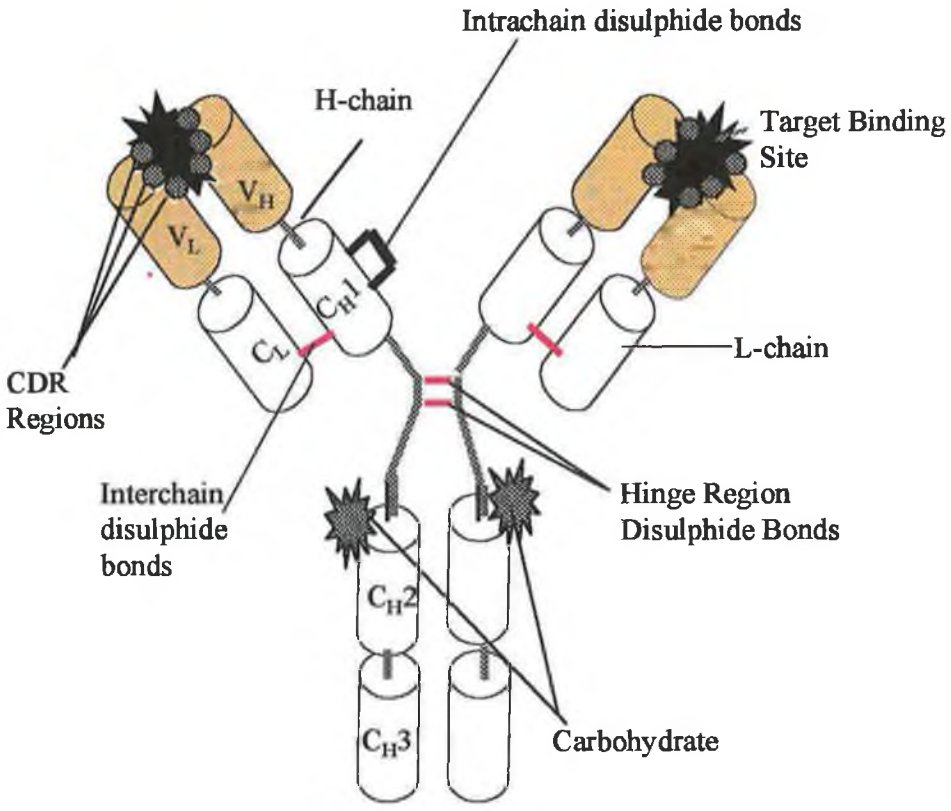

Figure 3.2: *The immunoglobulin molecule. The antibody is composed of two identical light (25 kDa) and heavy (50 kDa) chains. The heavy (H) chains are composed of five domains namely: one variable (V), three constant (C_H1, C_H2, C_H3), and one hinge region. The variable region is comprised of a single variable and constant domain. The hinge region provides the flexibility to allow for the individual antibody-binding sites to bind antigen. Interchain disulphide bridges connect the heavy and light chains; there are also intrachain disulphide bonds that form loops within the chain. The CDR regions confer the specificity to the particular antibody-binding site, and exhibit high amino acid sequence variability.*

3.1.4. Antibody Affinity:

The net interaction between an individual antibody's antigen binding site and the corresponding epitope dictates the affinity of the interaction between the two molecules. Antibody affinity is thermodynamically described in terms of the equilibrium constant, K_A, by the following expression:

where,

$$[Ag] + [Ab] \underset{k_d}{\overset{k_a}{\leftrightarrow}} [Ag{:}Ab] \qquad (1)$$

and

$$Ka = \frac{[AgAb]}{[Ag][Ab]} \qquad (2)$$

The term avidity is used to describe the overall affinity arising from the multivalent binding of the antigen-binding sites of an antibody to a multivalent antigen. As a result of the multivalent binding of an antibody to an antigen, such multivalent antibody-antigen interactions often exhibit extreme stability and reduced dissociation rates as a result of the multimeric interactions (e.g. IgM), although the individual dissociation rates would resemble the univalent interaction.

The affinity of the interaction between an antibody and antigen is the net result of the intermolecular forces between the two molecules, and four types of such intermolecular forces have been identified. They include hydrogen bonding, ionic interactions, Van der Waals forces and hydrophobic interactions. Hydrogen bonding involves the interaction of a H-atom covalently linked to an electronegative atom with the unshared electron pair of another electronegative atom. Ionic interactions are the result of the attraction between oppositely charged groups and consequently can be disrupted by changes in salt concentration or pH. Hydrophobic interactions involve the association of non-polar (hydrophobic) residues in aqueous environments. Van der Waals forces are the result of interactions between electron clouds of neighbouring molecules as two polar groups come in close contact. This results in the induction of oscillating dipoles between the two molecules resulting in a net attractive force. The strength of these particular forces is only effective over short distances, which can usually be disrupted by high ionic strength or extremes of pH.

The structure of antibody-antigen crystal complexes has also allowed for greater understanding of the formation of immune complexes. Crystal structures have revealed that following antibody-antigen binding that structural changes in the antibody upon complex formation include side chain rotations, movements of CDR loops and displacement of V_H

relative to V_L (Davies *et al.*, 1996). Crystal studies of a germline Fab fragment with its hapten were compared by Wedemayer *et al.* (1997) with the corresponding affinity-matured antibody fragment, which has a greater than 30,000 times greater affinity for antigen. The crystal studies of the antibody:antigen complexes revealed that the germ-line antibody combining site underwent significant structural changes following binding of hapten, whilst the hapten bound to the affinity-matured antibody by a 'lock and key' type mechanism. The gross structural changes observed were also accompanied by significant re-organization of the combining site residues. These results demonstrate that the germline antibody is pluripotential with respect to the possible number of recombinations it can assume in response to antibody binding, and that these mutations become fixed during the affinity maturation process to a particular high-affinity conformation that stimulates the immune response. It can therefore be seen that such flexibility within the germline can greatly expand the structural diversity of the primary immune repertoire.

3.1.5. The Genetic Basis of Antibody Diversity:

The variable region of the heavy and light chain of an antibody encodes for antibody diversity. It is the heterogeneity that exists within this sequence that is responsible for the generation of an effective immune response. Since the range of antigens is so diverse in both size and structure, the repertoire of antibodies must be correspondingly diverse, and four distinct processes encoding for this diversity have been identified (Tonegawa, 1983).

It has been shown that the genetic information encoding for the immunoglobulin polypeptide chain is contained in various gene segments in the chromosomes of a germ-line cell. During the development of the lymphocyte, these particular gene segments are recombined to give rise to a new functional gene (i.e. combinatorial diversity). Variable light chain genes are encoded by the V and J regions, whilst heavy chain gene sequences are composed of gene segments from the V, D and J loci. Following B-cell maturation, the various VDJ sequences on the heavy chain, and VJ sequences on the light chain recombine to form a complete functional gene. During the recombination process, to bring a D region adjacent to a V region, a process known as 'looping out' occurs, whereby the intervening gene segments are deleted by recombinase enzymes. Consequently, the number of different possible permutations in terms of sequence arrangement for each particular chain, is the product of the number of V, D and J sequences particular to each sequence.

The recombination of the various VJ and VDJ sequences also gives rise to what is known as junctional site diversity as a result of the imprecise joining ends of the various sequences which can lead to changes in amino acid sequences at junction sites altering the binding site

specificity. Junctional insertional diversity is the result of the insertion of small sets of nucleotides between the V-J and D-J sequences. Somatic mutations are also introduced at a high frequency in the amino terminal, which in turn creates additional diversity with regard to antibody specificity (Benjanimi *et al.*, 1996).

The process of class or isotype switching occurs in mature B-cells as a result of antigenic stimulation. Constant H regions are found downstream of the variable region genes, in the sequence μ, δ, γ, ε and α. Each constant region has at it's 5' end a repeating base sequence called the switch region, which allows for any of the VDJ sequences to recombine with the C_H regions (except for the δ gene which has no switch region). The influence of antigen and T-cell derived cytokines regulates this unique mechanism, allowing antibodies with a unique specificity to associate with a variety of effector functions as a result of their constant region sequence.

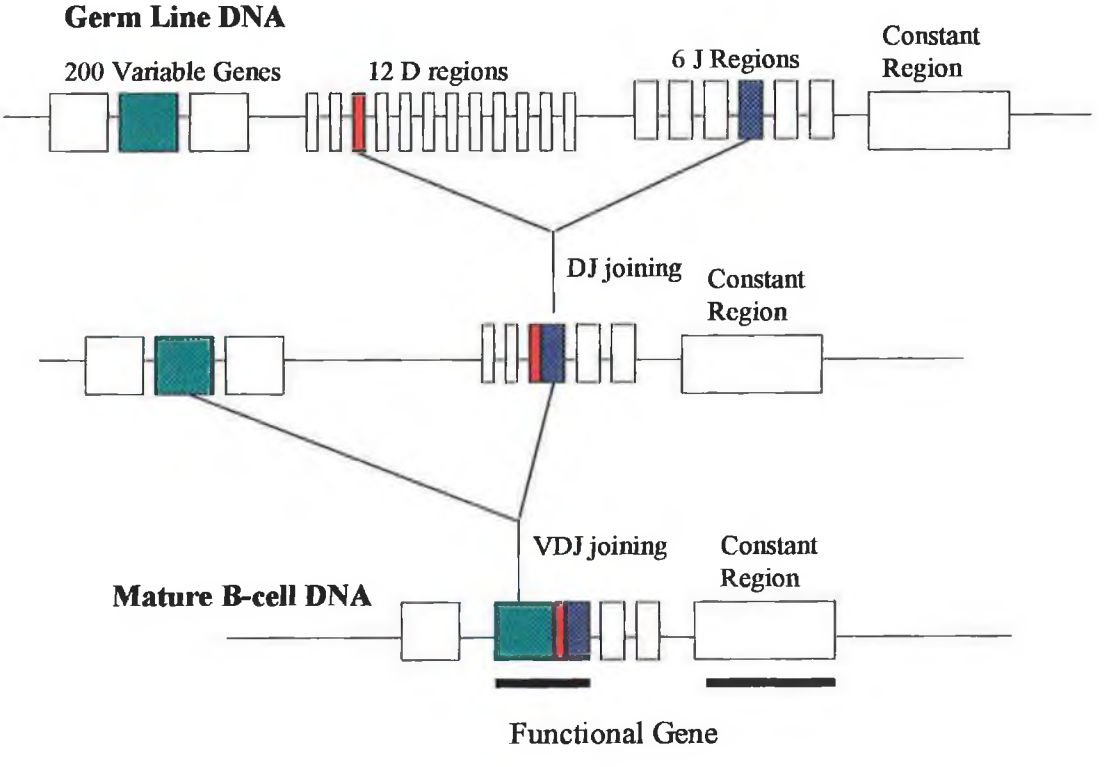

Figure 3.3: *Two separate processes are involved in the recombination of a heavy chain gene. Heavy chain gene segments are composed V (variable), D (diversity) and J (joining) segments. The constant regions encode for the antibody isotype. The first recombination step brings the D and J segments together, looping out the intervening DNA by recombinase enzymes, which introduce further variability at the point of cleavage. The second step brings the V region gene alongside the DJ sequence, thereby fixing the specificity of the antibody, and giving rise to a functional B-cell variable heavy chain gene.*

3.1.6. Purification of Immunoglobulins:

Immunoglobulins are relatively robust molecules capable of maintaining biological activity following exposure to extremes of pH for short periods of time, and storage for relatively long periods at –20°C. The purification of antibodies from serum, cell culture supernatants or cell lysates is often a necessity as the crude antibody preparations can often result in difficulties with particular assay systems. The degree of purity of antibody required for the particular purpose usually dictates the type of purification system employed. A variety of techniques have been developed for the isolation of immunoglobulin fractions from various matrices (Harlow & Lane, 1988), and the majority of these techniques exploit their differing solubilities in various solvent systems and their high isoelectric points (Steward, 1985).

The use of ammonium sulphate is commonly employed as an initial clean-up step for the isolation of relatively pure immunoglobulin fractions (Hudson & Hay, 1980). As the salt concentration increases, hydrophobic interactions between molecules increase, eventually leading to the precipitation of immunoglobulins at particular salt concentrations. The use of chromatographic separation systems such as DEAE anion-exchange columns, which exploits the basic nature of antibodies has also been described for the purification of crude antibody preparations (Carty & O' Kennedy, 1988). The partitioning and purification of antibodies in aqueous two-phase systems (e.g. aqueous solutions of PEG/salt) has also been demonstrated to be a powerful, economical system for the large-scale purification of immunoglobulins (Andrews *et al.*, 1996).

Protein A and G may also be used for the isolation of IgG. Protein G is a 30 kDa bacterial cell wall protein isolated from the group G streptococci, and binds to immunoglobulin molecules primarily through their Fc regions. Protein G binds with a higher affinity to particular immunoglobulin molecules such as mouse IgG_1 that do not bind particularly well to Protein A. Protein A is a 42 kDa cell wall component of several strains of *Staphylococcal aureus* and binds specifically to the Fc region of immunoglobulin molecules. The protein consists of four high affinity binding sites ($K_A = 10^8\ M^{-1}$), and is able to maintain activity after repeated exposure to extremes of pH rendering it suitable for routine purification procedures (Hermanson *et al.*, 1992). Protein A and G can be easily coupled to sepharose to produce solid supports with high immunoglobulin capacity, exhibiting low degrees of non-specific binding. Following application of the crude antibody preparation to such column supports and subsequent washing to remove non-specifically bound protein, the bound antibody can be eluted by exposure to high/low pH solutions.

Affinity-purification techniques involve the covalent coupling of the antigen of interest (e.g. 4'-aminowarfarin) to a solid support (e.g. Sepharose-4B), and offer a convenient means of obtaining antigen-specific antibody preparations of high purity, as not only extraneous non-specific protein is eluted but also non-specific immunoglobulin. The bound antibody can then be eluted using a combination of low pH and high salt buffers (e.g. Glycine-HCl buffer).

3.1.7. Immunoassays:

Immunoassays are the fastest growing analytical technique for the detection and quantification of a wide range of molecules (e.g. steroids, tissue markers), and have been extensively reviewed elsewhere (Wild, 1994; Price and Newman 1997).

One of the most commonly employed techniques for measuring antibody-hapten interactions, is the use of Enzyme-Linked ImmunoSorbent Assay (ELISA), which is now more commonly employed than radioimmunoassay techniques, primarily as a result of the hazardous nature and disposal of radioimmunoassay reagents. A schematic of the principle of the technique is shown in Figure 3.4., which is a modification of the immunoassay principle originally described by Yalow and Berson (1959). Such competitive ELISA assay formats describe the competition between free and immobilised forms of antigen for binding to a limiting quantity of antigen-specific antibody. Direct immobilisation of small molecular weight haptens to ELISA plates is often difficult and the use of hapten-protein conjugates is most commonly employed, which bind directly to the wells of γ-irradiated 96-well immunoplate, primarily through hydrophobic interactions. The use of conjugates employing different carrier molecules and coupling chemistries to those used for initial immunisation purposes is thus necessary to ensure specificity of the bound antibody towards the hapten only, and not the carrier molecule or a combined drug-protein epitope (Danilova *et al.*, 1994; Fasciglione *et al.*, 1996).

A wide variety of ELISA formats are possible (Price and Newman, 1997), however, the competitive ELISA format is described in the context of the assay format utilised for the detection and development of a competitive immunoassay for warfarin. The hapten of interest that is covalently coupled to a protein (e.g. 4'-azowarfarin-BSA), is added to the wells of a 96-well immunoplate, and binds to the immunoplate predominantly through hydrophobic interactions. Loosely bound protein is then removed by washing with a solution containing detergent (e.g. wash buffer section 2.3.). A blocking agent (e.g. 5% FCS in PBS-1) is then added to the wells to 'block' any remaining available adsorption sites on the surface of the plate. The use of such blocking agents is necessary to ensure that no non-

specific binding of either primary or secondary-labelled antibody to the wells of the plate occurs. A solution containing a limiting constant amount of antibody and varying known concentrations of antigen are then applied to the wells of the immunoplate, and incubated for a specified time interval. Competition then occurs between free antigen in solution and that immobilised to the immunoplate for binding to the antigen-specific antibody. The contents of the well are then removed and the plate washed to remove any non-specific antibody. The presence of antigen-specific antibody (i.e. affinity-purified rabbit anti-warfarin antibodies) in the wells of the immunoplate can then be determined using a species-specific secondary enzyme-labelled antibody for the primary antibody (e.g. alkaline phosphatase-labelled goat anti-rabbit immunoglobulin). Following washing of the plate wells, a substrate solution is added to the wells and converted to a coloured product in the presence of enzyme. The intensity of the colour solution formed is then measured spectrophotometrically at the appropriate wavelength. In such assay formats as the concentration of free antigen (i.e. warfarin) in solution increases, less antibody is available to bind to the solid-phase immobilised antigen (i.e. 4'-azowarfarin BSA). Consequently, an inverse relationship exists between the intensity of the coloured solution formed and the concentration of free antigen in solution. In this way, the concentration of warfarin in unknown solutions can be determined by reference to a suitable standard curve. The sensitivity of such competitive ELISA formats can be optimised using the appropriate dilution of antibody preparation and immobilised conjugate. However, the ultimate sensitivity of all immunoassay procedures is primarily a factor of the intrinsic affinity of the antibody preparation for the particular antigen.

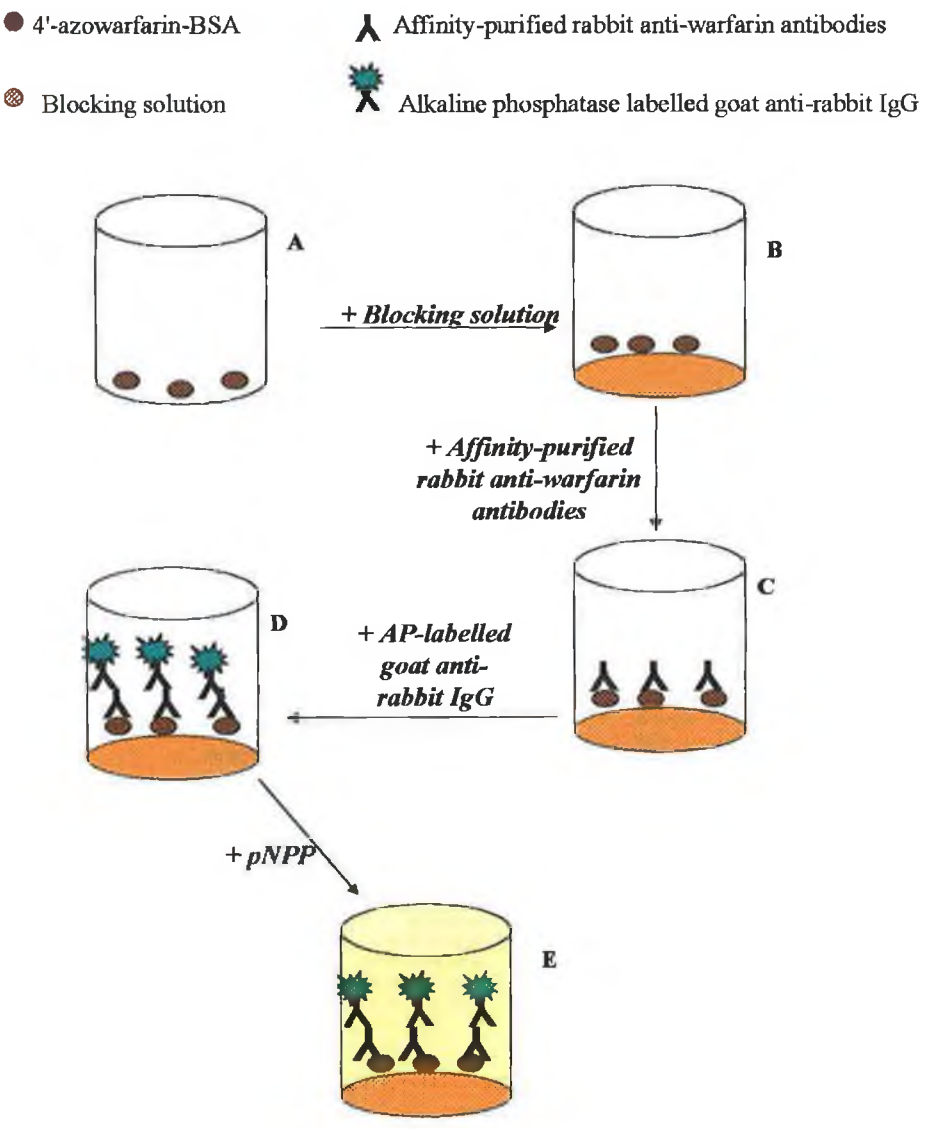

Figure 3.4: *Schematic of the principle of direct ELISA, as used for the measurement of antibody titres in purified samples. 4'-azowarfarin-BSA is used to 'coat' the wells of a 96-well immunoplate, and sticks to the γ-irradiated plate primarily by hydrophobic interactions (A). The wells of the immunoplate are then blocked with a suitable blocking solution (e.g. 5% (v/v) F.C.S. solution in PBS-1) to block any remaining absorption sites on the plate (B). The antibody-containing samples are then added to the wells of the immunoplate, and, following a suitable incubation step, washed (i.e. wash buffer section 2.3.) to remove non-specific protein(C). A species-specific secondary enzyme-labelled antibody is then added to the wells of the immunoplate and incubated for a suitable period of time (D). The wells are washed extensively again, and a substrate added to the wells of the plate, which in the presence of enzyme (i.e. secondary antibody) forms a coloured product whose absorbance can then be measured spectrophotometrically at the appropriate wavelength for the substrate (E).*

Results and Discussion:

3.2 Conjugate Synthesis and Characterisation

3.2.1. Synthesis and Characterisation of 4'-aminowarfarin

4'-aminowarfarin was synthesised by a modification of the method of Satoh *et al.* (1982) as outlined in section 2.4.1. This method involved the hydrogenation of acenocoumarin (4'-nitrowarfarin) in the presence of Raney nickel. This technique was initially modified to include the use of a palladium on carbon catalyst in the presence of hydrogen, due to the potentially explosive nature of the Raney nickel and hydrogen mixture. The reaction mixture was periodically analysed by TLC as described in section 2.4.2. to assess the extent of product formation. This particular reaction yielded 4'-aminowarfarin in relatively pure quantities, but took several days to reach completion. The slow rate of reaction was attributed to the reduced catalytic activity of the palladium catalyst compared to the use of Raney nickel as described by Satoh *et al.* (1982). Attempts were thus made to simplify the reaction procedure for the safe and relatively facile generation of relatively larger quantities of 4'-aminowarfarin for the production of drug-protein conjugates.

The initial proposed technique involved the reduction of the nitro group of acenocoumarin in the presence of tin and dilute hydrochloric acid (1 M). However, the reducing conditions for this particular technique were considered too harsh for the reduction of 4'-nitrowarfarin, as the procedure not only resulted in the reduction of the nitro group, but also what was believed to be the reduction of the ketone moieties on the parent compound yielding several reaction products as analysed by TLC (Figure 3.5). The use of zinc granules in the presence of dilute acetic acid (10%, v/v) proved to be the safest and simplest means of routinely producing the putative 4'-aminowarfarin product. However, the technique also suffered from some of the difficulties described for the reduction reaction in the presence of tin, namely, over reduction of the parent compound. It was then decided to proceed with the reduction procedure described, but to stop the reaction before reaching completion which may have resulted in the reduction of the ketone moiety groups on the parent acenocoumarin molecule (i.e. ketone group of 4-hydroxycoumarin ring and the ketone group attached to the aliphatic carbon). This resulted in a reaction mixture containing both the unreacted 4'-nitrowarfarin and also 4'-aminowarfarin. The separation of these two particular compounds was achieved by a combination of filtration and column chromatography. The initial filtration step removed the zinc granules from the reaction mixture, whilst it also allowed for the straight-forward separation of 4'-nitrowarfarin, which is only partially soluble in dilute acid, from the amine-containing 4'-aminowarfarin which is readily soluble in dilute acid solutions. The

reaction was monitored throughout by TLC analysis. However, visual inspection of the reaction mixture also afforded some knowledge of the extent of the reaction, which turned from a creamy white colour to a deeper orange colour as the reaction proceeded, due to the formation of the soluble 4'-aminowarfarin product. The dilute acid solution was then quickly back-extracted into ethyl acetate to protect the reaction product from further reduction. The relatively pure reaction mixture was then dried over anhydrous magnesium sulphate to remove any water remaining in the ethyl acetate fraction and evaporated to dryness on a rotary evaporator. The sample was then purified to homogeneity by column chromatography as described in section 2.4.3. The collected fractions containing 4'-aminowarfarin that were assayed by TLC (Figure 3.5) were pooled and evaporated to dryness on a rotary evaporator.

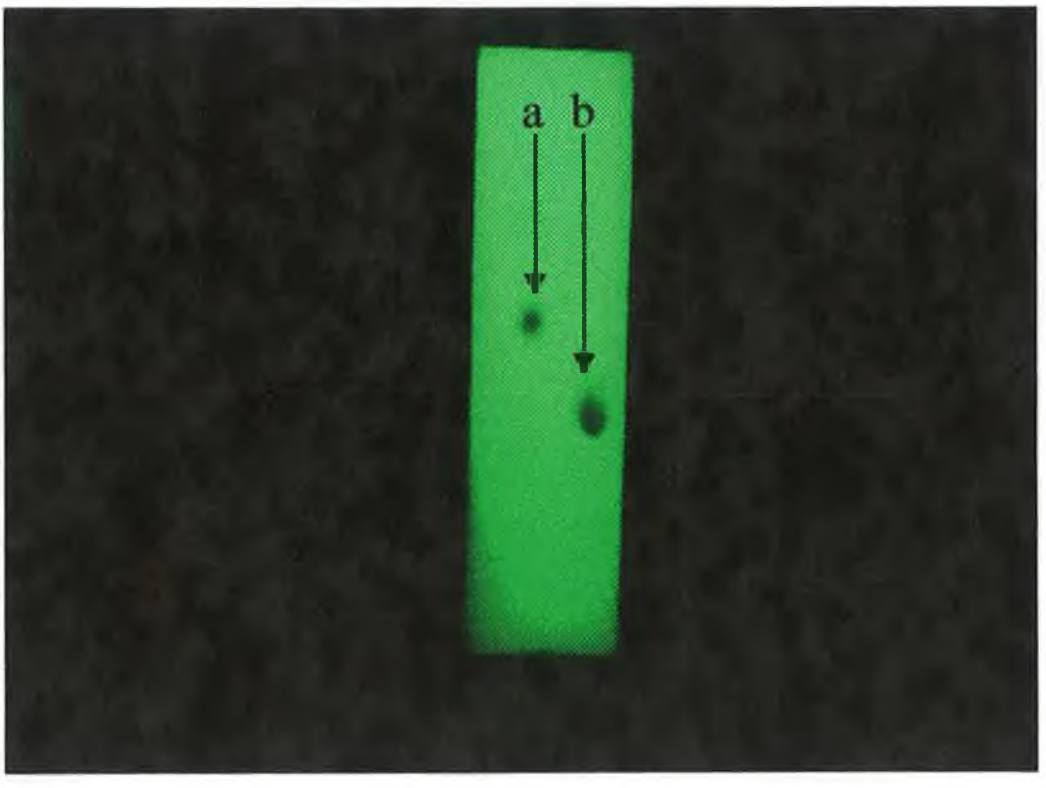

Figure 3.5: *Thin Layer Chromatography of starting material 4'-nitrowarfarin (a,Rf = 0.67), and 4'-aminowarfarin (b, Rf = 0.33) mixture viewed under a UV lamp following chromatography through a silica gel column. A mobile phase containing methanol and chloroform (2:98, v/v) was used to separate the reaction product from starting material. The presence of a single spot confirms the purity of the reaction mixture.*

3.2.2.1. Characterisation of 4'-aminowarfarin by Infra Red (IR) spectral studies:

The purity and character of the putative 4'-aminowarfarin compound was confirmed by a combination of infra-red (IR) and NMR (Nuclear Magnetic Resonance) studies as described in sections 2.4.4. and 2.4.5., respectively. The infra-red spectrum of a compound is essentially the superposition of absorption bands of specific functional groups, and IR studies may thus be qualitatively used for the confirmation of specific functional groups in a molecule. The chemical reduction of 4'-nitrowarfarin to 4'-aminowarfarin, involves the reduction of the nitro- group on position-4 of the phenyl substituent to the corresponding amine. The IR spectrum of both starting material and product are included in Figure 3.6. and Figure 3.7 for comparison. Analysis of the IR spectrum of 4'-nitrowarfarin shows two strong bands at 1350 and 1530 cm^{-1} corresponding to the symmetric and asymmetric stretches of the nitro-group, respectively. These bands are absent in the IR spectrum of 4'-aminowarfarin confirming the reduction of the functional groups. The stretch at ~1700 cm^{-1} corresponding to the carbonyl group evident in both infra-red spectra, is indicative of the presence of a carbonyl group in both molecules. An additional stretch is also evident at approximately 3400 cm^{-1} corresponding to the presence of a hydroxyl group in both starting material and reaction product. The IR spectrum of 4'-aminowarfarin shows a shoulder peak at 3300 cm^{-1} on the hydroxyl group confirming the presence of an amine group in the reaction product which is further confirmed by the presence of an amide stretch at ~1650 cm^{-1}.

3.2.2.1. Characterisation of 4'-aminowarfarin by Nuclear Magnetic Resonance (NMR) studies:

Nuclear magnetic resonance (NMR) permits the identification of atomic configurations of molecules from the absorption of energy of spinning nuclei in a strong magnetic field when irradiated by a second weaker field perpendicular to it. Absorption occurs when the nuclei undergo transition from one alignment to another one and such transitions depend on a number of factors including: the field strength, electronic configuration about the molecule, the type of molecule and intermolecular interactions. Consequently, NMR can be used to identify the presence of specific functional groups, and also their location in a particular molecule resulting in the delineation of atoms within a molecule. An important parameter of nuclear magnetic resonance is what is known as chemical shift. In different chemical environments, the same atom can be shielded from the applied field depending on the distribution of the surrounding electrons. It is the particular shifted resonance frequencies that characterize neighbouring molecules within an atom. Using chemical shift values, it can be seen that the presence of an amine and a nitro group on the phenyl ring will result in differing chemical shifts for the protons attached to this particular ring. The proton NMR

spectra of the starting material 4'-nitrowarfarin and product 4'-aminowarfarin are shown in Figures 3.8. and Figures 3.9, respectively. The aromatic protons in the starting material 4'-nitrowarfarin (acenocoumarin) are situated between 7.2 p.p.m and 8.2 p.p.m. The protons at 8.0-8.2 p.p.m. have been assigned as the protons adjacent to the nitro-group at the para-position on the phenyl susbstituent. Nitro groups have a deshielding effect, and result in pulling the aromatic protons downfield, and this could be used to describe the presence of the aromatic protons at 8.1-8.2 p.p.m. using the assigned J-values (i.e 7.27 +0.95 = 8.22).

Close examination of the aromatic portion of 4'-aminowarfarin reveals the absence of these two particular protons, and the presence of an additional peak at approximately 6.6. p.p.m. Amine groups have a shielding effect and result in the pulling the protons upfield, and this can be used to explain the positioning of the aromatic protons at these lower p.p.m. values (i.e. 7.27 – 0.75 = 6.5 p.p.m.). The proton NMR for the remainder of the molecule is essentially unchanged, as the remainder of the protons are unchanged as a result of this particular chemical reduction.

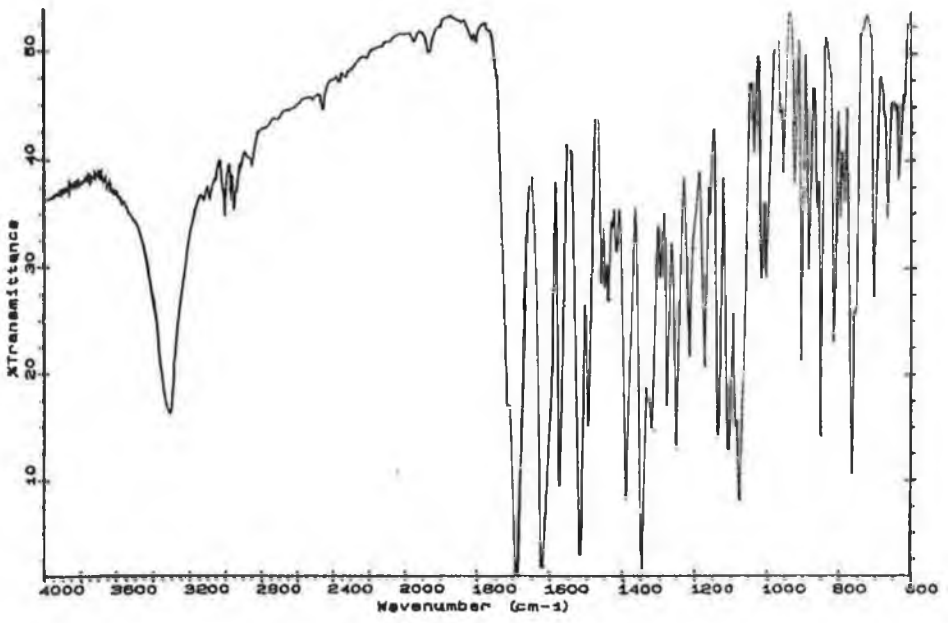

Figure 3.6: *IR spectrum for 4'-nitrowarfarin, prepared as described in section 2.2.4. The two strong bands at ~1530 cm^{-1} and 1350 cm^{-1} corresponds to the NO_2 asymmetric and symmetric stretches, respectively. The band at 3400 cm^{-1} corresponds to the presence of a hydroxyl group on the molecule, whilst the band at ~1700 cm^{-1} corresponds to the carbonyl group of the molecule.*

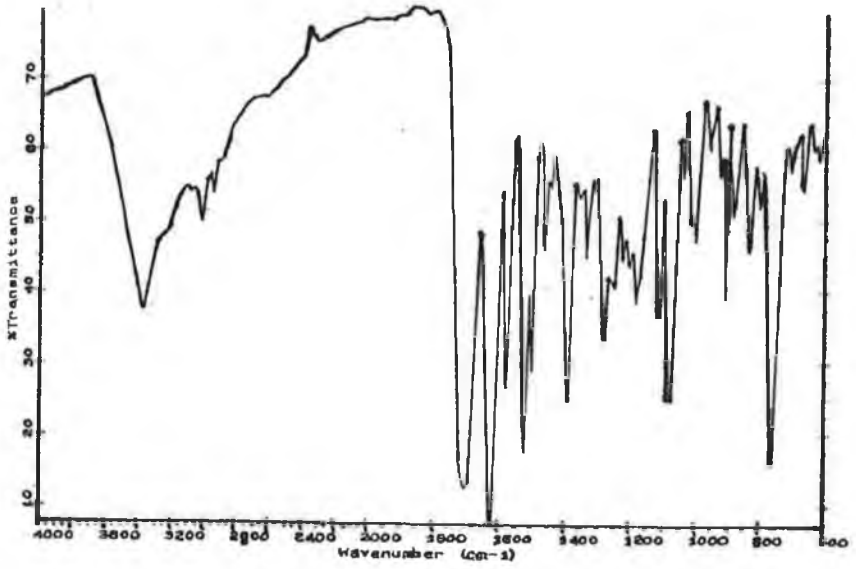

Figure 3.7: *IR spectrum for 4'-aminowarfarin prepared as described in section 2.2.4. The strong band at ~1650 cm^{-1} corresponds to the N-H stretch, which is also evident in the shoulder peak (~3300 cm^{-1}) on the hydroxyl band at 3400 cm^{-1}. The band at ~1700 cm^{-1} corresponds to the carbonyl group of the molecule.*

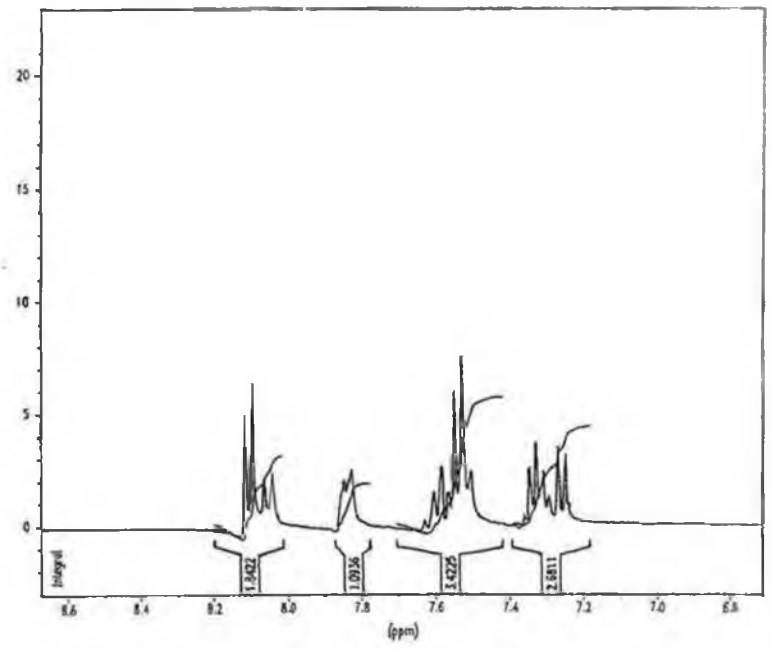

Figure 3.8: *NMR spectra of 4'-nitrowarfarin, which shows the aromatic protons of the molecule ranging from 8.2 - 7.2 p.p.m. which were shifted downfield as a result of the electron deshielding effect of the nitro group at the para-position on the phenyl substituent.*

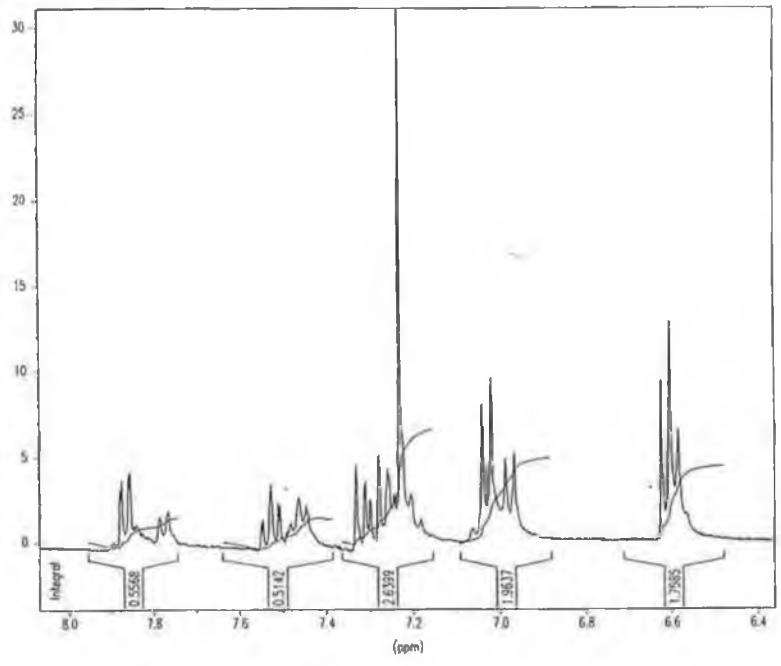

Figure 3.9: *NMR spectra of 4'-aminowarfarin, which shows the aromatic protons of the molecule ranging from 6.8 - 7.9 p.p.m. which were shifted downfield as a result of the electron withdrawing effect of the amine group at the para-position on the phenyl substituent.*

3.2.2. Production and Characterisation of warfarin-protein conjugates:

Various 4'-azowarfarin-protein conjugates were generated for the production and affinity-purification of polyclonal rabbit antibodies to warfarin, as warfarin (308 Da) is too small to elicit an immune response itself and so required conjugation to a carrier protein molecules in order to make it immunogenic. There are a variety of coupling chemistries available for coupling proteins to small molecules such as warfarin (Hermanson, 1996). The choice of coupling chemistry employed is generally selected as a result of the chemical residues available for coupling and whether or not spacer molecules need be employed to distance the molecule from the carrier protein.

The conjugation procedure for the coupling of 4'-aminowarfarin to various proteins (i.e. thyroglobulin, keyhole limpet haemocyanin (KLH), bovine serum albumin (BSA) and ovalbumin) was carried out according to the molar ratios described by Satoh *et al.* (1982) in section 2.5.2. Briefly, 4'-aminowarfarin was activated in an acidified sodium nitrite solution according to the reaction scheme outlined in section 2.5.1. to yield highly reactive diazonium ions. The activated diazonium ions then react with free amino groups on proteins to yield diazonium-coupled drug-protein conjugates. Drug-protein conjugates containing diazonium bonds yield highly coloured complexes that are also extremely stable due to the presence of the double bond chemistry. The conjugates produced were dialysed against several changes of PBS-1 to ensure complete removal of unconjugated 4'-aminowarfarin from the reaction mixture. In all cases the use of diazonium coupling resulted in the presence of dark-brown coloured solutions, which turned to a pale-tan colour following lyophilisation.

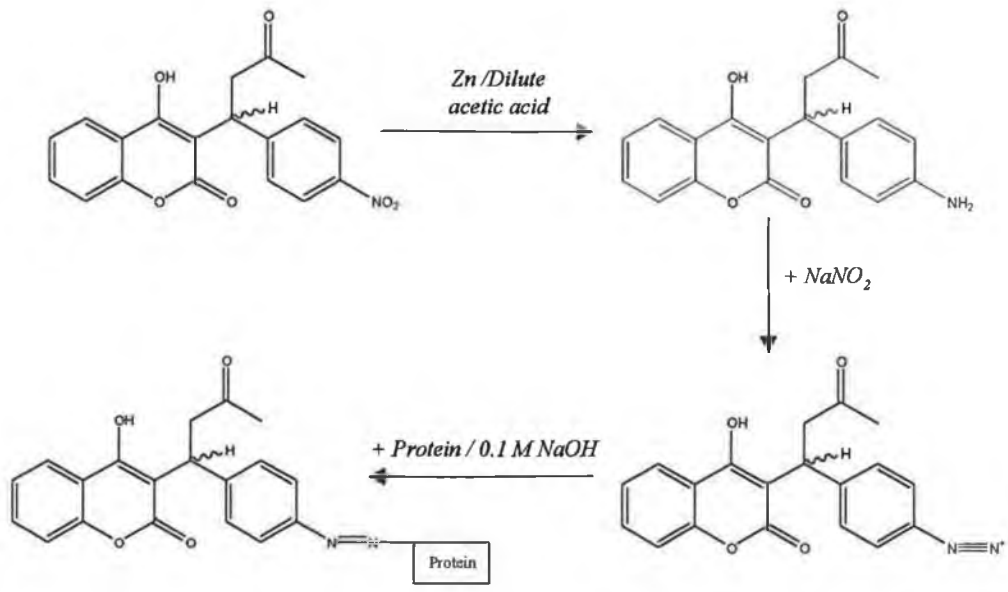

Figure 3.10: *Reaction scheme for the production of diazo-coupled drug-protein (e.g. 4'-azowarfarin-protein) conjugates as described in section 2.5.*

4'-aminowarfarin was also coupled to BSA and thyroglobulin using the homo-bifunctional N-hydroxysuccinimide ester, sulfo-disuccinimidyl tartrate (DST) as described in section 2.5.3. The drug-protein conjugates produced yielded a pure white powder upon lyophilisation. Sulfo-DST incorporates a four-atom spacer between the drug molecule and the carrier protein, and these particular conjugates were used primarily in the production and screening of monoclonal antibodies to warfarin (section 2.10.7.).

The conjugates were initially analysed by UV-spectroscopy from 200-400 nm, this allowed for the putative confirmation of the coupling procedure by direct comparison of the UV spectra for the drug-protein conjugates versus those for the unconjugated protein and drug molecules. The 'control' BSA sample (section 2.6.2.) shows a peak at approximately 280 nm corresponding to the protein peak. Comparison of the 'control' spectra (Figure 3.11.(a)) with that of the conjugate molecule (Figure 3.11.(b)), shows a second peak at approximately 310 nm which gives putative confirmation of the covalent coupling of 4'-aminowarfarin to the protein molecule, as a similar peak maxima is evident for the drug molecule itself (Figure 3.11.(c)).

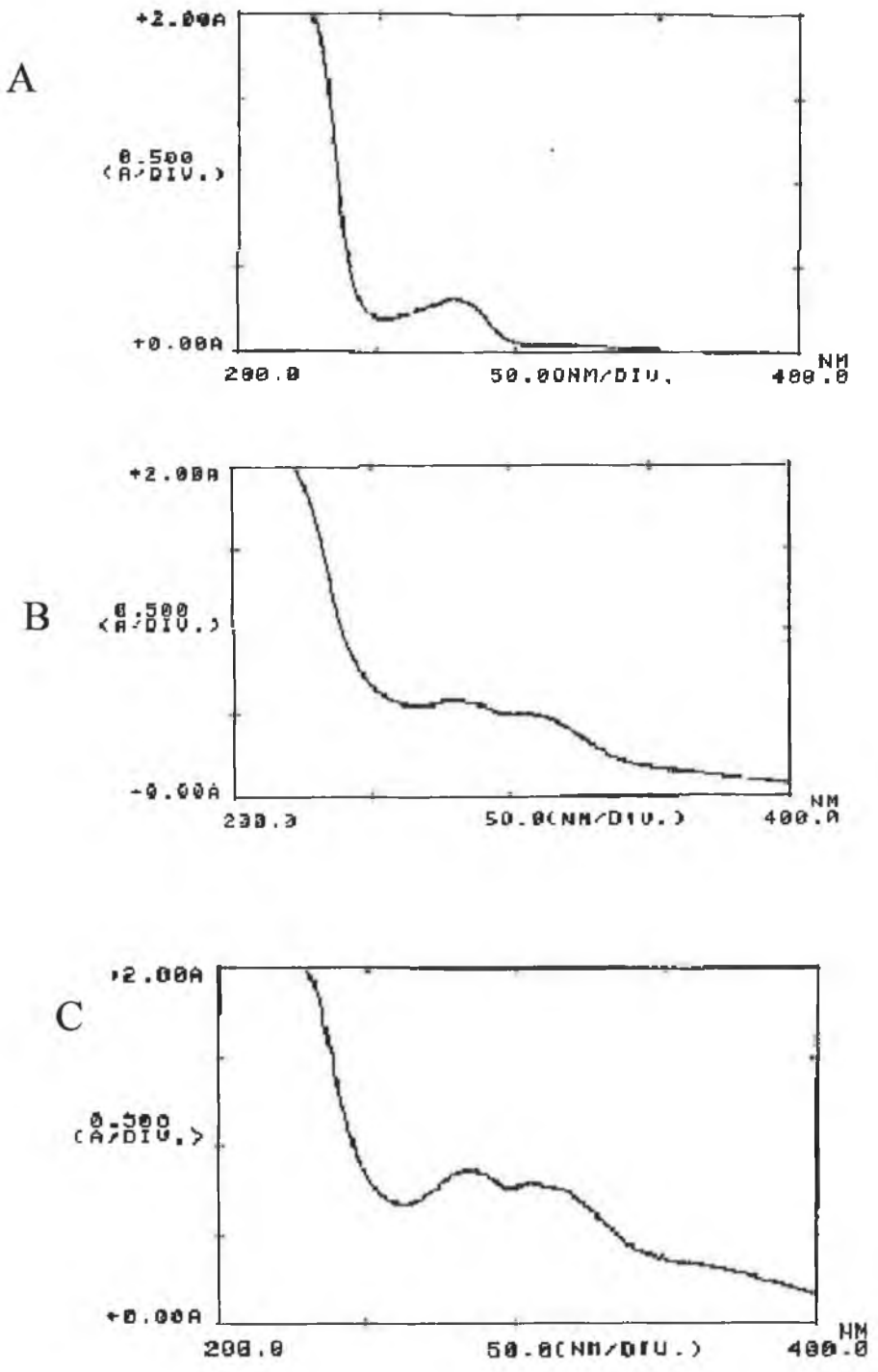

Figure 3.11: *UV spectra were measured for each drug-protein conjugate as described in section 2.6.3. Direct comparison of the UV spectra obtained for 'control' BSA (A)(section 2.6.2.) with those obtained for 4'-aminowarfarin-DST-BSA (B) and 4'-aminowarfarin shows a shoulder peak at approximately 310 nm for the drug-protein conjugate. A similar peak is evident at 310 nm for the drug itself which is indicative of the coupling of 4'-aminowarfarin to BSA using the DST crosslinker*

The drug-protein conjugates were then characterised using HPLC with photo-diode array (PDA) detection as described in section 2.6.1. Size exclusion chromatography allows for the separation of proteins on the basis of molecular size following passage through the size exclusion column, and has been described for the separation of protein mixtures and conjugate preparations (Carty & O' Kennedy, 1988). The use of photo-diode array detection allows the column effluent to be monitored across discrete wavelength bands. In this case all the spectra were analysed from 200-400 nm. The conjugates were analysed using a Beckman Gold software system. Following elution from the column, the drug-protein conjugates could be visualised 'on-screen' in terms of a contour map, and showed two particular absorption maxima at approximately 280 and 310 nm corresponding to the protein and drug portion of the molecule, respectively. The data from these particular chromatograms was transferred into Sigmaplot® software and 3-D contour plots were constructed for the conjugates analysed. The contour plots for 'control' BSA and 4'-azowarfarin-BSA are shown in Figures 3.15 and 3.16, respectively. Examination of the contour plot for BSA shows a peak maxima at 280 nm, whilst the conjugate reveals two peaks at approximately 280 nm and a shoulder peak at 310 nm on the main protein peak demonstrating the covalent coupling of 4'-aminowarfarin to BSA.

The conjugates were also analysed by SDS-PAGE as described in section 2.3. and the gel following electrophoresis is shown in Figure 3.14. The gel picture shows 'control' BSA and 4'-azowarfarin-BSA run in two adjacent wells, and demonstrates that the coupling procedure had no deleterious effect on the protein as one discrete band is seen for both protein samples. The conjugates were also analysed by HPLC with UV-detection at 280 nm as described in section 2.6.1. The void volume, Vo, of the size exclusion column was initially determined by passing Blue dextran through the column. The retention time of each sample was determined, Ve, and divided by the time taken for the sample to elute in the column void volume (i.e. Ve/Vo). The results are shown in Table 3.2. A calibration curve was then constructed of Ve/Vo versus the log of the molecular weight of the protein standards of known molecular weight, and from the constructed calibration plot shown in Figure 3.12. it was possible to estimate the molecular weight of the drug-protein conjugates. The molecular weight of 4'-azowarfarin-BSA was estimated to be approximately 85 kDa, which implies a high drug-protein ratio of approximately 60:1. The plot overlay (Figure 3.13) of the chromatograms for BSA and warfarin-BSA shows the conjugate eluting a fraction earlier from the column confirming the increased molecular weight. Estimation of the drug-protein coupling ratio was not possible using UV spectrometry due to the presence of the diazo bond, which would have distorted any possible measurements due to the coloured intensity of the sample and completely different molar extinction coefficients.

The 4'-aminowarfarin-DST-BSA protein conjugates produced were believed to have undergone a significant degree of protein-protein cross-linking as assessed from the retention time of the conjugate which was similar to that of thyroglobulin despite using a greater than 100-fold molar excess of antigen over protein in the conjugate preparation. SDS-PAGE studies also confirmed the high degree of cross-linking as assessed by the minimal migration of the protein sample following gel electrophoresis.

***Table 3.2:** Molecular Weight standards Calibration Curve:*

Sample	Mol. Wt. (Da)	Log Mol. Wt.	Retention Time, Tr (mins)	Ve/ Vo
Blue Dextran	2,000,000	6.301	5.75	1
Bovine Serum Albumin	66,000	4.819	8.55	1.487
Ovalbumin	45,000	4.653	9.03	1.571
Peroxidase	44,000	4.643	9.154	1.5924
Carbonic Anhydrase	29,000	4.4.62	9.568	1.664
Cytochrome C	12, 400	4.093	10.469	1.821

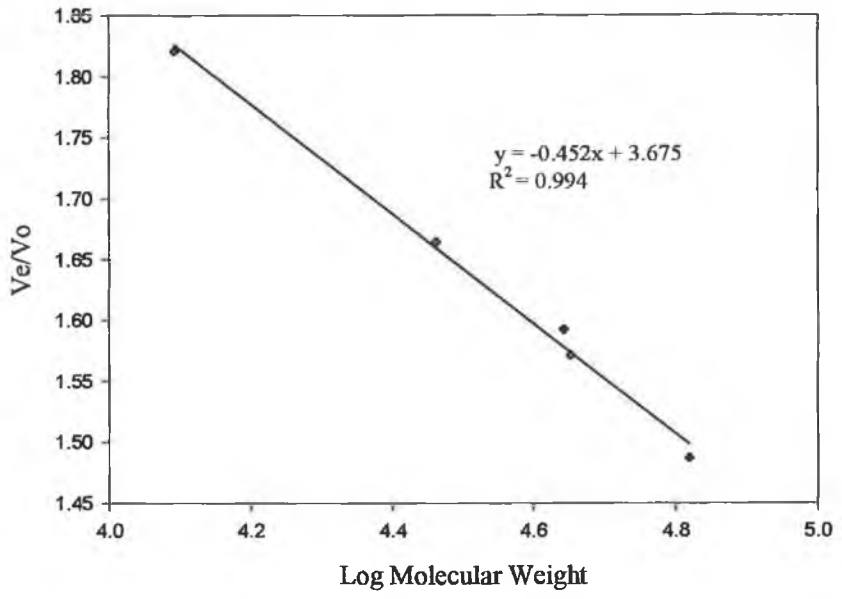

Figure 3.12: *Size exclusion chromatography of a set of protein standards of known molecular weight were passed down a Phenomenex 3000 SEC column using PBS-1 as mobile phase at a flow-rate of 1.0 ml/min with UV detection at 280 nm. The retention time, Tr, of each sample was recorded, and divided by the time taken for a sample to elute in the column void volume, Vo (Tr= Ve as flow rate = 1.0 ml/min). This value, Ve/Vo, was then plotted against the log of the molecular weight of the respective protein sample to construct the calibration plot. From the regression line, it was then possible to estimate the size of the 4'-azowarfarin-BSA and thyroglobulin conjugates. The 4'-azowarfarin-BSA conjugate was estimated to be approximately 85 kDa in size, implying a drug-protein coupling ratio of approximately 60:1, respectively.*

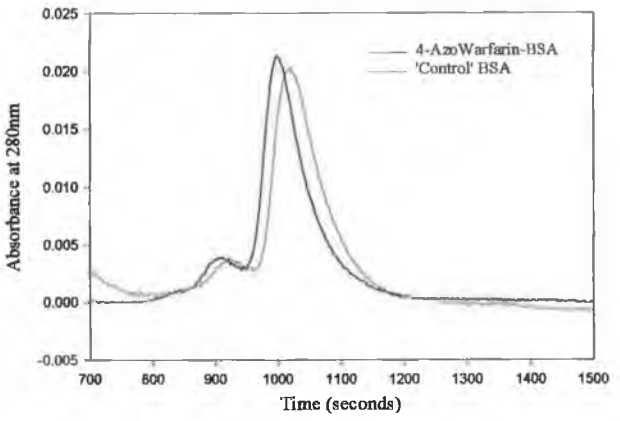

Figure 3.13: *Plot overlay of 'control' BSA and 4'-azowarfarin-BSA following chromatography on a Phenomenex SEC 3000 column using PBS-1 at a flow rate of 1.0 ml/min as mobile phase with UV detection at 280 nm. The conjugate shows a slightly shorter retention time of ~8.3 minutes compared to 'control' BSA which showed a retention time of approximately 8.62 minutes as a result of the increased molecular weight following the conjugation procedure.*

Figure 3.14: *SDS-PAGE analysis of 4'-azowarfarin-BSA (lane A) and 'control' BSA (lane B) as described in section 2.3. The drug-protein conjugate and 'control' protein showed that the conjugate had migrated slightly less than the 'control' BSA, as a result of the increased molecular weight.*

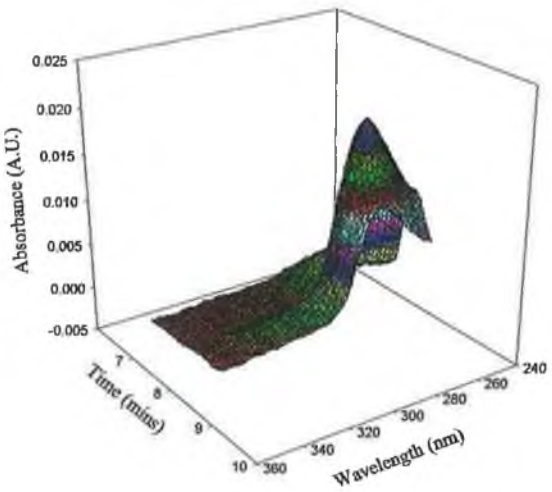

Figure 3.15: *3-D Contour plot for 'Control' BSA following Size Exclusion Chromatography with photo-diode array (PDA) detection as described in section 2.6.1. A large peak can be seen at 280 nm corresponding to the protein molecule.*

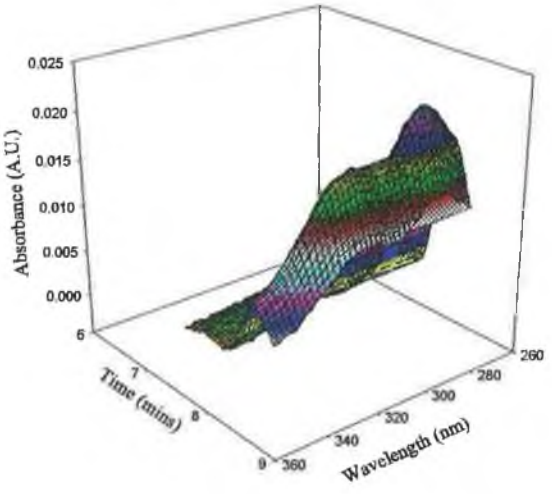

Figure 3.16: *3-D Contour plot for 4-azowarfarin-BSA following Size Exclusion Chromatography with photo-diode array (PDA) detection as described in section 2.6.1. A large peak can be seen at 280 nm corresponding to the protein molecule, with an additional shoulder peak with a maxima at 310 nm confirming the covalent coupling of 4'-aminowarfarin to BSA.*

3.2.3. Production and Affinity-Purification of anti-warfarin antibodies:

For the production of polyclonal anti-warfarin antibodies, rabbits were immunised intradermally with the characterised conjugates as described in section 2.8.3. The rabbits were initially immunised at various sites and the specific serum titre monitored as described in section 2.11.1. The titres following immunisation are shown in Figure 3.17. When the antibody titre has reached a sufficiently high titre the rabbit was sacrificed and the blood harvested by cardiac puncture.

The serum was then prepared as described in section 2.8.3. The rabbit serum was then partially purified using ammonium sulphate precipitation as described in section 2.9.1.1. to yield an immunoglobulin fraction of relatively high purity. This fraction was then dialysed extensively against PBS-2 and affinity-purified as described in section 2.9.1.2. Two immunoaffinity matrices were initially constructed for the purification of the rabbit serum employing the use of cyanogen-bromide sepharose-4B and Triazine agarose 4XL, as described in section 2.7.1. and 2.7.2., respectively. From immunoaffinity procedures carried out, the cyanogen-bromide activated sepharose column proved more effective in terms of affinity-purification, and this was considered to be due to a higher coupling ratio of ligand (i.e. 4'-azowarfarin-BSA) to the column as measured from the extracts following the coupling procedure. The levels of specific immunoglobulin were also slightly lower for the Triazine column than the sepharose immobilised ligand, despite the comparable total protein content. It was postulated that the use of triazole (2 M, pH 5.0, as per manufacturer's instructions) as a blocking agent to cap the excess active amine groups may have resulted in the generation of a very hydrophobic matrix given the molecular structure of triazole. The increased hydropbobicity in the column may have therefore resulted in increased non-specific binding to the column and overall reduced efficiency in terms of an affinity matrix. The bound antibodies were eluted from the column using 0.1 M glycine-HCl (pH 2.5) and collected in 1 ml eppendorf tubes containing 150 µl of 1 M Tris-HCl (pH 8.5), which neutralised the eluted acidic antibody fractions, thereby retaining the immunological activity of the eluted fractions. The affinity-purified fractions were then dialysed against several changes of PBS-2 at 4°C. The titre of the affinity-purified antibody following affinity-purification was determined as described in section 2.11.1 and showed a specific antibody titre of greater than 1/1,000,000 (Figure 3.18).

The purity of the affinity-purified fraction was determined by size exclusion chromatography as described in section 2.6.1. using a Phenomenex 3000 SEC column and PBS-1 as mobile phase at a flow rate of 0.5 ml/min with UV detection at 280 nm. The resulting chromatogram is shown in Figure 3.19, indicating the purity of the fraction whose molecular weight was made by reference to a calibration plot of known molecular weight standards.

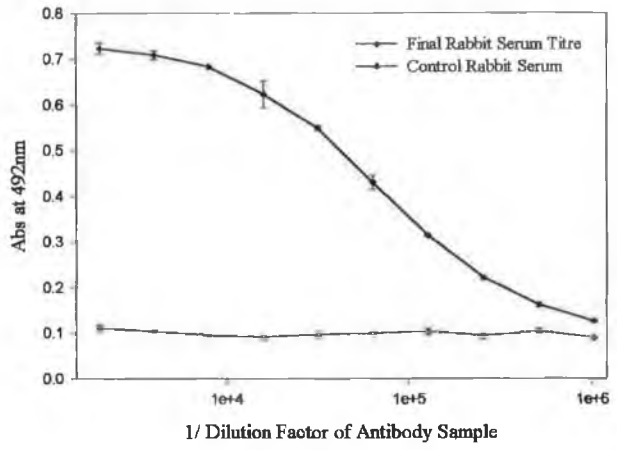

Figure 3.17: *Final rabbit serum titre as determined by direct ELISA as described in section 2.11.1. The final titre recorded was in excess of 1/500,000. The results shown are the mean of triplicate results ± standard deviation.*

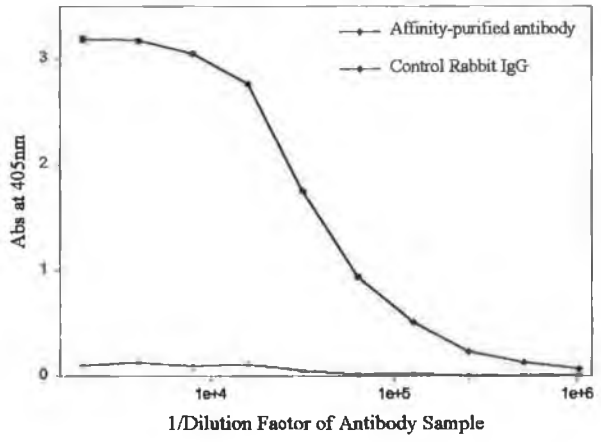

Figure 3.18: *Titre of affinity-purified antibody following affinity purification on a 4'-azowarfarin-BSA sepaharose-4B column as described in section 2.9.1.2. The dialysed fraction of ammonium sulphate-precipitated immunoglobulin was passed through the column several times. The bound anti-warfarin antibodies eluted with 0.1 M glycine-HCl (pH 2.5), and collected in eppendorf tubes containing 150 µl of 1 M Tris-HCl (pH 8.0). The fractions collected were then assayed spectrophotometrically at 280 nm and those fractions containing protein dialysed against several changes of PBS-2 at 4°C overnight. The dialysed fraction was then assayed for specific antibody (section 2.11.1.) and showed a specific antibody titre of greater than 1/1,000,000, as shown above. The results shown are the mean of triplicate results ± standard deviation.*

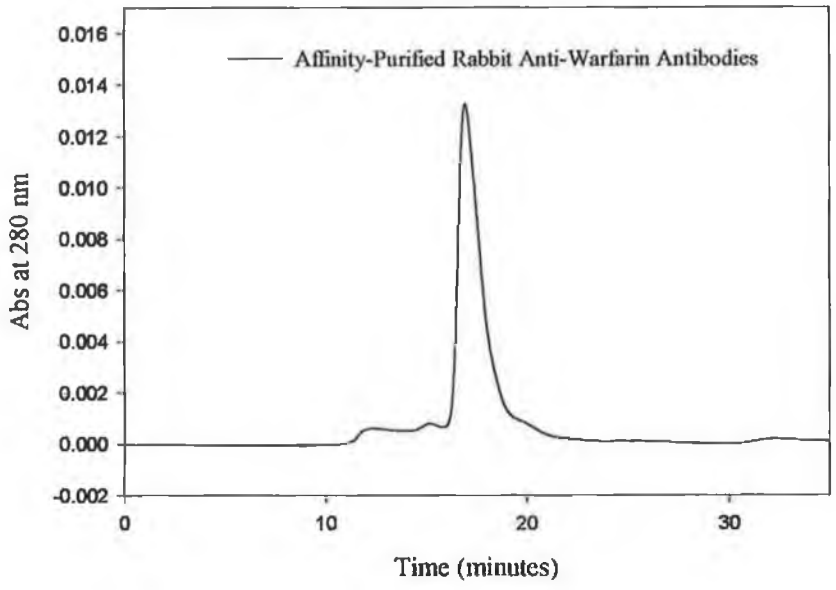

Figure 3.19: *Size exclusion chromatography of affinity-purified polyclonal rabbit anti-warfarin antibodies carried out as described in section 2.6.1. using a Phenomenex 3000 SEC column with PBS-1 as mobile phase at a flow rate of 0.5 ml/min with UV detection at 280 nm. The single peak on the chromatogram whose retention time corresponds to approximately 155 kDa by reference to a standard curve of proteins of known molecular weight shows the identity and purity of the immunoglobulin fraction*

3.2.4. Cross-Reactivity Studies:

Cross-reactivity may be defined as a measure of the antibody response to structurally related molecules, as a result of shared epitopes. Given the unique specificity of antibodies, one of the first steps in immunoassay design is the assessment of reactivity towards structurally related molecules that share such common epitopes (Wild, 1994). Assessment of the cross-reactivity of polyclonal antisera is limited to the analysis of binding specificity towards structurally related antigens (e.g. metabolites and structural analogues), and can be assessed by setting up serial dilutions of the competing antigen in parallel with the similar dilutions of the specific antigen as described in section 2.11.5. The cross-reactivity is often conveniently defined as the point where the reduction in signal recorded in the presence of a particular analyte concentration (A_x) gives a 50% reduction in the signal in the presence of zero analyte (A_0) (i.e. A_x/A_0=50%). This concentration value can then be expressed as a percentage of the analyte giving the same decrease in signal.

Therefore,

$$\% \text{ Cross-Reactivity} = \frac{\text{Concentration of analyte giving 50\% decrease in signal}}{\text{Concentration of cross-reactant giving 50\% decrease in signal}} = \frac{Z_1}{Z_2} \times 100\%$$

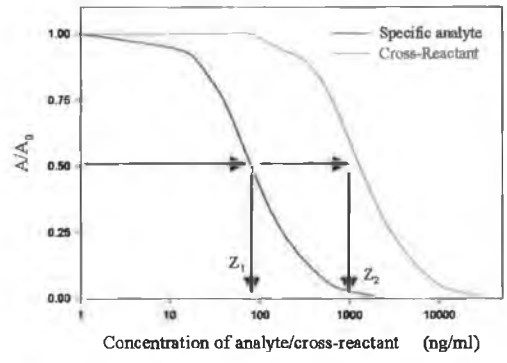

Figure 3.20: *The potential cross-reactivity of a particular antibody preparation towards a structurally related compound can be conveniently described as a percentage of the reactivity towards the specific analyte by expressing the concentrations of each reagent that gives 50% inhibition as shown in equation above.*

For the production of drug-protein conjugates the point of attachment of the drug to the carrier protein is of critical importance, as it will dictate the specific epitopes available for antibody-binding, and thus the specificity of the polyclonal antisera produced. The nitro-group on the parent molecule was chosen as the point of attachment for two particular reasons. Firstly, it provided a convenient means of conjugation. Secondly, as the major

human metabolites of warfarin involve hydroxylations of the 4-hydroxycoumarin ring structure and carbon side chain of the molecule (Figure 1.6), it was believed that conjugation via the phenyl substituent would confer a greater degree of specificity to the polyclonal antibodies produced against warfarin. The cross-reactivity towards the metabolites of warfarin available was determined and the ELISA developed as described in section 2.11.5.

The results from the cross-reactivity study are shown in Table 3.3 and Figure 3.21. The cross reactivity of the affinity-purified polyclonal antibodies demonstrates an almost identical cross-reactivity (≈ 98%) towards acenocoumarin, as expected given that the two compounds are essentially identical except for the presence of the nitro group. Given that this particular region does not confer any antibody specificity being the point of conjugation (Figure 3.10), this would explain the similar affinity of the polyclonal antibody preparation to acenocoumarin. The affinity-purified antibodies showed cross-reactivity of approximately 28 and 3% towards 6- and 7-hydroxywarfarin, respectively. Cross-reactivity studies were also carried out using 4-hydroxycoumarin (which comprises half of the molecule), coumarin, 7-hydroxycoumarin, and 7-hydroxycoumarin-4-acetic acid. Cross-reactivity towards these particular compounds in each case was negligible and typically of the order of <0.1%.

Table 3.3: *Cross-Reactivity of Affinity-Purified Rabbit Anti-Warfarin Polyclonal Antibodies with Structurally Related Analogues:*

Compound	% Cross Reactivity
Warfarin	100
Acenocoumarin	98
6-Hydroxywarfarin	28
7-Hydroxywarfarin	3
7-Hydroxycoumarin	<0.1
4-Hydroxycoumarin	<0.1
Coumarin	<0.1
7-Hydroxycoumarin-4-acetic acid	<0.1

The 3-dimensional geometrical structures of warfarin and it's major human metabolites analysed, namely 6- and 7-hydroxywarfarin were constructed using Hyperchem® molecular modelling software package. This particular package utilises molecular mechanics and a combination of algorithms to generate the geometrical shape of molecules based on the sum of the potential energies within the molecule, which is defined as the force field (Allinger *et al.* 1989). Using the software package the geometry of the molecule is systematically

adjusted to give the lowest potential energy state for a particular molecule. The constructed geometrical structures for (R)-7-hydroxywarfarin, (R)-warfarin, and (R)-6- hydroxywarfarin and are shown in Figure 3.22(a)-(c). It should be noted however, that the structural configurations displayed are the optimised configurations using the software package and are by no means an absolute configuration. Significant bond rotation can occur within a molecule, particularly at single bond residues which provide greater molecular flexibility to the molecule, implying that warfarin would be free to rotate about any of these particular bonds. From the models it can be seen that the 4-hydroxycoumarin residue and the carbonyl side chain appear to lie along the same plane, orthogonal to the phenyl substituent (i.e. the point of conjugation). It can be postulated therefore that the majority of the antibody-binding site is directed against the 4-hydroxycoumarin ring structure and carbonyl side-chain. Consequently, substitutions (e.g. hydroxylations to the coumarin ring) could lead to differing specificities of antibody binding pocket for the antigen, as the 'complementarity' of the binding domain is disturbed. In this context, the hydroxylation at position-7 of the 4-hydroxycoumarin ring could be expected in the context of a polyclonal antibody population, to have a more marked effect on the antibody affinity given the suggested epitope region, than a hydroxylation at position 6 of the 4-hydroxycoumarin residue, which would concur with the experimental observations noted. The fact that the degree of cross-reactivity towards the coumarin and it's hydroxylated metabolites is negligible implies that the antibodies require both the coumarin ring structure and the presence of the carbonyl side chain for antibody recognition. Unfortunately, as no other hydroxywarfarin metabolites were available for study, this hypothesis was unable to be substantiated. However, based on these stated assumptions, hydroxylations at position 8 and reduction of the carbonyl side chain to yield the warfarin alcohols would be expected to bring about corresponding changes in the affinity of the antibodies towards these metabolites.

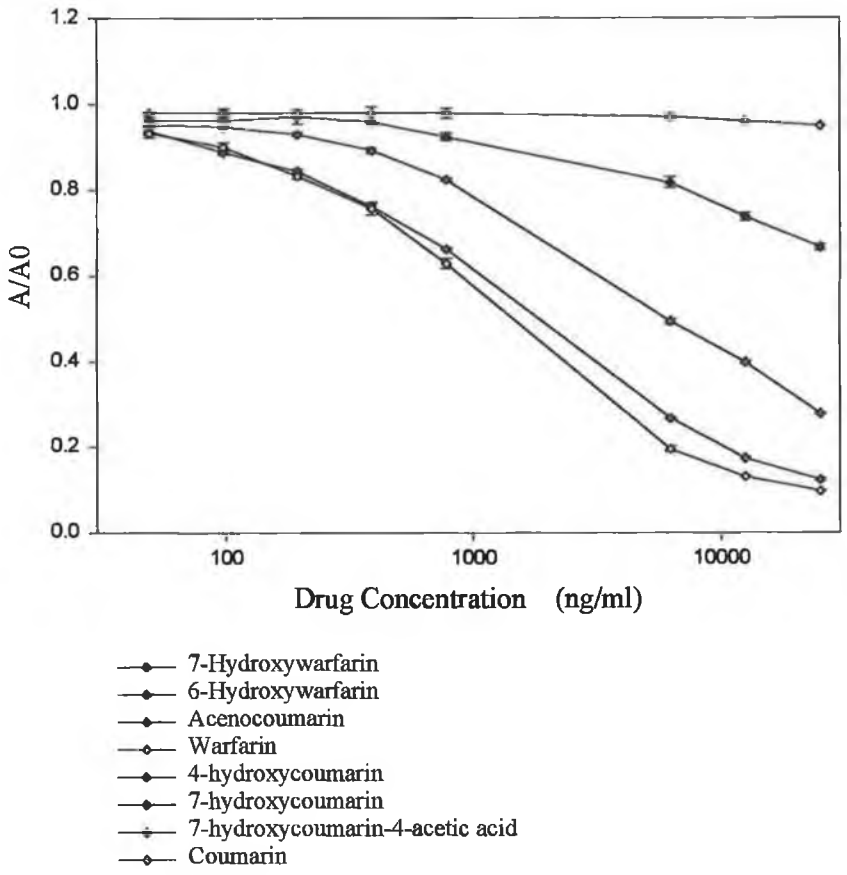

Figure 3.21: *Cross-reactivity studies of polyclonal antibodies. Cross-reactivity studies were carried out on the affinity-purified warfarin polyclonal antibodies as described in the text and section 2.11.5. to structurally related molecules of warfarin. The antibodies demonstrated little or no reactivity towards coumarin-based molecules suggesting that the presence of the carbonyl group and possibly the phenyl ring are also required for antibody recognition. The purified antibodies showed differing degrees of affinity towards both 6- and 7-hydroxywarfarin which could be explained by the substitution at position 7 of the 4-hydroxycoumarin ring structure which based on the optimised geometrical configurations of these molecules (Figure 3.22(a)-(c)) could play a more crucial role in terms of antibody recognition.*

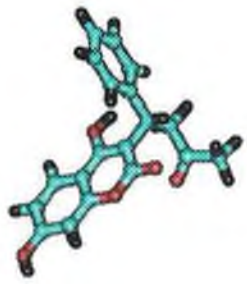

Figure 3.22.(a). 7-Hydroxy-R-Warfarin.

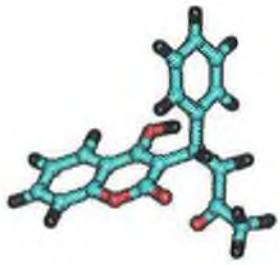

Figure 3.22.(b). R-Warfarin.

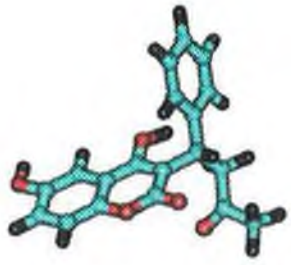

Figure 3.22.(c). 6-Hydroxy-R-Warfarin.

Figure 3.22: *The 3-dimensional geometrical structures of (R)-warfarin and 6- and 7-hydroxy-(R)-warfarin were constructed using Hyperchem ® software which determines the geometrical configuration of molecules using force-field algorithms that are continually systematically adjusted to give the optimal geometry of the particular molecule. From the constructed models the 4-hydroxycoumarin ring structure and the carbonyl substituent appear to lie in the same plane orthogonal to the phenyl ring substituent used as the point of conjugation, and provide the majority of the antibody-recognition site. Blue, red and black balls and lines correspond to carbon, oxygen and hydrogen molecules, respectively.*

3.2.5. Development of a competitive ELISA for Warfarin:

A competitive enzyme-linked immunosorbent assay (ELISA) was developed for the detection of warfarin in solution using the characterised drug-protein conjugates and the affinity-purified rabbit polyclonal anti-warfarin antibodies.

3.2.5.1. Determination of optimal conjugate coating density and antibody working dilution:

In competitive ELISA the highest degree of sensitivity in terms of detection limits, is achieved with the concentration of primary antibody approaching zero. The limits of detection in competitive ELISA are therefore a function of the intrinsic antibody affinity (or range of affinities as is the case with a polyclonal antibody preparation), and the equilibrium between both the free and immobilised forms of the antigen. Consequently, utilising too high a conjugate loading density (i.e. solid-phase form of immobilised antigen) will shift the binding equilibrium in favour of binding to the ELISA plate and cause reduced sensitivity to free antigen in solution (i.e. the desired detectable analyte). Similarly, utilising too high a concentration of antibody preparation, means that there will be greater free antibody in solution and the assay system will only be suitable for the detection of high concentrations of free analyte in solution (i.e. where antibody concentration approaches zero). It is essential therefore to optimise both the concentration of the solid-phase antigen and the optimal concentration of antibody (i.e. the working dilution of antibody) to be used for competitive ELISA techniques.

The optimal dilution of conjugate loading density was determined as described in section 2.11.4. Briefly, a range of conjugate loading densities ranging from 5 to 100 μg/ml of 4'-azowarfarin-BSA were prepared in PBS-1 and applied to the plate and antibody dilution curves constructed using serial doubling dilutions of affinity-purified antibody. The optimal conjugate loading density was defined as that conjugate coating density (μg/ml) that gave the widest linear detection range over the range of antibody dilutions used. A conjugate loading density of 50 μg/ml was found to be the optimal loading density for 4'-azowarfarin-BSA conjugates as shown in Figure 3.23. Similar determinations for the optimal conjugate loading densities for the various other drug-protein conjugates were made, as the concentration used for each conjugate preparation is a direct function of each particular drug-protein coupling ratio.

The optimal dilution of antibody to be used in competitive ELISA experiments was determined by setting up a standard curve of serial doubling dilutions of affinity-purified antibody as described in section 2.11.1. using the optimal conjugate loading density for the

particular immobilised solid-phase antigen. From Figure 3.18 it can be seen that using an antibody dilution taken from the asymptotes of the sigmoidal curve would be insensitive to small changes in antibody concentration. The working dilution of antibody for such competitive assay purposes is taken from the linear portion of the sigmoidal antibody dilution curve, where there is the greatest change in absorbance for a similar change in antibody dilution. For the affinity-purified antibody preparation used the working dilution of antibody was determined to be 1/25,000 (Figure 3.18).

3.2.5.2. Competitive ELISA for the detection of warfarin:

A series of warfarin concentrations ranging from 12.5-3125 ng/ml were prepared as described in section 2.11.5. 50 µl of each of these antigen concentrations was then applied to the wells of a coated ELISA plate (see section 2.11.1.). Affinity-purified rabbit anti-warfarin antibodies was then prepared at twice the working dilution of antibody, and 50 µl of this antibody preparation added to the wells of the ELISA plate so that the final antibody concentration on the plate was equal to that of the working dilution of antibody determined in section 3.5.1. The various warfarin concentrations were added to the wells of the ELISA plate in random order using a random number generator, to ensure there was no bias in any measurements conducted, as a result of thermodynamic effects within the plate. The mean normalised absorbance value was then determined at each antigen concentration (see Appendix 1A). The use of the mean normalised absorbance values (A/A_0) allowed for direct comparison between ELISA intra-assay results.

$$R = R_{HI} - \frac{R_{HI} - R_{LO}}{1 + \left(\frac{Conc}{A_1}\right)^{A_2}}$$

Where	R_{HI}	=	Response at infinite concentration
	R_{LO}	=	Response at zero concentration
	$Conc$	=	Analyte Concentration (ng/ml)
	A_1	=	Fitting constant
	A_2	=	Fitting constant

Four-parameter equations of the form above were fitted to the data sets of mean normalised absorbance versus warfarin concentration obtained for immunoassays curves using BIAevaluation 3.1 software. The constructed calibration curves also allowed for the determination of unknown values using the dedicated software package. In this way it was

possible to calculate the degree of precision of analytical measurements at different concentrations points relative to the fitted four-parameter equation. The inter-assay variation was calculated by performing the assay over three separate days, and a separate calibration curve constructed for each normalised absorbance (A/A_0) value versus the respective warfarin concentration for each assay. The mean back-calculated concentration at each antigen concentration was then used to calculate the inter-assay mean, standard deviation and coefficient of variation for the intra-assay curve. The inter-assay and intra-assay results are shown in Table 3.4 and Table 3.5, respectively.

The percentage accuracy values obtained for both the ELISA inter- and intra-assay variation were typically of the order of less than 7% which is well within the recommended guidelines for immunoassay calibration plots demonstrating the accuracy and reproducibility of the method (Findlay *et al.*, 2000). The low percentage coefficient of variation obtained also underlines the precision of the ELISA technique.

Table 3.4: *Inter-Assay variation for the determination of Warfarin by competitive ELISA (n=3).*

Actual Warfarin Concentration (ng/ml)	Mean Back-Calculated Warfarin Concentration (ng/ml)	% C.V.	% Accuracy
1562.5	1447.48	1.59	7.39
781.25	817.38	2.01	4.62
390.63	418.36	3.48	7.10
195.31	205.95	6.09	5.44
97.85	87.07	4.22	11.14
48.84	50.15	4.37	2.6
24.42	25.87	5.83	5.94

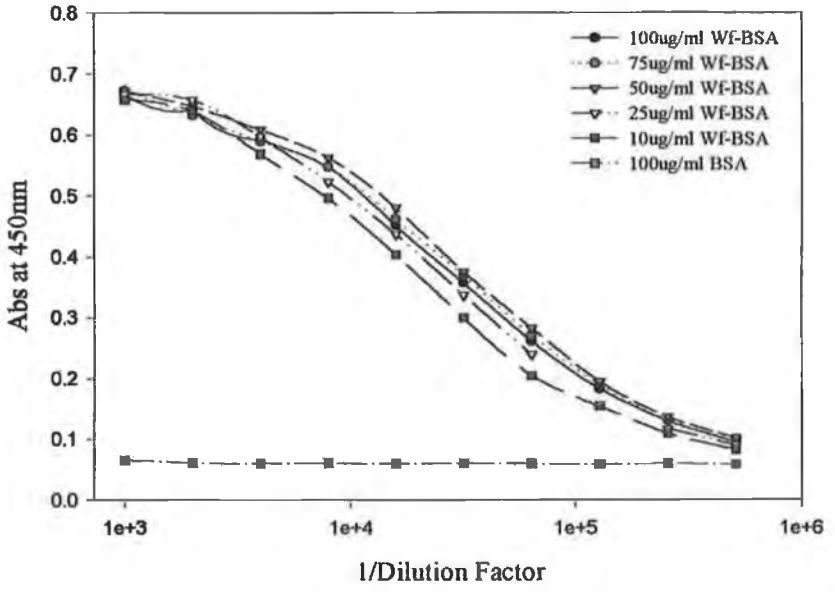

Figure 3.23: *Determination of optimal conjugate loading density. Wells of an immunoplate were coated with varying concentrations of conjugate ranging from 5-100 μg/ml. Serial doubling dilutions of affinity purified antibody were then added to the wells of the plate as described in section 2.11.4. The conjugate loading density that gave the widest linear detection range over the antibody dilution series used, and 50 μg/ml was chosen as the optimal conjugate loading density. The results shown are the average of duplicate results.*

Table 3.5: *Intra-Assay variation for the determination of warfarin using affinity-purified rabbit anti-warfarin antibodies (n=6)*:

Actual Warfarin Concentration (ng/ml)	Mean Back-Calculated Warfarin Concentration (ng/ml)	% C.V.	% Accuracy
1562.5	1429.85	6.63	8.54
781.25	836.92	4.84	7.12
390.63	422.15	1.76	8.02
195.31	195.85	6.99	0.28
97.85	89.26	4.02	8.64
48.84	49.95	5.39	2.28
24.42	22.72	4.85	6.96

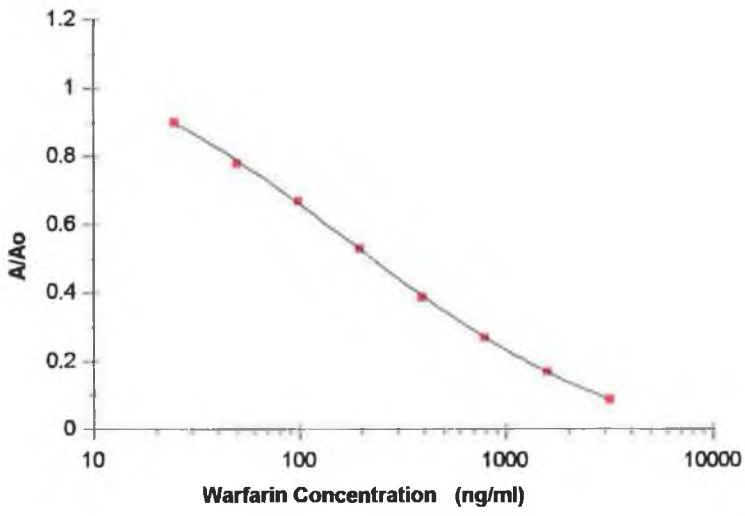

Figure 3.24: *Intra-Assay Variation for competitive ELISA for warfarin using affinity-purified rabbit anti-warfarin antibodies. A 4-parameter equation was fitted to the data set using BIA evaluation 3.1 software. The inter-assay mean and coefficient of variation were calculated and are tabulated in Table 3.5. Each point on the curve is the mean of six replicate measurements.*

3.3. Conclusions:

This particular chapter describes the chemical synthesis of the compound 4'-aminowarfarin following the reduction of acenocoumarin in the presence of dilute acid and the catalyst zinc. The modified reaction scheme provided a convenient, safe and reproducible means of routinely producing 4'-aminowarfarin without the need for an elaborate and potentially hazardous experimental setup as required for the hydrogenation reactions. Purification and subsequent characterisation of the reaction product provided unambiguous confirmation of the structure of the reaction product.

4'-aminowarfarin was then used for the production of a variety of drug-protein conjugates, which were subsequently characterised by a combination of size exclusion chromatography with UV and PDA detection, and SDS-PAGE analysis. The drug-protein coupling ratio for the diazo-coupled protein conjugates was particularly high (i.e. 60:1 for 4'-azowarfarin-BSA), and could be used to explain the extremely high antigen-specific titres (i.e. greater than 1/1,000,000) obtained, highlighting the immunogenicity of the conjugates produced.

The use of the immunoaffinity purification matrices provided a relatively simple means of obtaining an antibody preparation of high purity, free from extraneous protein and immunoglobulin. The use of such immunoglobulin preparations simplifies future experimental work where high protein concentrations in the antibody preparations used, can give rise to spurious errors associated with the non-specific binding of extraneous protein to wells of the immunoplate or chip surface in the context of BIACORE experiments (see Figure 4.12).

The purified antibodies were then used in the development of a competitive ELISA for the detection of warfarin in solution. The inter- and intra-assay variation for the competitive ELISA were typically of the order of 5-10%, and demonstrated the accuracy (intra-assay) and reproducibility (inter-assay) of the technique. These values are also well within the current recommended guidelines for immunoassay calibrations, that suggest that tolerance limits of 20% be applied to immunoassay curves with respect to assay precision (Findlay *et al.*, 2000). The cross-reactivity studies carried out demonstrated that the majority of the antibodies to the warfarin conjugate shared a common epitope between the 4-hydroxcoumarin ring structure and the carbonyl substituent as postulated from the 3-dimensional molecular structures constructed. The use of such modelling techniques provide intuitive information as to the probable geometrical configuration of small molecules such as drugs, which are not always evident from 2-dimensional configurations. Such tools should therefore be consulted before the synthesis of drug-protein conjugates, so that a clearer

picture of the possible epitopes can be identified, which can be subsequently utilised to confer molecular specificity, or alternatively, for the production of broad-spectrum specificity antibodies for a particular class of drugs through careful selection of the point of conjugation.

Chapter 4

Development and Validation of a BIACORE-based inhibition immunoassay for the detection of warfarin in biological matrices

4.1 Introduction:

The development of biosensor devices has grown enormously over the past two decades. Biosensors can be broadly described as sensing devices incorporating a biological sensing element coupled to a variety of transducing mechanisms (e.g. electrochemical, optical-electronic), which together relate the concentration of analyte to a measurable electronic signal (Rogers, 2000). The development of biosensors has been extensively reviewed elsewhere (Griffiths & Hall, 1993; Pancrazio *et al.*, 1999; Rogers, 2000). The current trend in biosensor technology is towards miniaturised, chip-based, microarrays capable of multi-analyte detection (Ekins, 1998; de Wildt *et al.*, 2000). The mode of operation and applications of several commercial SPR biosensors is reviewed with a particular emphasis on their applications as tools for the biopharmaceutical industry.

4.1.1. SPR Biosensors:

Surface plasmon resonance biosensors have become important tools in the biopharmaceutical industry, primarily because of their ability to generate a wealth of qualitative and quantitative information simultaneously. Qualitative information generated by molecular screening of small molecules can identify potential drug candidates (Markgren *et al.*, 2000), whilst 'ligand-fishing' experiments can identify possible interacting pairs of molecules and target agents (Catimel *et al.*, 2000). SPR systems can also be used as a means of monitoring purification procedures (Lackmann *et al.* 1996), and have been successfully used for the purification of the ligand for HEK (Human EPH-like Kinase). SPR instruments offer a unique means of monitoring immune complex formation and studying reaction kinetics and determining equilibrium constants, and also allow for the determination of active analyte concentrations (Karlsson *et al.*, 1993). Thermodynamic constants can also be generated by measuring reaction rates at different temperatures (Roos *et al.*, 1998), as well as studying reaction stoichiometry by careful experimental design (Morton & Myszka, 1998).
There are a number of SPR-based devices currently commercially available including: the BIAcore range of instruments (BIAcore AB), the BIOS-1 system (Windsor Scientific Limited), the IAsys instrument (Affinity Sensors), and the Texas Instruments SPR device (TI-SPR). A brief explanation of the mode of operation of each is described below.

4.1.1.1. Surface Plasmon Resonance:

For convenience the principle of SPR is described in the context of the BIACORE range of instruments that utilises the optical phenomenon of surface plasmon resonance to monitor biomolecular interactions in 'real-time'. When light is incident on two media of different refractive index (e.g. glass and water), a portion of the light coming from the medium of

higher refractive index is refracted and the remainder of the light is reflected (Figure 4.1). When the angle of incident light is greater than the critical angle of incidence, the light is totally internally reflected and no light is refracted across the interface between the two surfaces of different refractive index. Under conditions of total internal reflection (TIR), an electric vector component of the incident light known as the evanescent wave, propagates into the medium of lower refractive index a distance of approximately one wavelength. The evanescent wave decays exponentially with the distance travelled from the interface into the lower dense medium. In BIAcore the interface between the glass and water layer is coated with a thin layer of metal (e.g. gold, silver). The energy carried by the evanescent wave can be 'coupled' or transferred to electrons within the metal layer, causing the electrons to oscillate or resonate, resulting in the generation of a surface plasmon wave. This 'coupling' or 'resonance' effect occurs when there is a match between the energy of the surface electrons and the energy of the incident light photons. The coupling of energy between the surface electrons and the evanescent wave can be observed by measuring the amount of light reflected by the metal surface. All the light is reflected at most wavelengths, except for the surface plasmon resonance (SPR) angle where most of the light is absorbed, which can be observed by a dip in the intensity of the reflected light measured. The angle at which SPR occurs is dependent on a variety of factors including: the properties of the metal film (e.g. thickness, uniformity, composition), the wavelength of incident light and the refractive index of the medium either side of the metal film. As the wavelength of light and the properties of the metal film are constant, SPR can be used to probe the refractive index of the aqueous layer adjacent to the gold layer. Consequently, any interaction resulting in a mass effect will result in a refractive index change at the chip surface will be reflected by a corollary effect on the measured SPR angle. The displacement of the SPR angle as result of biological interactions occurring at the chip surface is measured in 'real-time' and interpolated as a sensorgram.

At the heart of the SPR measurement with the majority of commercial instruments (e.g. BIACORE and IAsys) is the sensor chip itself (Figure 4.2). There are currently a variety of chip surfaces available commercially available both from BIACORE and from IAsys which can be tailored for the intended general application (Rich & Myszka, 2000). The majority of applications on both instruments utilise a carboxymethylated (CM) dextran surface, which essentially forms a hydrogel at the sensor surface creating a hydrophilic environment with low non-specific binding, as well as providing a convenient means for immobilising various

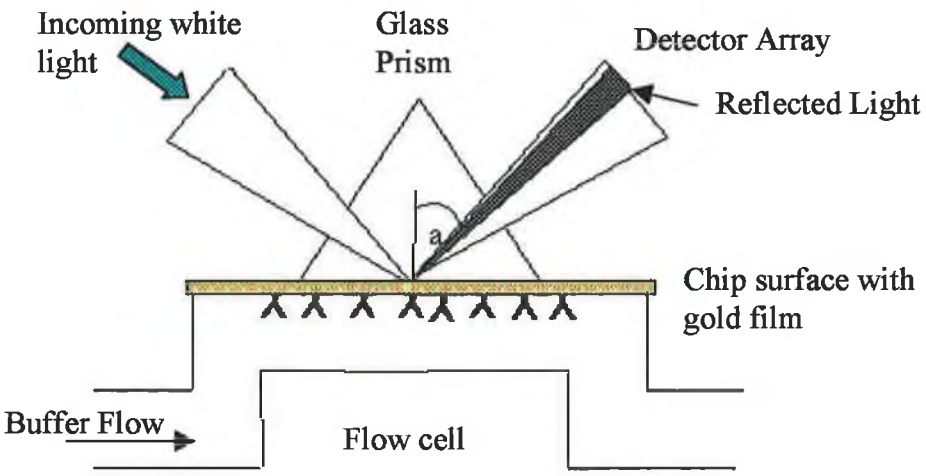

Figure 4.1 *Schematic of the basis of SPR measurements with the BIACORE instrument:*

(A) *In the example illustrated, antibody* (**Y**) *immobilised at the gold sensor chip surface using conventional coupling chemistries (e.g. EDC/NHS). Plane polarised light is emitted from a high efficiency light emitting diode and is focused onto the gold chip surface in the shape of a wedge shaped beam by means of a glass prism under conditions of total internal reflection. The reflected light is then measured by a two-dimensional photo-diode array. Under conditions of total internal reflection at a metal-coated interface an electromagnetic portion of the light known as the evanescent wave penetrates into the medium of lower refractive index. The angle at which this occurs is known as the resonant angle (i.e. SPR angle = angle a), and a sharp shadow or dip occurs in the reflected light at this particular angle (i.e. angle a), designated by the dark bold line in the reflected light. The angle at which SPR occurs is dependent on a number of factors including the refractive index of the layer adjacent to the metal film. SPR can thus be used to probe and monitor the interactions occurring at the chip-surface in 'real-time'.*

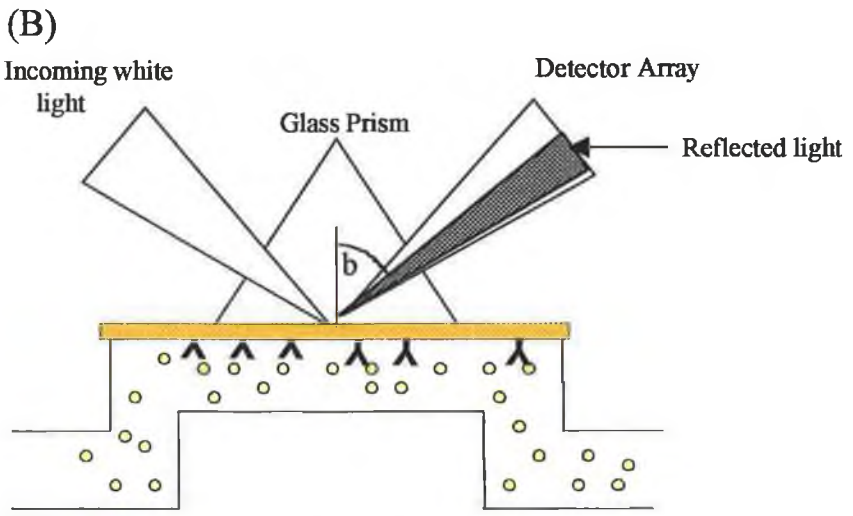

(B) Antigen (○) is then injected over the antibody-immobilised chip surface. Binding of antigen to immobilised antibody causes an increase in the mass bound at the sensor chip surface and a subsequent change in the refractive index at the sensor chip surface, causing a shift (θ) in the resonant angle of the reflected light (i.e. from angle a to angle b). The shift in the resonant angle is proportional to the change in the mass of analyte bound at the sensor chip surface.

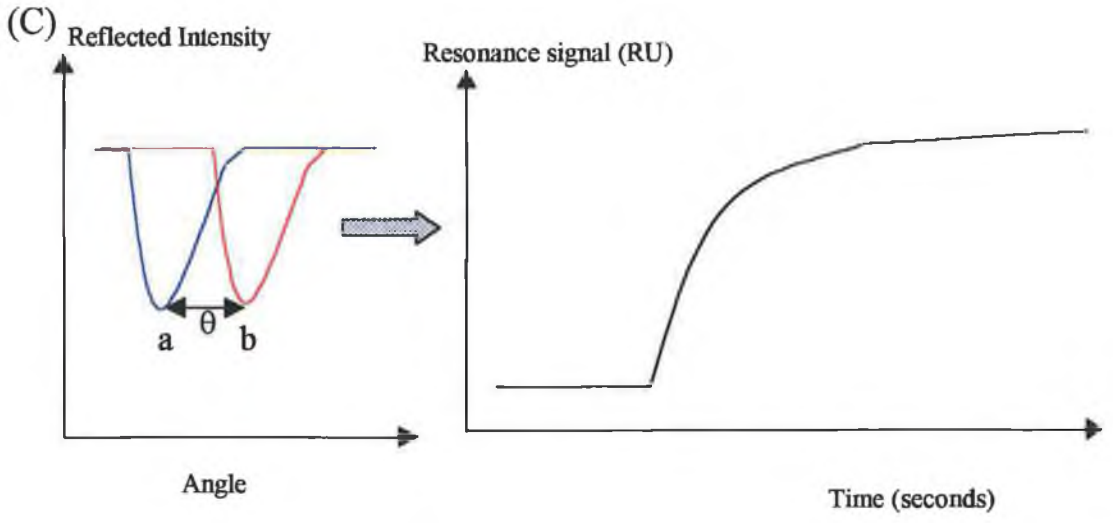

(C) A plot of the change in the resonant angle (θ) measured in 'real-time' following antibody: antigen binding versus time, is interpolated by the instrument software to generate the characteristic SPR response curve. The change in the SPR angle is converted to arbitrary response units by the instrument software. The response signal measured is proportional to the concentration of bound analyte. A change of approximately 1 kRU corresponds to a mass change in surface protein concentration of approximately 1 ng/mm^2.

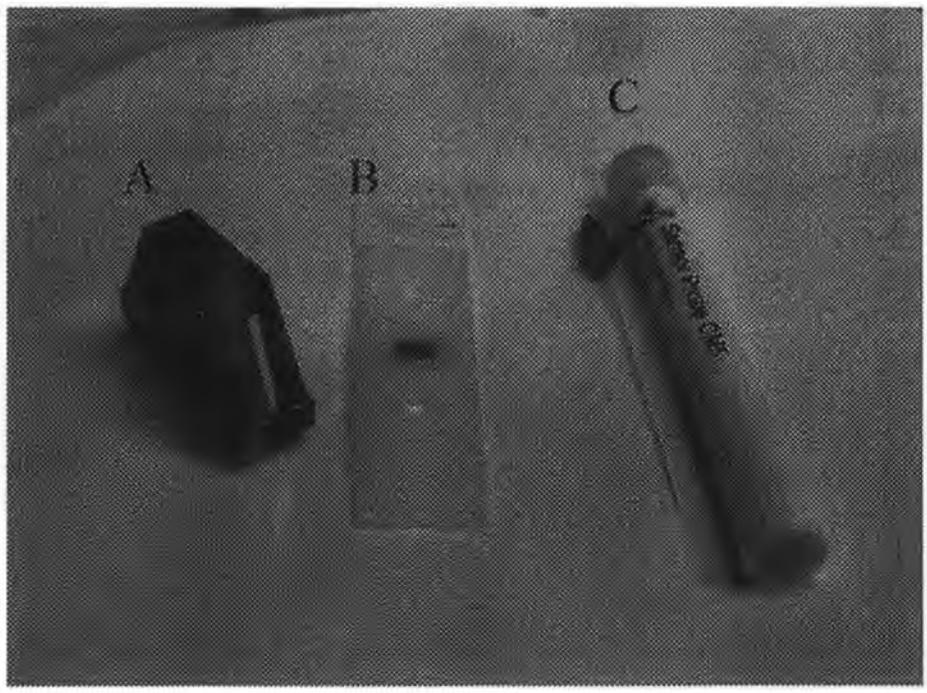

Figure 4.2: *Photographs of miniature TI-SPR device(a), CM5 dextran chip (b) and CM5 probe(c). CM-dextran provides a convenient means of attaching proteins and other molecules to the sensor surfaces for SPR analysis. The hydrophilic nature of the carboxymethyl dextran (CM) also provides an environment amenable to most biological reactions. The CM5 probe is utilised in connection with the BIAprobe device which is a manually operated device, which is operated in a pipette style configuration, and is ideally suited for the monitoring relatively crude matrices such as bacterial culture supernatants and blood (Quinn et al., 1997). The gold sensing layer on the TI-SPR device can be overlaid with disposable SPR chip.*

molecules. Direct immobilisation of proteins directly onto gold surfaces can result in significant denaturation of the immobilised protein. Carboxymethylation of the dextran layer also places a net negative charge on the dextran, which is fully charged above pH 7. This allows positively charged proteins (i.e. below their pI) to become electrostatically attracted to the bound dextran layer effectively 'pre-concentrating' the protein to the chip for subsequent protein immobilisation procedures.

4.1.1.2.Resonant Mirror Based devices:

An example of this type of technology is the commercial IAsys instrument, in which the polarised laser light is also totally reflected of the underside of the IAsys sensor surface. This particular instrument utilises a dielectric layer of high refractive index (e.g. titania) instead of the gold sensing layer in BIACORE (Cush *et al.*, 1993). The high refractive index layer is separated from the glass prism by means of a layer of low refractive index. A schematic of the system is illustrated in Figure 4.3. At certain incident angles there is a phase matching between the incident beam and resonant modes of the high index layer. At the point of resonance, light couples along the high index waveguide layer and propagates along the sensing layer before being coupled back into the prism. During resonance a phase shift occurs between the reflected electric (TE) and magnetic (TM) modes causing a phase shift (of the order of 2π) in the measured response which is observed as constructive interference and can be measured in 'real-time'. The angle at which resonance occurs is dependent upon the refractive index of the sensing layer. The IAsys instrument also utilises a cuvette-based design as opposed to a flow cell configuration, which is continually stirred to reduce mass transport effects and has a much larger surface area than the BIACORE chip.

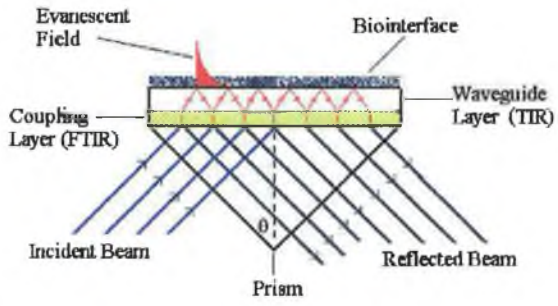

Figure 4.3: *Surface plasmon resonant based mirror device (IAsys). Incident light after passing through a prism undergoes total internal reflection at the boundary with the low refractive index layer and generates an evanescent layer at the sensing layer. The incident angle at which resonance occurs is dependent on the refractive index at the surface of the sensing layer. Binding interactions at the sensing surface causes a shift in the angle of reflected light, which are related to the mass change at the sensor chip surface.*

4.1.1.3.Input-Output Coupling devices:

The BIOS-1 instrument is an example of this type of system and it is comprised of a waveguiding film of high refractive index (e.g. SiO_2/TiO_2) on a glass support with a sub-micron diffraction grating that allows the diffracted light to propagate into the waveguide. Under conditions of TIR the waveguiding film can trap light, and the angle at which this occurs is again dependent on the refractive index of the surface layer in contact with the metal film. Consequently, the angle at which the light is coupled into the detector also changes according to the refractive index change at the sensor chip surface. The BIOS-1 system incorporates a laser whose angle of incidence is continually varied, and the angle at which surface plasmon resonance occurs is measured by an integrated optical scanner containing photodiodes at each end of the waveguide.

4.1.1.4.Miniature TI-SPR device:

Released by Texas Instruments in 1996, this fully integrated miniature SPR sensor contains a light emitting diode (LED), polarizer, thermistor (to allow for correction due to temperature fluctuations) and two 128 silicon photo diode arrays housed in an epoxy resin moulding which was designed in the form of the Kretschmann geometry prism (Figure 4.4(a)). Mirrored surfaces are thermally evaporated onto the internal surfaces of the device except for the SPR sensing portion of the device. The wedge shaped beam reflects off the SPR sensing layer and is reflected onto the PDA array by means of a mirror. The SPR minimum can then be measured in 'real-time' following dedicated signal processing (Kukanskis *et al.*, 1999). The system offers the capability for 'remote-sensing' and is available in a hand-held pipette-style format called the Spreeta™ device. A schematic of the device in illustrated in Figure 4.4(b) with the attached flowcell.

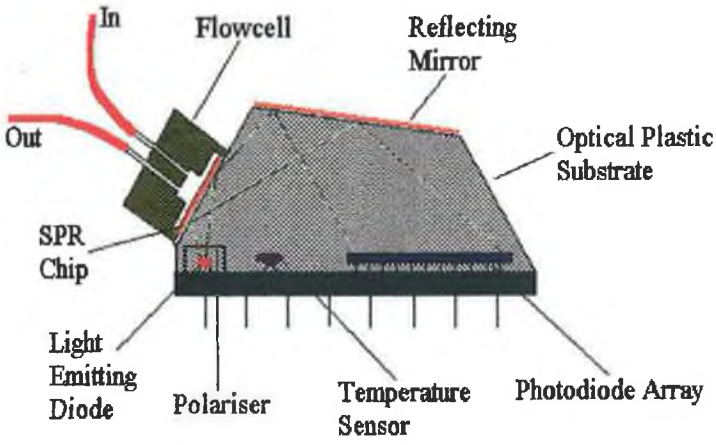

Figure 4.4(a): *Cross-section of miniature TI-SPR instrument. Mass changes are related to changes in the resonant angle and position of the reflectance minima, which can be detected using a dedicated software package in 'real-time'.*

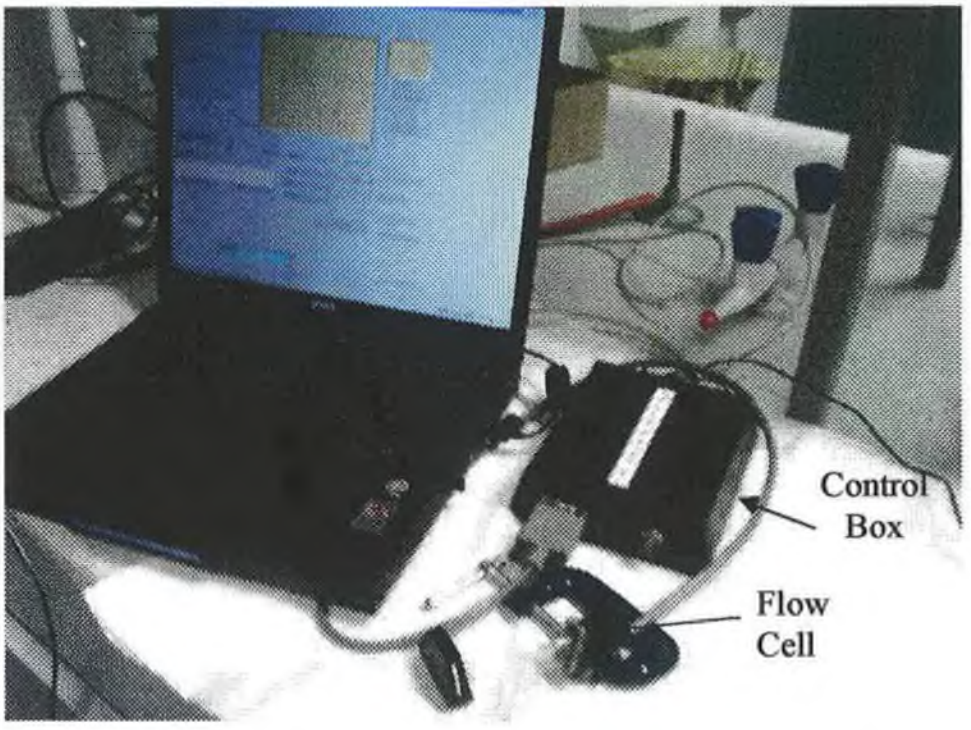

Figure 4.4(b): *Schematic of TI-SPR device fitted with flow cell. The control box interfaces with the device and allows the device to be installed onto a PC which together with dedicated software (SPR-MINI MS-Windows software) to allow control of data acquisition, processing and display as a virtual control panel as seen on the laptop.*

4.1.2. Applications of SPR technology:

Surface plasmon resonance detection allows for the label-free 'real-time' detection of interacting analytes. Labelling procedures can have a marked effect on the specificity and binding activity of antibodies (Høyer-Hansen *et al.*, 2000). The advantages of 'label-free' detection renders the system suitable as a screening device for unmodified ligands, particularly when screening for potential drug candidates and in 'ligand-fishing' experiments with relatively crude complex mixtures of proteins (Lackmann *et al.*, 1996). SPR biosensing systems have also been reported for the detection of blood group antigens in whole blood using immobilised antibodies (Quinn *et al.*, 1997). The potential applications of SPR technology are continually increasing with the development of miniaturised and more portable formats (Kukanskis *et al.*, 1999) making SPR instruments an increasingly more important device in modern biophysical analytical laboratories. Some of the more recent applications of SPR technology are described below:

4.1.2.1. Target Characterisation & Small Molecule Detection:

The use of SPR-based instruments is gaining increasing momentum in the area of biopharmaceutical discovery and the characterisation of biomolecules. Biosensors can be used to generate kinetic information regarding receptor-ligand interactions, and to assess the binding activity of different molecules, which is in turn related to their function. The growing number of potential therapeutic targets emerging from the field of functional genomics allied to economic and scientific advances has increased the need for enhanced drug-screening methodologies capable of high throughput. The lack of labelling, small sample consumption (50-100 µl) and high sample throughput (>500 per day) renders SPR-based biosensors extremely useful in high-throughput screening (HTS) for small molecular weight analytes in lead drug discovery. By providing kinetic binding data unattainable using more traditional equilibrium-based assays, useful information regarding complex information can be generated, allowing for the preferential selection of particular higher affinity 'binders'.

Developments in SPR technology, particularly with the latest BIACORE 3000 instrument with reduced flow cell size and on-line reference curve subtraction has greatly increased the feasibility of direct detection of small molecular weight analytes (Morton & Myszka, 1998). Markgren *et al.* (1998, 2000) utilised direct detection of small molecular weight analytes as a means of screening and ranking a panel of HIV-1 inhibitors. By immobilising HIV-1 proteinase directly onto the sensor chip, the authors were able to identify and rank potential inhibitors based on their association and dissociation rates. Kampranis *et al.* (1999) studied the binding interaction between wild-type and mutant DNA gyrases and a number of anti-

bacterial agents, including coumarin and cyclothialidine drugs. SPR analysis of the drug-protein interactions allowed the identification of the particular residues that were responsible for binding to the DNA gyrase.

4.1.2.2. Pharmacological Applications:

A great deal of time and money is spent in the pharmacological industry identifying new possible drug target molecules. For example, the average costs of developing a small molecule drug has been estimated to be approximately $500 million dollars with a lead-time to market of approximately 12-15 years; biopharmaceuticals costs are somewhat less ($200 million) with a development time of between 5-7 years (Hensley & Myszka, 2000). Following their identification, such targets must then be characterised in terms of their individual absorption, distribution, metabolism and excretion profiles (ADME). Such studies are generally speaking only carried out on a small number of potential drug molecules; the use of SPR biosensors can greatly facilitate such studies of larger numbers of molecules. The binding of a drug to serum proteins such as albumin and α–acid glycoprotein can greatly impact on the pharmacokinetic profile of such compounds, as a high degree of protein binding reduces the free drug concentration in the plasma pool and the desired therapeutic effect. Similarly circulating drug-protein complexes (e.g. warfarin-HSA) also serves to extend the duration of action of the drug following metabolism of the free-drug fraction (Wandell & Wilcox-Thole, 1983). The affinity of individual drug compounds to plasma proteins is therefore an important parameter of the compounds potential therapeutic usefulness, efficacy and potential side effects. Traditional methods for determining drug-protein binding which will be discussed in greater detail later include ultracentrifugation, equilibrium dialysis (Ferrer *et al.*, 1998) and chromatographic methods (Shibukawa *et al.*, 1990). The ability to determine as much as possible with respect to a drugs ADME profile as early as possible in the discovery process is becoming increasingly important with the larger number of potential drug candidates being identified. Frostell-Karlsson *et al.* (2000) investigated the interactions of a panel of 19 drug compounds with immobilised human serum albumin (HSA). The intensity of the binding response determined following injection of the drug compound over the HSA-immobilised surface was used as a means of determining the potential degree of HSA binding. The degree of drug-protein binding measured using biosensor techniques, correlated well with traditional techniques and comparable association constants were obtained.

Two new chips constructs released by BIACORE have made it possible to construct stable membrane surfaces within the flow cell. Evans & MacKensie (1999) have recently reviewed the different methods available for constructing lipid bilayers on chip surfaces. The

generation of such membrane surfaces offers several advantages over the conventional dextran-coated surfaces for studying membrane-bound proteins in that: the proteins are specifically orientated, and also that multivalent interactions can occur as a result of membrane fluidity which more closely resembles the *in vivo* environment.

An understanding of the intestinal absorption profile of new drug candidates is of importance when screening, particularly in being able to differentiate between drugs that demonstrate low, medium or high absorption. As the majority of drugs are administered orally, the fraction of drug absorbed from the intestine is of considerable significance. *In vivo* studies of drug absorption have been difficult to perform and the requirement for suitable *in vitro* models is growing. Several other recent techniques based on liposome-partitioning (Balon *et al.*, 1999) and liposome-chromatography (Liu *et al.*, 1995) has also been described to simulate drug absorption profiles from the intestine. Danelian *et al.* (2000) investigated the direct interaction of a panel of 27 drugs with a liposome-immobilised surface. The interaction between the immobilised liposomes and the various groups was monitored using a direct binding assay by SPR. The simulated absorption data produced correlated with previously reported oral absorption data, and allowed for the classification of the compounds absorbed by the transcellular route into low, medium and high membrane permeability based on the measured responses.

4.1.2.3. Proteomics

Recent interest has focused on more intensive proteomic studies, with technologies capable of screening up to 10, 000 compounds per day. Screening therefore is no longer the problem, instead it is the need to find new targets to fuel the expanding screening processes. Recent attention has thus been focused on identifying new ligand-receptor pairs and the characterisation of protein-protein interactions, making SPR systems the logical candidates for 'orphan' ligand screening procedures (Williams, 2000). 'Ligand-fishing' is the process by which 'orphan receptors' are screened against multitudes of compounds, cells and tissue extracts to identify putative targets. Traditional ligand-fishing techniques have relied on the use of immunoprecipitation, which suffers from a general lack of sensitivity. SPR biosensors can be seen thus to serve two purposes in the area of proteomic analysis: to be able to confirm detection and quantify direct binding of ligand from cell lysates and conditioned media. Secondly, they can also function as micropurification devices capable of recovery of sufficient quantities of analyte for subsequent analysis and characterisation (Williams & Adonna, 2000). Such ligand fishing procedures have been successfully applied and validated in micro-preparative scale by Catimel *et al.* (2000) for the recovery of sufficient quantities of bound ligand for subsequent characterisation using reverse-phase

HPLC and SDS-PAGE analysis. The concentration of bound ligand following elution from SPR instruments is also usually of sufficiently large quantity to allow for detection by mass spectrometry (MS). Sönsken *et al.* (1998) described an elaborate elution procedure for combined BIACORE-Maldi-MS analysis that allows for elution of bound analytes in as little as 4µl of eluant. This tandem format offers the benefits of sensitive affinity-capture, and subsequent fingerprint MS characterisation of the eluted analytes. Mass spectrometry offers several advantages such as specificity, sensitivity and rapidity over the majority of protein identification techniques which rely on proteolytic digestion of separated proteins and subsequent analysis of proteins by PAGE. The quantities of protein recoverable from most SPR biosensors are ideal for mass spectral analysis; whereby sequence information can be obtained at the femto (10^{-15}) and attomolar (10^{-18}) concentration range in seconds. Nelson *et al.* (1997(a)) performed MS analysis of analytes bound directly to the sensor chip surface, and also coupled MS with the use of the SPR probe instrument whose relatively large surface area allows for greater quantities of analytes to be recovered, and also given the exposed nature of the sensor surface collection and elution of analytes is also simplified (Nelson *et al.*, 1997(b)).

4.1.3. SPR Biosensors as a tool in Protein Engineering:

With the recent advances in genetic engineering the need for quick, precise analytical instrumentation capable of selecting antibodies of the desired specificity from the millions of specificities available becomes a prerequisite (Malmborg & Borrebaeck, 1995). SPR biosensors thus represent a unique, simple and rapid approach for analysing recombinant antibodies and phage displayed libraries from the screening and selection procedures right through to determination of kinetic constants and antibody specificity epitope mapping experiments. Given the relatively large number of candidates screened during panning procedures, ELISA is the most common format of analysis. However, as ELISA is an equilibrium process antibodies with high off rates may thus be lost, alternatively BIACORE-based selection procedures allow for the visualisation of the entire binding pattern. Marks *et al.* (1992) demonstrated that it is also possible to directly screen bacterial supernatants without any further purification procedures required. Selection procedures based on elution and re-screening of eluted phage could be used to increase specific phage titres and have demonstrated a 10-57% increase in specific phage titres (Malmborg *et al.*, 1996). The fact that biosensor-based technologies are also capable of measuring active antibody concentrations, which may be lower than the 'nominal' concentration as measured spectrophotometrically, is also of significance when determining association constants which consequently will be lower than the true value. Epitope mapping performed on biosensors offers the possibility of studying the stoichiometry and kinetic analysis of the binding of

several antibodies to the same antigen (Huber *et al.*, 1999), and is of importance when selecting antibodies to particular structural features of the antigen which may be related to its function. Biosensors are also useful as a means of monitoring complex fermentation mixtures and procedures on-line. They have been successfully used for the systematic change of overexpression conditions in *E.coli* bacterial supernatants and periplasm extracts, for the optimal generation conditions of an anti-angiogenesis antibody used for tumour targeting applications (Viti *et al.*, 1999) by monitoring the levels of antibody expression in 'real-time'.

The recent advances in protein engineering has facilitated the development and synthesis of novel enzymes with improved stability and catalytic performance, through the dissection of the role of individual amino-acids in catalysis and the use of site-directed mutant enzymes (Wilkinson *et al.*, 1984). Combinatorial mutagenesis has facilitated the task of producing such new products, and the role of biosensors will play a crucial role in the selection and characterisation of the desired catalytic activities from such libraries. Recent interest on enzyme engineering has focused on improving the catalytic properties and substrate specificities of existing enzymes. Biosensor selection procedures, based on catalysis and the physical selection of phage-enzymes which convert reaction substrate to product, have been successfully applied in a number of instances (Demartis *et al.*, 1999). Antibodies to the reaction product can then be used for the physical selection of phage-enzyme complexes having catalysed the reaction, which can then be selectively eluted and removed.

4.1.4. Drug-Protein Binding:

The degree of drug-protein binding can have a marked influence on the pharmacokinetic or pharmacodynamic profile of a drug, and ultimately the therapeutic efficacy of the administered drug. It is the 'non-protein' bound or essentially free drug fraction of the administered drug in plasma that dictates it's pharmacokinetic profile. The degree of drug-protein binding will thus determine its volume of distribution, plasma half-life and, eventually, the elimination of the drug from the body. Various disease states (e.g. uremia, malignancy), concomitant drug therapy, genetic and age-related factors have all been shown to influence the degree of drug-protein binding. Clinical conditions such as uremia, hypoalbuminemia and hepatic insufficiency have been related with reduced protein binding, whilst increased levels of drug-protein binding have been associated with acute myocardial infarction, renal transplant and malignancy (Wandell & Wilcox-Thole, 1983).

Plasma proteins such as albumin and α-acid glycoprotein bind reversibly to drugs primarily through hydrophobic and hydrophilic interactions, although Van der Waal's and hydrogen

bonding have also been implicated. The binding equilibrium between drugs and proteins can be described by the following expression:

$$[D] + [P] \underset{k_d}{\overset{k_a}{\leftrightarrow}} [DP]$$

$$K_A = [DP] / [D][P]$$

Where [D] = Plasma molar concentration of drug

[P] = Plasma molar concentration of protein

[DP] = Plasma molar concentration of drug-protein complex

K_A = association constant for drug-protein complex.

k_a = association rate constant

k_d = dissociation rate constant

Modification of the structure of albumin as is the case following the binding of aspirin to albumin results in acetylation of the albumin forming acetylalbumin, which can also alter the affinity of the interaction between particular drugs and proteins. The plasma binding of warfarin and it's analogues to human serum albumin (HSA) has been extensively studied (Chignell, 1970; Sellers & Koch-Weser, 1975; Bertucci *et al.*, 1999; Dockal *et al.*, 1999; Forstell-Karlsson, 2000). HSA is composed of three structurally similar globular domains IA, IB, IIA, IIB, IIIA and IIIB and is normally present in plasma at a concentration between 39 and 55mg/ml (Wandell & Wilcox-Thole, 1983). Dockal *et al.* (1999) recently dissected the binding of warfarin to HSA using various recombinant domains of human serum albumin in an attempt to elucidate the essential elements required for the formation of the warfarin binding site on HSA. Affinity constant determinations by fluorescence titration revealed that the warfarin binding site was located primarily on subdomain IIA, with a secondary binding site on domain I, and structural contributions on domain IIB. Bertucci *et al.* (1999) probed the binding of warfarin enantiomers to site I on HSA using a chiral stationary matrix to which HSA was anchored. Displacement studies demonstrated significant differences in the binding of the enantiomers to site I on HSA. Competitive binding displacement studies demonstrated that (S)-warfarin was a direct competitor for (R)-warfarin, confirming that the (S)-enantiomer has a higher affinity for HSA.

Warfarin is primarily bound to plasma albumin and any decrease in plasma albumin levels (e.g. hypoalbuminemia) as a result of reduced synthesis, excessive renal failure or increased catabolism will thus be reflected in an increased free drug concentration. Given the intended pharmacological effect of warfarin (i.e. prolongation of the prothrombin time (PT)) and its

narrow therapeutic window, any change in the equilibrium which results in an increased plasma free drug concentration can thus result in fatal consequences. A vast amount of literature has described potential inhibitory and potentiating factors in the overall metabolism of warfarin because of its narrow clinical window and widespread clinical use. Greater emphasis is now being placed on proper patient education with respect to potential interactions with foodstuffs (Wells *et al.*, 1994), and concomitant drug therapies (Chan, 1995; Harder & Thürmann, 1996). Any decrease in the plasma free drug concentration can result in reduced anti-coagulation and an increased incidence of thrombotic events, or alternatively, an increased free drug concentration can result in an increased likelihood of haemorrhagic complications as a result of increased anti-coagulation.

4.1.4.1 Methods for measuring free drug concentrations:

Many methods have been used to study drug-protein interactions, although many tend to lead to a particular bias with respect to the measured concentration of either free or protein-bound drug (Wandell & Wilcox-Thole, 1983). Equilibrium dialysis was traditionally the method of choice employed to assess the degree of drug-protein binding, and is based on the principle that an unbound drug will equilibrate across a semi-permeable membrane between protein and buffer containing solution by placing the drug-protein solution in buffer solution and allowing the solution to dialyse until equilibrium is attained. At equilibrium, the concentration of drug in the buffer solution is considered representative of the unbound drug fraction in the protein solution. For pharmacokinetic studies such a procedure is obviously limiting with respect to time constraints (i.e. the time taken to reach equilibrium is usually of the order of hours), the sample volumes required and the dilutional effects observed.

Ultrafiltration procedures, for the separation of free drug from the protein-bound portion, offer a relatively simple and rapid procedure that can be performed at physiological temperatures, without the dilutional effects observed with equilibrium dialysis. The procedure simply utilises a fine low molecular weight membrane (1-3kDa) to separate free drug from protein-bound drug following centrifugation. A detailed discussion describing the use of the two techniques with regard to free-drug concentration determinations is described elsewhere (Bowers *et al.*, 1984).

High performance frontal chromatography (HPFA) has also been used to assess the degree of binding of warfarin and other drugs to HSA (Shibukawa *et al.*, 1990). Using this chromatographic technique a sample of the drug-protein mixture at equilibrium is injected onto the HPLC column. The particular type of HPLC column utilised is comprised of a specially designed stationary phase that excludes large macromolecules such as albumin, but

retains smaller molecules such as warfarin on the hydrophobic ligands in the pores (Pinkerton *et al.*, 1989). When a sufficient volume of the drug-protein mixture is injected onto the column, a zone appears at the top of the column where the concentration of drug in the mobile phase reaches steady-state and the drug-protein binding in solution is reproduced in the column. The net result is that the drug is eluted as a trapezoidal peak with a plateau, which corresponds to the free drug concentration in plasma. The appearance of such a plateau is essential in HPFA. Several precautions should be taken when performing HPFA to ensure that the equilibrium of the drug-protein complex is not disrupted by careful selection of mobile phase conditions. The use of ion-pair reagents and buffers of different ionic strength to the equilibrium mixture should also be avoided when possible.

Parikh *et al.* (2000) described a method for the determination of the degree of drug-protein binding between potential drug candidates and serum proteins based on the quenching of the intrinsic tryptophan fluorescence of serum albumin and α-acid glycoprotein as measured by spectrofluorimetry. The dissociation constants measured for the complex compared well with those obtained using more traditional techniques such as equilibrium dialysis. The technique also has the added benefit that it does not involve membrane separations, lengthy dialysis procedures or chromatographic techniques for quantitation.

The use of ultracentrifugation that separates the fractions of plasma into concentration gradients based on their relative size, molecular weight and shape can also be employed to separate free drug from protein-bound drug. However, the technique is not widely used due to the time-consuming and expensive nature of the process. Cross-linked dextran gels that separate on the principle of size exclusion have also been used to separate free drug from protein-bound drug; however, the time-consuming and tedious nature are limiting factors for the routine use of this particular technique.

4.1.5. Analysis of warfarin:

There are currently a wide range of sensitive analytical methods available for the quantitative determination of warfarin and it's metabolites in human and animal biological samples, utilising various modes of detection ranging from chromatography to phosphorescence-based measurements (Table 4.1). The majority of techniques described in the literature require extensive sample pre-treatment (i.e. protein precipitation, liquid-liquid/ solid phase extraction, evaporation and reconstitution) to determine the plasma concentration levels of warfarin.

Early techniques described for the detection of warfarin in plasma were primarily based on thin-layer chromatography (TLC) of radiolabelled ligands followed by scintillation counting. Thin layer chromatography allows for the separation of organic molecules on a solid silica support by the capillary action of an organic solvent along the silica support. Separation of the migrating molecules can thus be achieved by selective change of the polarity of the organic solvent phase. Lewis and Trager (1970) described such a technique for the determination of warfarin and it's metabolites in biological fluids, identification of the resolved compounds was achieved by a combination of atomic spectroscopy and fluorescence analysis.

The development of high-performance liquid chromatography (HPLC) greatly advanced the study of a wide range of drug molecules, allowing for accurate determination of their pharmacokinetic profiles without the use of radiolabelled ligands. Chromatographic separation in HPLC, like TLC is the net result of specific interactions between sample molecules with both the stationary phase and the mobile phase. The variety of solid phase supports currently available (e.g. C2/8/12/18 and cat-/anion exchange columns) allows for greater variability in the types of interactions which is reflected in the degree of separation achieved. HPLC analysis of warfarin is predominantly carried out by reverse-phase HPLC, which employs the use of a suitable polar mobile phase and a non-polar stationary phase, typically employing hydrophobic C18 or C8 carbon chains. A list of many of the published chromatographic techniques and the detection methods employed is shown in Table 4.1.

A number of investigators have employed the use of derivatisation schemes to enhance the detectability of warfarin by ultraviolet and fluorescence detection methods and to allow for resolution of warfarin enantiomers (Banfield & Rowland, 1984). Post-column reaction techniques are carried out following the separation of the components on the analytical column, by mixing the column effluent with the desired derivatising reagent by means of a post-column reaction coil. The majority of post-column reaction techniques have employed the use of a suitable basic solution to utilise the native fluorescence of warfarin at high pH values (Steyn *et al.*, 1986). Recent advances in column chromatography have allowed for the development of various columns incorporating β–cyclodextrin molecules capable of enatiomeric resolution of the warfarin enantiomers (Ring & Bostick, 2000).

The pharmacokinetic profile of warfarin in man has been extensively reviewed (King *et al.*, 1995). Cai *et al.* (1994) studied the pharmacokinetic profile of 12 stroke patients on warfarin therapy by solid phase extraction of warfarin from plasma, and precolumn derivatisation to form diastereoiosmeric esters, followed by post-column reaction with fluorescent detection.

The authors reported the mean plasma concentration of (S)-warfarin to be 0.47±0.17 μg/ml, with that of the (R)-enantiomer to be equal to 0.69±0.18 μg/ml. Studies of the free drug fraction found the average protein-binding of (S)-warfarin to be equal to 99.67±0.33%, studies of the (R)-enantiomer demonstrated a slightly less plasma protein-bound concentration of 99.44±0.33%. For determination of free enantiomer concentrations, enhanced sensitivity was achieved by adjustment of the photomultiplier tube (PMT). The limit of detection for the free drug assay was found to be 8.05 ng/ml for the (S)-isomer and 6.21 ng/ml for the (R)-isomer. The limits of detection routinely attainable by the many published chromatographic publications are often unable to accurately determine the levels of free plasma concentrations of warfarin in patient samples, which in the majority of cases are at least an order of magnitude outside the desired quantification limits. The current trend in anticoagulant therapy is towards lower intensity treatment (Lodwick, 1999). Consequently, there is a need to develop newer more sensitive analytical techniques capable of detecting lower concentrations of warfarin in biological fluids, for the accurate determination of the physiologically free fraction of warfarin in plasma.

'Warfarin-like' anticoagulants have been routinely used as rodenticides, where repeated ingestion of the rodenticide results in death by haemorrhage. The determination of such residues is often important in cases of accidental ingestion by non-target animals. The anticoagulant residues are normally not present in the stomachs of poisoned animals. The liver is usually the most useful material for diagnostic analysis, where the residues are normally present in the livers of the affected animals at concentrations ranging below 1 μg/g (Jones, 1996). Langseth & Nymoen (1991) developed a HPLC method for the determination of brofadicoum, bromadiolone, coumateryl, difenacoum and warfarin in a variety of animal liver tissues. The procedure described involved the initial homogenisation of the liver samples, followed by liquid-liquid extraction and subsequent solid-phase extraction of the residues. The residues were detected using UV (ultraviolet) or fluorescence detection, with reported limits of detection for the rodenticides being 0.005 μg/g, with the exception of warfarin which had a limit of detection 0.08 μg/g. Jones (1996) described a similar method for the detection of the same rodenticides in animal liver tissues using gel-permeation chromatography (GPC) as a clean-up procedure followed by post-column reaction with fluorescent detection. The reported limit of detection for warfarin was 0.010 μg/g and 0.002 μg/g for each of the other rodenticides.

Capitál-Vallvey *et al.* (1999) recently described a phosphorescence-based assay for the detection of warfarin in plasma and water samples using solid-phase room-temperature

transmitted phosphorescence. Phosphorescence spectrometry involves a change in electron spin and consequently phosphorescence lifetimes are usually much longer than fluorescent lifetimes (i.e. of the order 10^{-4}-10 seconds). The technique described involves initially spotting the samples onto Whatman filter paper together with sodium hydroxide and iodide. The filters are then dried and the transmitted phosphorescence measured at 467nm using two quartz plates to reduce the quenching effect of oxygen. Interference produced by human serum was eliminated by the addition of sodium thiosulphate. A linear range of detection of warfarin between 300 and 4,000ng/ml was reported, with a lower limit of detection of 80 ng/ml.

Bush and Trager (1983) described a gas chromatographic-mass spectrometry (GC-MS) for the determination of warfarin and it's metabolites from microsomal incubations. The procedure developed involved two different extraction schemes that allowed for the selective separation of warfarin from its metabolites. Following the extraction procedure the compounds are reconstituted in BSTFA (*N, O*-bis- (Trimethylsilyl)-trifluoracetamide) that silylates the alcohol groups of warfarin alcohols, which serves to stabilise them prior to GC-MS analysis. The cited limit of detection for the GC-MS technique is of the order of 2 ng/ml with a reported lower limit of quantitation of 20 ng/ml.

Gareil *et al.* (1993) developed a capillary electrophoresis (CE) technique for the determination of warfarin enantiomers utilising a β-cyclodextrin column as a chiral selector, with reported lower and upper limits of detection of 200 ng/ml and 20 μg/ml, respectively. Computer-modelling studies by Armstrong *et al.* (1986) have shown that the coumarin moiety of warfarin penetrates into the hydrophobic cyclodextrin cavity with the phenyl substituent remaining outside the larger mouth of the cone.

Hutt *et al.* (1994) reported the development of an amperometric biosensor for warfarin utilising a platinum carbon felt to which the bacterium *Nocardia corallina* was chemically linked utilising carbodiimide chemistry. The electron mediator ferrocene was also coupled to the carbon electrode to improve electron transduction. *Nocardia corallina* was shown to stereospecifically reduce (S)-warfarin to the corresponding (S,S)-warfarin alcohol (see Figure 1.7). The biosensor was capable of detecting warfarin in the linear range 1.5-150 μg/ml.

Cook *et al.* (1979) developed a stereoselective radioimmunoassay (RIA) for the enantiomers of warfarin in rat-dosed subjects. 4'-carboxyethyl analogues of (R)- and (S)-warfarin were produced and analysed by an elaborate reaction scheme that involved the resolution of the d-

10-camphorsulfonate diastereoisomers for the production of optically pure radioligands. The synthesised 4'-carboxyethyl enantiomer analogues were subsequently coupled to bovine serum albumin (BSA) for the production of enantiomeric conjugates. The rabbit sera generated following injection of each enantiomeric conjugate produced enantiomeric antibodies with cross-reactivity to the opposite enantiomer of the order of 0.3-3.0%. The analytical procedure was based on a displacement radioimmunoassay (RIA) incorporating the use of tritium- labelled warfarin.

Table 4.1 Techniques and detection limits for warfarin analysis:

Detection Method	Limits of Detection/ Quantitation (ng/ml)	Reference:
Thin Layer Chromatography (TLC)	(Primarily Qualitative detection limits not reported)	Breckenridge & Orme (1973)
RadioImmunoassay (RIA)	L.O.D pg range	Cook *et al.* (1979)
Phosphorescence	300-4,000 ng/ml	Capitán-Vallvey *et al.* (1999)
Capillary Electrophoresis (CE)	200-20,000 ng/ml	Gareil *et al.* (1993)
HPLC- Total:		
Fluorescence-	L.O. D. ≈ 0.2 ng/ml	Lee *et al.* (1981)
	1-100 ng/ml (free)	Steyn *et al.* (1986)
	500-10,000 ng/ml (total)	Steyn *et al.* (1986)
	6.0-450 ng/ml	King *et al.* (1995)
Ultraviolet-	40-800 ng/ml	Fasco *et al.* (1977)
	100-5,000 ng/ml	De Vries *et al.* (1982)
	100-1000 ng/ml	Chan & Woo (1988)
HPLC-Enantiomeric:	12.5-2500 ng/ml	Naidong & Lee (1993)
Fluorescence-	100-6,000 ng/ml	Banfield & Rowland (1984)
Ultraviolet-	L.O. D. ≈ 20 ng/ml	De Vries & Schmitz-Kummer (1993)
	12.5-2500 ng/ml	Ring & Bostick (2000)
Surface Plasmon Resonance based Immunoassay		Fitzpatrick & O' Kennedy
Monoclonal:	0.5-500 ng/ml	
Polyclonal:	10-2000 ng/ml	
Amperometric biosensor	1,500 ng/ml-150 μg/ml	Hutt *et al.* (1994)
Gas-chromatography Mass Spectrometry (GC-MS)	L.O. D. ≈2 ng/ml	Bush *et al.* (1983)
	L.O. D. ≈10 ng/ml	De Vries *et al.* (1985)
		Kunze *et al.* (1996)

4.1.6. Measures of Analytical Performance:

When developing a new analytical assay procedure, various parameters of analytical significance must be considered, and these parameters for the validation of bioanalytical techniques by chromatographic techniques are particularly well defined and substantially reviewed (Karnes *et al.*, 1991; Braggio *et al.*, 1996; Hubert *et al.*, 1999). Until 1990 there were no real validation criteria outlined for the validation of immunoassays (Shah *et al.*, 1991), despite the increasing use of immunoassay procedures in the clinical setting (Gaines Das, 1999; George *et al.*, 2000). Findlay *et al.* (2000) recently addressed particular issues of bioanalytical validation peculiar to immunoassays, in an attempt to standardise the validation parameters for immunoassay procedures which the authors believed were not adequately described by the existing literature recommendations (Shah *et al.*, 1991). Bruno (1998) addressed the growing need for validation of immunoassays performed on BIACORE instruments, and described the relevant validation parameters according to current ICH guidelines (International Congress of Harmonisation).

Several differences exist between chromatographic and immunoassay assay procedures. Firstly and most importantly, chromatographic techniques rely on the measurement of a specific physicochemical property of the analyte in question whose measured response is usually directly proportional to the concentration of the analyte, and thus best described by a linear calibration model. Immunoassays rely on the antibody-antigen interaction for the specific analyte measurement, and the constructed calibration plot is inherently sigmoidal in shape and best fitted with a four-parameter logistical fit. The working range of immunoassays is as a result slightly limited when compared to chromatographic procedures. Also, depending on the source of the antibody preparation (i.e. polyclonal or monoclonal), there can be significant variation in reagent variability, although the development of monoclonal and recombinant techniques has obviated the majority of these difficulties. Despite these limitations, the use of immunoassays offers several advantages compared to chromatographic techniques when compared on an individual assay and capital cost investment. The sample throughput of immunoassays is significantly better than chromatographic techniques, which can also involve extensive sample pre-treatment and derivatisation steps. Generally speaking the inherent physicochemical properties of a molecule dictates the detection limits attainable chromatographically, and the lack of suitable chromophoric or electrochemically active functional groups can be limiting factors in the detailed analysis of the pharmacokinetics of a particular drug molecule. Given the recent advances in genetic engineering, the possibility of producing antibodies and fragments thereof with enhanced affinities ($K_D \approx 10^{-15}$M) (Boder *et al.*, 2000), has advanced the possibility of determining even lower analyte concentrations in complex matrices without the

need for extensive sample pre-treatment. Similarly, with the use of such antibody libraries and the unique specificity of the antibodies, common biosensor detection formats can be used for the analysis of a wide range of analytes, without the need for developing individual chromatographic assay separation techniques.

Findlay *et al.* (2000) commented that many of the existing recommendations with respect to the measured degrees of assay precision were too stringent given the inherently less sensitive nature of immunoassays compared to chromatographic assays. The authors suggested that the previous minimum acceptable limits of accuracy be increased from the previous published acceptable limits of 15% (20% at the lower limit of quantitation (LLOQ)) to 20% (25% at the LLOQ). Wong *et al.* (1997) recently described the validation of an immunoassay for the simultaneous detection of the concentrations of a humanised mouse antibody in mouse serum, and also for the presence of murine antibodies to the humanised antibody in the mouse serum. The main parameters addressed by the authors for the validation of the biosensor assay included: precision, accuracy, linearity, stability of the immobilised ligand, specificity and sensitivity. The stability of the immobilised ligand is an additional parameter that requires validation in the development of biosensor assays, unlike ELISAs. This must be determined prior to sample analysis through monitoring the binding capacity of the immobilised ligand by a series of consecutive binding-regeneration cycles. Depending on the nature of the immobilised ligand, the binding capacity may be drastically reduced by repeated regeneration exposure to mild acidic and basic pulses and/or the combined use of organic solvents (e.g. particularly for immobilised antibody molecules). Wong *et al.* (1997) suggested the use of independent positive controls to monitor the ligand surface-binding capacity, and to continue with the use of the immobilised surface when the binding capacity for the positive controls remains within 20% of the original measured binding response value.

4.1.6.1. BIACORE as an analytical detection device for the measurement of low molecular weight analytes:

Immunoassays are generally the method of choice for the detection of larger macromolecules and biomarkers. However, with recent developments in biosensor and antibody technology that has allowed for the standardisation of reagents, the use of immunoassays is continually growing for the measurement of smaller molecular weight molecules such as warfarin. Competitive immunoassays are generally the preferred assay format for such analytes, where the detection of analytes is based on competition between free and immobilised forms of the antigen (Figure 4.5). In equilibrium well-based ELISA systems, the measured response (i.e. absorbance) is inversely proportional to the concentration of competing analyte in solution.

The response measured using BIACORE and other SPR-based biosensors is the net result of analyte binding (i.e. mass effects at the chip surface). BIACORE utilises a flow cell as opposed to other SPR-based biosensors that incorporate a well-based system, which allows for the detection of analytes in solution as they pass over the derivatised sensor chip surface. For the detection of small molecular weight analytes, the most commonly employed assay format is the inhibition-based assay whereby an equilibrium drug-antibody mixture is passed over the derivatised chip surface. The measured binding response is thus inversely proportional to the analyte concentration as the greater free analyte in the antibody: drug mixture will 'inhibit' the binding of antibody to the chip surface (Figure 4.5).

The potential use of SPR-based biosensor assays in the food industry was demonstrated by Crooks *et al.* (1998) who developed and validated an assay for the detection of the antibiotics sulfamethazine and sulfadiazine in pig bile samples (n= 2081), which have been shown to be good determinants of the extent of sulfonamide accumulation in the kidney. The biosensor assay results reported the number of false positives for sulfamethazine and sulfadiazine, to be 0.14% and 0.34%, respectively, whilst simultaneous ELISA measurements reported the number of false positives for sulfamethazine and sulfadiazine, to be 1.54% and 1.44%, respectively. The biosensor assay also identified a number of false negatives missed by the ELISA procedure (frequency of false negatives by ELISA for sulfamethazine of 0.14% and for sulfadiazine of 0.24%, respectively).

Deckert & Legay (1999) developed a BIACORE assay for the determination of an immunoreceptor assay for the chimeric human/mouse antibody Simulect directed against interleukin-2 (IL-2). The inter- and intraday coefficients of variation for the assay were 1.6 and 1.7% respectively, with the overall accuracy for the assay was 98.5%±1.0.

The development of a biosensor-based immunoassay for the detection of warfarin in biological matrices is described with an investigation into the stability (i.e. binding capacity) of various immobilised ligands. Monoclonal and polyclonal antibodies were used to develop the inhibition-based SPR immunoassay, and a schematic of the interaction occurring at the sensor surface is shown in Figure 4.5. The ability of the assay to measure free warfarin concentrations in plasma ultrafiltrate was assessed, and the results obtained were correlated with HPLC analysis. Analytical issues regarding the accuracy, precision and robustness of the various immunoassays are also addressed. The developed immunoassay was subsequently used to measure the free-fraction of warfarin in patient plasma ultrafiltrate and used to determine the degree of plasma protein-binding of warfarin by comparison with the total plasma concentration as determined by HPLC techniques.

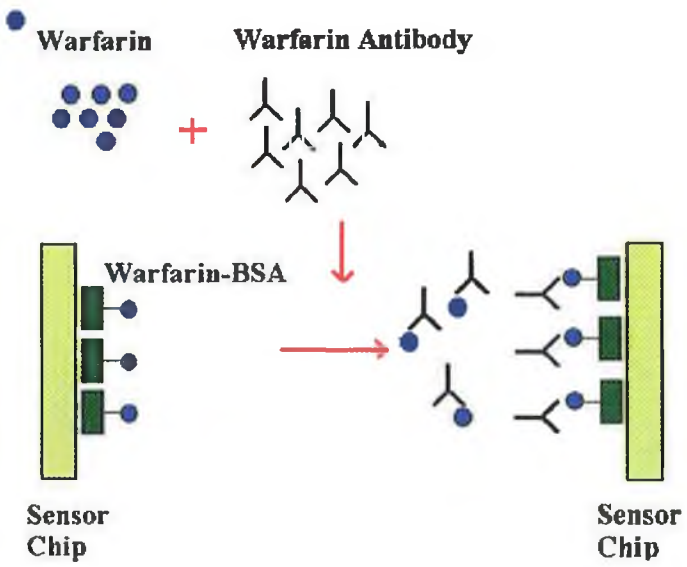

Figure 4.5. *Schematic of the antibody:antigen interaction occurring at the sensor chip surface. Equilibrated mixtures of antibody and antigen are injected over a functionalised sensor chip surface (e.g. 4'-azowarfarin-BSA, 4'-aminowarfarin). The amount of antibody available to bind to the chip surface will be 'inhibited' by the free warfarin concentration in solution (i.e. the greater the free analyte concentration in solution, the less free antibody available for binding to the chip surface).*

4.2 Results & Discussion:

4.2.1. Preconcentration of 4'-aminowarfarin-protein conjugates:

For the successful immobilisation of drug-protein conjugates at the sensor chip surface it is essential to maximise the interaction between the carboxymethylated dextran (CM-dextran) surface and the target drug-protein molecule, in this instance 4'-azowarfarin-BSA. At pH values greater than 7, the CM-dextran surface has a net negative charge, and proteins at pH values below their isoelectric point (pI) (i.e. will have a net positive charge) will be electrostatically attracted to the chip surface. Low ionic strength buffers (e.g. 10 mM acetate buffer) are employed for protein immobilisation procedures as they favour such electrostatic attractions between the dextran layer and the protein of interest. This 'preconcentration' step is an effective way of maximising the potential interaction between the hapten-protein conjugate and the CM-dextran layer for subsequent immobilisation, and increasing the potential yield of immobilised ligand.

A solution of 50 μg/ml 4'-azowarfarin-BSA was prepared in 10 mM acetate buffer and transferred into eppendorf tubes. The pH of each warfarin-BSA solution was adjusted to the desired pH value by the dropwise addition of a 10% (v/v) solution of acetic acid. Each protein was passed sequentially over an underivatised sensor chip surface at 10 μl/min for a period of 3 minutes as described in section 2.12.1. The differing degree of preconcentration can be measured by the response prior to the end of the injection for each protein solution at the various pH values. Following injection, the flow of running buffer over the chip surface is usually sufficient to dissociate the electrostatic attraction between the protein and CM-dextran surface (Figure 4.6). The degree of preconcentration illustrates a significant increase at pH values below 5. From these preconcentration experiments, it was possible to determine that the optimal pH for 4'-azowarfarin-BSA immobilisation procedures, was pH 4.8 in 10 mM acetate buffer.

4.2.2. Immobilisation of Hapten-protein conjugates:

Ligand immobilisation in BIACORE analysis involves the sequence of surface activation, ligand preconcentration/immobilisation and surface deactivation. Activation of the sensor chip surface usually results in the modification of up to 40% of the carboxyl groups in the hydrogel, and reducing the activation contact period is the simplest method for regulating the yield of immobilised ligand. There are a wide variety of immobilisation chemistries available for coupling proteins and drug molecules to the CM-dextran chip, depending on the residues available for coupling. The most commonly employed strategy is the use of EDC (N-ethyl-N'-(dimethylaminopropyl)carbodiimide) and NHS (N-hydroxysuccinimide)

chemistry. Using the water-soluble carbodiimide EDC, surface carboxyl groups can be transformed into active ester functional groups in the presence of NHS. The surface NHS esters then are available to react with suitable amine groups on the protein. The reaction works best between pH 6 and 9, whilst the efficiency of the reaction decreases rapidly below pH 4.5. Hapten-protein conjugates are often characterised by low isoelectric points, which can make adequate levels of surface immobilisation difficult using conventional EDC/NHS chemistry. In many such instances, the pH chosen for immobilisation procedures is often a compromise between the effective preconcentration pH and a pH level at which EDC/NHS chemistry works well (i.e. the pH chosen for immobilisation procedures may not always be the pH at which the most effective preconcentration occurred). Deactivation or 'capping' of unreacted NHS-esters was achieved by treatment with 1 M ethanolamine hydrochloride (pH 8.5), which also served to remove non-covalently bound protein by reducing the electrostatic attraction between the protein and CM-dextran surface.

For immobilisation of 4'-azowarfarin-BSA the procedure was carried out as described in section 2.12.2.1. Immobilisation of the drug 4'-aminowarfarin directly onto the chip surface was carried out as described in section 2.12.2.2., direct immobilisation of drug was performed external to the BIACORE instrument due to the relatively high concentration of DMSO (5-10%) in the coupling buffer. Following surface deactivation, the chip surface was pulsed with two 30 second pulses of 30 mM HCl, which ensured complete removal of non-covalently bound protein. A typical immobilisation strategy for the coupling of 4'-azowarfarin-BSA to the sensor chip surface is demonstrated in Figure 4.7. Routinely, it was possible to attain surface immobilisation of greater than 10,000 response units (RU) of 4'-azowarfarin-BSA. Immobilisation of 4'-aminowarfarin directly to the chip surface resulted in approximately ≈200 RU bound to the chip surface. Given the molecular weight ratio of 4'-aminowarfarin to 4'-azowarfarin-BSA (i.e. 318 Da to 84 kDa), this represents a significantly large increase in epitope concentration at the sensor chip surface, and is reflected in the 20-fold dilution of antibody required with such surfaces compared to conjugate surfaces. Immobilisation of high concentrations of analyte is essential for performing experiments under conditions of mass-transport limitation (MTL) (sections 5.1.11.2 and 5.2.4.2).

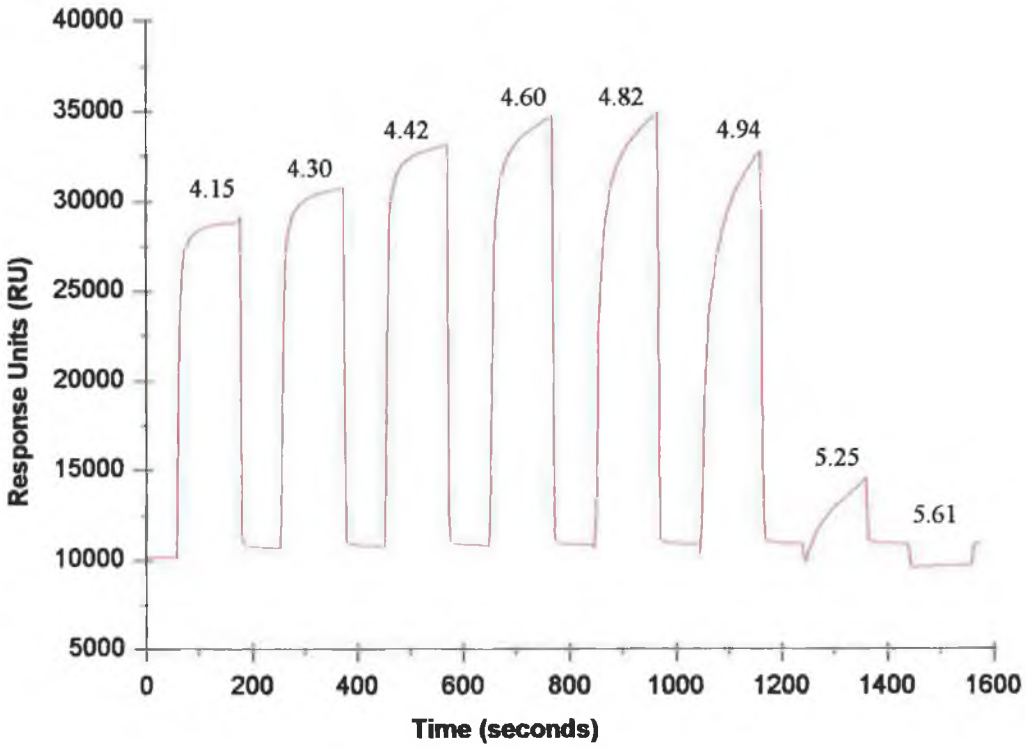

Figure 4.6: *Preconcentration of 4'-azowarfarin-BSA onto a CM-dextran chip surface. Solutions of 50 μg/ml of 4'-azowarfarin-BSA in 10 mM acetate buffer at various pH increments were passed over an unactivated CM-dextran surface at 10 μl/min for a period of 3 minutes. The low ionic strength of the buffer used favours the electrostatic attraction between the negatively charged dextran layer and the positively charged protein (i.e. below isoelectric point). The degree of 'preconcentration' was measured from the response prior to the end of each sample injection. The ionic strength of running buffer (150 mM NaCl) was sufficient to dissociate the electrostatically attracted conjugate from the chip surface. The optimal pH for immobilisation of 4'-azowarfarin-BSA onto a CM-dextran chip surface was calculated to be pH 4.8, and all subsequent immobilisation procedures of 4'-azowarfarin-BSA were thus prepared in 10 mM acetate buffer (pH 4.8).*

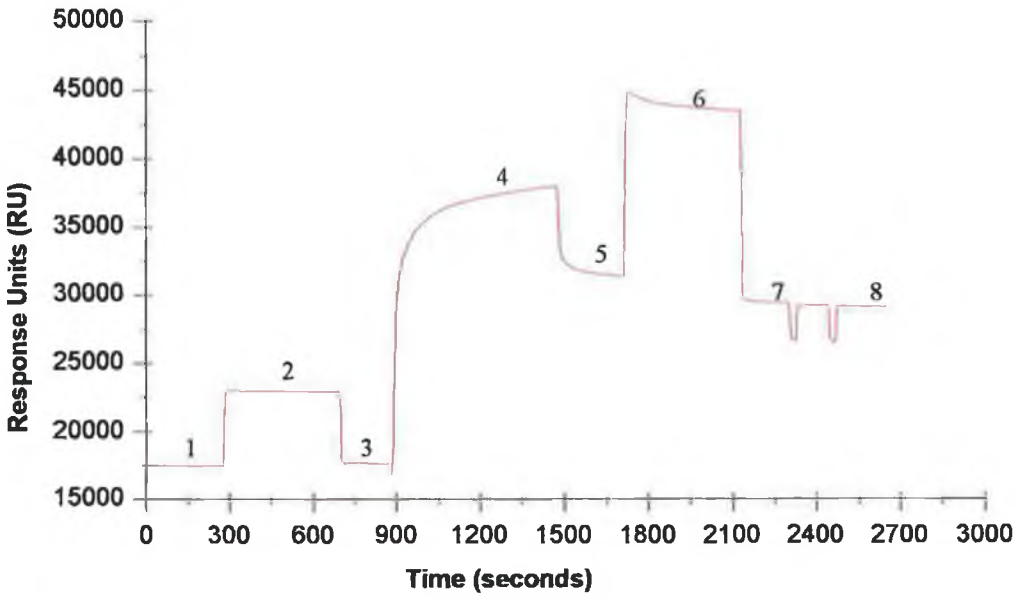

Figure 4.7: *Immobilisation of 4'-azowarfarin-BSA onto a CM-dextran chip surface:*

(1) HBS running buffer is initially passed over the chip surface and a baseline measurement recorded.

(2) Following mixing a solution containing 0.05 M NHS and 0.2 M EDC is passed over the chip surface to activate the chip, the large increase in SPR signal is due primarily to a bulk refractive index change.

(3) A small increase in baseline is recorded following activation of the chip surface (~200RU).

(4) A solution containing 50 μg/ml of 4'-azowarfarin-BSA in 10 mM acetate buffer (pH 4.8) is passed over the chip surface for a period of 10 minutes.

(5) The amount of bound ligand adsorbed is recorded whilst most of the non-covalently bound protein has been eluted.

(6) Deactivation of surface NHS-esters with 1M ethanolamine hydrochloride (pH 8.5), which also serves to elute non-covalently bound conjugate.

(7) Two regeneration pulses with 30 mM HCl serves to remove any remaining non-covalently bound conjugate.

(8) *12,500RU of 4'-azowarfarin-BSA remain bound following the immobilisation procedure.*

4.2.3. Development of an inhibition immunoassay for warfarin:

To establish effective working range concentration parameters for the detection of warfarin and suitable regeneration conditions for dissociation of the antibody-antigen complex following the binding of antibody to the derivatised chip surface, a model assay system was developed in running buffer (Hepes Buffered Saline, HBS). The analytical validation parameters as outlined by Wong *et al.* (1997) were initially used to assess the overall performance characteristics of the immunoassay, these included: accuracy, precision and the stability of the immobilised ligand. The use of directly immobilised 4'-aminowarfarin drug surfaces and 4'-azowarfarin-BSA conjugates were compared to ascertain which provided the optimal ligand binding characteristics and stability. The use of monoclonal and polyclonal antibodies to warfarin was also evaluated to determine which gave the more sensitive and reproducible assay performance.

4.2.3.1. Regeneration conditions:

An important characteristic of a biosensor assay unlike ELISAs that must be determined prior to sample analysis, is the binding capacity of the immobilised ligand. Ideally, it is preferable to be able to perform multiple measurements (>50) on a single derivatised chip surface to allow for routine sample analysis. Wong *et al.* (1997) suggested that the ligand binding capacity be maintained within 20% of positive control values, and be routinely checked throughout the course of the assay to monitor the ligand-binding capacity.

The binding-capacity of both directly immobilised drug surfaces and conjugate immobilised drug surfaces were determined by a series of binding and surface regeneration sequences to assess at which point the binding capacity deviated outside the desired performance range (<20%). Regeneration cycles of both monoclonal and polyclonal antibodies to warfarin were also compared on the two types of immobilised surfaces.

Affinity-purified polyclonal (4'-azowarfarin-BSA-sepharose-4B) and monoclonal (Protein-A/G) antibody samples were serially diluted in HBS running buffer as described in section 2.12.3. Antibody solutions (nominally a 1/100 dilution of each antibody preparation) were then repeatedly injected and the surface regenerated. Two 30 second pulses of 30 mM HCl was sufficient to dissociate the bound monoclonal antibody from the chip surface, whilst the bound polyclonal antibodies could be dissociated using mild acid (15-20 mM HCl) and base (10mM NaOH) pulses. Surface regeneration studies conducted demonstrated that the sensor chip surfaces to which the drug 4'-aminowarfarin was directly coupled were essentially 'in-exhaustible' with respect to antibody-binding capacity, and demonstrated no decrease in antibody-binding capacity over the course of greater than 140 cycles (Figure 4.8). Such

surfaces were in fact used for in excess of 1,000 cycles. The coefficient of variation of antibody binding over the course of 140 cycles was 0.82%. The binding capacity of 4'-azowarfarin-BSA surfaces was also assessed using both the monoclonal and polyclonal antibodies to warfarin. The conjugate surfaces displayed an initially relatively high decrease in binding capacity that began to plateau out after approximately 20 cycles (Figure 4.9). Consequently, studies performed with such conjugate immobilised surfaces were exposed to at least 25 regeneration cycles prior to sample analysis. The regeneration conditions needed to dissociate the polyclonal antibody:antigen complexes were not quite as harsh as those required for surface regeneration using the monoclonal antibodies, and an acid/base was usually sufficient to dissociate the complex. Also interesting to note is the slightly more variable binding response attained with the polyclonal antibodies compared to their monoclonal counterparts (Figure 4.10). The bound polyclonal antibodies showed a small slow dissociation rate from the immobilised surfaces that can be observed from the binding curve after the sample injection end in Figure 4.12. The monoclonal antibodies bound to the 4'-aminowarfarin immobilised chip surface demonstrated essentially no dissociation from the chip surfaces, which can be observed from the overlaid interaction curves at various antigen concentrations (Figure 4.13).

These results imply that the use of directly immobilised drug molecules should be employed whenever target molecules with suitable reactive groups (e.g. the amine moiety on 4'-aminowarfarin) are available for direct coupling to the chip surface. Firstly, such surfaces in this instance provided excellent stability of the immobilised ligand (although, the stability of the immobilised ligand molecule may vary with exposure to various pH extremes), and secondly extremely low coefficients of variation were observed over the course of binding studies (<1%). However, as the results demonstrate the use of drug-protein conjugates is applicable in many instances, provided the regeneration conditions maintain the binding capacity of the immobilised ligands. The use of drug-protein conjugates can be a limiting factor, particularly when trying to dissociate high affinity antibody: antigen interactions (Keating, 1998). The small molecular weight of the target analyte (308 Da) is somewhat restrictive in the type of immunoassay format available for the direct detection of analyte. Extremely high concentrations of IgG would need to be immobilised at the chip surface to attain any reasonable response for the direct detection of warfarin, which in turn would be reflected by a correspondingly large increase in the concentrations of analyte detectable. Direct chemical coupling of antibodies to the chip surface suffers from particular drawbacks; namely the regeneration conditions required too often result in significantly reduced surface binding capacity as a result of antibody denaturation. Secondly, direct immobilisation of antibodies does not afford any specific orientation of the antibody molecules for subsequent

binding to antigen. The most reproducible assay condition for such assay formats has been to employ the use of suitable affinity-capture surfaces, typically those incorporating Protein A/G. Protein A-coated surfaces specifically bind ($K_D \sim 10^{-9}$ M) and orientates the antibody molecules through their Fc regions, and have been shown to be capable of reproducibly being used for greater than 120 binding-regeneration cycles (Quinn *et al.*, 1999). The use of such affinity-capture systems is encouraged when the quantity of antibody utilised is not a limiting factor, and the target analyte is large enough for direct detection formats. Another notable feature of the use of directly immobilised drug surfaces is the substantially reduced quantity (i.e. 10-fold) of antibody required for assay purposes, a direct result of the increased surface epitope concentration, which again can be an important parameter given the high cost of many commercial antibody preparations. The use of guanidine hydrochloride was also routinely employed to dissociate bound antibody from the chip surface, typically at the end of analysis procedures prior to undocking the sensor chip for further analysis. Agents such as guanidine hydrochloride and guanidine thiocyanate are extremely effective regeneration solutions for dissociating high affinity antibody: antigen interactions and have been successfully used with directly immobilised drug surfaces (Nieba *et al.*, 1996).

4.2.3.2. Assessment of Non-Specific Binding:

The degree of non-specific binding of the monoclonal and polyclonal antibodies to both the dextran layer and the immobilised BSA portion of the drug-protein conjugate, was assessed by passing antibody at the requisite dilution (i.e. 1/100 dilution) over a blank CM-dextran and BSA-immobilised sensor chip surfaces as described in section 2.12.4. Figure 4.11 demonstrates the simultaneous injection of a 2 nM injection of monoclonal antibody over an immobilised 4'-aminowarfarin-BSA and BSA surface, respectively. The response following injection over the derivatised BSA surface is essentially negligible (~0.6RU) compared to the response measured over the 4'-azowarfarin-BSA surface (~243RU). Similarly, the binding responses measured when affinity-purified polyclonal antibody (~ 780RU) was passed over both BSA (~0.6RU) and blank dextran (~4.3RU) surfaces was also negligible. The low degree of non-specific binding observed for both the polyclonal and monoclonal antibodies can be attributed primarily to the immunoaffinity purification procedures employed that removed the majority of extraneous proteins (i.e. non-specific protein), resulting in highly purified immunoglobulin fractions (Figures 5.8 and 5.9). Recent advances in instrument hardware particularly with the BIACORE 3000 instrument, which has the capability for 'on-line' reference curve subtraction has overcome many of the difficulties associated with matrix effects and non-specific interactions. The use of 'on-line' reference curve subtraction can be used in situations where complete removal of the non-specific interaction cannot be achieved, or due to drifting baseline measurements, which can

be observed in particular with the affinity-capture assay formats previously described, allowing for visualisation of the specific biomolecular interaction only.

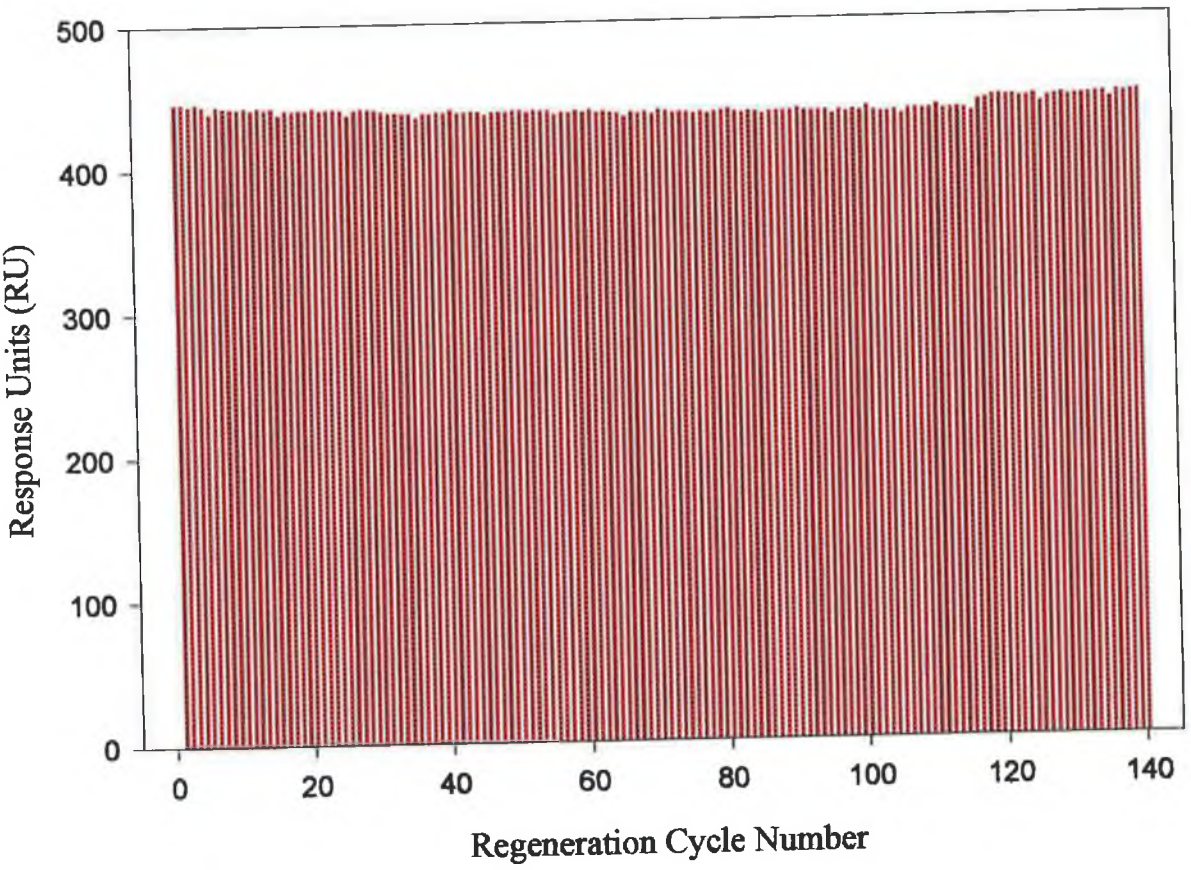

Figure 4.8: *140 consecutive regeneration cycles of a 4-minute binding of monoclonal antibody (3-2-19) to the directly immobilised 4'-aminowarfarin drug surface. The surface was regenerated with two 30-second pulses of 30 mM HCl. The binding response demonstrated a coefficient of variation of 0.82% over the course of 140 cycles and no decrease in the measured binding response over the course of the regeneration study (i.e. cycle 1= 446.2, cycle 140 = 446.4). Directly immobilised drug surfaces were essentially 'inexhaustible' with respect to antibody binding capacity and can be used for greater than 1,000 cycles.*

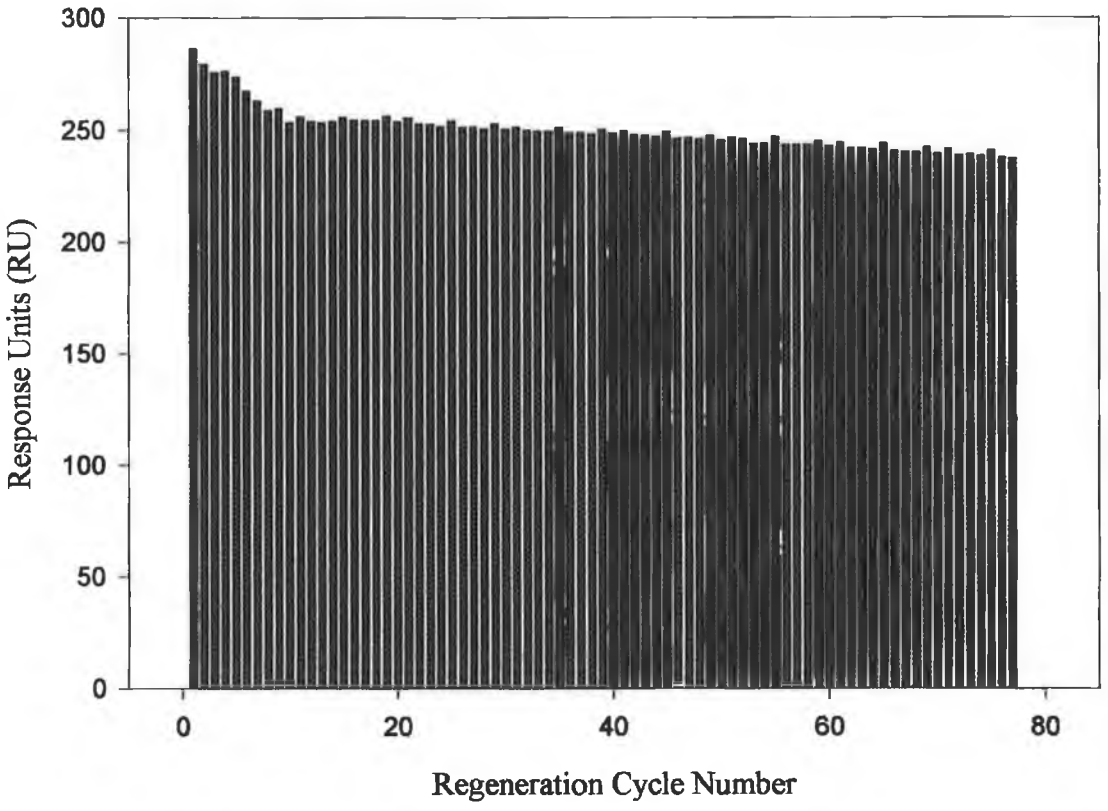

Figure 4.9: *75 consecutive regeneration cycles of a 4-minute binding of monoclonal antibody (3-2-19) to an immobilised 4'-azowarfarin-BSA surface. Surface regeneration was achieved with two 30-second pulses of 30 mM HCl. The binding response demonstrated a coefficient of variation of 3.82% over the course of 75 cycles. It can be observed from the plot that after approximately 20 regeneration cycles, the binding response began to plateau. Consequently, any assays performed using such conjugate surfaces were exposed to at least 20 regeneration cycles prior to sample analysis. After the first 20 regeneration cycles (i.e. from cycles 21-75), the coefficient of variation for the measured binding response decreased to 1.88%, with a decrease in the antibody binding capacity of the immobilised surface by approximately 7.2% over this regeneration cycle range.*

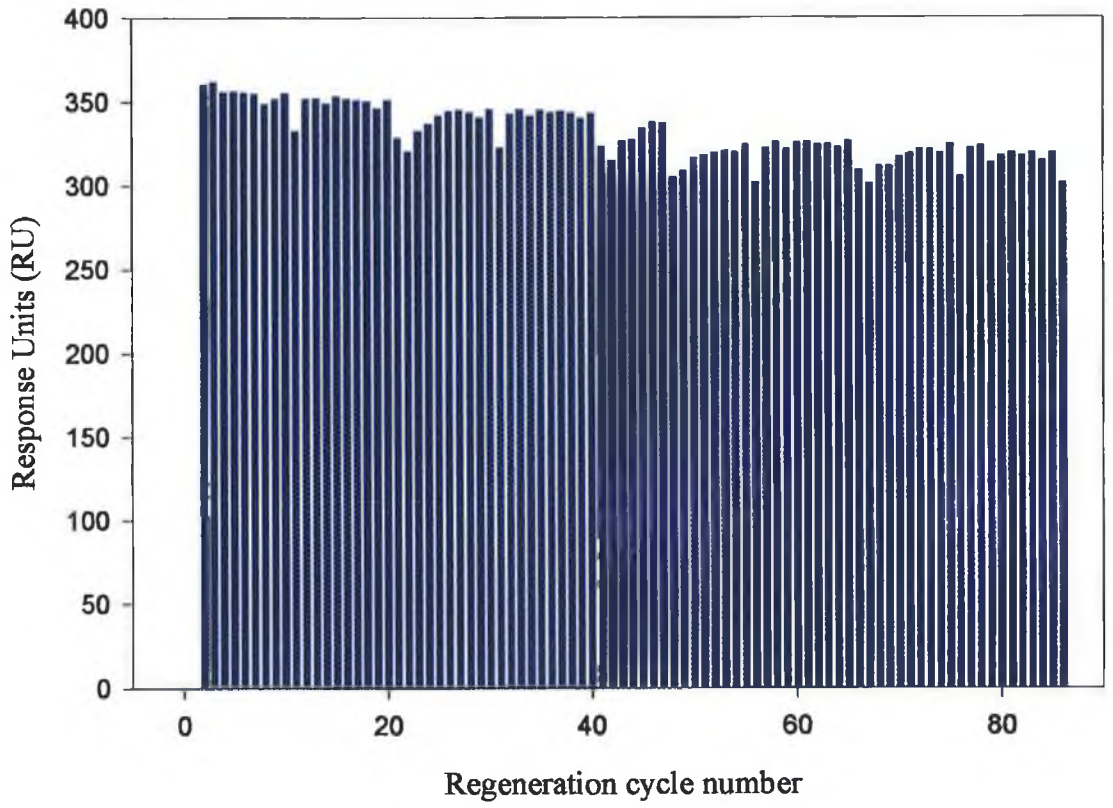

Figure 4.10: *Binding regeneration studies carried out using polyclonal antibodies on 4'-azowarfarin-BSA immobilised CM-dextran surfaces. Mild acid (15-20 mM HCl) and base (10 mM NaOH) pulses were sufficient to dissociate the bound polyclonal antibody from the conjugate surface. The ligand binding capacity was shown to decrease by approximately 16 % over the course of the regeneration cycle (n=86), and demonstrated a % C.V. of 4.8 % over the course of the binding study.*

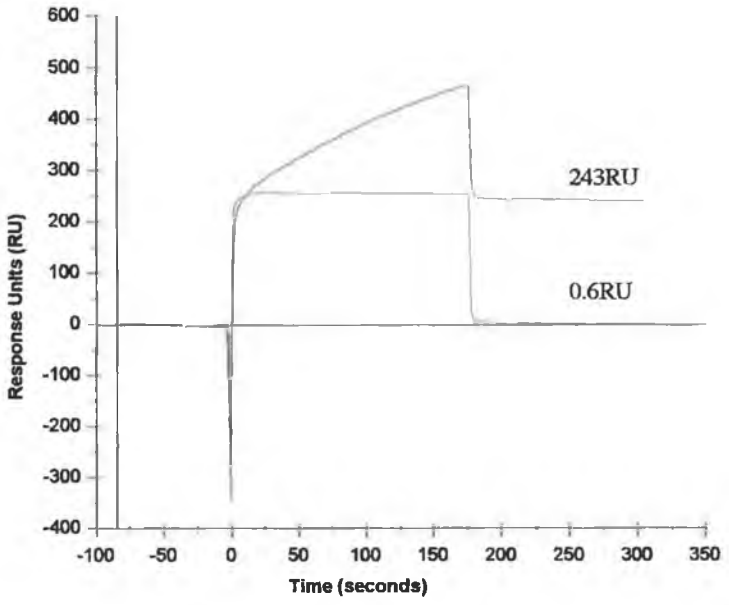

Figure 4.11: *Simultaneous injection of 2 nM monoclonal antibody (3-2-19) sample over immobilised 4'-azowarfarin-BSA (——) and BSA (——) surfaces. The negligible degree of non-specific binding to BSA immobilised surface (0.6RU) compared to the response recorded on the immobilised 4'-azowarfarin-BSA (246RU), can be attributed primarily to the particular immunoaffinity purification procedures employed.*

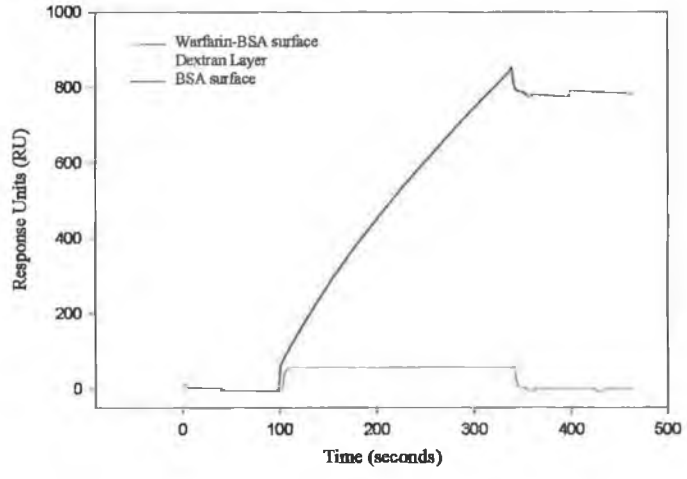

Figure 4.12: *Injection of a 1/100 dilution of affinity-purified (i.e. 4'-azowarfarin-BSA-Sepharose 4B) polyclonal antibodies over an immobilised 4'-azowarfarin-BSA surface at 10 µl/min for 4minutes, resulted in approximately 780RU of bound antibody. The amount of antibody binding which can be observed after the initial bulk refractive index change non-specifically to the dextran layer (4.3RU) or the immobilised BSA surfaces (0.8RU) was negligible.*

4.2.3.3. Determination of Working Range of Model Inhibition Assay Range in PBS:

Having established the binding capacity and the degree of non-specific binding associated with the binding interactions, the working range of the biosensor assay for each antibody type was then evaluated. The validation criteria described by Wong *et al.* (1997) in the development and validation of a biosensor-based immunoassay with regard to sensitivity, ligand-binding capacity, accuracy, and precision were assessed for the detection of warfarin for each antibody type (i.e. mono-/polyclonal) on the different immobilised (i.e. drug/drug-protein) surfaces. Two monoclonal antibodies (i.e. 3-2-19 and 2-5-16) to warfarin were also evaluated in terms of sensitivity. A brief description of the main definitions and terminology used in reference to bioanalytical methods is included in Appendix 1A.

For the determination of the working range of the inhibition immunoassay, dilutions of warfarin were firstly prepared in HBS buffer as described in section 2.12.6. to determine the working range of the biosensor assay for each antibody preparation. Dilutions of warfarin were prepared in HBS buffer ranging from 0.24 to 500 ng/ml for the monoclonal antibody inhibition assays, and from 1.22 to 5,000 ng/ml for the polyclonal antibody inhibition assays. The affinity-purified anti-warfarin antibody preparations were mixed with the corresponding dilution of warfarin using the autosampler, and allowed to equilibrate for a period of 5 minutes. The samples were then passed in random order, over the derivatised chip surface and regenerated using the appropriate predetermined regenerant for each antibody type (i.e. monoclonal/polyclonal). A typical antibody binding response curve is illustrated in Figure 4.13. The response measured following the binding of unliganded antibody from the equilibrated antibody: antigen mixtures could be thus determined. The binding response at each antigen concentration (R_{AG}) was subsequently divided by the antibody binding response determined in the presence of zero antigen concentration (R_0), to give normalised binding responses, which allowed for direct inter-assay comparison. Calibration curves for both the polyclonal and the two monoclonal antibodies were constructed as described in section 2.12.6. Examples of the calibration plots constructed for the various antibody preparations are illustrated in Figures 4.14.- 4.15. The intra- (precision) and inter-assay (reproducibility) variability was determined for each antibody preparation (Table 4.2.- 4.4). In this context, based on the degrees of precision, reproducibility, sensitivity and accuracy recorded, a direct comparison could be made with respect to each immobilisation format and particular antibody preparation. From the inter- and intra-assay studies, it was concluded that the monoclonal antibody preparation 3-2-19 on a directly immobilised 4'-aminowarfarin drug surface performed with the highest degrees of accuracy, reproducibility and precision, and was thus selected for the development of the biosensor assay for the determination of warfarin concentrations in plasma ultrafiltrate samples.

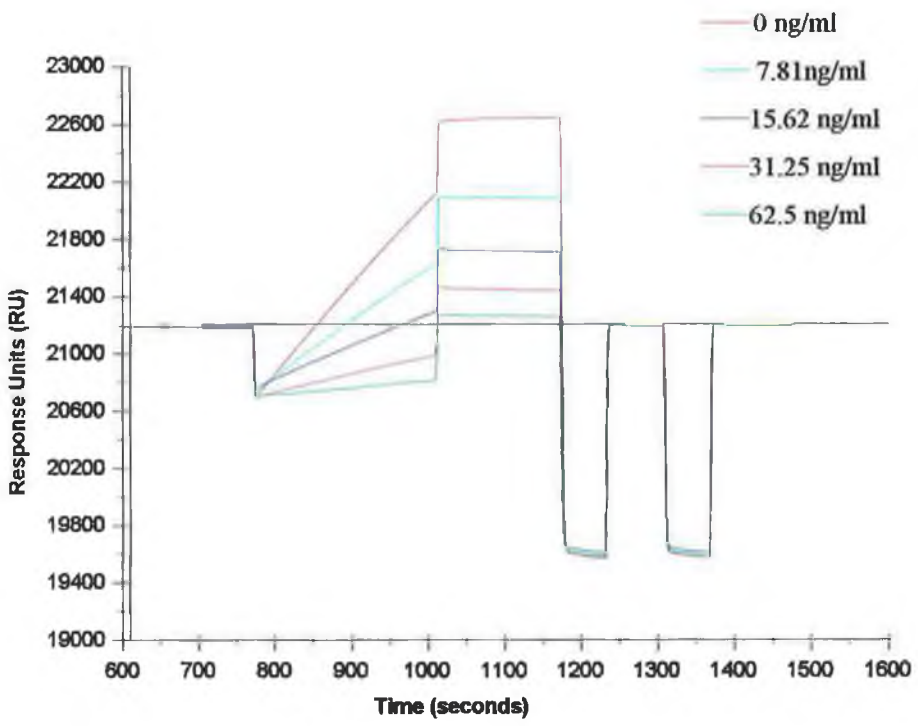

Figure 4.13: *Overlaid interaction curves for various equilibrated antibody: warfarin concentrations in plasma ultrafiltrate. The measured binding response was used to calculate the normalised binding response values, which were subsequently used to construct the calibration curves. The bound antibody showed essentially no dissociation from the sensor chip. The sensor chip could be easily regenerated using two 30 second pulses of 30 mM HCl.*

The intra-assay variation (precision/repeatability) for the SPR-immunoassay was calculated by calculating the coefficient of variation between samples assayed during a single assay run. The inter-assay variation (reproducibility) for each antibody preparation was calculated by performing the assay on three separate days and calculating the precision, or coefficient of variation between batches.

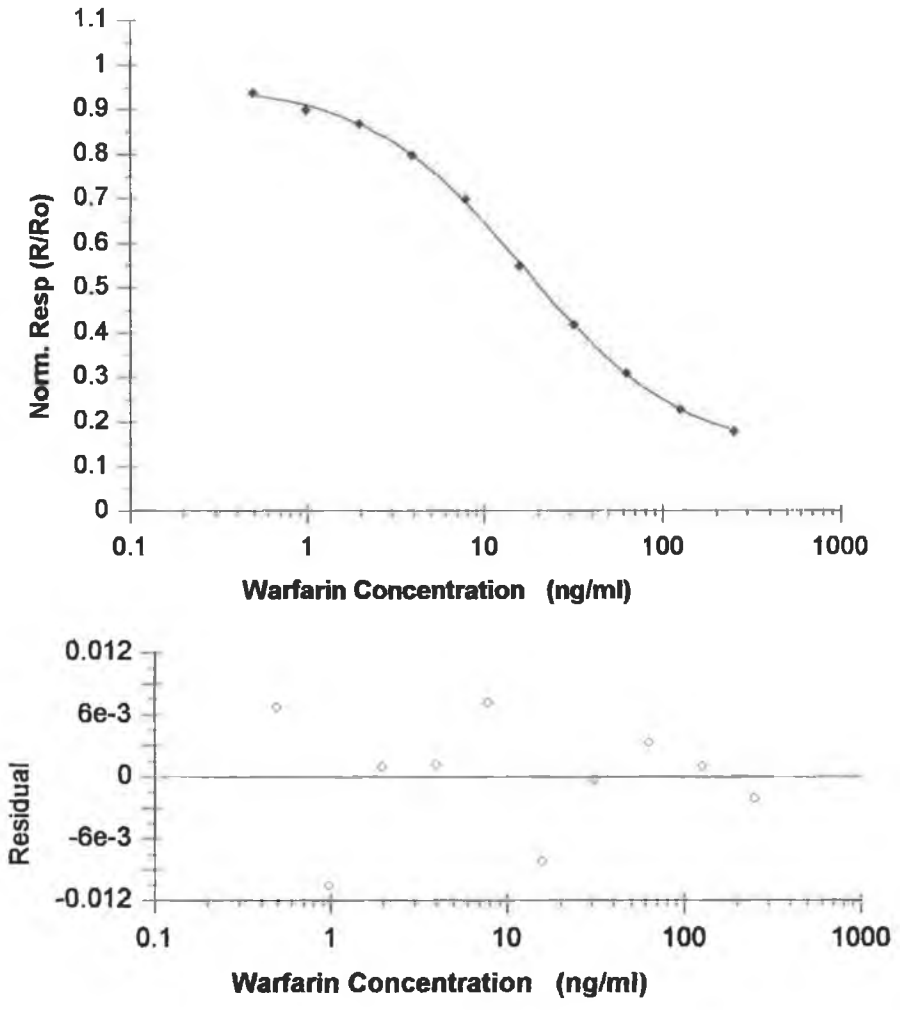

Figure 4.14: *Intra-Assay curve for warfarin in HBS using the monoclonal 2-5-16 on a 4'-aminowarfarin chip surface. The residual plot (precision profile) demonstrates the excellent correlation of the data set to the four-parameter model fit ($\chi^2 = 2.85 \times 10^{-5}$). The heteroscedastic nature of the precision profile illustrates the randomness of the associated error (i.e. no systematic bias). The calibration plot was constructed using BIAevaluation 3.1 software package. The results shown are the average of triplicate results.*

The intra- and inter-assay coefficients of variation are tabulated below for immunoassays studies performed using monoclonal 2-5-16 on a directly immobilised 4'-aminowarfarin chip surface. On the basis of results obtained from binding assays performed using the various antibody preparations on different immobilised surfaces, the antibody preparation and immobilised ligand, were selected for development of an inhibition immunoassay with respect to sensitivity and reproducibility of the antibody preparation and the stability/binding- capacity of the immobilised ligand.

Table 4.2: *Intra-Assay Variation (Precision) for monoclonal antibody 2-5-16 on a directly immobilised 4'-aminowarfarin chip surface (n=3):*

Actual Warfarin Concentration (ng/ml)	***Back-Calculated Warfarin Concentration (ng/ml)***	***% Accuracy***	***% Coefficient of Variation***
500	*501.26*	*0.25*	*3.15*
250	*249.12*	*0.35*	*3.97*
125	*126.13*	*0.90*	*2.32*
62.5	*60.67*	*2.93*	*2.04*
31.25	*32.02*	*2.47*	*1.13*
15.625	*15.95*	*2.05*	*1.14*
7.81	*7.52*	*3.68*	*0.17*
3.91	*3.87*	*0.86*	*0.58*
1.95	*1.84*	*5.85*	*0.43*
0.98	*1.19*	*21.92*	*0.61*
0.49	*0.53*	*7.59*	*1.11*

Table 4.3: *Inter-Assay Variation (Reproducibility) for monoclonal antibody 2-5-16 on a directly immobilised 4'-aminowarfarin chip surface (n=3):*

Actual Warfarin Concentration (ng/ml)	*Back-Calculated Warfarin Concentration (ng/ml)*	*% Accuracy*	*% Coefficient of Variation*
500	*551.364*	*10.27*	*2.91*
250	*261.78*	*4.71*	*3.40*
125	*118.87*	*4.91*	*4.31*
62.5	*60.86*	*2.62*	*9.46*
31.25	*31.65*	*1.28*	*8.46*
15.625	*15.78*	*0.97*	*6.77*
7.81	*7.75*	*0.84*	*5.09*
3.91	*4.06*	*3.94*	*3.65*
1.95	*1.79*	*8.10*	*0.78*
0.98	*0.94*	*4.14*	*0.83*
0.49	*0.48*	*0.02*	*0.44*

Table 4.4: *Intra-Assay Variation (Precision) for affinity-purified polyclonal antibodies on a 4'-azowarfarin-BSA chip surface (n=4):*

Actual Concentration (ng/ml)	*Back-Calculated Concentration (ng/ml)*	*% Accuracy*	*% Coefficient of Variation*
5000	*4824.90*	*3.50*	*6.76*
2500	*2687.46*	*7.50*	*4.82*
1250	*1316.87*	*5.35*	*4.76*
625	*618.66*	*1.01*	*2.47*
312.5	*285.21*	*8.73*	*1.81*
156.25	*141.46*	*9.47*	*0.98*
78.13	*78.75*	*0.80*	*0.89*
39.06	*43.83*	*12.21*	*0.73*
19.53	*22.64*	*15.94*	*0.80*
9.77	*10.15*	*3.93*	*0.39*
4.88	*4.13*	*15.36*	*0.55*

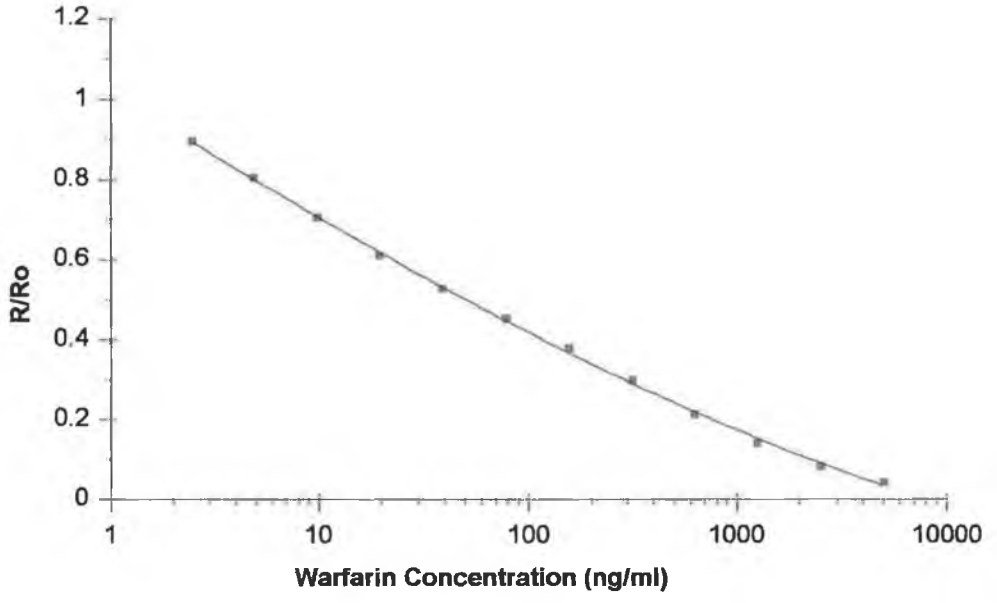

Figure 4.15: *Intra-Assay calibration curve for affinity-purified polyclonal antibodies on a 4'-azowarfarin-BSA chip surface. The results shown are the average of 4 replicates. The calibration curve was plotted using BIAevaluation 3.1 software package.*

4.2.3.4. Assessment of matrix composition on the antibody:antigen binding interaction:

The composition of human plasma is relatively homogeneous, and the approximate contributions of various plasma constituents to plasma osmolality are given in Table 4.5. (Zilva & Pannell, 1979). The major contributor to the ionic strength (> 90%) of human plasma is sodium and it's associated anions, whose ionic concentration is normally in the reference range from 0.133-0.145 M, with relatively lower contributions from other ions in solutions. Certain pathological conditions such as uraemia and hyperglycaemia can disrupt the normal plasma osmolarity.

Table 4.5: *Approximate Contributions of plasma constituents to plasma osmolarity:*

Constituent	Concentration mmol/l
Sodium	133-145
Potassium	3.5
Calcium	2.5
Magnesium	1

*Taken from Zilva & Pannell (1979)

To assess the potential effect of varying salt concentrations on the measured antibody response, a titration of salt concentration versus measured antibody response was constructed as described in section 2.12.9. Briefly, a fixed dilution of antibody (i.e. 1/100) was mixed with varying concentrations of sodium chloride spanning greater than twice the expected physiological ionic reference range for sodium (i.e. 0.120-0.155 M NaCl). A 20 µl sample of the respective salt concentration was allowed to equilibrate with 80 µl of antibody solution prepared in HBS buffer for 5 minutes with mixing on the BIACORE autosampler. The equilibrated samples were subsequently randomly injected in duplicate at a flow rate of 10 µl/min for 4 minutes over a directly immobilised 4'-aminowarfarin drug surface. The bound antibody was eluted and the remaining samples injected. The binding response measured at each salt concentration was measured and the results are illustrated in Figure 4.16. Over the range of concentrations for sodium chloride tested, there was no statistically significant difference in the antibody binding response measured under the experimental salt concentrations investigated as tested by ANOVA (Analysis of Variance) analysis (F-value = 0.506, $F_{crit\ 0.05,\ 7,\ 8} = 3.50$). A plasma dilution step (i.e. 1 part in 5) was employed, as this particular dilution factor was found to be optimal in serving to minimise differences in the measured binding responses, occurring as a result of the altered salt composition. Injection of plasma ultrafiltrate over the immobilised 4'-aminowarfarin drug surface demonstrated no non-specific binding as expected, given the essentially pure nature of the ultrafiltrate fraction.

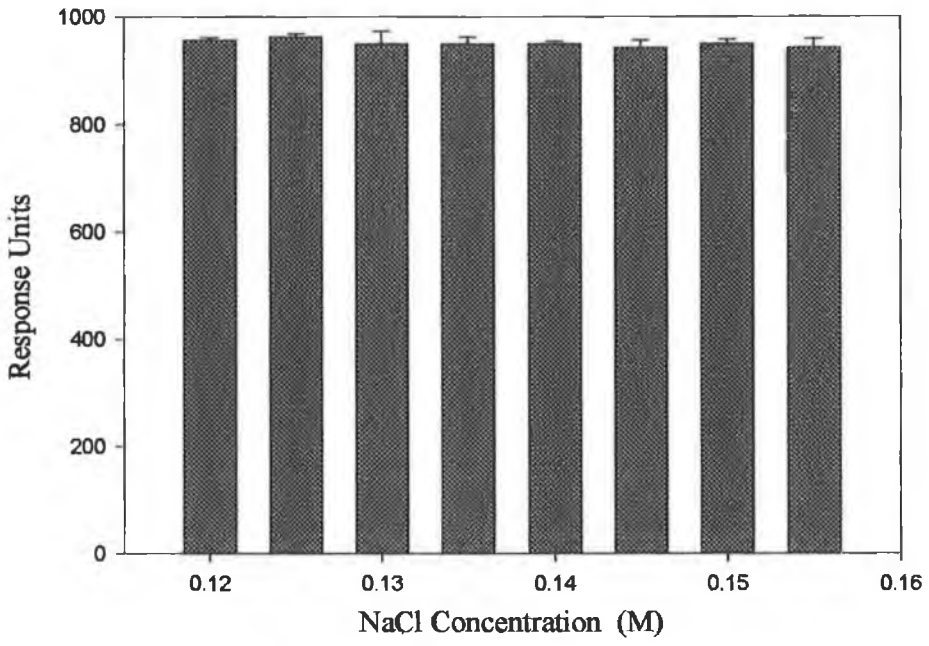

Figure 4.16: *Antibody (80 µl) was mixed with various concentrations of salt solution of known concentration and injected in random fashion over a 4'-aminowarfarin sensor chip surface at 10 µl/min for 4 minutes and the binding response recorded. The antibody binding signal measured over the salt concentration range tested (0.12-0.155 M NaCl), spans the physiological range of plasma salt concentration normally observed (i.e. Reference range 0.133-0.145 M NaCl, (Zilva & Pannell, 1979)). ANOVA analysis performed on the measured binding response, demonstrated that the differences in binding signal recorded are insignificant over the salt concentration range examined, under the described test conditions. Results shown are the average of duplicate measurements ± standard deviation. The coefficient of variation of the measured binding responses over the physiological reference range (0.130-0.145 M) was 0.38%.*

4.2.3.5. Determination of Working Range of Assay in Plasma Ultrafiltrate:

Plasma ultrafiltrate was prepared by ultrafiltration of blank human plasma through an Amicon separation device containing a 1 kDa molecular weight cut-off membrane under positive pressure as described in section 2.13.1. Dilutions of warfarin of known concentration were prepared in the concentration range 0.48-500 ng/ml in the ultrafiltrate of blank plasma. Dilutions of antibody solution (i.e. nominally 1/100) were then mixed with 20 µl of warfarin-spiked plasma ultrafiltrate of known concentration, and allowed to attain equilibrium for five minutes on the BIACORE autosampler. The equilibrium mixtures were then serially passed over the derivatised drug surface in random sequence, to ensure there was no bias in the recorded measurements. The normalised responses were then used to construct a calibration curve of the normalised response versus warfarin concentration (ng/ml) and a four-parameter logistic fit modelled to the data set using BIAevaluation™ 3.1 software. The working range of the bioassay was calculated to be from 0.48-250 ng/ml (Figure 4.17). The intra-assay degrees of precision and accuracy are tabulated in Table 4.6. The coefficients of variation for the assay were typically of the order of 2-3%, except as expected towards the asymptotes of the spline curves where the degree of precision decreased to 13.54% at the lower limit of quantitation. The coefficients of variation for the complete curve including the lower limit of quantitation (LLOQ)(i.e. 0.48 ng/ml) are all well within the current recommended validation guidelines for immunoassay procedures (Findlay *et al.*, 2000).

4.2.3.6. Validation of the Analytical Biosensor Assay for warfarin in Plasma Ultrafiltrate:

For the validation of the immunosensor assay developed for warfarin, the assay was carried out over three separate days at 12 different analyte concentrations spanning the working range of the calibration curve from 0-500 ng/ml, with each analyte concentration value determined in duplicate. The inter-assay degrees of precision and accuracy are tabulated in Table 4.7 (Figure 4.18). Additionally, 8 independent standards of known concentration were also prepared in plasma ultrafiltrate for each calibration curve. From the calibration curves that were constructed for each assay procedure, the concentration of the independent standards could be determined by back-calculation from the constructed spline plot using the BIAevaluation™ 3.1 software. The reproducibility of the assay as measured by the inter-assay variation, demonstrates that the assay is robust and reliably reproducible as observed from the degree of inter-assay variation which is typically of the order of 2-6%. At the asymptotes as noted previously, the coefficient of variation is approximately ~12%.

4.2.3.7. HPLC Analysis of Warfarin plasma ultrafiltrate samples:

HPLC analysis of the warfarin-spiked plasma ultrafiltrate samples and independent standards was carried out as described in section 2.13.4. The samples were analysed by HPLC with a slight modification of the method of King *et al.* (1995), using a mobile phase flow rate of 1 ml/min with ultraviolet detection at 308 nm (the absorption maxima for warfarin in the particular mobile phase). The post-run analysis of the chromatograms was conducted using Varian Star software (version 5.1). The retention time of warfarin on the column under the specified conditions was approximately 5.7 minutes (Figure 4.19). The peak heights of the injected warfarin standards were calculated using the dedicated software package, and a plot of the peak height versus warfarin concentration (ng/ml) constructed (Figure 4.20). Linear calibration models were fitted to the data sets, and from the regression lines it was possible to calculate the concentration of the independent standards from each of the calibration curves. The limit of detection using the current HPLC technique described was 5 ng/ml (section 2.13.4). Several attempts to reduce the limit of detection by the use of post-column reaction were made, by altering the flow rate and the basic post-column reagents used (e.g. triethanolamine and triethylamine). Although there are reports in the literature citing lower limits of detection below 1 ng/ml (Steyn *et al.*, 1986), the lowest limits of warfarin detectable using the post-column detection procedure described (section 2.13.5) were of the order of approximately 5 ng/ml when the photomultiplier tube was at the highest sensitivity setting. These results are in agreement with those reported by other authors employing post-column reaction with fluorescent detection (Cai *et al.*, 1994; King *et al.*, 1995). Consequently, many of the independent standards (i.e. below 5 ng/ml) that were quantifiable by the SPR-based immunoassay were below the limit of detection of the HPLC technique.

4.2.3.8: Comparison of the independent analytical techniques:

To assess whether or not there was any statistical difference between the two analytical techniques, ANOVA analysis of the back-calculated concentration of the independent standards (n=8) run in conjunction with each assay (n=3) procedure was performed. The back-calculated concentrations using the two analytical techniques are tabulated in table 4.8, and the % accuracy determined for each sample using the appropriate calibration plot. ANOVA analysis demonstrated that over the concentration range assayed, that there was no significant difference between the values determined using the two different analytical techniques. An X-Y correlation plot of the back-calculated values for each analytical technique demonstrated excellent correlation (R^2= 0.990).

The use of ultrafiltration has been reported by a number of authors for the determination of the free-drug fraction of various drugs (Menguy *et al.*, 1998; Jortani *et al.*, 1999) and is

gaining increasing use primarily because of it's simplicity of use and the speed of sample preparation (~20 minutes). The BIACORE inhibition immunoassay developed illustrates the potential of utilising SPR as a comparable analytical technique to HPLC for the quantitation low-molecular weight analytes. The results presented demonstrate the sensitivity attainable with the presented immunoassay format (<0.5 ng/ml), which has limits of detection at least an order of magnitude lower and in many cases two, lower than those reported for the detection of warfarin using HPLC with UV detection (Table 4.1, L.O.D. 5-50 ng/ml). The majority of fluorescence-based techniques utilise elaborate derivatisation and post-column schemes to exploit the native fluorescence of warfarin at basic pH values (Steyn *et al.*, 1986; Cai *et al.*, 1994), and the reported limits of detection of such techniques are comparable to the biosensor assay developed.

The biosensor assay developed for the analysis of warfarin is by no means exclusive, but instead should be considered as the development of a generic sensing platform for the development of low molecular weight analytes (unlike the majority of chromatographic assays which must be tailored to suit individual molecules). The validated assay format can be suitably modified for the detection of indeed any particular molecule by simply altering the immobilised ligand and the particular antibody. With the variety of coupling chemistries and chip surfaces available, almost any particular ligand can now be conveniently immobilised. The surface regeneration conditions can also be routinely modified depending on the chemical stability of the immobilised ligand. For example, for molecules that are labile or unstable at high/low pH values, the use of organic solvents could be employed or alternatively, the use of agents such as guanidine hydrochloride could also be used to remove the immobilised high affinity antibodies from the chip surface.

The current assay format described was developed for the detection of warfarin in biological samples, namely plasma ultrafiltrate. Warfarin as a drug of therapeutic utility can be considered somewhat unique in terms of it's pharmacokinetic profile, given that it is almost exclusively plasma protein-bound, and the fact that it is extremely potent physiologically despite its extremely low free drug concentration in the plasma pool. The intensity of warfarin treatment (1-2 mg/daily) is also considerably less than that administered for the majority of drug therapies, which are usually administered at considerably higher dosage levels (e.g. 10-250 mg). It is evident, therefore, that the assay developed for a drug with such a low circulatory plasma concentration, could easily be extrapolated as a tool for the analysis of the pharmacokinetic profile of particular drug candidates for which current methodologies are inadequate (e.g. many of the penicillin compounds: ampicillin/amoxicillin). Indeed, allied with the use of ultrafiltration for drugs that are not

plasma protein-bound, patient plasma samples could be routinely analysed in the order of 10-15 minutes, which is considerably less than many of the existing chromatographic techniques that require in many cases extensive sample pre-treatment.

The concentration of warfarin determined in the plasma ultrafiltrate samples using the inhibition immunoassay was comparable to the concentrations obtained by existing HPLC methodologies. The lower limit of detection (i.e. an order of magnitude lower than that of the HPLC technique) of the immunoassay format made direct comparisons between standards at the lower end of the calibration range impossible. As Table 4.8 illustrates excellent correlation (R^2= 0.990) was achieved between the independent assay results over the concentration range sampled. Similarly, the accuracy of the independent measurements which was assessed by direct comparison with constructed calibration curves for each assay technique revealed that the accuracy of the inhibition immunoassay was in all cases comparable and many instances better than that recorded for the HPLC assay procedure.

Table 4.6: *Intra-Assay variation for warfarin in plasma ultrafiltrate (n=2):*

Actual Concentration (ng/ml)	*Back-Calculated Concentration (ng/ml)*	*% Accuracy*	*% Coefficient of Variation*
250	*208.46*	*16.61*	*2.20*
125	*127.23*	*1.78*	*0.27*
62.5	*66.47*	*6.35*	*4.40*
31.25	*32.01*	*2.43*	*0.87*
15.625	*15.86*	*1.50*	*1.31*
7.81	*7.13*	*8.71*	*1.41*
3.91	*4.50*	*15.08*	*2.77*
1.95	*2.21*	*13.33*	*10.18*
0.49	*0.40*	*17.45*	*13.54*

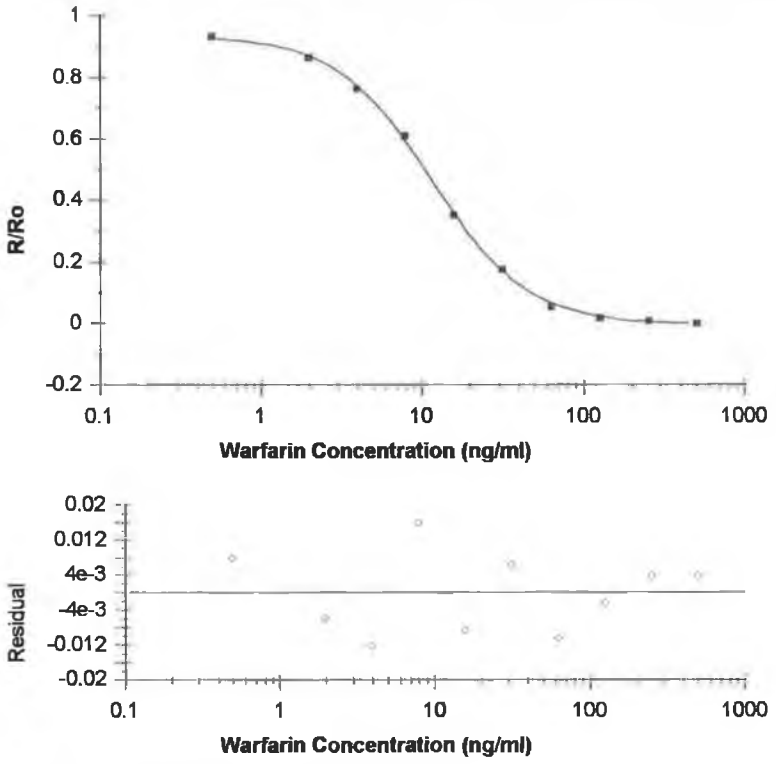

Figure 4.17. *Calibration plot of normalised response versus plasma warfarin ultrafiltrate concentration constructed using BIAevaluation™ software. The use of BIAevaluation™ software allowed for the determination of the concentration of warfarin in the independent standards run in conjunction with the calibration curve from the determined normalised response values. Results shown are the average of duplicate results. The low Chi² value (χ^2) obtained ($\chi^2 = 3.14x10^{-7}$) illustrates the 'goodness of the fit' using the logistic four parameter equation fit.*

Table 4.7: *Inter-Assay variation for warfarin in plasma ultrafiltrate (n=3):*

Actual Concentration (ng/ml)	*Back-Calculated Concentration (ng/ml)*	*% Accuracy*	*% Coefficient of Variation*
125	*129.89*	*3.91*	*2.17*
62.5	*69.64*	*11.42*	*4.54*
31.25	*31.09*	*0.50*	*2.77*
15.625	*15.68*	*0.35*	*2.96*
7.81	*7.50*	*3.94*	*5.61*
3.91	*4.20*	*7.41*	*6.76*
1.95	*2.10*	*7.53*	*4.98*
0.98	*0.90*	*7.53*	*12.38*

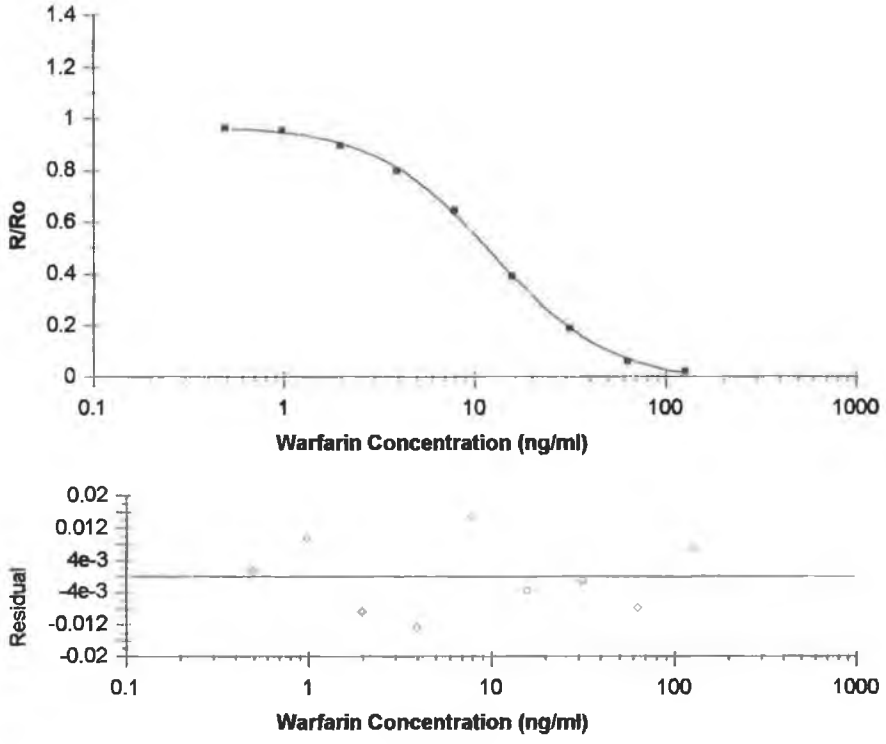

Figure 4.18: *Inter-assay (Reproducibility) variation for warfarin in plasma ultrafiltrate (n=3). The mean normalised response value at each antigen concentration from three independent assays was used to calculate the calibration curve and to determine the intra-assay variation. Results shown are the mean of triplicate results.*

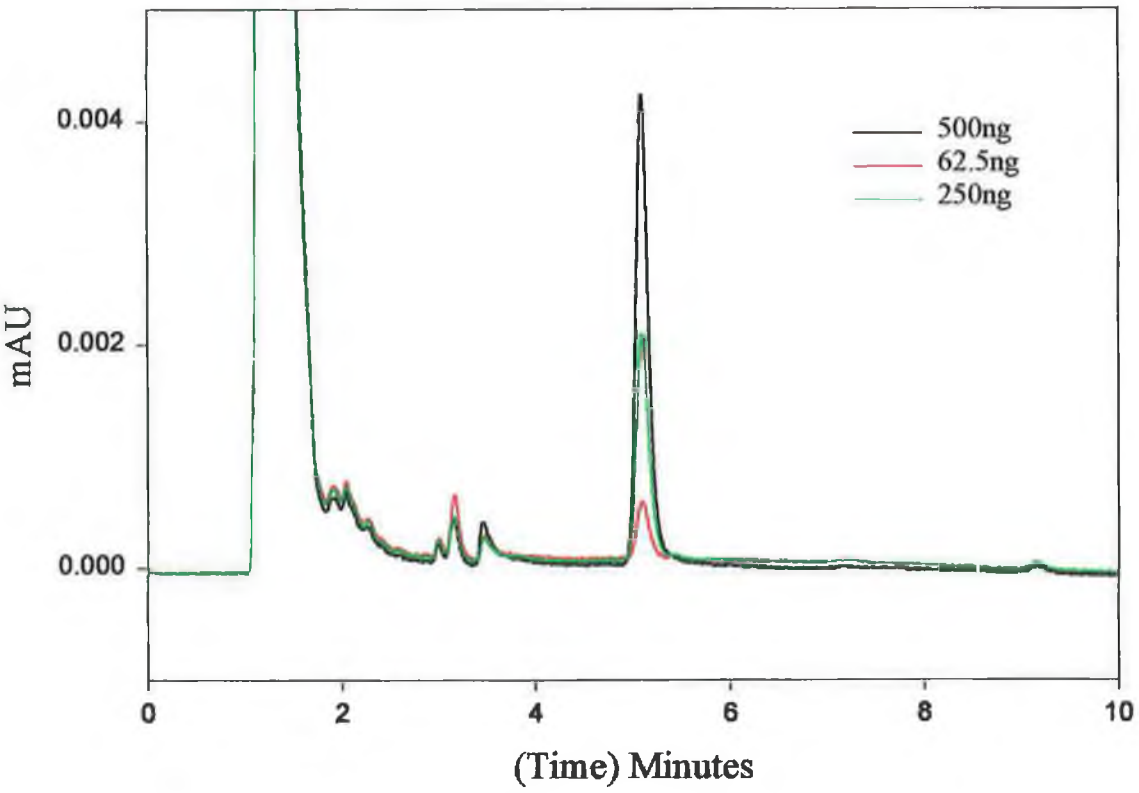

Figure 4.19: *Plot overlay of three different warfarin concentrations in plasma ultrafiltrate separated using a C-18 HPLC column with a mobile phase flow rate of 1.0 ml/min and UV detection at 308 nm. The peak area counts for each chromatogram were calculated using Varian Star 5.1 software (version 5.1) and used to construct a calibration plot of peak area versus warfarin concentration in plasma ultrafiltrate (Figure 4.20) as described in section 2.13.4.*

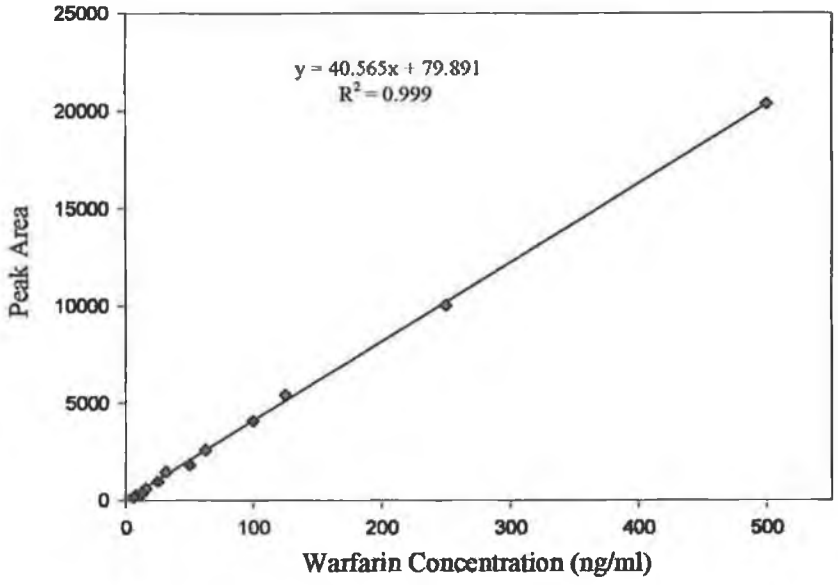

Figure 4.20: *Standard curve for warfarin (♦) (0-500 ng/ml) in plasma ultrafiltrate as determined by HPLC. The peak area determined at each warfarin concentration was plotted against the respective warfarin concentration (ng/ml). From the linear calibration plot constructed, the concentration of warfarin (ng/ml) in the independently prepared set of standards (♦) was back-calculated using the equation for the regression fit line.*

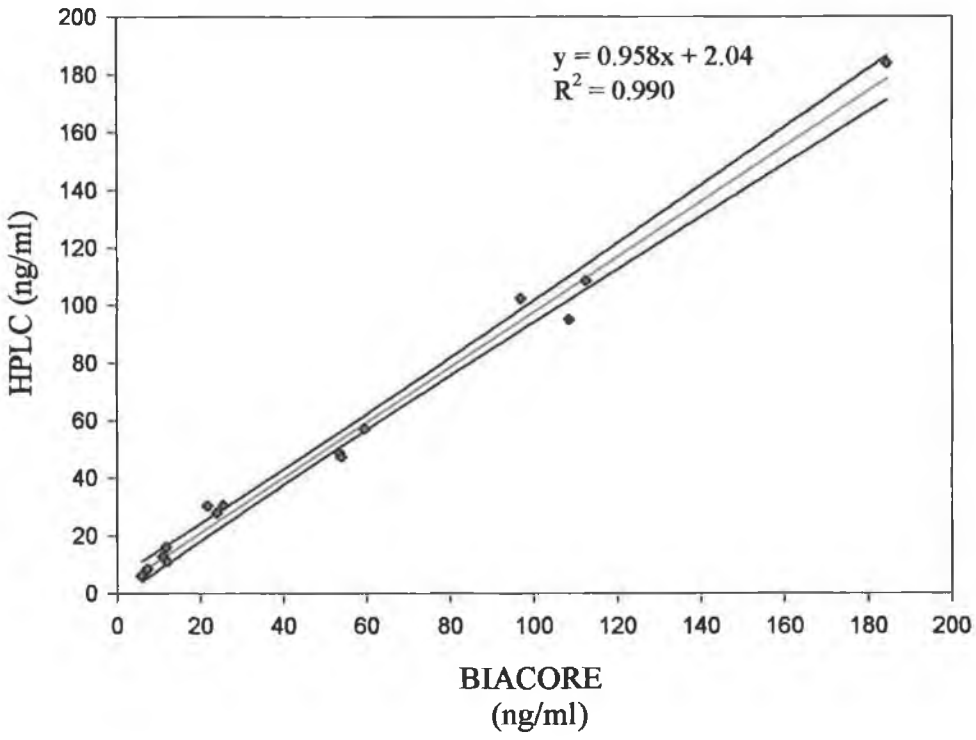

Figure 4.21: *The back-calculated warfarin concentration (ng/ml) for an independent set of standards were determined from the calibration curves constructed on the day the samples were analysed by the two independent analytical techniques (HPLC and BIACORE). The back-calculated concentration values were then plotted against each other and a correlation coefficient of R^2 =0.990 was determined between the two data sets. ANOVA analysis of the data sets demonstrated no significant difference between the two analytical techniques for the determination of warfarin in plasma ultrafiltrate samples.*

4.2.3.9. Determination of the degree of plasma protein binding:

The degree of protein binding of warfarin has been described by a number of techniques as described previously (Cai *et al.*, 1994; Ferrer *et al.*, 1998). The degree of plasma protein binding of warfarin was assessed in patient samples (n=20), by calculating the free drug concentration of warfarin human plasma and comparing this value with the total concentration of warfarin in human plasma measured by HPLC with UV-detection.

4.2.3.9.1. Determination of the total plasma concentration of warfarin samples:

Extraction of warfarin from plasma samples was carried out as described in section 2.13.2. Determination of the total plasma concentration of warfarin in human plasma was carried out as described in section 2.13.4. using a modification of the method of King *et al.* (1995). Briefly, 50 µl of internal standard *p*-chlorowarfarin was added to 1.0 ml of human plasma. 1.0 ml of 1 M sulphuric acid was then added to the plasma samples, which precipitated the protein fraction, releasing the drug from the bound drug-protein complex. The samples were then placed with constant rotation on a carousel for 30 minutes. 5 ml of ethyl acetate was then added to each plasma sample, and the patient samples were placed on the rotary carousel at 30 r.p.m. for a further 60 minutes. 4.5 ml of the organic layer was then removed to a clean test-tube and evaporated to dryness under nitrogen. The patient plasma samples were reconstituted in mobile phase prior to sample injection onto the HPLC column. Quantitation of the plasma warfarin concentration of the patient samples was made by reference to a calibration curve of peak height ratio (*p*-chloro-warfarin: Internal standard) versus warfarin concentration. The total plasma concentrations demonstrated considerable variance in the patient plasma pool analysed, and the mean patient plasma concentration was determined to be 1,015±383.59 ng/ml. Two of the patient samples analysed for plasma warfarin concentrations (patient identification: 11328, 11387) demonstrated a plasma warfarin concentration of zero in the samples analysed and it was suggested that this might have been due to poor patient compliance. Unfortunately, no patient records were available with respect to the dosing regimen of each patient and this could explain for the wide inter-patient variability in the plasma concentrations recorded (Table 4.9).

The HPLC method described was also routinely used in the analysis of patient plasma samples following suspected ingestion of warfarin and particular suspected cases of Munchausen's syndrome. HPLC analysis of such samples was performed to confirm the presence of such residues in the patient plasma and so to rule out other possible haematological complications. An example of such a typical patient chromatogram is illustrated in Figure 4.23. The peak height ratio of warfarin to internal standard was used to

construct the linear calibration curve (Figure 4.22) from which the total plasma warfarin concentrations were calculated.

4.2.3.9.2. Determination of the free warfarin concentration in the plasma ultrafiltrate of warfarin patient samples:

Patient plasma samples (500 µl) were placed in Nanosep™ devices and centrifuged at 6,500 r.p.m. for 30 minutes using an ultracentrifuge device. The plasma ultrafiltrate was then analysed by BIACORE immunoassay as described in section 2.12.6. The patient plasma ultrafiltrate was also analysed by HPLC as described in section 2.13.4. The concentration of warfarin in the patient plasma ultrafiltrate samples was calculated from constructed calibration plots. The degree of patient plasma protein binding was calculated by comparing the concentration of warfarin in the plasma ultrafiltrate samples to the total plasma concentration. The mean free drug concentration of warfarin was calculated to be 99.72±0.24%. This value is in accordance with that described by Cai *et al.* (1994) who found the mean plasma concentrations of (R)- and (S)-warfarin to be 99.4±0.33% and 99.67±0.33%, respectively. The samples analysed by immunoassay were also analysed by the HPLC technique described in section 2.13.4. However, the concentrations of warfarin in the plasma ultrafiltrate were below the limit of quantitation for the existing method. The percentage degree of protein-binding for warfarin in patient plasma calculated (99.72±0.24%) is in agreement with that previously reported elsewhere employing the use of radiolabelled ligands (99.03±0.20%) (Mungall *et al.*, 1984). However, Mungall *et al.* (1984) described several discrepancies between the results obtained using both ultrafiltration and equilibrium dialysis and found that the observed discrepancies were due to radiochemical impurities in the radiolabelled ligand. The inhibition immunoassay system described employing the use of ultrafiltration offers a simple, accurate and rapid means of assaying free warfarin concentrations in plasma ultrafiltrate.

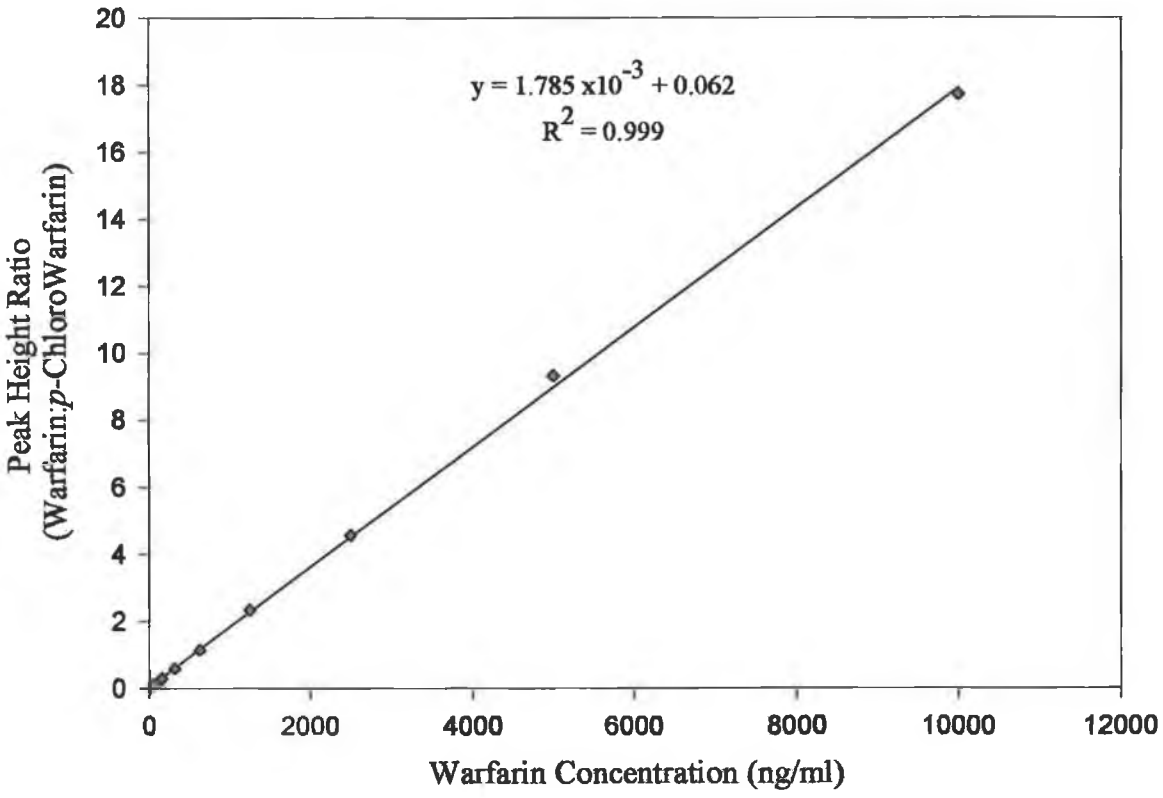

***Figure 4.22**: Standard curve of warfarin concentration versus peak-height ratio of warfarin: p-chlorowarfarin as determined by HPLC. The constructed standard curve was used to calculate the concentration of warfarin in patient samples. The plasma concentrations of the patient samples are demonstrated in Table 4.9. The free fraction of warfarin as determined by BIACORE immunoassay was then used to calculate the degree of plasma-protein binding in the patient samples assayed.*

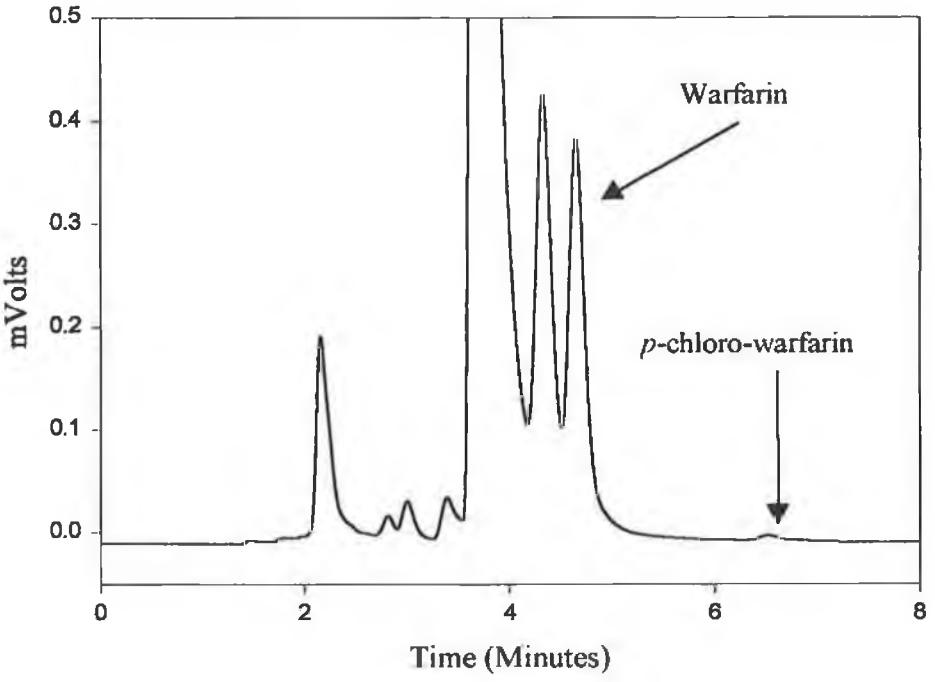

Figure 4.23: *Patient plasma chromatograms of 'suspected' warfarin ingestion. The patient was admitted with extensive bleeding episodes and a prothrombin time of greater than 100 seconds (normal reference range 12-16 seconds). 'Suspected' warfarin ingestion was confirmed by HPLC analysis, the patient was administered vitamin K intra-venously and subsequently discharged. The actual plasma concentration of warfarin determined in the above sample by reference to a calibration curve of peak height ratio (warfarin:internal standard (p-chloro-warfarin) versus warfarin concentration (ng/ml) was calculated to be approximately 38.5 μg/ml, almost 30 times the average patient plasma concentration.*

Table 4.8 *Concentration of back-calculated standards determined using HPLC and BIACORE immunoassay:*

Actual Concentration (ng/ml)	*BIACORE back-calculated concentration (ng/ml)*	*% Accuracy of BIACORE Immunoassay*	*HPLC assay back-calculated concentration (ng/ml)*	*% Accuracy of HPLC assay*
187.5	*184.47*	*1.61*	*183.93*	*1.90*
112.5	*112.46*	*0.03*	*108.55*	*3.51*
100	*96.99*	*3.00*	*102.35*	*2.35*
93.75	*108.42*	*15.65*	*95.12*	*1.46*
56.25	*59.42*	*5.63*	*57.10*	*1.51*
50	*53.90*	*7.8*	*47.35*	*5.3*
46.88	*53.37*	*13.85*	*48.90*	*4.31*
28.13	*25.47*	*9.45*	*30.55*	*3.86*
25	*23.91*	*4.34*	*27.98*	*11.92*
23.44	*21.70*	*7.41*	*30.43*	*29.82*
14.06	*11.64*	*17.22*	*16.09*	*14.44*
12.5	*11.94*	*4.52*	*11.04*	*11.68*
11.72	*10.98*	*6.33*	*12.87*	*9.81*
7.03	*7.22*	*2.75*	*7.22*	*2.63*
6.25	*5.85*	*6.39*	*6.28*	*0.48*
5.86	*5.99*	*2.27*	*6.16*	*5.66*
3.52	*3.85*	*9.52*	*<L.O.D.*	*N/A*
3.13	*3.35*	*7.05*	*<L.O.D.*	*N/A*
2.93	*3.24*	*10.45*	*<L.O.D.*	*N/A*
1.47	*1.71*	*16.58*	*<L.O.D.*	*N/A*

The limit of detection of the HPLC assay was determined to be approximately 5 ng/ml.

The degree of accuracy of the developed inhibition immunoassay was comparable to the HPLC technique over the concentration assayed and excellent correlation was achieved between the two data sets ($R^2 = 0.990$).

Table 4.9: *Measurement of degree of plasma protein binding in patient samples (n=20).*

Patient Identification Number	***Total Plasma Warfarin concentration (ng/ml) as determined by HPLC***	***Free Warfarin Drug concentration in plasma (ng/ml) as determined by BIACORE immunoassay***	***% Protein-Bound Drug in plasma samples***
11328	*642.22*	*BLQ*	*NQ*
11346	*2022.22*	*2.08*	*99.89*
11350	*757.22*	*BLQ*	*NQ*
11313	*625.55*	*0.46*	*99.93*
11377	*973.89*	*1.56*	*99.84*
11323	*983.33*	*5.05*	*99.49*
11321	*792.22*	*4.42*	*99.44*
11327	*1150.56*	*2.85*	*99.75*
11458	*1398.89*	*4.49*	*99.68*
11378	*474.44*	*0.23*	*99.95*
11436	*882.22*	*2.36*	*99.73*
11390	*857.22*	*BLQ*	*NQ*
11320	*1679.44*	*2.28*	*99.86*
11333	*930.00*	*1.03*	*99.88*
11366	*1217.78*	*BLQ*	*NQ*
11331	*900.00*	*2.58*	*99.71*
11328	*0.00*	*0*	*NA*
11387	*0.00*	*0*	*NA*
11315	*802.78*	*7.24*	*99.10*
11326	*1185.00*	*0.45*	*99.96*

NA = *Not Applicable*
NQ = *Not Quantifiable*
BLQ = *Below Limit of Quantitation*

The mean plasma concentration of the patient plasma samples assayed was found to be 1,015±383.59 ng/ml, whilst the average degree of plasma protein binding for the samples for which the degree of drug-protein binding was estimable was calculated to be equal to 99.72±0.24%.

4.2.3.10. Urine analysis of samples:

The inhibition immunoassay was also used for the detection of warfarin in urine as described in section 2.12.6. The ionic composition of urine can illustrate considerable variation depending on the individual liquid volume intake. To compensate for the potential wide inter-individual variability in the salt composition of urine, the antibody sample was prepared in HBS of twice the normal ionic strength (i.e. 2 x [HBS]). Similarly, a dilution step (i.e. 1 in 5 urine dilution) was also employed to reduce the potential effect on the measured binding response due to the altered salt composition. The coefficients of variation for the inhibition immunoassay over the assayed concentration range (%C.V. range 2-11% (Table 4.10)), were well within the recommended validation guidelines for immunoassay procedures (Findlay *et al.*, 2000). The working range of the assay for the detection of warfarin in urine using the affinity-purified polyclonal antibodies to warfarin was from 10-5,000 ng/ml (Figure 4.24).

The polyclonal antibodies demonstrated a much broader dynamic range than their monoclonal counterparts, a reflection of the widely differing antibody affinities from the purified serum fraction. The polyclonal antibodies also showed increased cross-reactivity to warfarin and metabolites, and this could be exploited in the current immunoassay format, which as shown can be used for the detection of warfarin and it's metabolites in urine samples. Proper patient compliance is extremely important in the management of warfarin anticoagulation, as dosage adjustments are made based on the pharmacological end-point of warfarin therapy (i.e. Prothrombin time measurements). Consequently, any dosage adjustments made on the basis of improper patient compliance can have extremely serious consequences upon return of the patient to the recommended dosage regime. The current system could therefore be used an immunoassay screening technique to guarantee adequate patient compliance prior to dosage adjustment. A similar strategy could also therefore be used in cases of suspected warfarin ingestion similar to those outlined in section 4.2.3.9.1. A similar approach to monitoring patient compliance has been described by George *et al.* (2000) for monitoring methadone compliance in patient urinary samples by immunoassay. Such screening procedures could be used for rapidly determining substance abuse to a wide range of residues, by employing broad spectrum antibodies (poly-/monoclonal) capable of detecting particular classes of drugs of abuse (e.g. amphetamines). By immobilising different residues of abuse on the various flow cells (i.e. flow cell 1-4) in the BIACORE 3000 instrument, a single injection of patient sample (urine/plasma or saliva) could be rapidly used to identify the presence of such residues of abuse in the order of minutes. Such rapid screening techniques are essential to allow for rapid identification of the offending agent so that a suitable antidote may be administered.

Table 4.10: *Intra-Assay variation for warfarin in urine samples (n=5):*

Actual Warfarin Concentration (ng/ml)	*Back-Calculated Warfarin Concentration (ng/ml)*	*% Accuracy*	*% Coefficient of Variation*
5000	*4448.42*	*11.03*	*9.53*
2500	*2674.02*	*6.96*	*6.57*
1250	*1239.53*	*0.83*	*7.55*
625	*658.67*	*5.39*	*11.25*
312.5	*330.63*	*5.80*	*6.52*
156.25	*135.48*	*13.29*	*5.33*
78.12	*75.98*	*2.74*	*2.16*
19.53	*16.27*	*16.67*	*2.43*
9.77	*10.09*	*3.28*	*3.19*

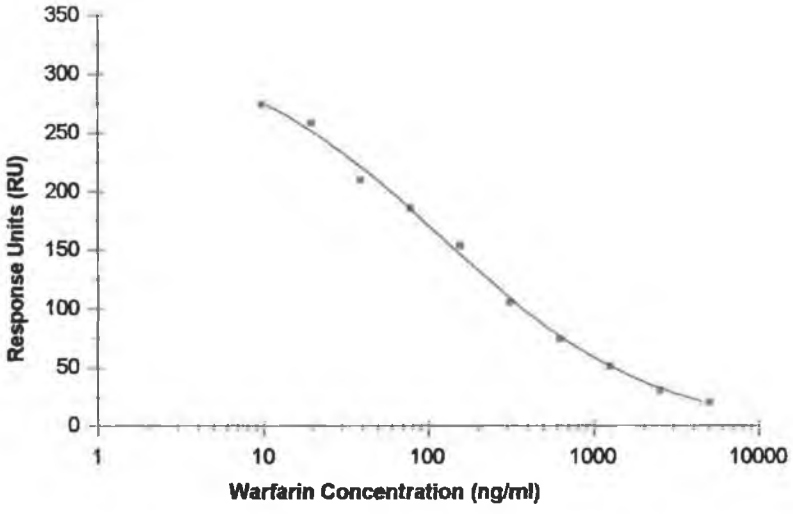

Figure 4.24: *Calibration curve for the detection of warfarin in urine using affinity-purified polyclonal antibodies. The results shown are the average of (n=5) replicates. The spline curve was constructed using BIAevaluation™, which allowed for the determination of the relative accuracy of the data set from the fitted 4-parameter logistic fit.*

4.2.4. Conclusions:

This chapter has described the development and validation of an inhibition-based immunoassay for the detection of warfarin in biological samples. The use of directly immobilised drug surfaces and the use of drug-protein conjugates were initially compared in terms of ligand-binding capacity. It was demonstrated in this instance, that the directly immobilised drug surface offered considerably better binding reproducibility (% C.V. = 0.82%) over the binding-regeneration cycles studied (i.e. >140 cycles), which is primarily related to the exceptional stability of the immobilised drug molecule (4'-aminowarfarin) on the dextran surface. Whilst the immobilised 4'-azowarfarin-BSA was not comparable to the directly immobilised drug surface, the use of hapten-protein conjugates do offer an alternative when suitable reactive groups are not available for direct immobilisation of the drug. However, the use of hapten-protein conjugates can prove difficult particularly when trying to dissociate high affinity antibody:antigen interactions, where the use of adequately harsh regeneration solutions to regenerate the sensor surface, too often results in denaturation of the immobilised ligand. Similarly, immobilisation of sufficiently high yields of conjugate for routine sample analysis can sometimes prove difficult using EDC/NHS chemistry, as many hapten-protein conjugates are characterised by very acidic isoelectric points.

The validation of the inhibition assay with conventional chromatographic techniques demonstrated excellent correlation between the back-calculated concentrations for the independent standards using the two different analytical techniques described ($R^2 = 0.990$). The limits of detection attainable with the developed inhibition immunoassay were more than an order of magnitude below those attainable using HPLC with UV detection (i.e. L.O.D. inhibition immunoassay = < 0.3 ng/ml, HPLC with UV-detection ≈ 6ng/ml). The assay performance as measured by the conventional measures of analytical performance, namely precision, accuracy, reproducibility and robustness demonstrated that the assay performed comparably in every respect to the conventional chromatographic techniques.

The developed and validated inhibition immunoassay system was then used for the detection of warfarin in patient plasma ultrafiltrates. The free fraction of a drug determines the pharmacokinetic profile of many drugs is in the body, and so is the fraction of the most considerable significance pharmacologically. The use of ultrafiltration is the most convenient method of preparing such plasma ultrafiltrates because of the non-dilutional effects observed (Bowers *et al.*, 1984). The matrix contribution to the measured binding response could be overcome by the suitable buffering and use of an appropriate dilution of sample. The mean free-drug concentration in the patient plasma samples assayed demonstrated that the degree of protein binding was approximately 99.72 ± 0.24%. This

value correlates well with other values cited in the literature which found plasma protein-bound fractions of the order of ~ 99.5% (Mungall *et al.*, 1984; Cai *et al.*, 1994).

SPR systems have traditionally been used to monitor bio-molecular interactions in 'real-time'. The use of the present system could be regarded as the development and validation of a generic quantitative SPR inhibition immunoassay for the detection of a wide range of analytes in various matrices, as relatively facile manipulation of the experimental parameters (i.e. immobilised ligand, regeneration parameters and choice of antibody) can be achieved to tailor the assay for the detection of different analytes. The development of the majority of chromatographic assays requires individual manipulation of mobile phases, extraction schemes and detection techniques for the detection of particular drug molecules. In many circumstances the limits of detection with such techniques are a factor of the physicochemical properties of the individual molecule, which can be limiting when particular suitable chromophoric or electroactive groups are not available. Alternatively, recent advances in genetic engineering with the development of phage-displayed libraries and various *in-vitro* affinity maturation techniques, has realised the potential of generating antibodies of extremely high affinities ($K_D \sim 10^{-15}$M, Boder *et al.*, 2000) to almost any molecule. Allied with the sensitivity of current SPR devices, the ability to accurately quantitate sub-picogram quantities of analytes for detailed pharmacokinetic/environmental studies is now a reality.

Chapter 5

Production, Characterisation and Applications of Monoclonal Antibodies to Warfarin

5.1. Monoclonal Antibodies:

Monoclonal antibodies were first produced over 25 years ago, following the fusion of a myeloma cell with that of an immune lymphoblast expressing a specific gene (Kohler and Milstein, 1975). The resulting fusion product a hybridoma (*hybrid*-myel*oma*) exhibits the immortality of the myeloma and the antibody producing properties of the splenocyte, thereby producing a virtually limitless supply of antibody of predetermined specificity and affinity.

Prior to the production of monoclonal antibodies by Kohler and Milstein, the lack of availability of antibodies of predefined specificity and affinity hampered the development and standardisation of many new emerging techniques such as ELISA and flow cytometry whose potential as diagnostic tools were being recognised. Indeed, Kohler & Milstein themselves may not fully have recognised the magnitude of their work for which they received the Nobel prize by concluding that:

"Such cultures could be valuable for medical and industrial use".

Monoclonal antibodies have today, become an important tool: in basic research, in clinical laboratories as therapeutic agents, as components of diagnostic kits, in affinity chromatography and as carriers in drug-targeted therapy (de Geus & Hendriksen, 1998).

5.1.1. Production of Monoclonal Antibodies following in vivo immunisation:

For the production of monoclonal antibodies an animal (e.g. rat, mouse) is initially immunised with the antigen of interest. The serum response of the animal is closely monitored for antibody production to the antigen of interest, and when a sufficiently high serum titre has been achieved the animal is sacrificed and the splencocytes may be harvested for cell fusion procedures. A variety of myeloma cell lines are available as suitable fusion partners the most commonly employed being X63-Ag8.653 and Sp2/0-Ag14 cell lines, which were produced from a myeloma cell line developed following the injection of mineral oil into the peritoneal cavity of mice. The technique pioneered by Kohler and Milstein, employed the use of the HAT selection system described by Littlefield (1964). Myeloma cell lines lacking the enzyme hypoxanthine guanine phosphoribyl transferase ($HGPRT^-$) are unable to proliferate in the presence of HAT (Hypoxanthine, Aminopterin and Thymidine) medium. Aminopterin blocks the *de novo* biosynthesis of purines and pyrimidines required for DNA synthesis, and the $HGPRT^-$ cells lines are incapable of using the salvage pathways for DNA synthesis as they do not possess the requisite enzyme systems (Figure 5.1).

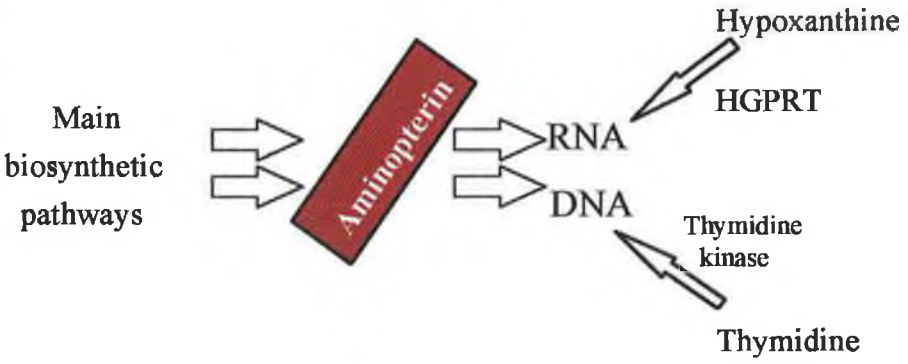

Figure 5.1: *Principle of the HAT system.*
Aminopterin blocks the main biosynthetic pathways for nucleic acid synthesis. Cells can use the salvage pathways for nucleic acid synthesis by incorporating thymidine and hypoxanthine. Cells lacking either of the enzymes HGPRT or thymidine kinase (e.g. Sp2/0-Ag14) are incapable of nucleic acid synthesis and die off in HAT culture medium.

Splenocytes carry the functional enzyme ($HGPRT^+$), but are incapable of proliferation in culture and naturally die off. In this context, HAT medium may be considered to be 'semi-selective'. Following the fusion procedure, a variety of cell fusion products exist, however only splenocyte-myeloma fusion products (i.e. hybridomas) which carry the functional enzyme ($HGPRT^+$), are capable of proliferation in the HAT medium. A variety of agents ('fusogens') have been used for cell fusion procedures, the most commonly used agent is polyethylene glycol, a polywax which promotes cell fusion and transfer of nuclei (Hurrell, 1985). The above technique although most commonly applied for the production of rat and mouse monoclonal can also be used for other species including human hybridomas. Tonsils and other lymphoid tissues can be used as a source for B lymphocytes, instead of the spleen. Due to the lack of human non-secreting myeloma cell lines, murine meyloma cell line are used as fusion partners and tend to produce unstable hybridomas which rapidly lose the ability to produce immunoglobulin, although some success has been had using human CLL as a fusion partner (Hurrell, 1985). A schematic of the procedure is illustrated in Figure 5.2

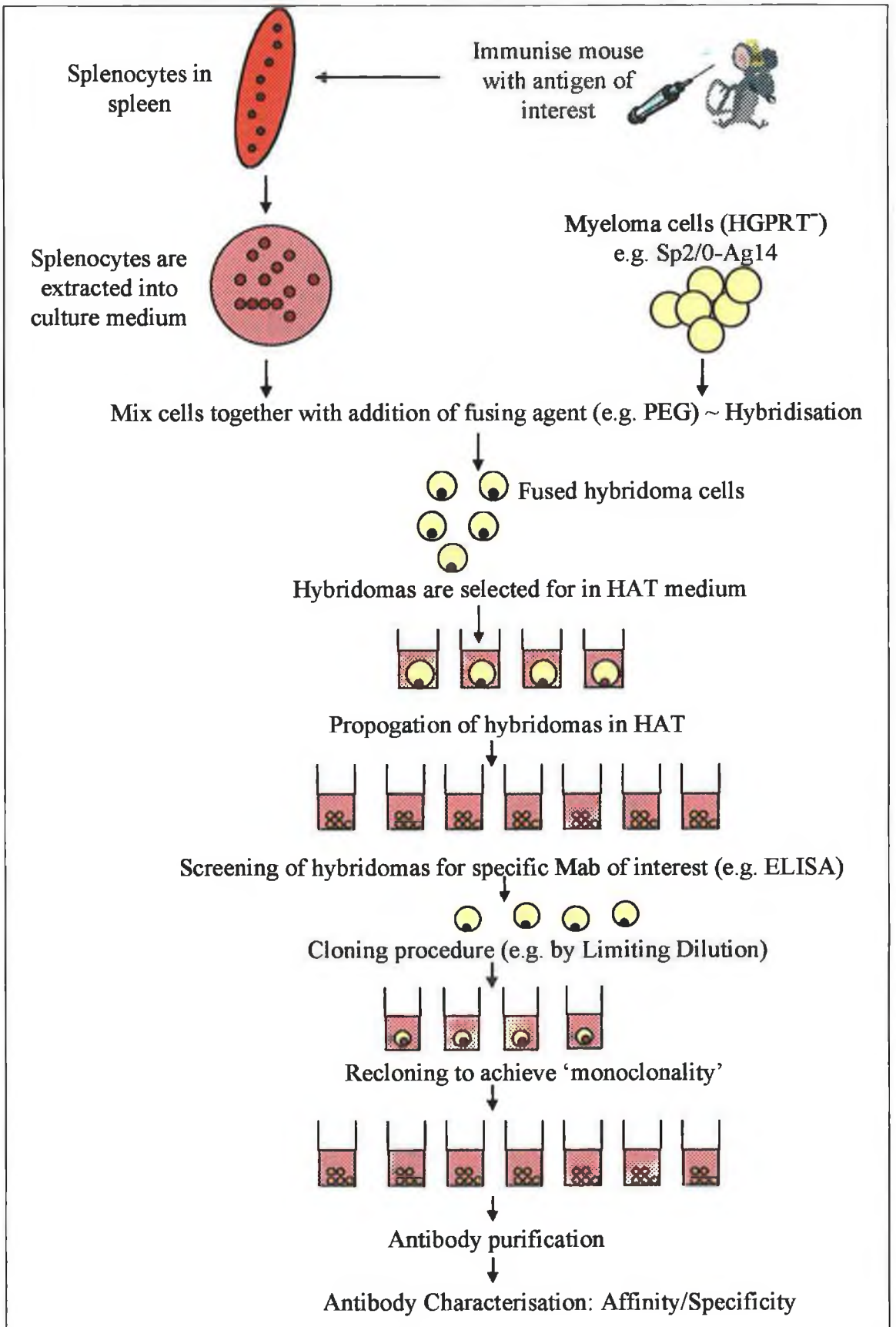

Figure 5.2 : Principle of Monoclonal Antibody Production

5.1.2. Production of Monoclonal Antibodies following in vitro immunisation:

Monoclonal antibodies can also be produced by *'in vitro'* stimulation of an antibody response (Borrebaeck *et al.*, 1983). B-lymphocytes are harvested from the spleens of naïve (i.e. non-immunised) animals and incubated for a period of typically 5-9 days, with the antigen of interest, prior to somatic cell fusion procedures. The technique offers the advantages of reduced immunisation schedules and quantity of antigen required, but suffers from the disadvantage that the majority of antibodies raised to the antigen of interest are the result of a primary immune response (predominantly IgM in nature with reduced quantities of IgG), and the antibodies are consequently of lower affinity, typically in the micromolar range. Wallen & Borrebaeck (1991) demonstrated a statistically significant correlation between the antigen concentration employed and the affinities of monoclonal antibodies generated. The use of a primary *in vivo* immunisation followed by a secondary *in vitro* stimulation (IVB, *in vitro* boost) has also been shown to produce greater quantities of IgG antibodies of increased affinity (De Boer *et al.*, 1989). To date, little success is reported in the literature with respect to *in vitro* forms of immunisation, particularly for monoclonal antibody production to small haptens. Bonwick *et al.* (1996) generated monoclonal antibodies to the pesticides flucofuron and sulcofuron, following *in vitro* immunisation. However, although the antibodies demonstrated specificity with respect to binding to drug-conjugates on ELISA plates, concentrations of free pesticide up to 1 mg/ml were unable to prevent binding to solid phase antigen. It was suggested that the effects of multi-specific, low affinity interactions (i.e. IgM) would be favoured and, therefore, negate the effect of free pesticide (Borrebaeck, 1989). Conventional *in vivo* immunisations are still required to produce antibodies of sufficiently high affinity, particularly to small molecular weight molecules. The use of IVI may provide a useful source of mRNA for recombinant work.

5.1.3. Production of Monoclonal antibodies to small haptens:

Coupling of haptens to carrier proteins is generally required for an anti-hapten antibody response. Fasciglione *et al.* (1996) identified three critical factors for the production of specific immunoconjugates. These include: the hapten conjugation method employed, the choice of carrier molecule and the amount of neodeterminants introduced. The conjugation method should increase the specific antibody response to the hapten. Fasciglione *et al.* (1996) found that the choice of carrier protein specifically modulates the serum titre and affinity of clones generated. It was also demonstrated that hydrophobic haptens can modify the tertiary structure of carrier proteins and become hidden in the core of protein, thereby limiting the interaction with the immune response and serum response generated. The use of specific hydrophilic carriers such as poly-L-lysine and sepharose was thus suggested for small hydrophobic haptens (Fasciglione *et al.*, 1996).

The chemical link employed between small molecular weight analytes and carrier proteins is responsible for the changes in the structure of small haptens, and ultimately their antigenicity and immunogenicity. The use of a different coupling chemistry via different amino acid residues is recommended for the selection of antibodies to small haptens to maximise the selection of positive clones specific for the hapten, and not a combined protein-hapten epitope (Danilova, 1994).

The importance of the appropriate immunoassay format employed for determining the specificity and affinity of antibodies must also be addressed. Delcros *et al.* (1995) found that the affinity of a particular monoclonal antibody, SPM8-2, appeared to depend on the whether the polyamine was free in solution and the type of conjugate immobilised. The discrepancy between relative affinities in solution and bound to the solid phase, was attributed to the different mode of linkages employed in the production of conjugates (EDC versus glutaraldehyde). Coupling using EDC chemistry resulted in a different polyamine structure (i.e. transforms a diamine to a monamine), and, as a result, the affinities for solid phase bound EDC-coupled antigen and antigen in solution were completely different. These examples serve to highlight the importance of an understanding of how the different coupling chemistries employed, and chemical nature of the hapten can directly impinge on the primary structure of proteins and small molecules and their subsequent interaction with antibodies.

5.1.4. Cloning Techniques:

Kohler and Milstein used a plaque assay technique to screen for antibody-producing clones. Today most hybridoma supernatants are screened using conventional ELISA or biosensor-based techniques (de Wildt *et al.*, 2000). Following screening, 'positive' (i.e. hybrids secreting specific antibody of interest) clones are propagated, and the hybridomas are then cloned to isolate the individual cells secreting the specific antibody of interest. The most commonly used method for cloning is that of limiting dilution, which involves repeated dilution and selection of 'positive' clones following screening (Harlow & Lane, 1988). After several rounds of cloning the hybridoma can be considered to be statistically 'monoclonal' in nature (Lietske & Unsicker, 1985). Difficulties associated with the limiting dilution method of cloning have been reviewed in detail elsewhere (Underwood & Bean, 1988). There are a number of traditional techniques available for cloning (Davis *et al.* 1982; Bell *et al.*, 1983), and one of the more sophisticated current technologies involves the transfer of single cells by means of a Peltier controlled pipette (Wewetzer & Seilheimer, 1995). The transfer of cells into wells of a microtitre plate is microscopically visualised and in this manner, the accurate transfer of individual hybridoma cells is assured. The transfer of individual cells greatly

reduces the time required for cloning procedures compared to the cloning by the traditional limiting dilution method.

5.1.5. Propagation Techniques for Monoclonal antibody production:

Monoclonal antibodies can be propagated by either *in vivo* or *in vitro* techniques. The underlying principle and developments that have taken place with respect to these two forms of antibody production are outlined below:

5.1.5.1 In-vivo antibody production:

Hybridoma growth as ascites fluid was initially the primary technique employed when monoclonal antibodies were required in larger quantities, because there were very few efficient and cost effective *in vitro* techniques available at the time. The peritoneal cavity of syngeneic mice is initially 'primed' with either Freund's Incomplete Adjuvant (FICA) or pristane (2,6,10,14-tetramethypentadecane), which serve as immunostimulants attracting monocytes, lymphoid cells and other nutrients into the peritoneal cavity, thereby creating a suitable environment for hybridoma growth. Approximately 7-10 days later, hybridoma cells (typically ~10^6 cells) can be injected into the peritoneal cavity. The peritoneal cavity of mice provides a continuous supply of oxygen, permanent inactivation of metabolites and active phagocytosis of dead cells and cell debris, where the cells can multiply to high cell densities secreting antibody into the ascitic fluid (Marx, 1998). The age, sex and strain of the mice can affect the yield of antibody recorded. Higher concentrations of antibody have been recorded in male mice which have been shown to have a longer period of secretion and greater volume of ascites, whilst mice between 43-75 days of age have also been shown to produce higher antibody concentrations (Brodeur *et al.,* 1984). The ascites fluid containing the hybridoma cells and antibodies can then be collected aseptically by 'tapping' the peritoneal cavity (i.e. draining the ascites fluid from the periteonal cavity by means of a needle and syringe), and the hybridoma cells cultured *in vitro* or passaged to another animal if required.

The advantages of using an *in-vivo* form of antibody production is that cell densities up to 10^{10} cells/ml with antibody yields in the mg/ml range can be routinely produced, without the need for elaborate techniques or equipment in a mycoplasma free environment (Hendriksen & de Leeuw, 1998). There are several disadvantages associated with the procedure, including contamination with biochemically identical immunoglobulins of the host. However, the use of SCID mice allows the production of antibodies free of endogenous Ig (Pistillo *et al.,* 1992). There are risks associated with product contamination by viruses

pathogenic to humans, which becomes increasingly important if the antibodies are required for therapeutic or prophylactic purposes. The potential for genetic alteration of hybridoma cells grown *in vivo* has also been reported, and conformational changes have also been observed in DNA from cells passaged in mice and correlated with cell-associated pristane (Garrett *et al.*, 1987). Human hybridoma cells grown as ascites in nude mice have also exhibited gross morphological change and alteration in DNA content compared to cells grown *in vitro* (Truitt *et al.*, 1984). The growing public, ethical and legal pressures to replace *in-vivo* forms of animal experimentation with comparable *in-vitro* techniques, has led to the development of numerous *in-vitro* technologies for monoclonal antibody production (Falkenberg, 1998(a); Lipski *et al.*, 1998).

5.1.5.2. In-vitro antibody production:

The primary objective in the development of suitable *in-vitro* technologies was to simulate an environment, similar to that of the peritoneal cavity of mice capable of producing large quantities of antibody in a concentrated form similar to ascitic fluid. *In-vitro* production systems can be categorised according to the principle of the culture system employed (Marx, 1998):

- Static and agitated suspension culture systems
- Membrane-based and matrix-based suspension systems
- High-cell density bioreactors

The quantity and purity of the MAb required, generally speaking will dictate the type of production method employed (Peterson, 1998).

Cells grown *in vitro* culture have two basic needs: a constant supply of gaseous and water-soluble nutrients, and to be able to remove toxic metabolites from (e.g. gaseous CO_2 and soluble lactic acid and ammonium ions) the culture medium. The principle behind the various means of *in vitro* cell culture are described below:

Static and Agitated suspension culture systems:

For the small-scale production of antibody sufficient to meet those of most academic research laboratories, tissue culture flasks provide adequate levels of antibody production. Hybridomas typically yield from 5-50 μg/ml of antibody depending on the individual hybridoma growth characteristics. Transfer of gaseous nutrients is achieved by diffusion, whilst withdrawal and replacement of media is required to replace water-soluble nutrients and remove waste metabolites. Consequently antibody concentrations achieved using static culture systems are lower, in the 1-100 μg/ml range. The osmolality of the growth medium has also been reported to have a direct correlation on the rate of antibody production of

certain hybridoma cell lines (Oh *et al.*, 1993). Oyaas *et al.* (1994) found that when particular hybridoma cell lines were placed in media made hyperosmotic through the addition of NaCl or sucrose, the rate of antibody production approximately doubled compared to cell lines maintained at physiological osmolality. The use of osmotic stress decreased the maximal cell densities attainable, which to some degree negated the positive effects on the overall rate of antibody production. However, when an osmoprotective compound such as glycine betaine was added to the NaCl or sucrose-stressed cultures, the overall concentration of antibody recorded was more than double that of control cells. These results suggest that the use of osmotic stress and osmoprotective compounds (e.g. glycine betaine, sarcosine and proline) may have potential future benefits for *in vitro* systems to enhance specific rates of antibody production.

One of the more recent commercial additions to this type of culture technology is the use of gas permeable membranes, such as the commercially available i-MAB™ gas permeable bag. The system is comprised of a gas permeable bag that allows for greater exchange of gaseous molecules. The cells do not achieve significantly higher numbers but appear to produce more antibody yield per cell in tests carried out to date (Lipski *et al.*, 1998). The system also offers the advantage that once initiated it is a completely enclosed system thereby reducing the possibility of contamination, whilst the system can be maintained for up to 3 weeks.

Agitated culture systems such as those employing roller bottle flasks achieve higher levels of antibody production through greater levels of oxygenation as a result of culture agitation and removal of CO_2 from the culture medium. The cells multiply at a greater rate and use up media faster, achieving higher antibody concentrations.

Membrane based and matrix-based suspension systems:
Early devices of this nature constructed included Milsteins' 'oscillating bubble chamber' (Pannell & Milstein, 1992) which employed a piece of dialysis tubing placed at a diagonal in a roller bottle flask. During rolling the bubble moves back and forth, thus mixing and keeping the cells in culture. The 'Berlin tumbling chamber' (Jaspert *et al.*, 1995) and the 'Bochum glass mouse' employed similar dialysis type constructions and provided the solutions for some of the more recent commercial constructions (e.g. miniPERM®, CELLine®) (Trebak *et al.*, 1999; Falkenberg, 1998(a)).

Devices belonging to this category typically employ two chambers, one housing the cells and products (i.e. antibodies), and another containing the medium reservoir (Nagel *et al.*, 1999).

In such systems, the cells are contained in a chamber separated from the medium reservoir by means of a dialysis membrane. Efficient exchange of nutrients and excretion of toxic metabolites is achieved by means of diffusion of medium through the dialysis membrane. The low oxygen content of aqueous media and the high oxygen consumption rate of hybridoma cells *in vitro* limited the growth of cells. Falkenberg (1998) overcame this difficulty by employing the use of a semi-permeable silicone rubber seal on the culture unit with agitation that allows for sufficient transfer of oxygen into the culture system to meet the high oxygen requirement within the culture system. CELLine 1000™ membrane systems are capable of producing antibody concentrations from 0.7-2.5 mg/ml, during periods of culture up to 40 days (Trebak *et al.*, 1999).

High-cell density bioreactors:

Hollow fibre vessels are the most advanced technology for the production of antibodies, which is reflected in their cost and operation requirements. Hollow fibre bioreactors are comprised of two main units: the cell culture reservoir, and the hollow fibre bioreactor (Figure 5.3). The hollow fibre bioreactor unit is composed of a unit containing a bundle of semi-permeable fibres with a molecular weight cut off (MWCO) of 10-50 kDa. Cells are inoculated into the hollow fibre core and bathed in culture medium passing through the hollow fibres. The molecular weight cut-off of the membranes permits the transfer of small molecular weight molecules (e.g. nutrients and toxic metabolites), but excludes the movement of cells and antibodies, which grow to high cell density in the bioreactor unit, capable of producing antibody in the mg/ml range. Culture medium is pumped back to the cell culture reservoir after passage through the hollow fibres. An evaluation of hollow fibre systems compared to other *in vitro* methods of antibody production by Gorter *et al.* (1993) revealed that the amounts of bispecific antibody produced by the hollow fibre bioreactor, were equal to that from ascitic fluid from 200 mice, or 38L of tissue culture supernatant.

One of the major difficulties with hollow fibre systems is achieving adequate levels of oxygen aeration to meet the high cellular requirement in the bioreactor core. Oxygen saturated media is pumped through the hollow fibre under high flow rates to meet the oxygen requirements within the bioreactor. Several attempts have been made to overcome these difficulties by incorporating oxygen carriers such as stabilised haemoglobin and perfluorocarbons into the culture medium, in an attempt to overcome this limiting factor with the use of hollow fibre systems. A recent study investigated the advantages of incorporating various oxygen carriers originally designed as blood substitutes into the cell culture medium as a means of increasing the dissolved oxygen content, and consequently, the antibody

production capacity of hollow fibre bioreactors. Levels of antibody production were increased from 20-104% depending on the particular hybridoma line and oxygen carrier chosen. Of the carriers evaluated, Erythrogen™-1, a chemically stabilised form of haemoglobin proved to be the most efficacious additive, more than doubling the concentration of antibody achieved compared to control cells at a final concentration of 0.1% (w/v) (Shi *et al.*, 1998).

One disadvantage of all the *in vitro* systems described, is that to date none of the devices are capable of active elimination of dead cells and cell debris, which can be a limiting factor with respect to cell growth and maximal antibody concentrations attainable.

Table 5.1: Summary of various forms of antibody production

Method	Advantages	Disadvantages
In-Vivo: Ascites	Cost (£/mg antibody) Antibody concentrations mg/ml range Ease of production 'Mycoplasma-free' environment	Concern (legal/ethical) with the use of live animals Variability in yield from animal to animal Separate facility required Possibility of contamination with murine viruses
In-Vitro: Tissue Culture Flasks	Technically easy Consistent yield Relatively cost effective	Large volumes of media for processing Time-consuming with respect to feeding and passaging hybridoma cell lines
Gas Permeable Bags (e.g. i-MAB™)	Technically easy Consistent yield Cost effective in terms of media consumption and labour required Culture periods up to 30 days Reduced operator handling Enclosed system	Large volumes of media for processing
Membrane based systems (e.g. miniPERM, CELLine).	Higher antibody concentrations attainable in relatively small volumes Culture periods up to 40 days	Increased medium consumption depending on cell concentrations achieved
Hollow fibre Cartridges	Antibody concentrations of mg/ml range achieved in small volume Culture periods up to 30 days Media may contain high concentration of FCS without contamination of product	Large volumes of media expended Initial investment high Possibility of mechanical faults associated with high flow rates/pressures (e.g. leakages within system)

5.1.6. Chimeric/Humanised Antibodies:

The development of MAbs has had a considerable impact on the area of clinical diagnostics, but the expected success in the area of human therapy to date has not been fully realised (Clark, 2000). Three problems were initially encountered with the use of monoclonal antibodies in human therapy: they did not always trigger the requisite effector function, they had a short life span *in vivo*, as the antibodies often elicited a HAMA (Human Anti-Mouse Antibody) response. The HAMA elicited results in the increased clearance of the antibody from the circulation thereby negating the therapeutic potential; and has been reported to cause severe allergic reactions (Jaffers *et al.*, 1986). To try and circumvent this particular response, chimeric antibodies were constructed where the mouse variable regions were joined to human constant regions (Boulianne *et al.*, 1984). Chimerisation solved some of the initial problems associated with murine Mabs: as it allowed for increased half-life in the circulatory system through interaction with the Brambell receptor (FcRn), which protects the IgG from catabolism thereby recycling it back to the serum pool (Ghetie & Ward, 2000); and the ability to recruit effector cells such as complement and cytotoxic cells (Glennie and Johnson, 2000). V-region humanisation has also been carried out to try and humanise the antibodies even further by changing some of the amino acid sequences thought to be non-critical to antigen binding to more 'human-like' sequences whilst retaining the murine CDR sequences necessary for antigen binding (Riechmann *et al.*, 1988).

Two new strategies that have evolved for the production of 'fully human antibodies' involve the use of recombinant antibody technology through the expression of naïve variable regions expressed on the surface of bacteriophage and the use of transgenic mice. Recombinant methods of human antibody production generally speaking require successive rounds of panning and mutagenesis to produce antibodies of sub-nanomolar affinities comparable to conventional MAbs (Vaughan *et al.*, 1998).

Transgenic mice (Xenomouse™) have also been constructed whereby the mice immunoglobulin genes have been replaced with human Ig genes on YAC (Yeast Artificial Chromosomes) transgenes, which carry the majority of the human variable repertoire as well as the possibility of undergoing class-switching from IgM to IgG and efficient affinity maturation. Xenomouse™ strains of mice recognise human antigens as foreign, and are capable of producing antibodies with sub-nanomolar affinities (Mendez *et al.*, 1997). Human antibodies from mice can be differentiated from their human cell counterpart by the glycosylation pattern, which contains the Galα1-3Gal residue. Human serum antibody titres of up to 100μg/ml against Galα1-3Gal residue have been recorded, and it has been argued

(Borrebaeck, 2000), that the *in vivo* administered transgenic antibody would not survive long in human circulation following complexation with anti-Galα1-3Gal antibodies. However, antibodies from transgenic mice have shown promising results in a number of clinical trials to date, with plasma half-lifes similar to normal Ig and no detectable anti-human antibody responses recorded (Green, 1999). Xenomouse antibodies are also adaptable to production directly from hybridomas, transgenic plants or recombinant cell lines.

5.1.7. Recombinant Antibodies:

The development of phage display technology has realised the possibility of producing 'tailor-made' antibodies of high affinity to any particular antigen (Hoogenboom & Chames, 2000). The connection between genotype (antibody V regions) and phenotype (binding specificity) allows for selection and enrichment of specific phage with the desired specificity. The principle involves cloning DNA into phage genome as a fusion to one of phage coat proteins. Following expression the antibody fragments are presented on the surface of the phage with the encoding DNA residing inside the phage. The phage display library can then be panned by selection of phage with specific binding affinity towards a particular immobilised target ligand. The affinity of the antibodies created has been reported to be proportional to the size of the antibody library (Sblattero & Bradbury, 2000).

The antibody libraries may be constructed from naïve or immunised donors, and also from synthetic libraries. Immunised donors will already be enriched for specific immunoglobulin, some of which will have undergone affinity maturation. Naïve libraries from which high affinity antibodies may be selected are particularly useful for selection of human antibodies (Hoogenboom *et al.*, 1998).

The affinity of the selected antibodies is very often not sufficiently high enough and may require *in vitro* affinity maturation to produce antibodies of suitable affinity (Hemminki *et al.*, 1998). This can be achieved in a variety of ways from the use of mutator strains, the use of error prone PCR (Harayama, 1998), chain or oligonucleotide directed mutagenesis shuffling (Jirholt *et al.*, 1998). The introduction of diversity into the V genes allows for the creation of a 'mature' secondary library from which higher affinity variants may be selected. BIACORE-based selection procedures allows for the selection of particular variants with respect to specific affinity and kinetic rate constants (Dueñas *et al.*, 1996). ScFvs with femtomolar association constants, the highest yet reported for monovalent ligands have been produced using a similar approach of 'molecular breeding' involving repeated cycles of affinity mutagenesis (Boder *et al.*, 2000). The potential applications of such higher affinity

variants with association constants 1000 fold greater than possible by *in vivo* maturation, is particularly interesting for developing areas such as immunotherapy and tumour targeting.

5.1.8. Alternative Expression systems for antibody production:

A variety of expression systems are available for the production of antibodies and antibody fragments, including the use of bacteria, yeast, plants, insect cells and mammalian cells. Each has it's own advantages and limitations with respect to ease of production, and the glycosylation pattern of antibodies recorded, two potentially relatively low cost antibody expressions systems are described.

5.1.8.1. 'Plantibodies':

Hiatt *et al.* (1989) was the first to report genetically engineered tobacco plants capable of synthesising correctly folded immunoglobulin heavy and light chains. A variety of 'plantibodies' have since been constructed, three of which are currently in use as immunotherapeutic products for the treatment of caries and cancer (Larrick *et al.,* 1998). Plantibodies offer several advantages as potential protein sources compared to other mammalian and bacterial systems: including the production of antibodies on an agricultural low-cost scale, and potential increased safety as plants do not serve as human pathogen hosts (e.g. HIV, prions). Ma *et al.* (1995) produced secretory IgA (sIgA) plantibodies in tobacco plants (CaroRx™), which recognises and binds the oral pathogen *Streptococcus mutans*, with yields of antibody up to 0.5 mg/gram of fresh weight of tobacco recorded.

5.1.8.2. Transgenic Milk:

The possibility of using the mammalian milk gland as a means of producing antibodies in transgenic dairy animals is currently being investigated (Pollock *et al.*, 1999). Expression vectors containing the gene encoding the specific protein fused to milk specific regulatory genes can be introduced by microinjection into one embryo cells. Following a period of *in vitro* culture the embryos can be transferred to pseudopregnant animals and development to full term (Little *et al.*, 2000). Following integration into the germline, the transgene is transmitted in Mendelian fashion and if expressed, will become a dominant characteristic to offspring which can be tested for the transgene. The identified animals can then be bred or induced to lactate. Dairy goats have been shown to be excellent animals for the production of transgenic milk, capable of producing between 1 and 5 g/l of recombinant antibody (Pollock *et al.*, 1999). The efficiency of microinjection has limited the development of this technology as the integration into the genome of specific transgenes is typically low, 0.1% in cattle to 5% in mice. The antibodies can be separated from the majority of milk proteins by

standard dairy procedures to relatively pure antibody (~60%) which can be further purified by traditional chromatography procedures (e.g. Ion exchange, Protein A/G chromatography). A variety of antibodies have been produced in the milk of transgenic animals, and in particular cases been shown to be produced at levels 160,000 fold times those recorded in cell culture systems whilst retaining all biological activity (Newton *et al.*, 1999).

5.1.9. New Antibody Constructs

5.1.9.1.'Plastibodies' -Molecular Imprinted Polymers (MIPs):

The technique of molecular imprinting polymers allows for the generation of specific recognition sites in synthetic polymers that mimic the binding sites of antibodies. A target molecule provides a template for the polymerisation process, whereby monomers carrying specific functional groups are arranged around the template molecule through covalent and non-covalent interactions, and secured into position by the crosslinking process. Following removal of the template molecule from the polymer, a cavity remains in the polymer whose shape, size and arrangement of functional groups closely resemble that of the target molecule. MIPs are rigid and insoluble, and consequently cannot compete with antibodies for procedures that rely on antibody solubility, such as immunodiffusion and immunoelectrophoresis. Areas of application where plastibodies have shown potential application include immunoaffinity procedures and immunoassays (Haupt and Mosbach, 1998). The high stability of MIPs renders them suitable for sample pre-treatment and solid state extraction procedures particularly those employing organic solvents. MIPs have already been used for the extraction of herbicides from beef-liver extracts and various drugs from dilute serum and urine (Muldoon & Stanker, 1997). Molecular Imprint Sorbent Assays (MISA) have also been developed for the detection of various drugs, herbicides and corticosteroids (Ramstrom *et al.*, 1996). Results for the MISA correlated very well with those for conventional ELISA for theophylline, the cross reactivity profile of the plastibodies closely resembling that of the MAb. MIPs have also been used in biosensors employing field-effect transistors (Hedborg *et al.*, 1993), electrochemical (Piletsky *et al.*, 1995) and optical (Levi *et al.*, 1997) transducers. MIPs also give rise to a heterogeneous mix of antibody binding sites similar to polyclonal antibodies, with the frequency of high affinity sites (Kd ~ nanomolar range) between 0.1-1.0% (Andersson *et al.*, 1996). The majority of molecular imprinting to date has been developed using non-polar solvents, and work is currently under going to develop imprinting in polar solvents such as water, which can disrupt the prepolymerisation complex during imprinting, and polymers with more homogenous binding sites similar to MAbs through stabilisation of the polymer complex.

5.1.9.2. Diabodies:

Diabodies are constructed by two functional scFv joined by a short polypeptide linker. Careful selection of the linker length dictates the size (kDa), and thus the valency of the scFv multimer formed (Hudson & Kortt, 1999). The production of monomeric scFv requires that the linker employed be at least 12 residues in length. By selecting a residue of 3-10 residues in length, the scFv cannot fold into a functional scFv and associates with a second scFv to form a diabody (60 kDa). Reducing the linker length below 3 residues forces the scFv to form triabodies (90 kDa) or tetramers (120 kDa). As a result of the increase in valency, scFv multimers exhibit very high avidity and reduced off rates as a result of multiple binding and re-binding when one Fv dissociates (Pluckthhun & Pack, 1997). In BIAcore studies conducted, Iliades *et al.* (1997) found that the trimers produced from a scFv exhibited an approximate 4-fold apparent slower off-rate compared to the monomeric unit.

The association of two different scFv molecules from different parent IgG will result in the formation of bispecific diabodies (Hollinger *et al.*, 1993), which have been successfully used for ELISA, immunohistochemistry and immunoblotting procedures (Kontermann *et al.*, 1997).

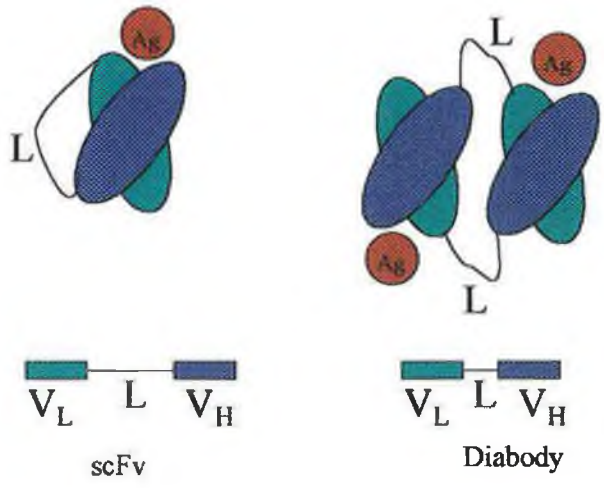

Figure 5.4: *Schematic diagram of scFv and diabodies showing antigen binding sites. When joined by a peptide linker (L) at least 12 residues long scFv's are predominantly monomeric, diabodies (~60Kda) are formed by selecting linkers between 3 and 12 residues. Reducing the linker length below 3 residues can force scFv into triabodies (~90 kDa) and tetramers (~120 kDa).*

The use of diabodies has gained increasing interest particularly in the areas of immunotherapy and tumour imaging. The reduced size of diabodies compared to whole Ig for tumour targeting has the advantage of increased tumour penetration and faster clearance rates *in vivo*. Bispecific diabodies have also been shown to induce cytotoxic and 'vaccine effects' *in vivo* (van Spriel *et al.*, 2000), and a number are currently under trial for the treatment of various cancer cell types.

5.1.9.3. 'Affibodies':

The combination of genetic engineering and advanced selection techniques has led to the development of a novel range of protein ligands, 'affibodies' (affinity ligands) with specific binding capacities similar to natural antibodies. Knottins, are a small group of small disulphide-bonded proteins capable of binding to target molecules. Smith *et al.* (1998) have created knottin scaffolds with binding capacities in the micromolar range for target antigens such as alkaline phosphatase. Nord *et al.* (1997) have also created 'affibodies' from the α-helical bacterial receptor domain Z derived from staphylococcal protein A, which does not depend on disulphide bridges for stability, that has been shown to be exceptionally stable to pH extremes and harsh regeneration conditions and thus potentially useful in areas such as affinity purification (Nord *et al.*, 2000). The potential for improving binding affinity has also been exploited through the use of *in vitro* affinity maturation strategies, such as α-helix shuffling strategy employed by Gunneriusson *et al.* (1999) which resulted in a 20-30-fold increase in functional affinity.

5.1.10. Applications of Monoclonal Antibodies:

Monoclonal antibodies have become the cornerstone of most diagnostic kits, immunoaffinity procedures and found extensive use for the detection of a wide variety of target antigens ranging from pesticides, illicit drugs and toxins to blood markers (Fitzpatrick *et al.*, 2000). Coupled with the development of biosensing platforms they have led to the development, standardisation and automation of the majority of previously laborious laboratory procedures. Their use in the monitoring of enviromental (e.g. pesticides, pollutants) and food (e.g. growth promoters) residues have been recently reviewed (Fitzpatrick *et al.*, 2000). The diagnostic market, is today almost completely reliant on the use of monoclonal antibodies which allowed for the standardisation of laboratory reagents with regard to affinity and specificities. Indeed, one has only to browse the antibody catalogues available to witness the greater than 100,000 monoclonal antibodies currently commercially available. Some of the potential clinical uses and developing areas of monoclonal antibody technology are described below:

5.1.10.1. Clinical Applications of Monoclonal Antibodies:

The application of monoclonal antibodies for the treatment of a variety of clinical disorders has not fully developed following the initial potential shown in 1982; with the complete response of an individual with lymphoma following a brief treatment with a murine antibody (Miller *et al.*, 1982). However, the expected progress that Mabs brought to diagnostics and basic research, did not occur as quickly as expected in the area of therapeutics. The advances of genetic engineering which has allowed for the development of fully functional human antibodies has overcome many of the initial difficulties associated with murine MAbs: namely their inability to elicit the requisite effector functions and notably short half-life. Currently there are 8 FDA licensed MAbs and numerous others at various stages of clinical trials for use against cancer, transplant rejection and a variety of other diseases including Rheumatoid Arthritis and Crohn's disease (Glennie & Johnson, 2000).

The most successful murine antibody to date, OKT3 (anti-CD3), approved by the FDA in 1986, for acute allograft rejection prevents tissue rejection by binding to CD3, thereby blocking the action of T-cells. Two other recently licensed anti-CD25 Mabs (Zenapax® Chimeric IgG1, Simulect® Humanized IgG1) are also currently available for allograft rejection therapy which prevent binding of inteleukin-2 to CD25, blocking the transduction of IL-2 and suppressing the action of T-cells.

Currently successful anti-cancer Mabs include the use of rituximab (anti-CD20) and trastuzumab (antiHER2/neu). The binding of trastuzumab to it's receptor (antiHER2/neu) has been shown to induce a number of signalling events believed to play a role in tumour growth (Goldenberg, 1999). Rituximab also induces a number of signalling events, and has been shown to induce apoptosis in a number of B-cell lines. However, the median recurrence interval in patients with low grade B-cell malignancies is approximately 1 year (McLaughlin *et al.*, 1998), suggesting that this particular Mab therapy may be useful as an adjunct therapy to surgery. Clynes *et al.* (2000) has recently shown that the direct interaction between antibodies and Fc receptor is responsible for the cytotoxic anti-tumour effects of both rituximab and trastuzumab in therapy, suggesting that greater efforts should be made to maximise particular Fc receptor interactions to increase the efficacy of various immunotherapies.

Current therapies are focusing on the use of conjugated MAbs to deliver toxins selectively to tumour bearing antigen cells, with the potential for increased efficacy of treatment while minimising systemic toxicity (Trail & Bianchi, 1999). Calicheamin conjugates are among the most potent antitumour compounds used to date and produce double-stranded breaks in

DNA. Clinical trials of CMA-676, an immunoconjugate of calicheamin and anti-CD33 Mab have shown a 20% response rate in patients with AML (Acute Myeloid Leukemia). BR96-DOX, an immunoconjugate coupled to the antibiotic doxorubicin which binds to a Le^y-related tumour antigen expressed on most carcinomas has shown partial remissions in phase 1 clinical trials. The immunotherapy conjugate was also shown to induce cures of multiple carcinoma types, in athymic rats and mice (Trail & Bianchi, 1999).

Radioimmunotherapy (RIT) offers the possibility of delivering 3-50 times the normal radiation dose to tumour cells (DeNardo *et al.*, 1999), and has been shown to be particularly useful in the treatment of Non-Hodgkins' Lymphoma. One of the more interesting developments in RIT, is the Pretarget® system that exploits the streptavidin-biotin interaction and makes use of a three-step system for targeting radionuclides to the tumour cell, with promising results to date. Streptavidin-conjugated Mabs are initially administered and localise at the tumour antigen site. A second 'chase' reagent is then added to complex any unbound tumour Mab. Radiolabelled biotin is then administered and binds to the streptavidin complex. The small size of the biotin conjugate enables its quick elimination from the kidneys (DeNardo *et al.*, 1999).

The use of bispecific antibodies and newer recombinant antibody constructs are also under investigation, to exploit the potential signalling potential of these particular antibodies as therapeutic agents with the ability of recruiting specific effector molecules to tumour cells (Segal *et al.*, 1999; Hudson, 1999). The potential for development in the field of immunotherapy is enormous, which combined with developments in antibody engineering, an increase in our understanding of cellular signalling pathways, the development of newer more potent anti-tumour agents, augurs well for the concept of Ehrlich's 'magic bullets' being finally realised in the new millennium.

5.1.11.1. Basic Antibody:Antigen Reaction Kinetics:

The equilibrium between an antibody, antigen and immune complex can be described by the following expression:

$$[Ag] + [Ab] \underset{k_d}{\overset{k_a}{\leftrightarrow}} [Ag:Ab] \qquad (1)$$

Where [Ag] = Antigen

[Ab] = Antibody

[Ag:Ab] = Immune Complex

k_a = Equilibrium association rate constant

k_d = Equilibrium dissociation rate constant

The overall association rate constant can thus be described by the following expressions:

$$\frac{k_a}{k_d} = K_A = \frac{1}{K_D} \qquad (2)$$

Where $[K_A]$ = Equilibrium Association rate constant

$[K_D]$ = Equilibrium Dissociation rate constant

Various techniques are available for the determination of the antibody affinity constants including equilibrium dialysis (Lehtonen & Eerola, 1982), polyethylene glycol precipitation (Stanley *et al.*, 1983), affinity chromatography (Chaiken *et al.*, 1992) and those involving the use of enzyme-linked immunosorbent assay (Friguet *et al.*, 1985; Chu *et al.*, 1995). These techniques rely on the concentration measurement of either analyte or antibody:antigen complex at equilibrium for determination of overall affinity constants.

Liquid phase affinity constants for monovalent antigens are based on the use of enzyme-linked immunosorbent assays, and partitioning of antibody between solid and liquid phase antigen offer a relatively simple procedure for the determination of overall affinity constants (Nieto *et al.*, 1984; Friguet *et al.*, 1985). The procedure described by Friguet *et al.* (1985) has the advantage that affinity determinations may be made with crude antibody preparations, whose exact antibody concentration does not need to be known.

Two antibodies with similar affinity constants (K_A) may possess completely different kinetic rate constants, and consequently vary considerably in their time taken to reach equilibrium which can be of considerable significance depending on the intended use of the antibody. The use of 'real-time' biomolecular interaction analysis (i.e. BIACORE) is a useful means of affinity ranking antibodies, and can also be used early in the selection process as a screening device for the selection of particular antibodies (monoclonal/scFv) based on their individual

kinetic rate constants (Deuñas *et al.*, 1996). For a detailed description of the theory and practice of this instrument, the reader is referred to sections 2.12. and 4.1.2.

For a one-to-one interaction in solution the rate of complex formation at the sensor chip surface at time t between reactants *[A]*, and *[B]* to form the complex *[AB]* can be described by the following equation (Fagerstam & O' Shannessy, 1993):

$$\frac{d[AB]}{dt} = k_a[A]_t[B]_t - k_d[AB]_t \qquad (3)$$

Where

$[AB]_t$ = Molar concentration of complex at interaction surface at time t

$[AB]$ = Molar concentration of complex at interaction surface

$[A]_t$ = Molar concentration of analyte at interaction surface at time t

$[B]_t$ = Molar concentration of immobilised ligand at interaction surface at time t.

However, the concentration of ligand at time t, $[B]_t$, equals the initial concentration $[B]_0$ minus the formed complex $[AB]_t$ at time t:

$$[B]_t = [B]_0 - [AB]_t \qquad (4)$$

therefore equation (3) becomes:

$$\frac{d[AB]}{dt} = k_a[A]_t([B]_0 - [AB]_t) - k_d[AB]_t \qquad (5)$$

In BIAcore, the ligand, B, is immobilised and the analyte is continually replenished over the sensor chip surface. The response signal measured, R, is related to the formation of the complex, AB, at the chip surface. The maximal response attainable, R_{max}, will therefore depend on the immobilised surface concentration of ligand and equation (5) can therefore be rewritten as:

$$\frac{dR}{dt} = k_a[A]_t(R_{max} - R_t) - k_d[R_t] \qquad (6)$$

Where R_t = Response measured at time t

R_{max} = Maximal response if all ligand binding sites are occupied

The concentration of analyte passing over the ligand surface is continually replenished by fresh analyte, and the concentration at interaction surface $[A]_t$, can thus be approximated to be equal to the injected analyte concentration $[A]_i$:

$$[A]_i \approx [A]_t \tag{7}$$

Equation (6) can therefore be rewritten as:

$$\frac{dR}{dt} = k_a[A]_i(Rmax - R_t) - k_d[R_t] \tag{8}$$

Rearranging equation (8):

$$\frac{dR}{dt} = k_a[A]_i(R_{max}) - (k_a[A]_i + k_d)(R_t) \tag{9}$$

The integrated form of the rate equation can be described by the following relationship:

$$R_t = \frac{k_a[A]_i R_{max}(1 - exp[-ka[A]i + kd]t)}{ka[A]i + kd} \tag{10}$$

and used to calculate the values of R_{max}, k_a and k_d.

A plot of dR/dt versus R_t from equation (9) yields a line of slope, k_s, which is equal to $(k_a[A]_i + k_d)$.

$$k_s = (k_a[A]_i + k_d) \tag{11}$$

By calculating the slope, k_s, at different analyte concentrations $[A]_i$, the quadratic equation (11) can be used to construct of k_s versus $[A]_i$ whose slope is equal to k_a and intercept is k_d. Following withdrawal of the analyte ($[A]_i = 0$) from the interaction surface allows for visualisation of the dissociation phase and equation (11) can be simplified to (i.e : as $[A]_i = 0$).

$$\frac{dR}{dt} = -k_d R_t \tag{12}$$

5.1.11.2. Conditions of Mass Transport Limitation (MTL):

Mass transport limitations (MTL) conditions have been exploited in BIACORE for the development of novel quantitative assays, capable of determining the 'active' antibody concentration in solution. The Universal curve technique utilises low flow rates and high immobilised ligand concentrations to establish conditions of MTL (Karlsson *et al.*, 1993). Under such conditions the antibody-binding rate (dR/dt) becomes proportional to the active analyte concentration [C_A] (equation 16). A similar MTL technique for the quantitative determination of antibody concentrations has been described by Christensen (1997), exploiting the flow rate dependence of the binding rate under MTL conditions. Consequently, an understanding of the basic fundamentals of MTL is important before such useful quantitative techniques may be implemented.

In BIACORE, the binding response measured can be described by two distinct processes occurring at the sensor chip surface following introduction of an analyte into the flow cell:

$$[A]_{bulk} \xleftrightarrow{Lm} [A]_{surface} \qquad (13)$$

and

$$[A]_{surface} + B \xrightarrow{k_a} [AB] \qquad (14)$$

Where $[A]_{bulk}$ = Bulk Analyte concentration (M)

$[A]_{surface}$ = Surface Analyte concentration (M)

AB = Complex

B = Ligand

L_m = Mass-transport Coefficient

The mass transport coefficient, L_m, is dependent on flow cell geometry and flow rates into the flow cell and is described by the following relationship:

$$Lm = 1.21\sqrt[3]{\frac{D^2 F}{h^2 bl}} \qquad (15)$$

Where F = Flow rate (m^3/s)

h, b, l = height, breadth and length of flow cell (m)

D = Diffusion coefficient for the analyte in solution (m^2/s)

If mass transfer of analyte from the bulk flow to the immobilised surface ligand is greater than the binding of ligand to the analyte, then the concentration of analyte in the bulk flow will be essentially the same as that at the immobilised ligand (i.e. $[A]_{bulk} \approx [A]_{surface}$). The measured response will, therefore, reflect the reaction kinetics (i.e. k_a / k_d). If the reaction is mass transport controlled the rate of binding reflects the mass transport, which is influenced by flow rates, diffusion coefficients, the flow cell dimensions and active analyte concentrations (Christensen, 1997). For a particular molecule at a given flow rate in a particular flow cell these conditions of mass transport will be constant. Provided sufficient ligand is immobilised at the chip surface for the reaction to be mass transport limited, the binding rate will reflect the active analyte concentration and can be used for concentration determinations (Karlsson *et al.*, 1993).

Under conditions of mass transport limitation (MTL), if the kinetic association rate is high, the mass transfer rate becomes limiting and the maximal slope attained (dR/dt) can be described by the following expression (Piehler *et al.*, 1997):

$$\frac{dR}{dt} \approx \frac{D[C_A]}{d} \qquad (16)$$

Where D = Diffusion coefficient for the analyte in solution (m^2/s)

$[C_A]$ = Concentration of analyte within the boundary layer (M)

d = Thickness of the boundary layer (m)

In other words, the rate of antibody binding dR/dt is dependent on the diffusion of analyte to the sensor chip surface and independent of kinetic rate constants and identity of the immobilised ligand and therefore reflects the active analyte concentration in solution.

Mass transport Limitation (MTL) can be quantitatively described by the following expresssion:

$$MTL = \frac{Lr}{Lr + Lm} \qquad (17)$$

Where

Lr = Onsager coefficient of reaction flux (m/s)

The Onsager coefficient reaction Flux is described by the following relationship:

$$Lr = k_a[B] \qquad (18)$$

From equation (17) it is evident that % MTL can be reduced by decreasing the ligand concentration [B] (i.e. decrease *Lr*), and increased by increasing the mass transfer coefficient (*Lm*) by simply increasing the flow rate of analyte into the flow cell. Inspection of equations (17) reveals that for kinetic experiments (i.e. low % MTL) the value for mass transport coefficient, *Lm*, should be high to ensure that equation (7) is maintained (i.e. ($[A]_{bulk} \approx [A]_{surface}$, use high flow rates), and also that the Onsager reaction coefficient is low (i.e. reduce surface ligand concentration [B]). To ensure mass transport limiting conditions (i.e. 100% MTL) the converse logic should be applied, that is maximal concentrations of immobilised ligand employed and the analyte introduced to the flow cell under low flow rates.

5.2 *Results & Discussion:*

5.2.1. Production of a panel of monoclonal antibodies to warfarin

Mice were initially immunised with a panel of conjugates including 4'-azowarfarin (4'-AW) thyroglobulin, 4'-AW-DST-BSA (DiSuccinimidyl Tartrate) and 4'-AW-KLH (Keyhole Limpet Haemocyanin) prepared in Freund's Complete Adjuvant. Conventional ELISA as described in section 2.11.1. was used to measure the specific antibody titre of each animal for the production of antibodies to warfarin. Dilutions of mouse serum were prepared as described in section 2.11.1. from 1/200 to 1/50,000, using the serum from pre-immunised animals as a control. The titre was described as that dilution of immunised serum giving a response greater than the control at the same dilution + 3 standard deviations. The specific antibody response to warfarin for the mice receiving the combined conjugate injection of 4'-azowarfarin-thyroglobulin/KLH, illustrated a marked increase in titre as illustrated in Figure 5.5. compared to immunisation with the individual conjugates alone. The mice were boosted and immunised approximately 4 weeks later with the same drug-protein conjugate as used for the initial immunisation. The serum antibody responses elicited in the animals receiving the combined drug-protein conjugate (i.e. 4'-AW-Thyroglobulin/KLH) were again significantly higher than immunisation with the individual conjugates alone and the conjugate mix was thus used for all subsequent immunisation procedures. The warfarin-DST crosslinked proteins were used primarily for subsequent screening steps, as the use of conjugates with different coupling chemistries is highly recommended when screening for antibodies to small haptens (Danilova, 1994).

The mice were immunised at 3-monthly intervals, and the antibody titres of four mice that had been immunised for greater than a 12-month period is illustrated in Figure 5.6. The specific antibody titres of all mice was greater than 1/250,000, a 10-fold increase in titre as compared to the initial antibody titres, and the titres measured after the first boost which were 1/25,000 and 1/35,000, respectively.

Spleen cells were then harvested from immunised mice and fused with Sp2/0 myeloma cells as described in section 2.10.7. Following the fusion procedure, hybridoma supernatants were screened approximately 10 days post fusion for specific antibody by ELISA as described in section 2.11.1. 'Positive' wells were scored on the basis of a positive result being > normal background reading + 3 standard deviations, and scaled up to 48-well plates. At this stage, supernatants were screened using 4'-aminowarfarin-DST (Disuccinimidyl tartrate) protein conjugates in a competitive immunoassay format to ensure selection of hybrids secreting

antibody specific for the hapten molecule only. Sulfo-Disuccinimidyl tartrate is a homobifunctional *N*-hydroxysuccinimide ester, which reacts with protein and target molecules via primary amine groups, resulting in a covalent bond with the release of *N*-hydroxysuccinimide. The use of a spacer arm employing a different coupling chemistry and via different amino acid residues is essential when screening supernatants for antibodies to low molecular weight compounds to ensure recognition of free antigen in solution and not a combined drug-protein epitope (Danilova, 1994; Fasciglione *et al.*, 1996).

Positive wells were then grown up in 24-well and 6-well plates and finally in culture flasks and frozen down in liquid nitrogen as described in section 2.10.5. An aliquot of cells was cloned using the method of limiting dilution (Harlow & Lane, 1988) until all of the wells demonstrating growth were shown to be secreting antibody of the desired specificity, at which stage they were considered to be statistically 'monoclonal' in nature (Lietske & Unsicker, 1985). During the screening protocol for fusion procedures, two 'positive' clones were also identified that bound to immobilised conjugate, but not free hapten in solution, although the supernatants were screened using a different carrier protein and via a different coupling chemistry. These supernatants were further screened using a variety of conjugates in an attempt to determine the particular specificity of these antibodies. The supernatant binding profiles interestingly showed increased binding to the hapten-protein conjugates over the native protein at similar coating densities, probably occurring as a result of electrostatic interactions between the antibodies and hapten-protein conjugates (Figure 5.7). The binding of these particular 'sticky'immunoglobulins to protein on ELISA plates also identified by Breen (1987) and Keating (1998), highlights the importance of screening for hapten-specific antibodies in a competitive assay format.

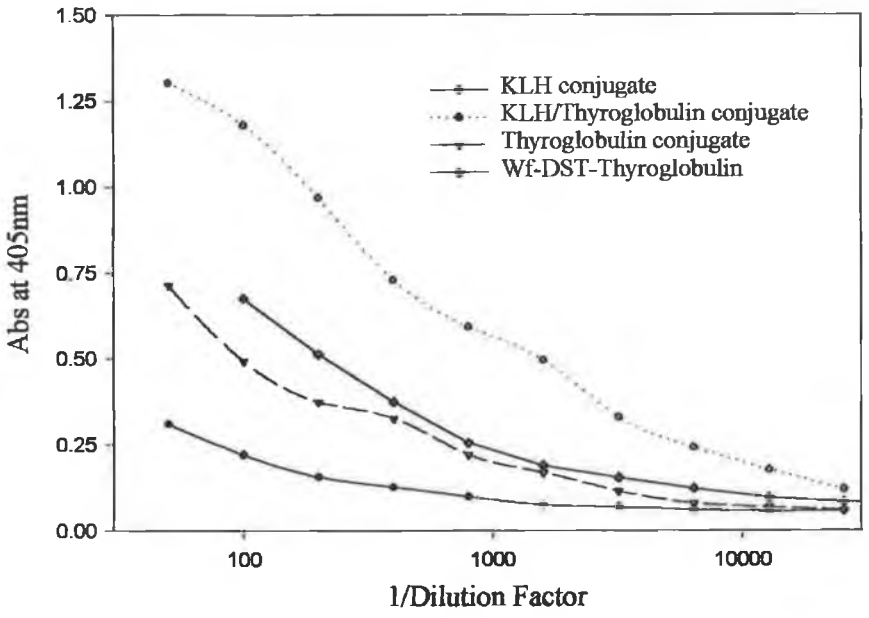

Figure 5.5: *Specific antibody titres following the initial immunisation of mice with the various warfarin-protein conjugates, namely: 4'-azowarfarin-KLH, 4'-azowarfarin-thyroglobulin, 4'-aminowarfarin-DST-thyroglobulin and a combined emulsion of 4'-azowarfarin-thyroglobulin/KLH. As the results demonstrate, mice immunised initially with the combined conjugate emulsion 4'-azowarfarin-thyroglobulin/KLH elicited a significantly greater titre than those immunised with the individual conjugates alone, showing a titre of greater than 1/30,000. These results were also evident following the second immunisation, and the combined conjugate mix was thus used for all subsequent immunisations. The results illustrated are the average of duplicate measurements.*

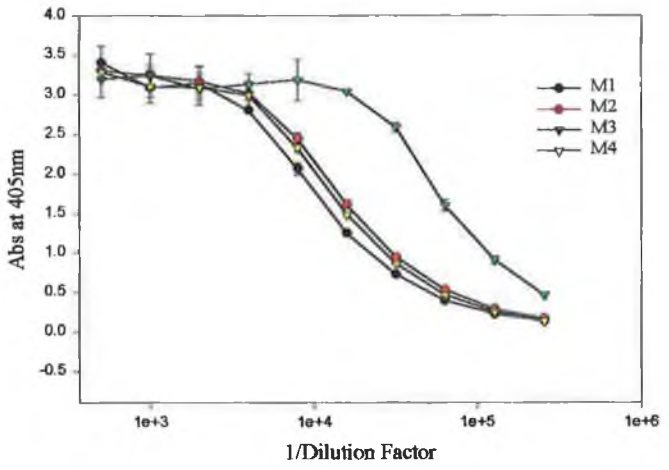

Figure 5.6: *Specific antibody titres to warfarin from mice (n=4) which had been previously immunised for greater than >12month period. The mice were boosted intraperitoneally 5 days prior to the somatic cell fusion procedure. Specific antibody titres greater than 1/250,000 were recorded for each mouse. The results shown are the average of triplicate measurements (± S.D.). Legends M1, M2, M3 and M4 correspond to the antibody titres from mice 1,2, 3, and 4, respectively.*

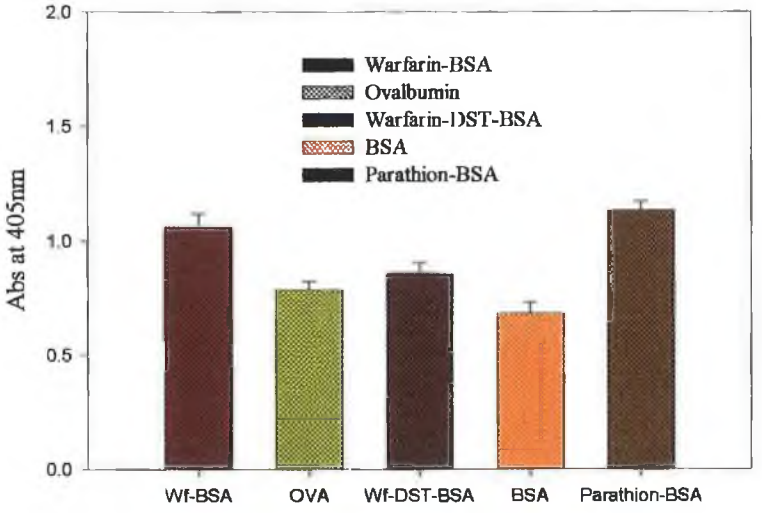

Figure 5.7: *Binding profile of clone 48-12 to various immobilised conjugates, highlighting the importance of screening in competitive assay formats to ensure selection of hapten-specific clones only. Results shown are the average of (n=6) results ± standard deviation. A similar binding profile for clone 48-13 was observed.*

5.2.2. Monoclonal Antibody Purification:

200mls of 'spent' hybridoma supernatant from each clone were concentrated using an Amicon™ filtration device as described in section 2.9.2.1. The concentrate was then passed through a Protein G/A column as described in section 2.9.2.2. The fractions were then assayed using a spectrophotometer at 280 nm, and the fractions containing protein were pooled and dialysed against several changes of PBS-2. The elution profile illustrated in Figure 5.7 for the purification of monoclonal 3-2-19 murine IgG2a on a Protein-G column is typical of that recorded for other purified clones.

The purity of the IgG fractions was assessed by HPLC-SEC (Size Exclusion Chromatography). The affinity-purified antibody fraction was analysed by size exclusion chromatography as described in section 2.6.1. The molecular weight of the antibody was estimated to be approximately 150,000 Da, by reference to a calibration curve containing standards of known molecular weight. A plot overlay of the chromatograms for affinity-purified hybridoma supernatant and standard IgG is shown in Figure 5.9 demonstrating the purity and character of the dialysed fraction.

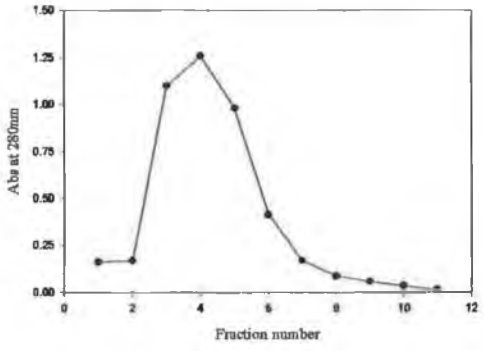

Figure 5.8: *Elution profile of monoclonal 3-2-19 following purification on a Protein G column. 20 ml of concentrated 'spent' hybridoma supernatant were applied to the Protein G column which was then washed with two column volumes of wash buffer. 0.1 M Glycine-HCl (pH 2.5) was then applied to the column and 850 µl extracts were collected in eppendorf tubes containing 150 µl of 1 M Tris-HCl (pH 8.0). The samples were then measured for protein content by recording absorbance 280 nm, and those fractions (i.e. fractions 2-7) containing immunoglobulin were pooled and dialysed against several changes of PBS-2 at 4°C.*

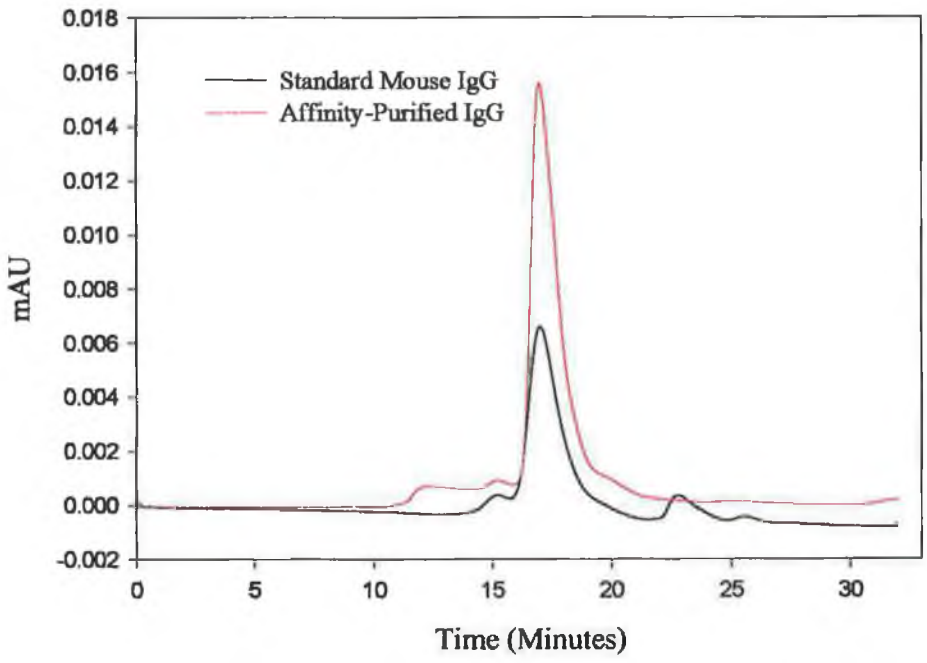

Figure 5.9: *Size exclusion chromatography of purified hybridoma mouse IgG and standard mouse IgG run on a Phenomenex SEC 3000 column (Size Exclusion Column) according to section 2.6.1. The column effluent was measured at 280 nm, using PBS-1 as mobile phase at a flow rate of 0.5 ml/min. The molecular weight of the purified immunoglobulin was estimated to be approximately 150,000 Da by reference to a calibration curve of standards of known molecular weight, the plot overlay of the purified fraction and standard mouse IgG preparation confirms the purity and identity of the purified fraction.*

5.2.3. Screening of Hybridoma supernatants:

The purified antibody fractions were then assayed for antibody activity as described in section 2.11.1. Titres of the hybridoma supernatant prior to, following concentration, and after affinity purification are shown in Figures 5.10-5.13, for each of the 4 clones characterised. The levels of antibody secreted from clones W1 and 48-5 as measured by antibody titre (Figure 5.10-5.11) were significantly lower than that of the other clones assayed, namely 2-5-16 and 3-2-19 (Figure 5.12-5.13). Clones W1 and 48-5, were 'recloned' by limiting dilution several times in an attempt to isolate 'stable' clones from the hybridoma colonies. The results showed that the number of wells producing antibody as measured by ELISA, decreased significantly following cloning at one cell per well, however, they appeared to produce 'adequately' following cloning at 10 cells per well. It was thought that the low levels of antibody production may have been a result of mycoplasma infection and the hybridoma cells were cultured in antibiotic-free media and screened for mycoplasma. The results following staining with Hoechst 33258 showed no evidence of infection.

Attempts were also made to enhance the levels of monoclonal antibody production by growth as an ascitic fluid in mice. The antibody titre following ascitic fluid development shown in Figure 5.10 demonstrates a 10-fold increase in the antibody titre obtained, giving a final titre of greater than 1/50,000. Hybridoma growth as ascitic fluid has also been shown to be useful as a means of ridding cells of mycoplasma infection (Carroll & O'Kennedy, 1988). Following growth as ascitic fluid, the hybridoma cells were aseptically collected and cultured *in vitro* and recloned by limiting dilution. There was a slight increase (~15%) in the levels of antibody production achieved following cell culture of the hybridoma cells grown as an ascitic fluid as seen in Figure 5.14, compared to cells cultured *in vitro* continually. Cloning of the hybridoma cells following growth as ascitic fluid and *in vitro* culture did not prove successful, however, in increasing the number of positive antibody-secreting clones in the masterwells, and it was thus concluded that these two particular hybridomas were 'low secretors' in terms of antibody production.

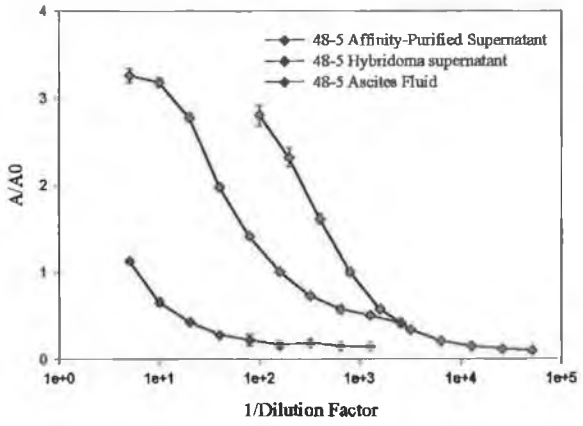

Figure 5.10: *Typical antibody titres from 'spent' hybridoma medium from clone 48-5 were approximately 1/600, which increased to 1/6000 following concentration and affinity purification. Following growth of the hybridomas as an ascitic fluid the antibody titre increased to over 1/50,000. However, this was still considerably lower than that obtained with other hybridoma lines (Figure 5.12-5.13). The results shown are the average of triplicate results ±S.D.*

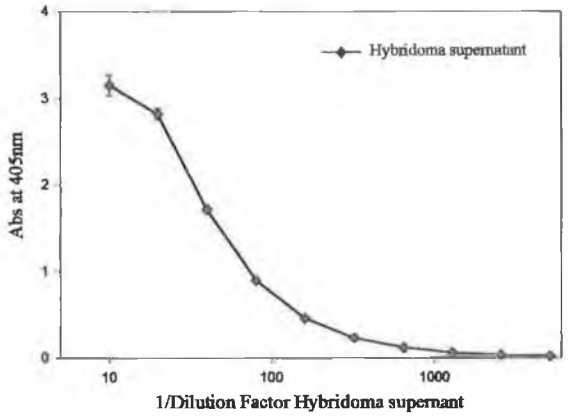

Figure 5.11: *Typical hybridoma supernatant titre for clone W1, which was greater than 1/1200. This titre was considerably less than that obtained with other clones assayed (namely 3-2-19 and 2-5-16) and various attempts to increase the levels of secretion through repeated cloning to try and isolate stable clones proved unsuccessful. W1 and 48-5 were thus considered to be 'low secretors' in terms of antibody production. The results shown are the average of triplicate results ±S.D.*

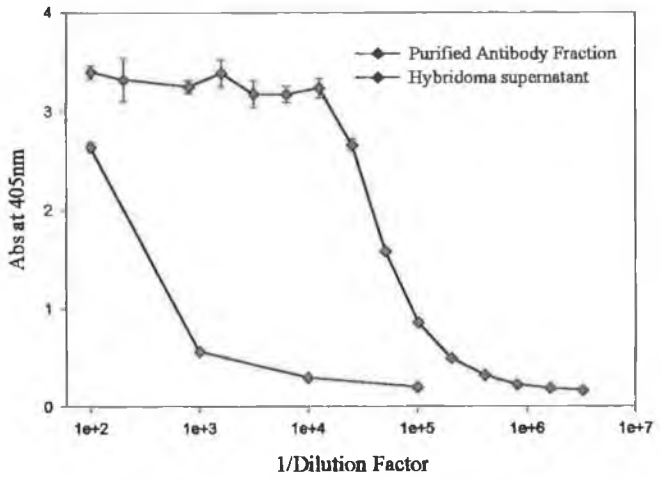

Figure 5.12: *Typical antibody titre for clone 2-5-16 from 'spent' hybridoma supernatant and affinity-purified antibody sample were greater than 1/10,000 and 1/200,000, respectively. Results shown are the average of triplicate measurements ± S.D..*

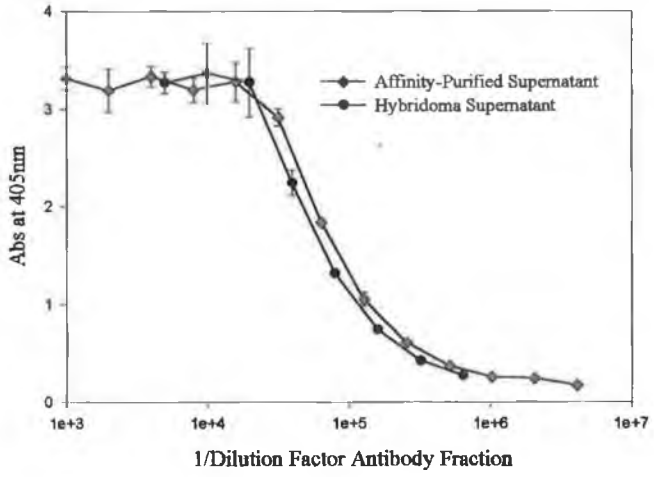

Figure 5.13: *Typical antibody titre for clone 3-2-19 from 'spent' hybridoma supernatant and affinity-purified antibody sample were greater than 1/10,000 and 1/200,000, respectively. Results shown are the average of triplicate measurements ± S.D. Clone 3-2-19 was a particularly high secretor, with typical antibody 'spent' hybridoma antibody concentrations ≈ 35 μg/ml (section 5.2.4).*

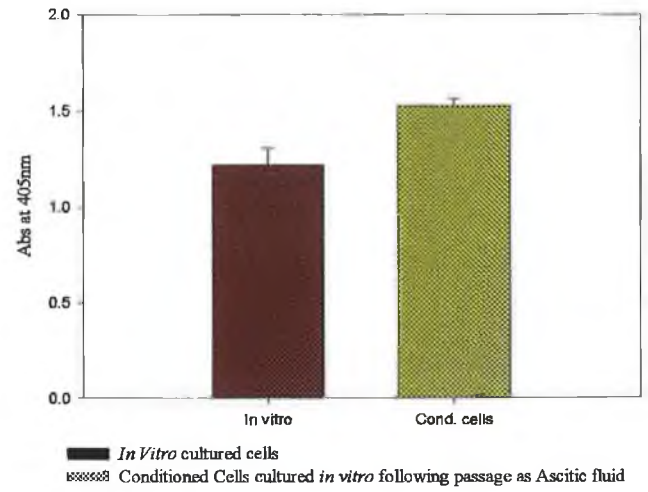

Figure 5.14: *Titres from cells from clone 48-5 cultured in vitro, and conditioned cells following growth as ascitic fluid and cultured in vitro. Dilutions (1/10) of supernatants from both sets of cells were titrated for antibody as described in section 2.11.1. Results show an increase (~15%) in antibody titre and although statistically significant ($\alpha = 0.05$), the levels of antibody recorded were still significantly less than those recorded for other clones, and no significant increase in the number of 'positive' antibody-secreting clones following cloning by limiting dilution was achieved. This clone, 48-5, and clone W1, were thus concluded to be 'low secretors' of antibody.*

5.2.4. Antibody Concentration Determinations:

The exact concentration of antibody must be initially known for accurate determinations of equilibrium affinity constants on BIACORE. Affinity-based techniques such as ELISA and other biosensor-based techniques provide a unique means of determining the biologically active concentration of antibody, unlike spectroscopic techniques that provide total protein concentrations, and consequently inaccurate thermodynamic constants. Antibody concentrations in purified and neat hybridoma supernatants were determined using the Universal Standard Curve method of Karlsson *et al.* (1993) on BIAcore described in section 2.12.5, and also using a well-based ELISA capture system employing purified polyclonal anti-mouse immunoglobulin (M6149) as the capture antibody described in section 2.11.7.

5.2.4.1. Mouse IgG Determination by Antibody Capture ELISA:

Goat anti-mouse immunoglobulin (M6149) was initially purified on a Protein-G sepharose column as described in section 2.9.2.2. The concentration of protein in the purified fraction was estimated by means of UV absorbance at 280 nm (1 mg/ml IgG $O.D._{280\ nm} \approx 1.35$) (Hudson & Hay, 1988). The wells of an ELISA microtitre plate were coated with a solution containing approximately 10 µg/ml anti-mouse immunoglobulin (M6149) in PBS-1, and blocked as described in section 2.11.1. Serial dilutions of murine IgG of known concentration ranging from 3.90-1000 ng/ml were prepared in blocking buffer. Dilutions of affinity-purified antibody and 'spent' hybridoma supernatant ranging from 1/2000 to 1/16000, and 1/1000 to 1/4000, respectively, were also prepared. The known concentrations of murine IgG and the dilutions of hybridoma supernatant and affinity purified antibody were then added to the wells of the microtitre plate and the ELISA was then developed as described in section 2.11.1. The concentration of antibody in both the purified antibody fraction and the hybridoma supernatant were calculated by constructing a standard curve of known mouse immunoglobulin concentration (µg/ml) versus absorbance at 405 nm. A cubic spline calibration plot was constructed using BIAevaluation 3.1 software™, and a linear standard curve was also constructed. From the results from the cubic spline calibration plot concentration of antibody in the affinity-purified fraction for clone 3-2-19 was calculated to be approximately 0.56 ± 0.04 mg/ml, and the concentration in the hybridoma supernatant to be approximately 35.70 ± 0.7 µg/ml. Linear regression analysis determined the concentrations of immunoglobulin for purified antibody and the hybridoma supernatant to be 0.62 ± 0.04 mg/ml and 30.25 ± 6.4 mg/ml, respectively, as shown in Table 5.2:

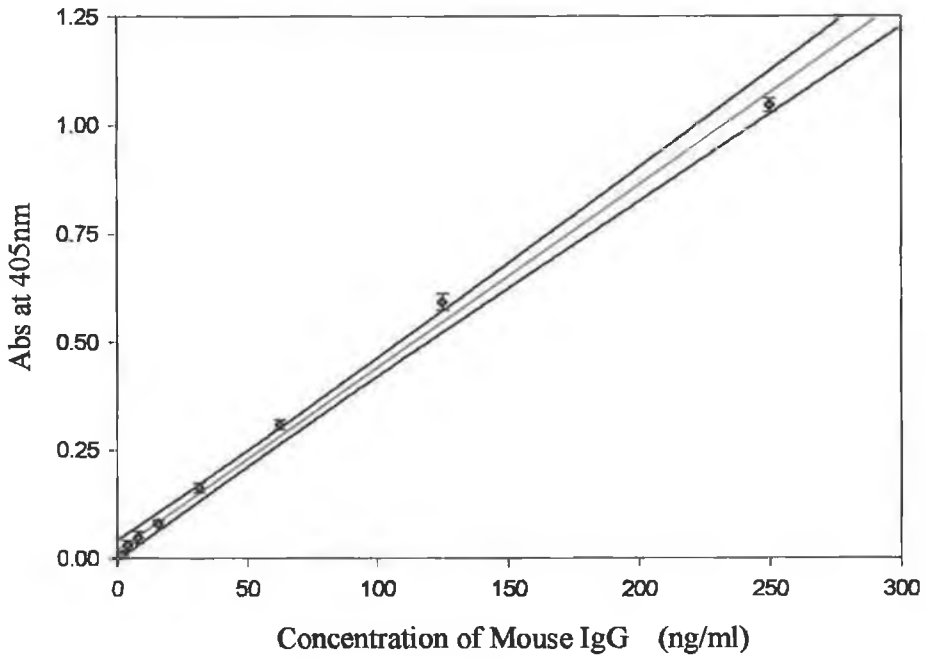

Figure 5.15: *Calibration plot for the determination of mouse IgG concentrations in Protein G-purified antibody fractions and 'spent' hybridoma supernatant. Goat anti-mouse IgG was used as capture antibody. Dilutions of mouse IgG of known concentration from 1,000 to 3.90 ng/ml were prepared, as were serial dilutions of purified antibody (1/1,000-16,000), and 'spent' hybridoma supernatant (1/1,000-4,000), and applied to the wells of an ELISA plate as described as in section 2.11.7. Using regression analysis the concentration of mouse IgG in the purified antibody fractions and that of 'spent' hybridoma supernatant were calculated and shown in Table 5.2. Each point on the calibration curve is the average of three replicates ±S.D.*

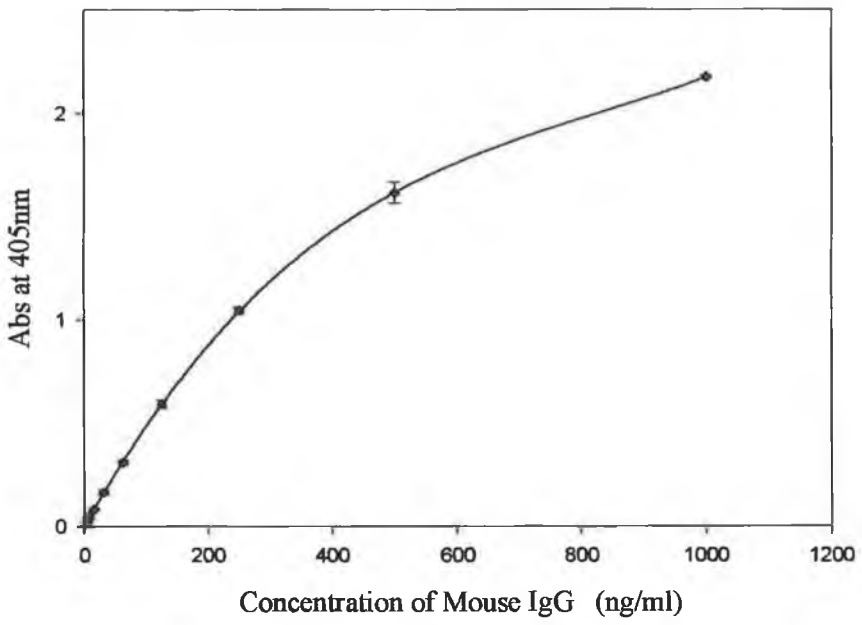

Figure 5.16: *Mouse IgG calibration plot constructed using BIAevaluation™ software. A spline is fitted to the data set for non-linear plots, allowing for the calculation of the mouse IgG in the affinity-purified and neat hybridoma fractions. Each point on the curve is the average of three replicates ± S.D.*

5.2.4.2. Universal standard Curve:

Under conditions of mass transfer limitation (MTL) the rate of antibody binding (dR/dt) is independent of the identity and concentration of the immobilised antigen and can be used for the evaluation of active antibody concentrations in solution (Karlsson *et al.*, 1993). Conditions of MTL may be confirmed by comparing the antibody binding rates on surfaces with different immobilised ligand densities, which should be identical under conditions of mass transport limitation. The technique can also be used as a means of monitoring specific antibody titres, and able to discriminate between the specific antibody class (Karlsson *et al.*, 1993).

The concentrations of the Protein G affinity-purified antibody and neat hybridoma supernatants were evaluated using the Universal standard curve method as described in section 2.12.5. 4'-aminowarfarin was directly immobilised as described in section 2.12.2.2., in order to attain as high as possible a ligand density on the sensor chip surface to fulfil

conditions of MTL. Immobilisation of a sufficiently high ligand density to fulfil conditions of MTL can be difficult to achieve with hapten-protein conjugates with low isoelectric points (e.g. 4'-azowarfarin-BSA). The purified antibody fraction and the neat hybridoma supernatant were serially diluted in HBS buffer (running buffer) and passed sequentially over the derivatised sensor chip surface and regenerated between antibody pulses by 25mM HCl. To assess the degree of non-specific binding of media to the sensor chip surface, dilutions were also made of fresh tissue culture media. These values were then subtracted from the values obtained for 'spent' hybridoma supernatant.

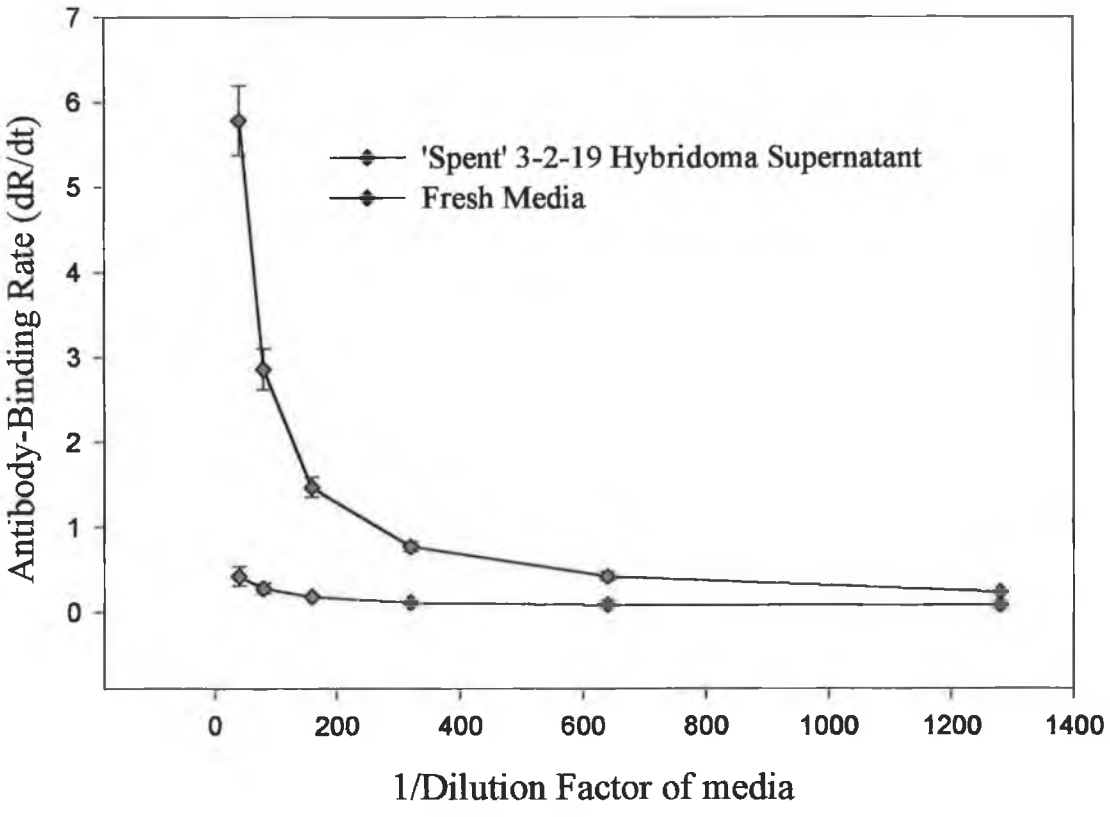

Figure 5.17: *Plot of antibody-binding rate (dR/dt) versus dilution factor of media used. Dilutions of 'spent' hybridoma supernatant and fresh media were passed over the surface at 10 µl/min under conditions of mass transport limitation, and the binding rate dR/dt calculated. The non-specific binding rate was subtracted from the measured hybridoma binding rate for the purpose of active antibody concentration determinations.*

The slope of each binding curve (dR/dT) was calculated, and a plot of binding rate (dR/dt) versus the log of antibody dilution (Log(DF)) constructed, from which the slope, m, could be calculated. According to Karlsson *et al.* (1993) the following mathematical model can be applied to concentration measurements.

$$Log\frac{dR}{dT} = mLog(C_A)(nM) \qquad (19)$$

Where

m = slope of regression line

$$Log\frac{dR}{dt} = mLog(DF) \qquad (20)$$

where DF = Antibody Dilution factor

From the constructed plots of log of antibody-binding rate (dR/dt) versus log dilution factor, the concentration of antibody in the purified fractions and neat hybridoma supernatant were determined by substituting the slope of regression line into equation (19). The antibody concentration of hybridoma supernatant and affinity-purified samples are tabulated in Table 5.2. Under similar conditions of MTL, a single antibody curve can thus be used for various antibody concentration determinations. The slope of the line is dependent on mass transfer coefficients (Lm), and will thus have to be recalculated under different flow rates and flow cell dimensions as described in equation (15).

The calculated concentration measurements for the purified antibody fraction and hybridoma supernatant for hybridoma 3-2-19 correlate closely with the values measured using the mouse IgG capture ELISA. The Universal standard Curve method of Karlsson *et al.* (1993), has several advantages over the ELISA capture assay in that active antibody concentrations can be determined over a much shorter time interval, as measurements can be taken in early part of binding curve (i.e. under conditions of MTL during first 30 seconds) versus hours for the ELISA, and also that the procedure is fully automated. One drawback of the Universal standard curve method is that conditions of MTL may be difficult to establish for antibodies with low association rates ($<10^{-5}\,M^{-1}s^{-1}$).

Table 5.2. *Antibody Concentration Determinations:*

Sample	***Affinity Capture Antibody Assay (μg/ml ± S.D.)***	***Universal Standard Curve Method (μg/ml ± S.D.)***
3-2-19: Hybridoma supernatant	35.70 ± 0.70 (S) 30.25 ± 6.40 (L)	36.98 ± 1.09
3-2-19: Purified Antibody fraction	560.0 ± 40.0 (S) 620.0 ± 40.0 (L)	570.0 ± 35.0

The concentration of antibody was determined using an affinity capture ELISA and the Universal Standard curve method. The concentration of antibody in the two fractions was determined by ELISA using two different calibration curves, namely a cubic spline (S) and a linear regression line (L). The mean antibody concentration in the affinity-purified and hybridoma supernatant fractions were 583.33± 32.14 μg/ml and 34.31 ± 3.57 μg/ml, respectively.

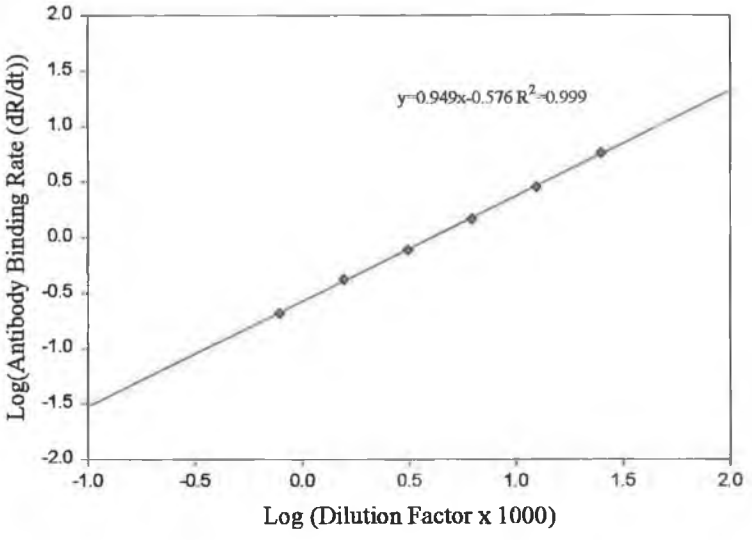

Figure 5.18: *Antibody concentration were determined using the Universal standard curve method of Karlsson et al. (1993). The slope of the regression line was substituted into equation (19) and used to determine the concentration of active antibody in 'spent' hybridoma supernatant for clone 3-2-19. Results shown are the average of 5 replicate measurements.*

5.2.5. Use of panel of monoclonal antibodies in competitive ELISA:

Protein G affinity-purified monoclonal antibody from each of the individual hybridoma clones was used in a competitive ELISA format for the detection of warfarin in solution as described in section 2.11.5. The optimal working dilution of antibody to be employed for competitive immunoassay procedures was determined from the antibody dilution curves obtained for each clone from Figures 5.10-5.13.

Immunoassay response curves are inherently non-linear and adopt a sigmoidal bell shape on log-linear plots (Findlay *et al.*, 2000). Immunoassays are generally best modelled using a four-parameter fit equation, of the form:

$$R = R_{HI} - \frac{R_{HI} - R_{LO}}{1 + \left(\frac{Conc}{A_1}\right)^{A_2}} \qquad (21)$$

Where R_{HI} = Response at infinite concentration

R_{LO} = Response at zero concentration

$Conc$ = Analyte Concentration (M)

A_1 = Fitting constant

A_2 = Fitting constant

Four-parameter equations of the form above were fitted to the data sets obtained for immunoassays curves using BIAevaluation 3.1 software. Such calibration curves also allowed for the determination of unknown values from the constructed plot. In this way it was possible to calculate the degree of precision of analytical measurements at different concentrations points relative to the fitted four-parameter equation.

Fitting a four-parameter curve to the data set as opposed to utilising the straight line portion of the sigmoidal plot conventionally obtained with ELISAs, greatly extends the working range of the plot at the asymptotes of the curve for both ends of the concentration range employed. 4-parameter curves were fitted to the data obtained using BIAevaluation software™. A comparison of the extended working range obtained can be observed in Table 5.3 and 5.4 and Figures 5.19 and 5.20, which illustrates that the working range of the ELISA has been extended by a factor of 4 at each end of the calibration plot with no significant effect on the degree of assay precision.

To determine the intra-assay variation of the ELISA, 4 replicate measurements per concentration point were used. These absorbance values (A) were then divided by the absorbance measurement in the presence of zero antigen concentration (A_0) to give normalised absorbance values (A/A_0)(Appendix 1A). A calibration plot of the mean normalised absorbance value versus warfarin concentration in ng/ml was then constructed using BIAevaluation software™. From the calibration curve it was possible to calculate the mean, standard deviation, coefficient of variation and precision for intra-assay measurements. The results are shown in Table 5.3 for clone 3-2-19.

The inter-assay variation was calculated by performing the assay over three separate days. A separate calibration curve plotting normalised values (A/A_0) versus concentration values (ng/ml) was then constructed for each assay curve. The normalised values from each curve for each concentration determination were then back-calculated using the calibration curve and BIAevaluation software. The mean back-calculated concentration from each of the calibration curves was then used to calculate the mean, standard deviation and coefficient of variation for the inter-assay curve. Residual plots for the calibration curves are included for each calibration curve, which illustrate the 'goodness of the fit' of the applied 4-parameter equations. The residual plots also illustrate the precision profile of the calibration curves over the assayed concentration range and illustrate that the 4-parameter equation demonstrates no bias over the assayed concentration range, unlike linear plots which have a tendency to demonstrate increased bias at the extremities of the linear plot.

Table 5.3: *Intra-Assay results for Clone 3-2-19 (n=4) curve:*

(From 4-parameter fit curve constructed using BIAevaluation software)

Actual Warfarin Concentration (ng/ml)	Mean Back Calculated Warfarin Concentration from calibration curve (ng/ml)	% C.V.	% Difference Accuracy
312.50	315.84	5.99	1.07
156.25	161.22	8.02	3.18
78.13	73.43	21.95	-6.01
39.06	39.24	9.10	0.45
19.53	21.02	1.12	7.62
9.77	8.81	2.23	-9.79
4.88	5.32	1.00	8.95
2.44	2.36	1.80	-3.33
1.22	1.21	3.23	-0.87

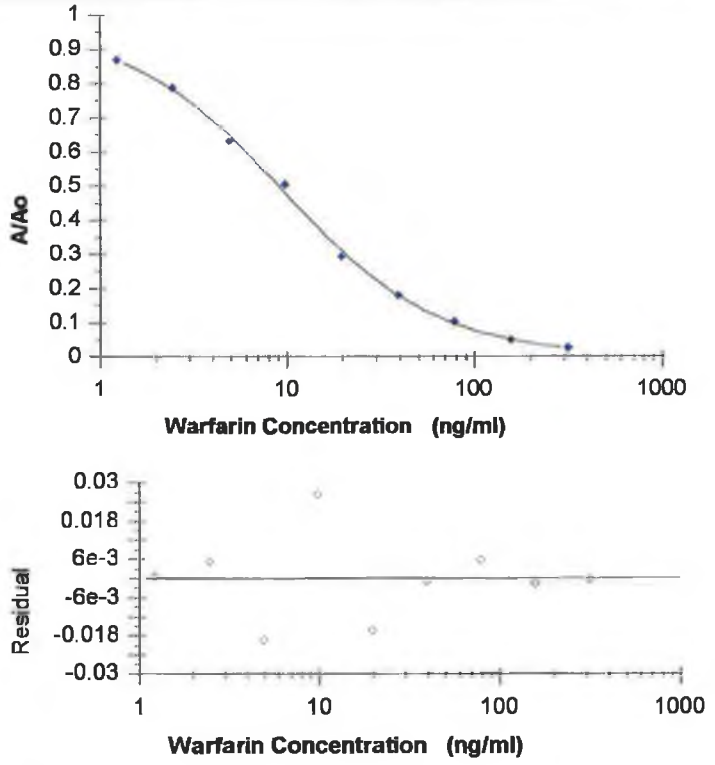

Figure 5.19*: Intra Assay Spline Curve & Residual plot:*

A 4-parameter equation was fitted to the data using BIAevaluation software™, from which the intra-assay mean, coefficient of variation and precision were calculated and shown in Table 5.3. Each point on the curve is the mean of (n=4) replicate measurements. The residual plot and low χ^2 value obtained (2.80×10^{-4}) demonstrates the 'goodness of the fit' of the 4-parameterfit applied to the data set.

Table 5.4: *Intra-Assay results for Clone 3-2-19 (n= 4) using linear regression:*

Actual Warfarin Concentration (ng/ml)	Mean Back Calculated Warfarin Concentration (ng/ml)	% C.V.	% Difference Accuracy
39.06	37.28	9.10	-4.78
19.53	22.27	0.30	12.3
9.76	8.76	0.51	-12.6
4.88	4.99	0.63	2.10
2.44	2.46	0.78	0.75

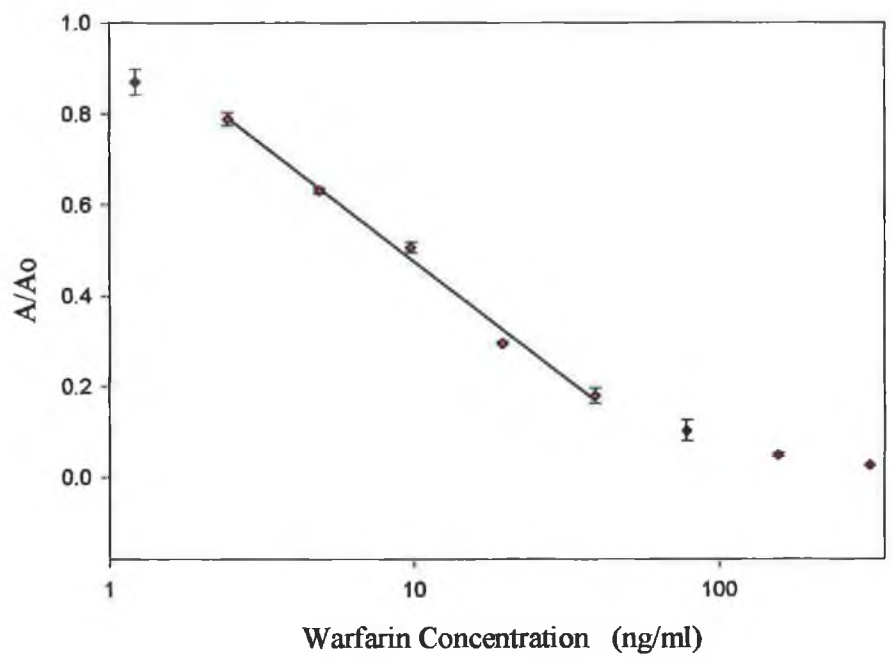

Figure 5.20*: Intra Assay Curve:*

Linear regression analysis was applied to the data set giving the line of best fit, from which the intra-assay mean, coefficient of variation and precision were calculated and shown in Table 5.4. Each point on the curve is the mean of (n=4) replicate measurements ± standard deviation.

Table 5.5: *Inter-Assay results for Clone 3-2-19 (n=3):*

Actual Warfarin Concentration (ng/ml)	Mean Back Calculated Warfarin Concentration from spline curve (ng/ml)	% C.V.	% Difference Accuracy.
500.00	494.80	13.39	1.04
250.00	239.10	14.37	4.36
125.00	125.92	12.44	-0.74
62.50	62.56	9.68	-0.10
31.25	31.90	9.90	-2.09
15.63	15.48	8.32	0.92
7.81	7.62	8.98	2.41
3.91	3.92	4.07	-0.32
1.95	2.23	4.82	-14.36

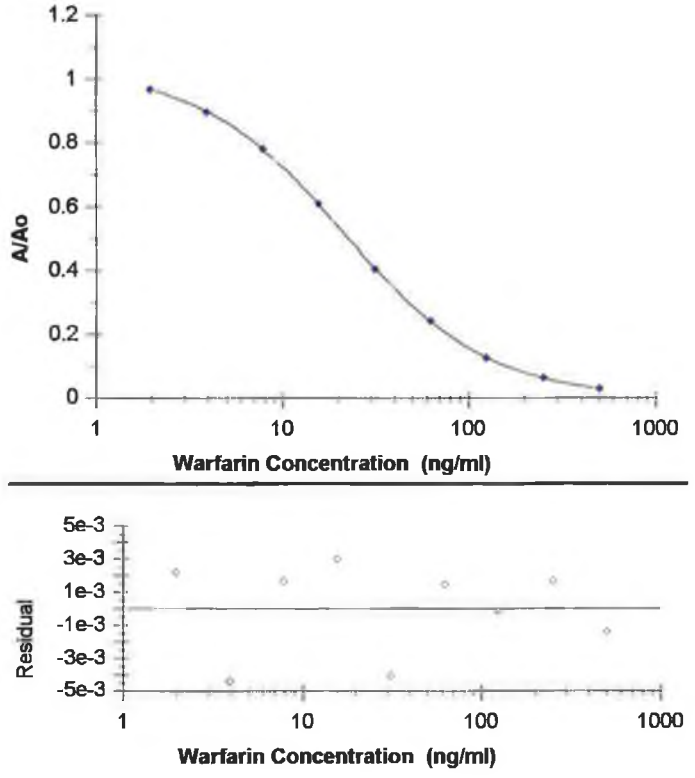

Figure 5.21: *Mean Inter-assay calibration curve*

The mean normalised absorbance value at each drug concentration was calculated for each of the intra-assay curves (n=4), was then used to calculate the inter-assay mean (n=3), coefficient of variation and precision. Each point on the curve is the mean of triplicate measurements ± standard deviation (n=3).

Table 5.6.:Intra-Assay results for Clone 48-5 (n= 4):

Actual Warfarin Concentration (ng/ml)	Mean Back Calculated Warfarin Concentration from spline curve (ng/ml)	% C.V.	% Difference Accuracy
3125	3369.56	4.14	7.83
1562.50	1546.82	2.99	-1.00
781.25	753.64	1.79	-3.53
390.63	400.34	1.26	2.49
195.31	196.53	1.26	0.62
97.656	95.10	1.39	-2.61
48.828	45.74	1.83	-6.28
24.4	22.93	1.17	-6.02

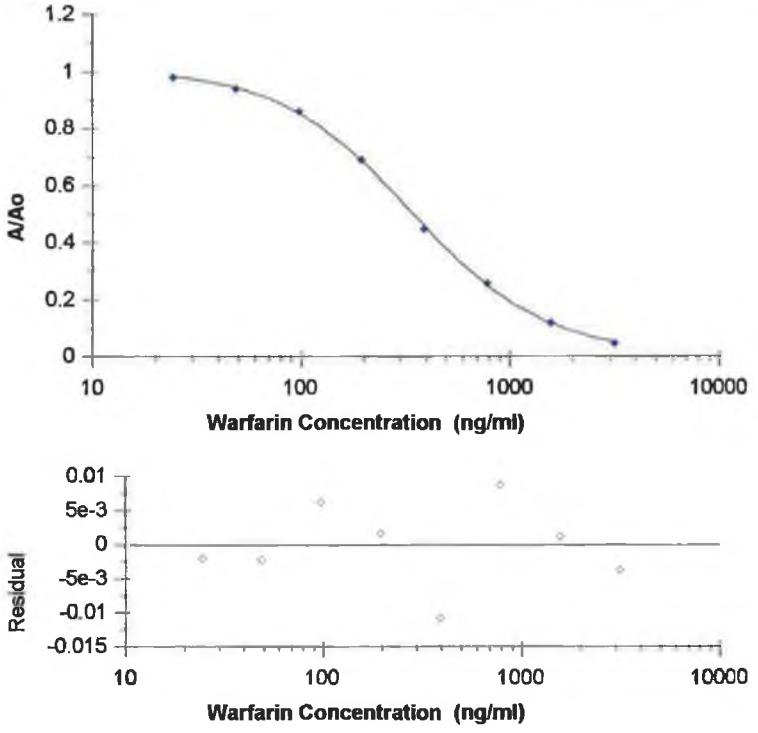

Figure 5.22: *Intra Assay curve for warfarin with clone 48-5*

The intra-assay mean, coefficient of variation and precision were calculated from the calibration curve using the software and shown in Table 5.6. Each point on the curve is the mean of (n=4) replicate measurements ± standard deviation

Table 5.7:*Intra-Assay results for Clone W1 (n= 3):*

Actual Warfarin Concentration (ng/ml)	Mean Back Calculated Warfarin Concentration from spline curve (ng/ml)	% C.V.	% Difference Accuracy
3.91	3.92	1.23	0.37
7.81	7.80	0.10	-0.12
15.62	15.32	0.13	-1.95
31.25	33.06	2.70	5.78
62.5	59.08	2.99	-5.46
125.0	120.77	9.11	-3.38
250.0	273.76	8.44	9.50
500.0	502.35	12.49	0.46

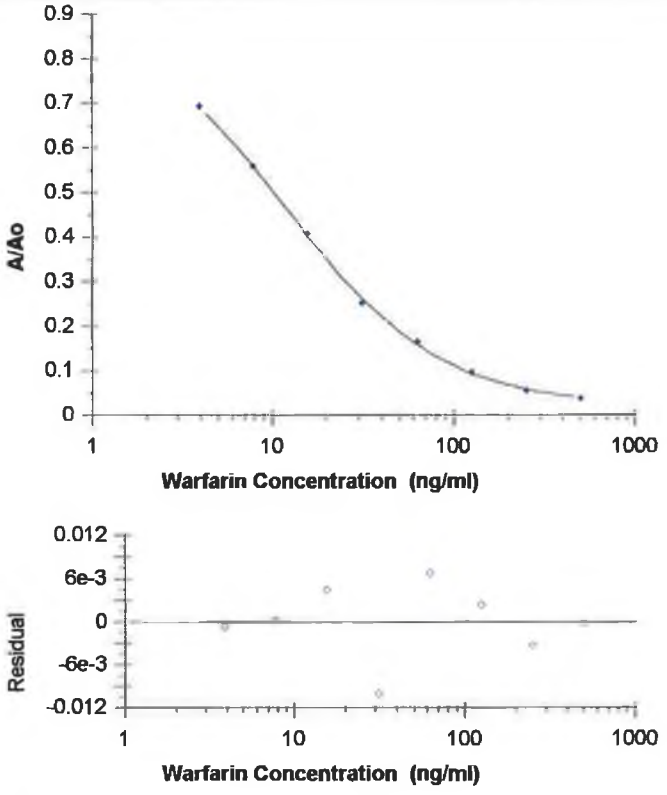

Figure 5.23:*Intra assay spline curve for clone W1*

Each point on the curve is the mean of triplicate measurements (n=3). The intra-assay mean, coefficient of variation and precision were calculated from the calibration curve using the software and shown in Table 5.7.

5.2.6. Affinity Constants determinations:

Various techniques are available for the determination of antibody affinity constants including equilibrium dialysis (Lehtonen & Eerola, 1982), polyethylene glycol precipitation (Stanley *et al.*, 1983), affinity chromatography (Chaiken *et al.*, 1992), and those involving the use of enzyme-linked immunosorbent assay (Friguet *et al.*, 1985; Chu *et al.*, 1995). These techniques rely on the concentration measurement of either analyte or antibody:antigen complex at equilibrium for determination of overall affinity constants.

Two antibodies with similar affinity constants (Ka) may possess completely different kinetic constants, which can be of considerable significance depending on the intended use of the antibody. The use of 'real-time' biomolecular interaction analysis is a useful means of affinity ranking antibodies, and can also be used early in the selection process as a screening device for the selection of particular antibodies (monoclonal/scFv) based on their individual kinetic rate constants (Deuñas *et al.*, 1996).

5.2.6.1. Method of Friguet et al. (1985):

The method described by Friguet *et al.* (1985) was used to assess the affinity of the monoclonal antibodies raised to warfarin and structurally related analogues, by calculation of the dissociation constant (K_D) of antibody:antigen mixtures at equilibrium in solution. For determination of overall affinity constants, antibody at a constant concentration is mixed with solutions of antigen of varying concentration. The antibody: antigen mixtures are allowed to attain equilibrium and the 'bound' concentration of antibody (V) can then be calculated by indirect ELISA as described in section 2.11.6. by the expression:

$$V = \frac{A_0 - A_1}{A_0} \qquad (22)$$

Where A_0= Absorbance in the absence of antigen

A_1= Absorbance in the presence of antigen

The concentration of bound antibody can be related to the antigen concentration by the following equation:

$$\frac{1}{V} = \frac{KD}{Ag} + 1 \qquad (23)$$

A plot of 1/(V) versus 1/[Ag] will thus yield a straight line graph with a y-intercept of 1, with the slope of the regression line (K_D), describing the overall equilibrium constant for the antibody: antigen interaction at equilibrium.

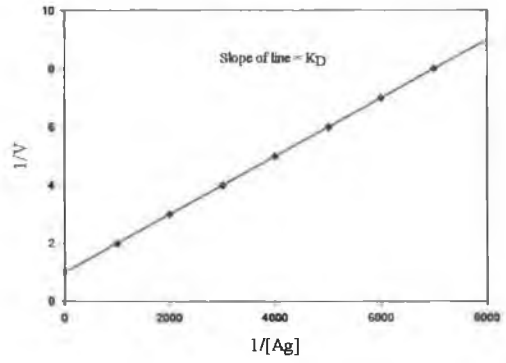

Figure 5.24: *Typical plot attained using the method of Friguet et al. (1985). A plot of the reciprocal of bound antibody (1/V) versus the reciprocal of antigen concentration (1/[Ag]) should yield a straight line plot with a y-intecept of 1 and whose slope defined the dissociation constant for the particular antibody: antigen interaction at equilibrium.*

For the method to provide reliable dissociation constants two prerequisites must firstly be met. The first prerequisite is to demonstrate the correlation between 'free' (i.e. unbound) antibody concentration in solution and enzymatic activity, and adding various dilutions of antibody to antigen-coated wells of an ELISA plate as described in section 2.11.6 and constructing a calibration plot of nominal antibody concentration versus absorbance. A straight line plot similar to that in Figure 5.26 of 'nominal' antibody concentration (i.e. 1/dilution factor) versus enzymatic activity at 405 nm is attained, demonstrating the linear correlation between antibody concentration and enzymatic activity. This calibration plot can then be used to calculate the concentration of antigen bound antibody at equilibrium in the antibody: antigen mixtures.

The 'free' antibody concentration, i, following incubation with the antigen can be related to absorbance by the following equation:

$$\frac{i}{i_0} = \frac{A}{A_0} \qquad (24)$$

Where A_0 = absorbance in the absence of antigen.

A = absorbance in the absence of antigen.

i_0 = total antibody concentration.

The second prerequisite is that no readjustment of the antibody: antigen equilibrium mixture should occur during the incubation in the antigen-coated wells. This can be demonstrated experimentally by placing serial dilutions of antibody into the wells of an antigen coated ELISA plate for a specified time interval, and then transferring the contents of the well into the adjacent antigen coated wells on the ELISA plate for a similar incubation period. An overlay of the plots for the developed ELISA of wells 1 and 2, as shown in Figure 5.25 should demonstrate no significant decrease in the antibody bound in the second set of wells, implying that the amount of antibody bound by the solid phase antigen is negligible compared to the amount of antibody in solution, and therefore unlikely to cause any significant displacement of the antibody:antigen mixture at equilibrium. The fraction of antibody retained by the first set of wells, f, can be calculated by the following equation:

$$f = \frac{A_1(c) - A_2(c)}{A_1(c)} \qquad (25)$$

Where

f	=	fraction of antibody retained
$A_1(c) / A_2(c)$	=	enzymatic activities in the first and second set of wells, respectively. (i.e. absorbance measurements)
c	=	initial concentration of antibody

The antigen concentration has been shown to have the greatest effect on the solid phase disruption of fluid phase equilibrium in affinity assays (Hetherington, 1990). Reducing the incubation period in the antigen-coated wells also minimises the disruption of the fluid phase equilibrium. The incubation period for each clone was determined individually, and the incubation periods on the plate were typically of the order of 15-20 minutes. The value of f calculated for clone W1, as shown in Figure 5.25, was approximately = 0.01, demonstrating that the amount of bound antibody is negligible compared to overall antibody concentration. By calculating the amount of unbound antibody at equilibrium by reference to the antibody concentration calibration plot, the amount of ligand-bound antibody (V), can thus be estimated and used to calculate the overall affinity constant.

***Table 5.8**: Calculation of free antibody concentrations.*

[Warfarin] mol/l	1/[Warfarin] l/mol 1/[Ag]	Abs at 405nm	Nominal Antibody concentration. NC	1/V
$3.246\ e^{-6}$	308000	0.029	0.022	1.02
$1.623\ e^{-6}$	616000	0.053	0.041	1.04
$8.12\ e^{-7}$	1232000	0.074	0.056	1.06
$4.06\ e^{-7}$	2464000	0.129	0.098	1.10
$2.03\ e^{-7}$	4920000	0.219	0.167	1.19
$1.015\ e^{-7}$	9840000	0.333	0.254	1.32
$5.07\ e^{-8}$	19680000	0.564	0.430	1.69
$2.54\ e^{-8}$	39380000	0.774	0.590	2.26
0	∞	1.387	1.057	∞

***Table 5.8**: Calculation of free antibody concentrations.*

The nominal concentrations of antibody were calculated by reference to the constructed antibody standard curve and substituting the value obtained into equation (22). The value for bound antibody was calculated to yield the values of 1/V, from which a plot of 1/[Ag] versus 1/V was constructed, whose slope (K_D) defined the dissociation constant K_D of the overall interaction.

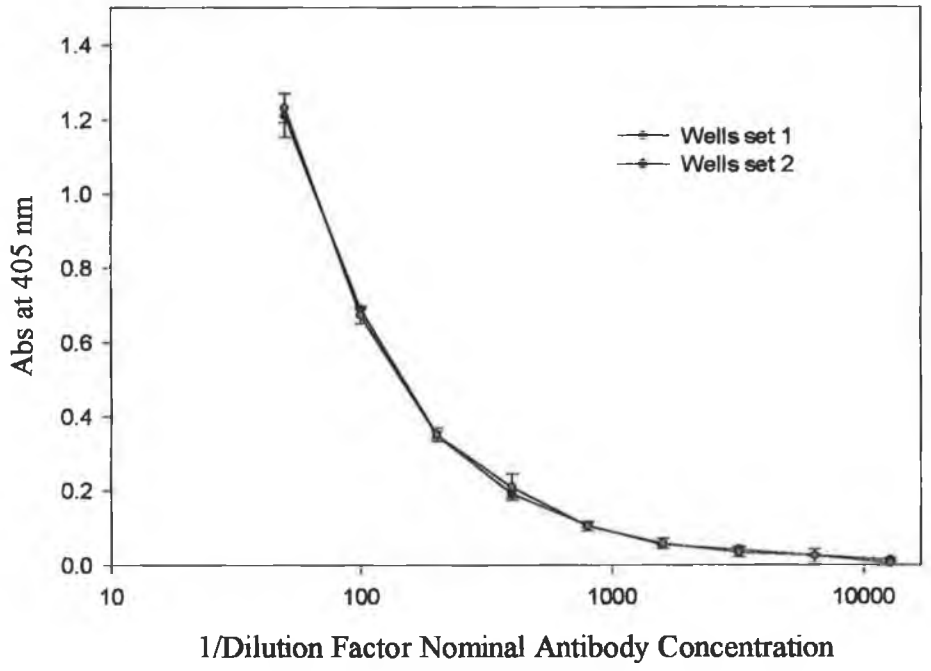

***Figure 5.25**: Antibody was applied to the wells of a microtitre plate as described in section 2.11.6. for a predetermined incubation period. A prerequisite of the Friguet assay is to ensure that there is the minimal disturbance of the antibody:antigen equilibrium mixtures in solution when transferring the equilibration mixtures to the microtitre plate. This can be determined experimentally by firstly preparing a set of antibody dilutions and applying these to a set of wells in a microtitre plate for a specified incubation period. The contents of these wells would then be transferred to a second set of wells on the same microtitre plate and the ELISA developed as described previously. The value of f, as described in equation (25), could then be calculated from the graph. By ensuring that this value is kept as close to zero as possible it can be stated that the amount of antibody bound by the plate is negligible compared to the total antibody concentration and will not disturb the fluid phase equilibrium of the the antigen:antibody complex. The results shown are the average of triplicate measurements $\pm$ standard deviation.*

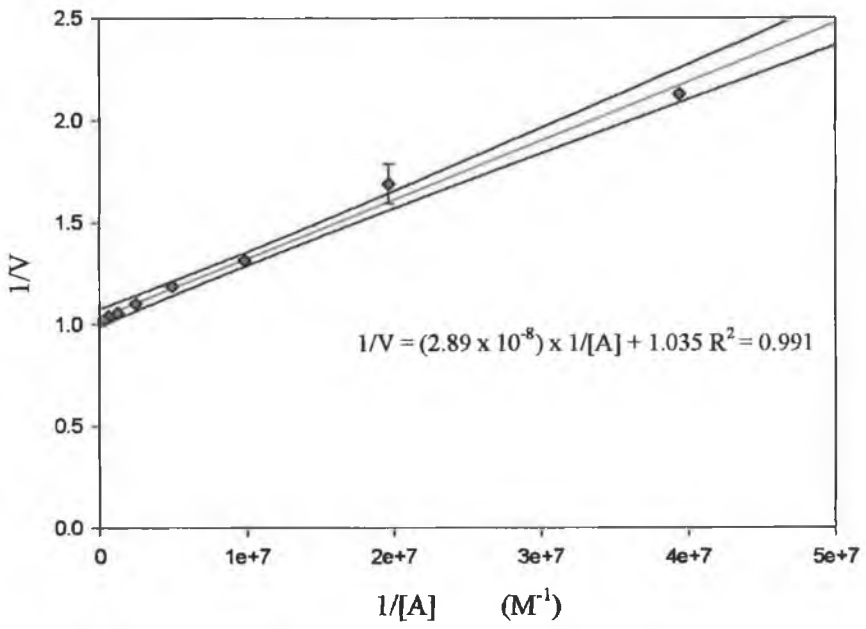

Figure 5.27: *Determination of the equilibrium dissociation constant for the interaction between warfarin and clone W1 by the method of Friguet et al. (1985). The nominal unbound antibody concentrations were calculated using the standard curve constructed in Figure 5.26, and equation (22) from which the values of 1/V were subsequently determined at the respective antigen concentrations as shown in Table 5.8. The calculated equilibrium dissociation constant for the interaction between warfarin and monoclonal antibody W1 was calculated to be 2.89 x 10 $^{-8}$ M.*

However, an antibody whether monovalently bound or completely unbound with respect to its specific antigen, will be able to bind to an ELISA plate. The concentration of antibody complex measured at equilibrium does not take into account the fact that monovalently bound antibodies may also bind to the plate. The apparent binding constant measured will therefore not equal that of the corresponding antibody Fab fragments. Stevens (1987) developed a 'correction factor' based on the binomial distribution theory to provide the 'correct' concentration of liganded antibody binding sites to allow for the calculation of the 'correct' thermodynamic constant. Stevens (1987) postulated that if the probability that a Fab binding site is bound is taken as, *z*, then the probability that the binding site is free can then be interpreted as 1-*z*. For the case of an intact IgG molecule, the following relationships

can be used to describe the three populations of antibody fractions existing within the equilibrium complex:

Completely Unbound:	$(1-z^2)$	
Monovalently bound:	$2z\ (1-z)$	
Bivalently bound:	z^2	(26)

On the basis of binomial distribution, assuming that the binding of one Fab does not preclude the binding of a second Fab (which is the case for small haptens, not necessarily true for larger molecular weight haptens due to steric hindrance factors (Quinn & O'Kennedy, 2001)), of the three antibody populations present at equilibrium, only the bivalently bound antibody, (z^2), is incapable of binding to the ELISA plate. The fraction of free antibody assayed by ELISA (m) is therefore equal to $1-z^2$.

$$m = 1 - z^2 \tag{27}$$

and

$$z = \sqrt{1-m} \tag{28}$$

represents the corrected fraction of liganded binding sites in terms of the apparent free IgG. The method of Friguet *et al.* (1985) measures the 'bound' fraction of unbound IgG (V), using the relationship:

$$V = \frac{A_0 - A_1}{A_0} \tag{23}$$

It can be seen therefore that as the concentration in equation (26) represents the bivalently bound antibody fraction, the corrected fraction of occupied antibody binding sites at any antigen concentration is given by:

$$z = \sqrt{V} \tag{29}$$

Stevens (1987) found that overall association constants were overestimated by a factor of at least 2, with the level of error inversely proportional to the level of binding site occupancy. By substituting the corrected value of liganded binding sites a more 'realistic' value of association constants is determined which takes into account the bivalent nature of the antibody giving association constants for whole IgG that closely mirror those for Fab fragments.

Table 5.9: *'Corrected' Free Antibody Concentrations according to Stevens (1987):*

[Warfarin] mol/l	1/[Warfarin] l/mol 1/[Ag]	Nominal Antibody concentration. NC	1/V	Corrected Free Antibody concentration $1/z = (1/V)^{1/2}$
$3.246\ e^{-6}$	308000	0.022	1.02	1.01
$1.623\ e^{-6}$	616000	0.041	1.04	1.02
$8.12\ e^{-7}$	1232000	0.056	1.06	1.03
$4.06\ e^{-7}$	2464000	0.098	1.10	1.05
$2.03\ e^{-7}$	4920000	0.167	1.19	1.09
$1.015\ e^{-7}$	9840000	0.254	1.32	1.15
$5.07\ e^{-8}$	19680000	0.430	1.69	1.30
$2.54\ e^{-8}$	39380000	0.590	2.26	1.50
0	∞	1.057	∞	

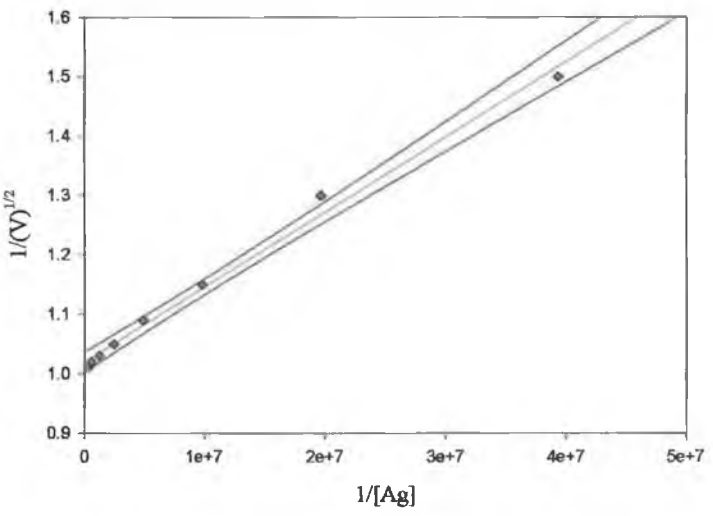

Figure 5.28: *Friguet assay for warfarin with clone W1 using 'corrected' IgG concentrations described by Stevens (1987) to account for bivalency of IgG. The corrected overall dissociation constant (K_D=1.26 x 10^{-8} M) shows a 2.3 fold increase in estimation of overall affinity constant compared to that observed for the 'uncorrected' IgG concentration shown in Figure 5.27 (K_D=2.88 x 10^{-8}M).*

The method of Friguet *et al.* (1985) it could be argued only works particularly well for high affinity antibodies, as the incubation step in ELISA must be sufficiently short not to perturb the antibody: antigen equilibrium complex, for low affinity antibodies (high off rates) such a condition can be difficult to achieve in practice. Friguet assays for the various other clones with particular antigens are shown in Figures 5.29 to 5.41 and overall affinities shown in Table 5.10.

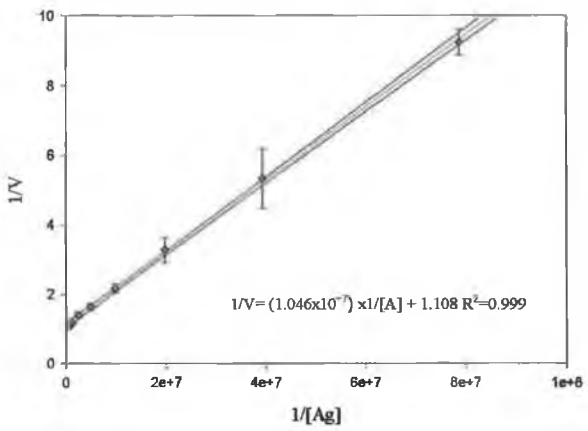

Figure 5.29: **48-5:4-Hydroxycoumarin**

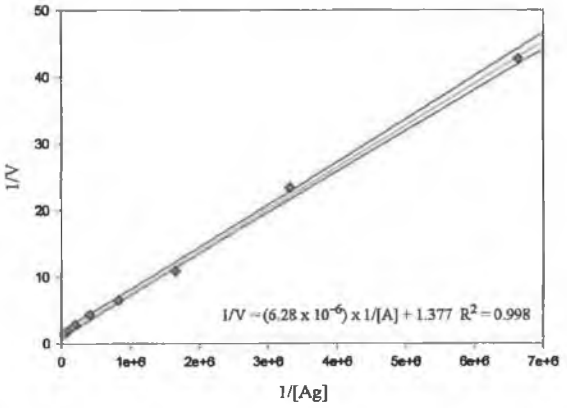

Figure 5.30: **48-5:6-Hydroxywarfarin**

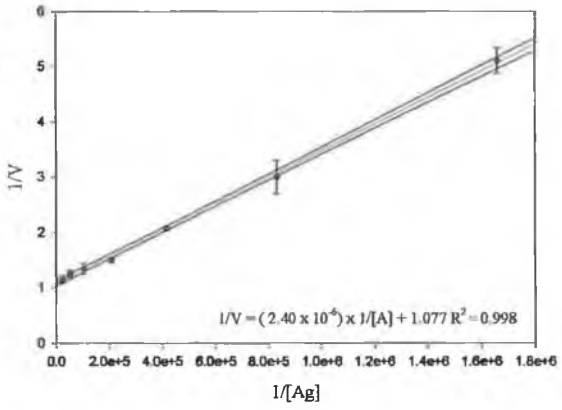

Figure 5.31: **48-5:7-Hydroxywarfarin**

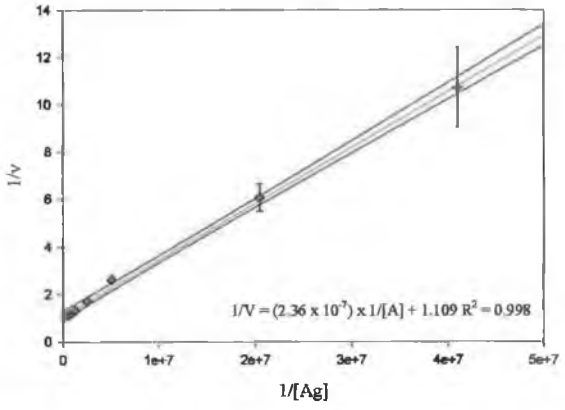

Figure 5.32: **48-5:Acenocoumarin**

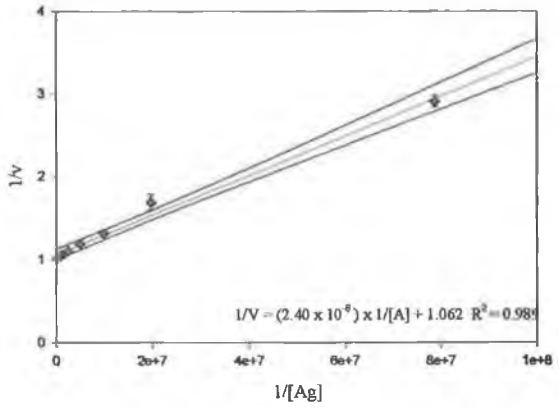

Figure 5.33: **48-5:Warfarin**

Figure 5.29-5.33: *Friguet affinity determinations of equilibrium dissociation constants for the interaction between clone 48-5 and the antigens 4-hydroxycoumarin, 6-hydroxywarfarin, 7-hydroxywarfarin, acenocoumarin and warfarin, respectively.*

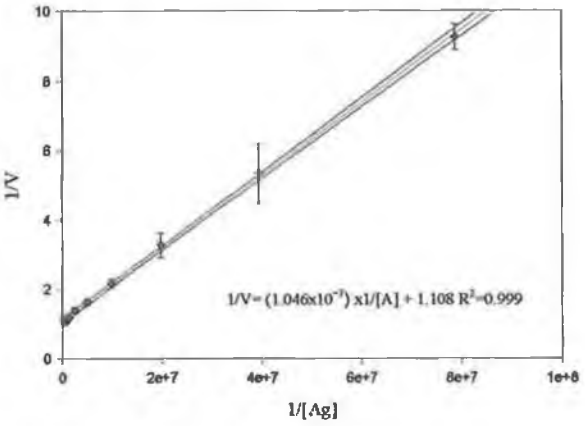

Figure 5.34: **W1:6-Hydroxywarfarin**

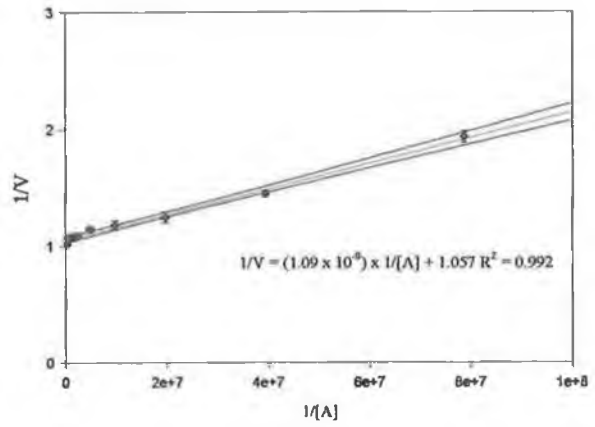

Figure 5.35: **W1:7-Hydroxywarfarin**

Figure 5.34-35: *Friguet affinity determinations of equilibrium dissociation constants for the interaction between clone W1 and 6- and 7-Hydroxywarfarin.*

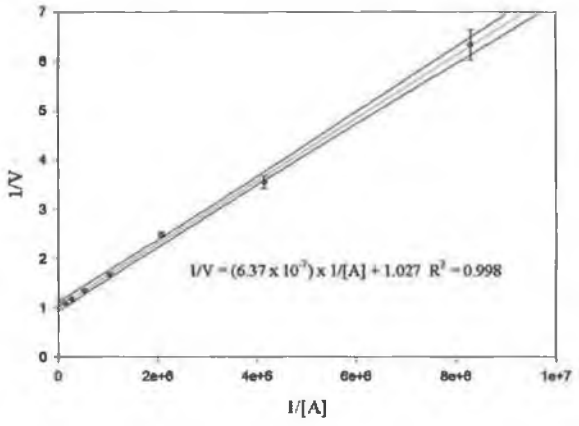

Figure 5.36: **2-5-16:4-Hydroxycoumarin**

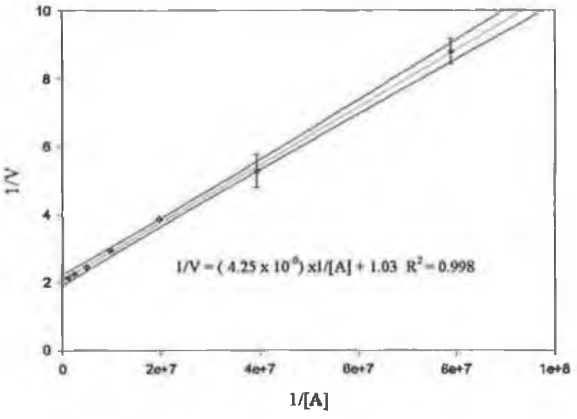

Figure 5.37: **2-5-16:Warfarin**

Figure 5.36-37: *Friguet affinity determinations of equilibrium dissociation constants for the interaction between clone 2-5-16 and 4-Hydroxycoumarin and warfarin*

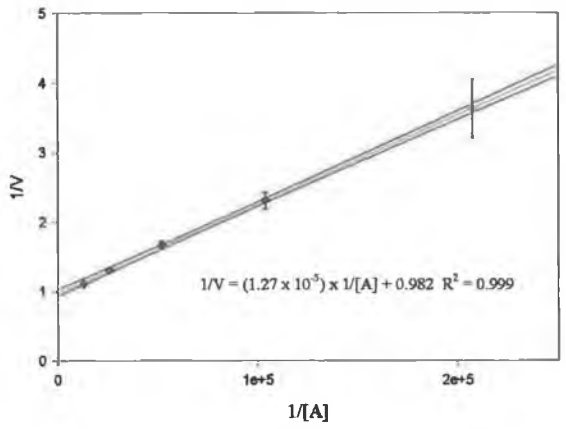

Figure 5.38: **3-2-19:4-Hydroxycoumarin**

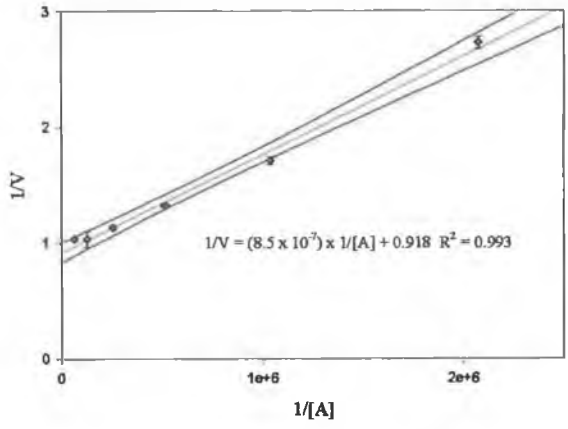

Figure 5.39: **3-2-19:6-Hyroxywarfarin**

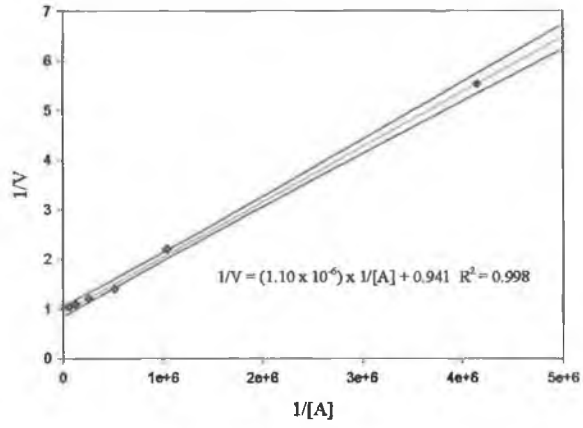

Figure 5.40: **3-2-19:7-Hydroxywarfarin**

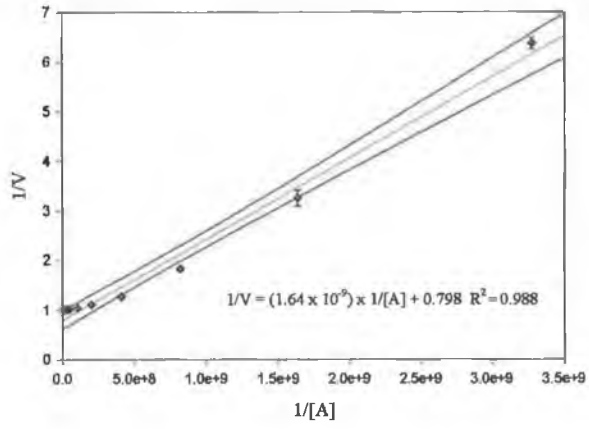

Figure 5.41: **3-2-19:Warfarin**

Figure 5.38-5.41: *Friguet affinity determination of equilibrium dissociation constant for the interaction between clone 3-2-19 and 4-hydroxycoumarin, 6-hydroxywarfarin, 7-hydroxywarfarin and warfarin, respectively.*

Table 5.10.: *Equilibrium dissociation constants (K_D) determined using the method of Friguet et al. (1985) for the interaction between warfarin and four particular monoclonal antibodies. The affinity of the monoclonal antibodies to structurally related molecules of warfarin was also measured, and the equilibrium dissociation constants determined are tabulated below:*

Antigen	***Clone W1***	***Clone 48-5***	***Clone 3-2-19***	***Clone 2-5-16***
Warfarin	2.89×10^{-8}	2.39×10^{-8}	1.64×10^{-9}	4.25×10^{-8}
6-Hydroxywarfarin	1.05×10^{-6}	6.28×10^{-6}	8.50×10^{-7}	ND
7-Hydroxywarfarin	1.09×10^{-8}	2.40×10^{-6}	1.10×10^{-6}	ND
Acenocoumarin	ND	2.36×10^{-7}	ND	ND
4-Hydroxycoumarin	ND	6.85×10^{-6}	1.28×10^{-5}	6.37×10^{-7}

ND = Not determined

5.2.6.2. Solution Phase Steady State Affinity determinations:

The use of BIAcore technology was employed to determine and compare the dissociation constants obtained using 'real-time' biomolecular interaction with those determined using a well-based ELISA analysis for the interaction between anti-warfarin monoclonal antibodies and specific target antigens. The method employed utilises the same principle as that employed in the ELISA method of Friguet *et al.* (1985), but has several advantages over the ELISA technique. The short contact time of the antibody:antigen equilibrium mixture in the flow cell (compared to incubation step in the ELISA) and continual flow of fresh equilibrium mixture over the warfarin-coated sensor chip limits the possibility of a re-equilibration of the antibody:antigen mixture, and subsequent underestimation of the affinity constant. The method also does not require additional labelling of either reagent, or the addition of secondary reagents, which may affect the intrinsic thermodynamic binding constants.

A known concentration of anti-warfarin antibodies were serially doubly diluted in HBS buffer and used to construct a calibration curve of free antibody concentration versus response as described in section 2.12.7. and shown in Figure 5.42. A known concentration of antibody (nM) was then mixed with serial doubling dilutions of antigen of known concentration and allowed to attain equilibrium. Each equilibrium mixture was then assayed for 'free-unliganded' anti-warfarin antibodies by passing the equilibrated mixtures over a warfarin-coated sensor chip surface. The concentration of free antibody at equilibrium was determined by reference to the standard curve.

The model described below is used to calculate the solution equilibrium dissociation constant:

$$B_{free} = \frac{B - A - Kd}{2} + \sqrt{\frac{(A + B + Kd)^2}{4} - A\,B} \qquad (30)$$

Where B_{free} is the free concentration of anti-warfarin IgG.

A is the total concentration of warfarin

B is the total anti-warfarin IgG concentration

K_d is the equilibrium dissociation constant.

The equilibrium dissociation constant can be calculated by constructing a plot of free anti-warfarin antibodies versus warfarin concentration as shown in Figure 5.43. Equation (30) describing the model for solution phase affinity assumes that the antibodies are monovalently bound. The assay format utilised is capable of detecting free and monovalently bound antibody, and a correction similar to that applied to the ELISA measurements may be applied, so that the concentration of free antibody in the equilibrated antibody:antigen mixture is not overestimated giving an underestimated affinity constant. Piehler *et al.* (1997) amended the solution phase

model based on the binomial distribution principle described by Stevens (1987), and expressed the 'corrected' concentration of free antibody with at least one antibody binding site free by the expression:

$$B_{free} = \frac{B}{2} - \frac{\left[\frac{B+A+K_d}{2} - \sqrt{\frac{(A+B+K_d)^2}{4} - AB}\right]^2}{2B} \qquad (31)$$

The symbols have the same meaning as described for equation (30).

The model described in equation (31) assumes that the sensor responses for free and monovalently occupied antibody are similar. The assumption that the sensor responses measured would be similar for free and monovalently liganded antibodies particularly with larger target antigens is obviously incorrect, however with small molecules such as warfarin, the response measured for monovalently bound antibodies and free antibodies would be similar, given the small molecular weight of warfarin compared to an intact IgG molecule. The bivalent model when fitted to the data resulted in a higher association constant, deriving an equilibrium dissociation constant of, $K_D = 8.57 \times 10^{-9} \pm 1.31 \times 10^{-9}$ M. The data does not fit the bivalent model particularly well as seen in Figure 5.44, and the monovalent fit appears to describe the interaction better between the antibody and the conjugate-immobilised drug surface.

The likelihood of a monovalently ligand-bound (i.e. 4'-azowarfarin-BSA) antibody molecule encountering a second free warfarin molecule bound to the conjugate within the 'sweep of the arm' of the monovalently conjugate-bound antibody molecule could be regarded as low, given the relatively low epitope density of warfarin molecules on the protein. This assumption implies with the use of conjugates that the incidence of bivalent antibody binding to the immobilised conjugate surface would also be low. Given the inhomogeneity of the surface ligand (4'-azowarfarin-BSA) immobilised, it is impossible to predict what conformation the conjugate bound warfarin molecules would adopt when immobilised, and whether or not bivalent analyte binding is sterically possible with the use of protein conjugates. The possibility of bivalent binding would therefore be a function of the drug epitope density, and given the manner in which such drug-protein conjugates are synthesised, conformity of structural epitope density would be impossible to control.

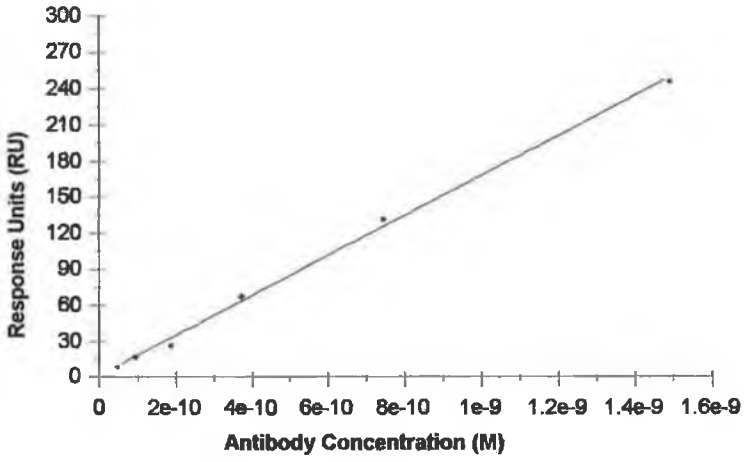

Figure 5.42: *Serial doubling dilutions of anti-warfarin antibodies of known concentration (nM) were passed sequentially over a warfarin-coated (i.e. 4'-azowarfarin-BSA or 4'-aminowarfarin) sensor chip surface. A calibration plot was constructed of anti-warfarin antibodies (nM) versus response measured (RU). The calibration plot was then used to calculate the concentration of free antibody at equilibrium. Results shown are the average of triplicate measurements.*

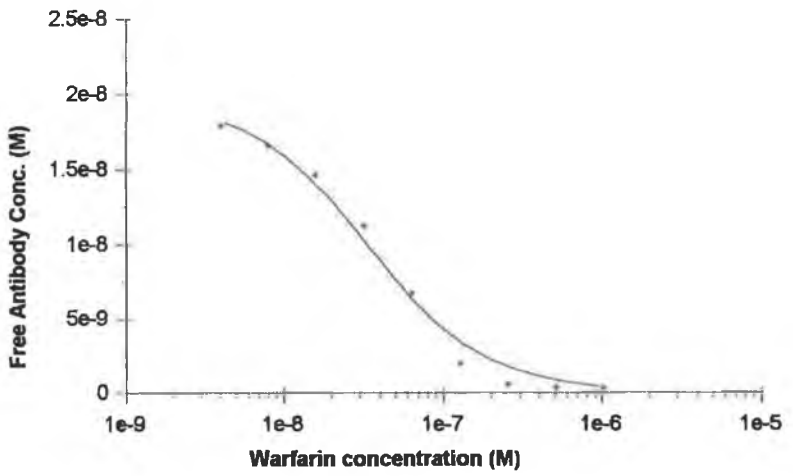

***Figure 5.43**: Determination of overall solution equilibrium affinity constant between clone 3-2-19 and warfarin on a 4'-azowarfarin-BSA-coated chip surface. Warfarin concentrations were plotted against free anti-warfarin antibody concentration, determined by reference to a calibration plot of anti-warfarin antibodies. A 1:1 interaction model was used to describe the interaction (equation (30)), and fitted to the data set using BIAevaluation software, deriving an equilibrium dissociation constant of K_D=2.44 x 10^{-8} M, for the interaction between clone 3-2-19 and warfarin.*

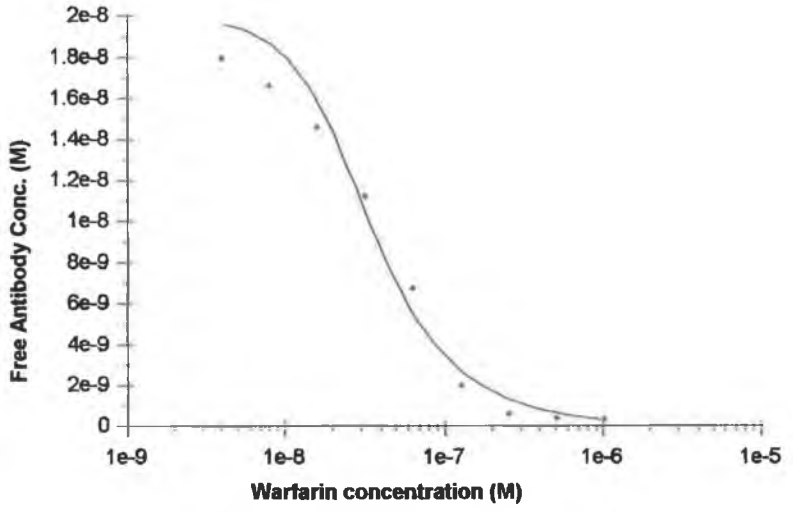

***Figure 5.44**: Solution phase affinity for warfarin and clone 3-2-19 on 4'-azowarfarin-BSA - coated chip surface. The model describing bivalent binding was applied to the data set, giving an overall, equilibrium constant of K_D = 8.57 x 10^{-9} $\pm$ 1.31 x 10^{-9} M. The bivalent model described in equation (31) fitted to the data using BIAevaluation software, does not describe the interaction particularly well as seen from the plot.*

To assess the effect that immobilisation of drug-protein conjugates had on the dissociation constants determined solution phase assays were replicated using directly coated drug surfaces prepared as described in section 2.12.2.2. In this context, the homogeneity and orientation of the surface ligand warfarin molecules was assured. The assays were replicated over a similar inhibitor concentration range. A 20-fold less concentration of antibody was required for experiments with the use of the directly immobilised 4'-aminowarfarin drug sensor chip surfaces (i.e. 20nM for conjugate surface and 1nM for directly immobilised drug surface). The concentration of free antibody for the equilibrium mixtures was determined as previously described, and the models for monovalent and bivalent binding applied. The models fitted to the data generated on directly immobilised drug surface, describe the interaction better than those employing the use of drug protein conjugates, upon inspection of the fitted data set. Interesting to observe is that the model for bivalent binding fits the data set better than the monovalent model, as shown from the fit and residual values obtained. Given the high surface ligand concentration of warfarin directly immobilised, the likelihood of a monovalently surface-ligand bound antibody binding a second warfarin ligand-bound molecule would be extremely high, and thus bivalent antibody binding to the chip surface would most probably be the net result, resulting in increased association constants as a result of avidity effects. The dissociation constant obtained for bivalent model is 2.6 fold lower than that obtained for the monovalent model. The value obtained for the bivalent model, $K_D = 1.53 \times 10^{-9} \pm 8.66 \times 10^{-11}$ M, results in a dissociation constant almost identical to that recorded for the ELISA based Friguet assay ($K_D = 1.64 \times 10^{-9}$ M). The monovalent fit results in a dissociation constant of, $K_D = 4 \times 10^{-8} \pm 3.72 \times 10^{-10}$ M. Avidity effects and rebinding occurring as a result of the high ligand density at the sensor chip surface could, therefore, be used to explain the deviation obtained between the equilibrium dissociation constants determined using drug-protein and directly immobilised drug sensor chip surfaces. An investigation into the affinity constants determined for the corresponding Fab fragments for each clone would have given the 'true affinity' for each antibody binding site. This would also have reduced the complexity of the fits as a result of bivalent antibody binding, and illustrated how well each of the binding models and affinity constants determined with the correction factors employed resemble that of the corresponding Fab fragment. The solution phase equilibrium constants for clones 3-2-19 and 2-5-16 with structurally similar analogues of warfarin were also determined using the immobilised conjugate and drug surfaces. The results are tabulated in Table 5.11 and 5.12 and the corresponding equilibrium dissociation plots illustrated in Figures 5.47-5.53.

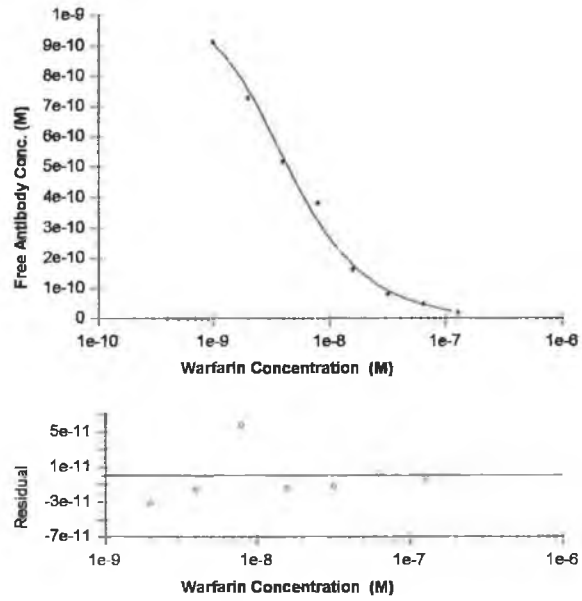

***Figure 5.45**: Determination of solution affinity for interaction between warfarin and clone 3-2-19 on a chip surface directly immobilised with 4'-aminowarfarin. The bivalent model fitted to the data set describes the interaction particularly well as seen from the residual plot, and derives a dissociation constant, $K_D = 1.53 \times 10^{-9} \pm 8.66 \times 10^{-11}$ M for the interaction.*

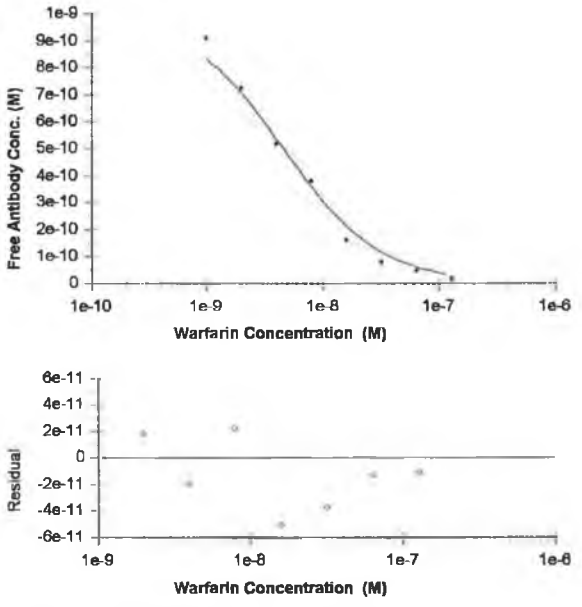

***Figure 5.46**: Determination of solution affinity for interaction between warfarin and clone 3-2-19 on a chip surface directly immobilised with 4'-aminowarfarin. The monovalent binding model was fitted to the data set and derives a dissociation constant, $K_D = 4.08 \times 10^{-9} \pm 3.72 \times 10^{-10}$ M for the interaction. This value is slightly lower than that obtained for the bivalent fit as would have been expected based on the binomial model described by Piehler et al. (1997).*

The binding interaction models described previously were fitted to the relevant data sets, and used to calculate the equilibrium dissociation constant, K_D, for the interaction between anti-warfarin antibodies from clone 3-2-19 and particular antigens. The results are shown below in Figures 5.47-5.50, and the calculated dissociation constants based on the fitting of both monovalent and bivalent models to the data set are shown in Table 5.11.

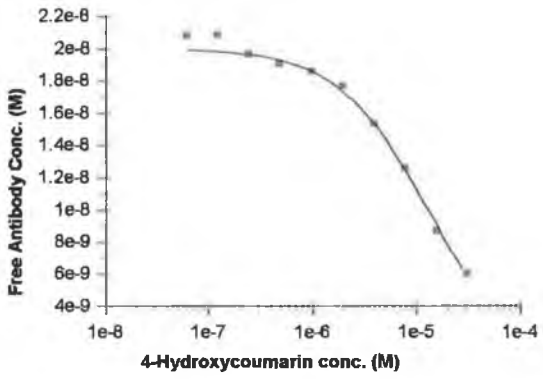

Figure 5.47: *Determination of equilibrium dissociation constant between clone 3-2-19 and 4-hydroxycoumarin on a 4'-azowarfarin-BSA-coated chip surface. The solution phase affinity models were fitted to the data using BIAevaluation software, deriving an equilibrium dissociation constant for the interaction of* $1.29 \times 10^{-5} \pm 6.94 \times 10^{-7}$ *M using equation (30).*

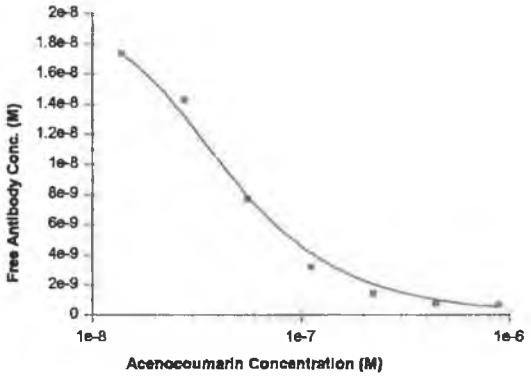

Figure 5.48: *Determination of equilibrium dissociation constant between clone 3-2-19 and acenocoumarin on a 4'-azowarfarin-BSA-coated chip surface. The solution phase affinity models were fitted to the data using BIAevaluation software, deriving an equilibrium dissociation constant for the interaction of* $3.19 \times 10^{-8} \pm 6.02 \times 10^{-9}$ *M using equation (30).*

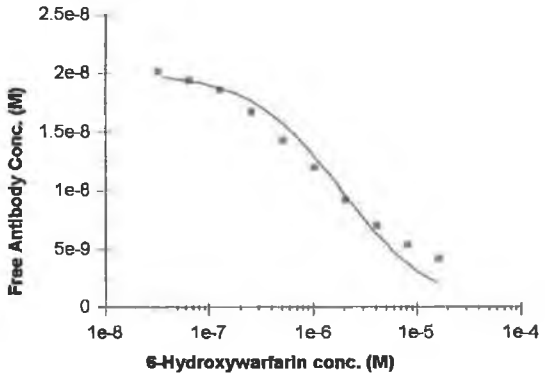

Figure 5.49: *Determination of equilibrium dissociation constant between clone 3-2-19 and 6-hydroxywarfarin on a 4'-azowarfarin-BSA-coated chip surface. The solution phase affinity models were fitted to the data using BIAevaluation software, deriving an equilibrium dissociation constant for the interaction of* $1.86 \times 10^{-6} \pm 2.23 \times 10^{-7}$ *M using equation (30).*

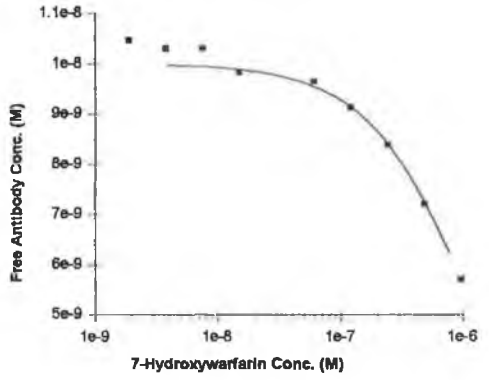

Figure 5.50: *Determination of equilibrium dissociation constant between clone 3-2-19 and 7-hydroxywarfarin on a 4'-azowarfarin-BSA-coated chip surface. The solution phase affinity models were fitted to the data using BIAevaluation software, deriving an equilibrium dissociation constant for the interaction of* $1.27 \times 10^{-6} \pm 8.94 \times 10^{-8}$ *M using equation (30).*

Table 5.11: *Equilibrium solution phase dissociation constants (K_D) determinations for clone 3-2-19 with particular antigens. The dissociation constants were determined using both the monovalent (equation 30) and bivalent models (equation 31) using BIAevaluation software.*

Antigen	*K_D Monovalent model $\pm$ S.E.*	*K_D Bivalent Model $\pm$ S.E.*
(a) 4-hydroxycoumarin	$1.29 \times 10^{-5} \pm 6.94 \times 10^{-7} M$	$4.88 \times 10^{-6} \pm 3.47 \times 10^{-7} M$
(b) Acenocoumarin	$3.19 \times 10^{-8} \pm 6.02 \times 10^{-9} M$	$1.14 \times 10^{-8} \pm 9.24 \times 10^{-10} M$
(c) 6-Hydroxywarfarin	$1.86 \times 10^{-6} \pm 2.23 \times 10^{-7} M$	$6.95 \times 10^{-7} \pm 1.10 \times 10^{-7} M$
(d) 7-Hydroxywarfarin	$1.27 \times 10^{-6} \pm 8.94 \times 10^{-8} M$	$4.4 \times 10^{-7} \pm 3.95 \times 10^{-8} M$
(e) 4-hydroxycoumarin (*4'-aminowarfarin-coated sensor chip)*	$1.13 \times 10^{-5} \pm 7.46 \times 10^{-7} M$	$4.35 \times 10^{-6} \pm 5.13 \times 10^{-7} M$

The binding interaction models described previously were fitted to the relevant data seta and used to calculate the equilibrium dissociation constant, K_D, for the interaction between anti-warfarin antibodies from clone 2-5-16 and the corresponding antigens. The results are shown below in Figure 5.51-5.53 and tabulated below in Table 5.12.

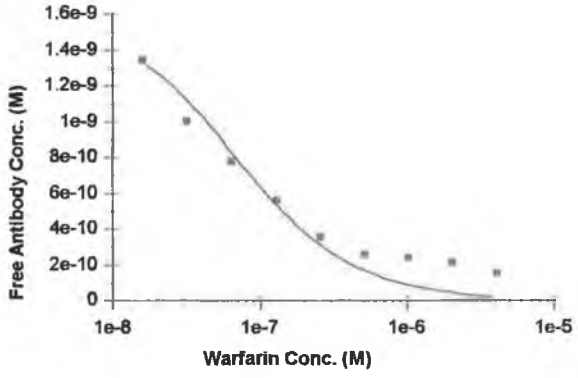

Figure 5.51: *Determination of equilibrium dissociation constant between clone 2-5-16 and warfarin on a 4'-aminowarfarin-coated chip surface. The solution phase affinity models were fitted to the data using BIAevaluation software, deriving an equilibrium dissociation constant for the interaction of $8.26 \times 10^{-8} \pm 3.16 \times 10^{-9} M$ using equation (31).*

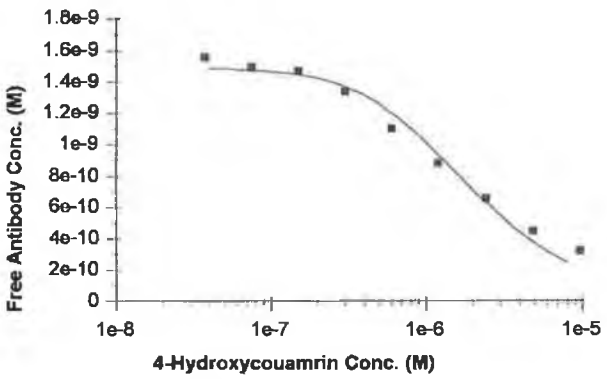

Figure 5.52: *Determination of equilibrium dissociation constant between clone 2-5-16 and 4-hydroxycoumarin on a 4'-aminowarfarin-coated chip surface. The solution phase affinity models were fitted to the data using BIAevaluation software, deriving an equilibrium dissociation constant for the interaction of* $2.06 \times 10^{-6} \pm 3.16 \times 10^{-9} M$ *using equation (31).*

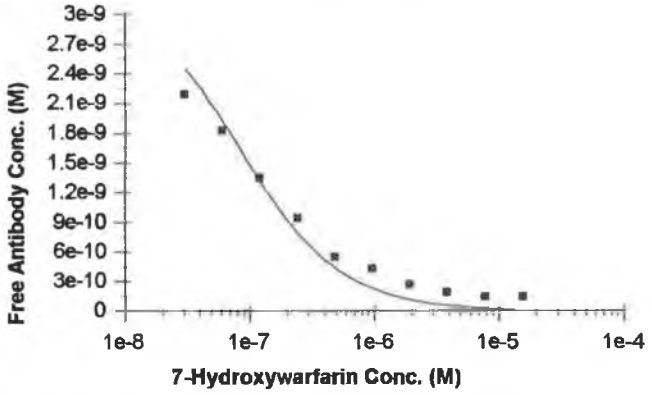

Figure 5.53: *Determination of equilibrium dissociation constant between clone 2-5-16 and 7-hydroxywarfarin on a 4'-aminowarfarin-coated chip surface. The solution phase affinity models were fitted to the data using BIAevaluation software, deriving an equilibrium dissociation constant for the interaction of* $1.03 \times 10^{-7} \pm 8.07 \times 10^{-9} M$ *using equation (31).*

Table 5.12: *Equilibrium solution phase dissociation constants (K_D) determinations for clone 2-5-16 with particular antigens on a 4'-aminowarfarin-coated chip surface and determined using both the monovalent and bivalent models using BIAevaluation software.*

Antigen	K_D *Monovalent model* $\pm$ *S.E.*	K_D *Bivalent Model* $\pm$ *S.E.*
(a) 4-hydroxycoumarin	$2.06 \times 10^{-6} \pm 1.87 \times 10^{-7} M$	$2.06 \times 10^{-6} \pm 6.73 \times 10^{-8} M$
(b) Warfarin	$8.26 \times 10^{-8} \pm 1.17 \times 10^{-8} M$	$3.16 \times 10^{-8} \pm 4.52 \times 10^{-9} M$
(c) 7-Hydroxywarfarin	$1.03 \times 10^{-7} \pm 8.07 \times 10^{-9} M$	$4.03 \times 10^{-8} \pm 4.22 \times 10^{-9} M$
(d) 6-Hydroxywarfarin	$2.00 \times 10^{-5} \pm 5.19 \times 10^{-6} M$	$7.35 \times 10^{-6} \pm 1.98 \times 10^{-6} M$

5.2.6.3. Steady-State Affinity Determinations:

4'-azowarfarin-BSA was immobilised at a sufficiently low surface concentration to give a maximum response of approximately 200 RU on the sensor chip surface using conventional coupling chemistry. Direct immobilisation of 4'-aminowarfarin at a sufficiently low ligand density on the chip surface was difficult to control, and consequently drug-protein conjugates were immobilised. BSA was immobilised on a second flow cell at a similar surface concentration. BIACORE 3000 is capable of on-line reference curve subtraction, thereby removing matrix effects, and baseline jumps due to sample injection and refractive index changes. Ideally, it would have been preferable to immobilise the antibody to the chip surface by affinity capture using Protein A/G. Direct immobilisation of the antibody would remove the complexity arising from a bivalent analyte binding to the drug surface, and possible avidity effects at the chip surface resulting in elevated affinity constant determinations. However, the surface concentration of antibody required to achieve a quantifiable response signal following binding of warfarin to the affinity captured antibody proved to be a limiting factor and consequently the use of drug-protein conjugates was employed. For example, affinity capture of 10,000RU of anti-warfarin antibody via protein G, (which is difficult to achieve in practice) would only result in a maximal saturation response of 41RU even when taking antibody bivalency into account given the ratio of the molecular weights of the antibody (~150,000Da), and warfarin (308Da). Given the large concentration of antibody required to generate such a quantifiable signal, the time taken to reach equilibrium and saturation of the surface would have been extremely long.

The steady state affinity for a surface interaction can be described by the expression:

$$\mathrm{Re}q = \frac{Ka.(C_A)i.R\max}{Ka.n.(C_A)i + 1} \qquad (32)$$

Where n = Steric hindrance factor and represents the average number of ligand sites occupied per analyte molecule.

Req = Response at equilibrium

$(C_A)i$ = Injected concentration of analyte (M)

Rmax = Maximal response

Ka = Equilibrium association constant

The value for steric hindrance factor, n, can be determined experimentally by calculating the fraction of the response measured versus the theoretical maximal response attainable given a specific immobilised ligand surface concentration. The value of n, could therefore not be

calculated using drug protein conjugates and was set to 1, for the purposes of modelling experiments.

Serial dilutions of anti-warfarin antibody of known concentration were simultaneously injected over warfarin-BSA and BSA coated surfaces at a flow rate of 2 µl/min for 40 minutes, using 'on-line' reference curve subtraction as illustrated in Figures 5.54 and 5.55. A plot of the equilibrium response (Req) measured versus the injected antibody concentration was constructed, and the steady state affinity model described in equation (32) was fitted to the plot deriving an association constant (K_A) value of $1.78 \times 10^8 \pm 0.28 \times 10^8$ M^{-1} for the steady-state interaction between clone 3-2-19 and warfarin.

The steady-state affinity model derives an association constant higher than that obtained for the solution phase constant using immobilised drug conjugates, but less than that obtained with directly immobilised drug surface. One would expect the solution phase affinity constant to yield a slightly higher value for the association constant, given that both interacting molecules (i.e. antibody and antigen) are free in solution. The overall reaction flux (L_r) would therefore be greater, compared to the steady state experiments where one of the interacting molecules is immobilised (i.e. warfarin-BSA). The low molecular weight of the target analytes and difficulties involved in immobilising a sufficiently low ligand density of 4'-aminowarfarin directly (i.e. Rmax < 200RU), restricted the various types of immunoassay format possible. Similar to the solution phase assays, the possibility of bivalent analyte binding to the chip surface also exists. However, given the low surface ligand concentration of warfarin-BSA employed, and for similar but highly more probable reasons than those discussed for the solution phase assays, the likelihood of a monovalently bound antibody bound to the conjugate surface, encountering a second free ligand site would be particularly small, given also the saturating concentrations of antibody employed. In this context, the restrictions enforeed by the small molecular weight of the analyte and the use of drug conjugate surfaces allows for approximations of overall association constants, given that values for the steric hindrance factor, n, were impossible to calculate given the in-homogeneity of the surface ligand.

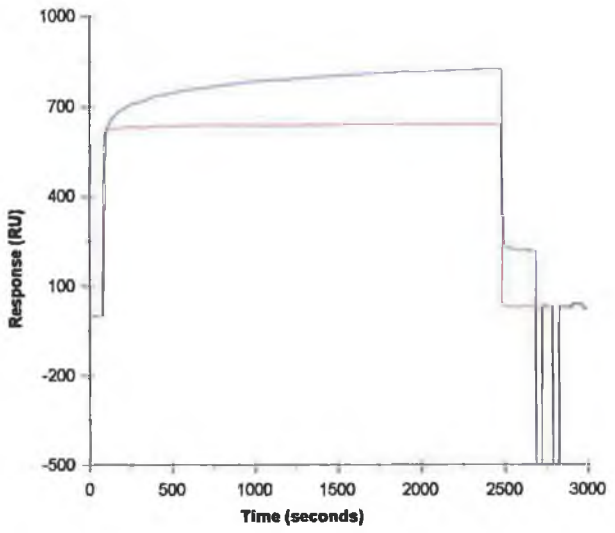

Figure 5.54: *Warfarin-BSA (——) and BSA (——) were immobilised onto two flow (Fc) cells of a sensor chip surface, namely Fc2 and Fc1, respectively. 80nM of affinity-purified anti-warfarin antibodies were injected over the two sensor chip surfaces and monitored simultaneously using 'on-line' reference curve subtraction (i.e Fc2-Fc1).*

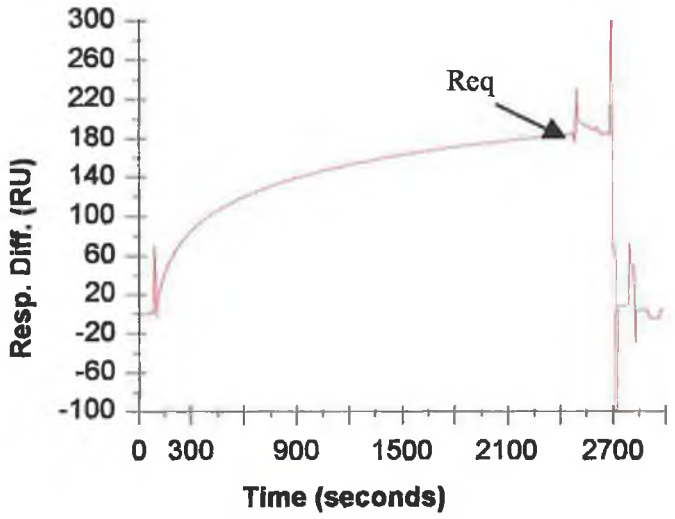

Figure 5.55: *The interaction curve from figure 5.54 following 'on-line' reference curve subtraction is shown. The equilibrium binding response was measured at a variety of injected antibody concentrations, and used to plot a curve of the binding response at equilibrium (Req) versus injected antibody concentration (Figure 5.57).*

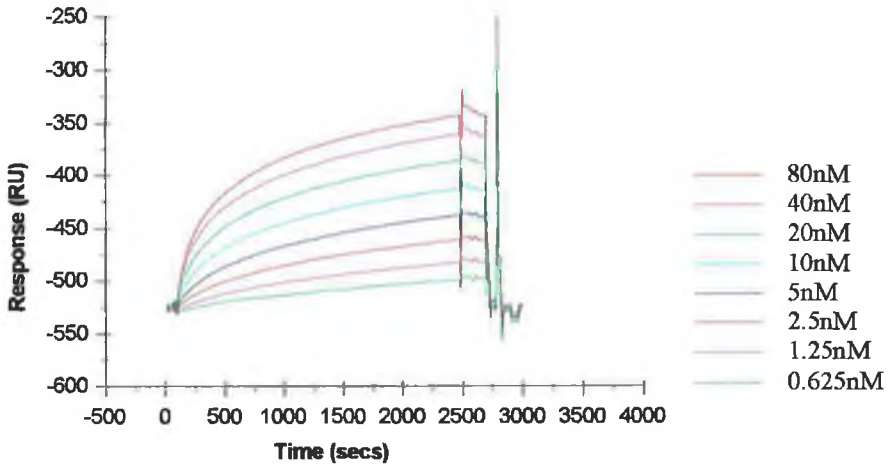

Figure 5.56. *Reference curve subtracted binding curves for various concentrations of anti-warfarin antibodies and a warfarin-BSA-coated chip surface, following injection over the surface at a flow rate of 2 µl/min for 40 minutes.*

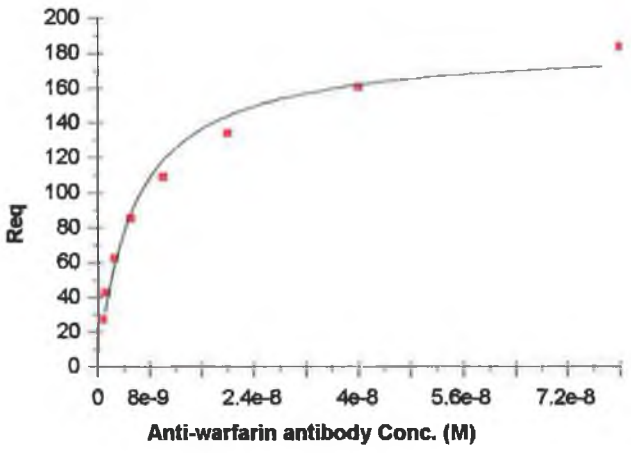

Figure 5.57: *The value obtained for Req was plotted against the molar concentration of antibody injected. The steady state model described in equation (32) was fitted to the data, and assuming a value of n=1, the value for the association constant, Ka, for the interaction between warfarin and affinity-purified antibodies from clone 3-2-19 was determined using BIAevaluation software to be* $1.78 \times 10^8 \pm 0.28 \times 10^8\ M^{-1}$.

5.2.7. Conclusions:

The results presented in this chapter describe the production and characterisation of a panel of monoclonal antibodies to the small hapten molecule, warfarin (Mol. Wt. 308 Da). Balb/C mice were initially immunised with a variety of immunogens to assess which of the conjugates would be the best immunogen. The results show that the use of a combined 'cocktail' of conjugates proved to be the most effective. Difficulties in generating sufficiently high titres against small hydrophobic haptens have been reported in the literature, and attributed to protein modifications of the carrier protein with the hapten molecule reassociating with hydrophobic residues within the protein core, thereby reducing the surface epitope concentration of hapten and subsequent interaction with the immune system (Fasciglione *et al.*, 1996). No such difficulties were encountered in the generation of an immune response to warfarin, and results demonstrate a >10 fold increase in the final antibody titres recorded compared to the initial antibody titres measured over the course of the immunisation schedule (> 15 months).

Hapten-specific clones were selected by ELISA, and cloned by the method of limiting dilution. The fusion efficiency measured in terms of the number of wells containing hybridomas, was in all cases relatively high (> 70%). However, the 'relative' success of the fusion procedure measured in terms of hapten-specific clones following the cloning and scale-up procedure was low, ranging from individual to multiple clones isolated for the various fusion procedures carried out. The final fusion procedure generated 7 hybridomas and highlights the importance of extended immunisation procedures for the generation of high serum titres (> 250,000) and high affinity monoclonal antibodies ($\sim K_D = 10^{-9}$ M). Other authors have reported difficulties associated with the selection of antibodies to small molecular weight haptens during screening procedures, resulting in the selection of antibodies sharing a combined drug-protein epitope (Danilova, 1994; Keating, 1998; Killard, 1998). The use of conjugates employing different coupling chemistries and carrier protein homology than those used for immunisation procedures is thus strongly recommended. Whilst it may not be logistically possible initially given the large number of wells screened during an initial hybridoma screening procedure (> 600 wells), the use of a competitive immunoassay format is highly recommended as early as possible into the screening procedure. The use of such a competitive selection system can generally be employed after the initial screen when the number of 'positive' wells is logistically more manageable. Competitive screening procedures thus ensure the selection of hybrids secreting antibody specific for the free hapten. Despite the fact that different conjugates were used in screening procedures, several 'positive' wells were identified which bound to the conjugate but not free hapten. Further analysis of these clones identified that the 'sticky' immunoglobulins produced demonstrated a non-specific binding profile to a variety of conjugates and native

proteins, highlighting the importance of such competitive immunoassay screens so that reagents, labour and time will not be wasted cultivating such useless clones.

The cloned hybridomas were cultured *in vitro* and the supernatants collected and purified for further analysis. Two of the clones (i.e. W1 and 48-5) demonstrated significantly lower titres than those recorded for the other hybridomas. Attempts to increase the levels of specific antibody production were made by repeated cloning by limiting dilution to try and isolate more stable clones, which proved unsuccessful. Propagation of these hybridomas as ascites increased the antibody titres recorded. However, *in vitro* culture of the cells following growth as ascites and subsequent cloning by limiting dilution produced only slightly elevated levels of antibody production and no significant increase in the number of antibody-secreting wells. It was thus concluded that these clones were considered to be genetically unstable or 'low secretors' of antibody. A practical decision should thus be made at this stage with respect to such clones as to whether or not the levels of antibody recorded from such clones are sufficiently high for the desired purposes before performing new fusions.

The levels of antibody produced by the hybridoma cells were measured using a well-based ELISA affinity-capture assay and on BIAcore using the Universal standard curve method of Karlsson *et al.* (1993). The results obtained using these two techniques correlated extremely well, and showed clone 3-2-19 to be a high secretor of antibody with levels of ≈35 μg/ml culture media recorded. The Universal standard curve method offers several advantages over the ELISA-based system in that once a single calibration curve has been constructed for a particular molecule under specific conditions of MTL, it can be used repeatedly under the same conditions for subsequent concentration determinations. In this context, the use of BIAcore and namely the Universal standard curve should be encouraged as a means of monitoring serum responses and screening supernatants for the presence of monoclonal antibodies/scFvs. Using the Universal standard curve as a screening tool can also give a wide range of information with regard to particular clones. For example, a single injection will not only identify 'positive' hybrids, but also yield important protein concentration information. A second follow up injection based on this initial positive result, where the antibody could be mixed with a competing antigen, could then be used as a means of affinity ranking antibodies in a similar fashion to IC_{50} values. All this information could be generated in two simple injection procedures in the order of minutes, as opposed to carrying out several independent ELISAs, each of which is based on the previous result and can thus take many days to conduct. The technique could thus prove very valuable in laboratories where a large number of hybridomas may warrant screening and further identification.

Each of the hybridomas was then used to develop a competitive immunoassay for warfarin. For all immunoassay calibration plots the use of a spline function in BIAevaluation™ software was adopted which fitted an advanced smoothed curved cubic polynomial to the data set. Immunoassay curves are inherently non-linear in origin and adopt a familiar sigmoidal bell shaped curve on log-linear plots. The fitting of linear plots to such data sets ignores the inherent shape of the plot, with the resulting 'linear' plots showing a greatly reduced dynamic range with reduced precision at both the upper and lower ends of the calibration set. Fitting 4-parameter equations to immunoassay curves offers a much more realistic fitting of the data set, and as shown can increase the detection range by 4-fold at both ends of the linear range increasing the dynamic range considerably with no significant effect on the degree of assay precision or performance.

The method of Friguet *et al.* (1985) was used to assess the overall dissociation constants for each of the hybridomas to warfarin and structurally related analogues. All of the conjugates used for immunisation and screening utilised the same point of attachment (i.e. the amine group on position 4 of the benzyl ring). This particular point of attachment was chosen for a number of reasons: primarily because it offered a convenient means of protein conjugation. Secondly, as the majority of warfarin metabolites involve various hydroxylations of the coumarin part of the molecule, it was suggested that a point of conjugation away from this area might confer extra specificity to the monoclonals produced, as antibody specificity is directed primarily at the area of the hapten most sterically accessible (Landsteiner's principle)(i.e. the 4-hydroxycoumarin moiety of warfarin). The affinity profile of the monoclonals produced measured by the equilibrium dissociation constants, was generally of the order:
warfarin ≥ acenocoumarin > 7-/6-Hydroxywarfarin >> 4-hydroxycoumarin with the exception of clone 2-5-16 which showed increased affinity for 4-hydroxycoumarin. These results suggest that the majority of the antibodies were directed against an epitope on the coumarin portion of the molecule. However, when tested for reactivity against a series of coumarin-based molecules including: coumarin, 7- and 6-hydroxycoumarin, esculetin and 7-hydroxy-4-acetic acid none of the clones exhibited any affinity towards these coumarin-based molecules with the exception of clone 2-5-16. This implies that the monoclonal antibodies produced from clones W1, 3-2-19 and 48-5 were directed against a combined epitope near the 4-hydroxycoumarin residue and the branched keto substituent at position 3 part of the coumarin molecule. This also explains why there was a reasonably high degree of affinity of the antibodies for the hydroxylated metabolites. Clone 2-5-16 exhibited increased affinity relative to the other clones to 4-hydroxycoumarin, suggesting that the majority of the specificity of this particular antibody is directed against the 4-hydroxycoumarin residue. The dissociation constants measured by the method of Friguet *et al.* (1985)(despite it's many limitations) correlate well with those

determined using steady state and solution phase affinity analysis on BIAcore over a wide range of antibody affinities studied (i.e. K_D 10^{-5} – 10^{-9} M). Using BIAcore analysis affinity determinations were made using both directly immobilised drug and conjugate surfaces. All of the assay formats employed an immobilised monovalent ligand (warfarin-BSA, 4'-aminowarfarin) with a bivalent analyte (antibody) in solution, with the potential, therefore, of bivalent analyte binding. Dissociation plots fitted to the data generated on drug-protein conjugate surfaces appeared to conform to the fit of monovalent binding better than bivalent model, whilst the plots generated on directly immobilised drug surfaces fitted the bivalent model better. The reality is that the dissociation fit lies somewhere between the modelled mono- and bivalent fit. The increased affinity constants measured on the directly immobilised drug surfaces compared to the conjugate bound surfaces are in all probability the net result of bivalent antibody binding at the chip surface as a result of the high ligand concentration immobilised. The high ligand concentrations employed would thus encourage rebinding events within the flow cell and avidity effects at the chip surface resulting in the observed elevated association constants. The likelihood of an antibody being bound to two immobilised conjugate bound warfarin molecules simultaneously would be small as a result of the lower epitope concentration and possible steric hindrance factors at the chip surface, giving slightly lower association constants. The lower dissociation constant values generally obtained using solution phase assays compared to steady state analysis, agrees with what one might have predicted. Given that for solution phase assays both interacting molecules (i.e. antibody and antigen) are free in solution and hence have an increased collision frequency, thus affecting the kinetic rate constants and the measured affinity constants, unlike steady state analysis where one of the interactants is immobilised.

In conclusion, for the generation of high affinity monoclonal antibodies to small haptens the use of extended immunisation schedules and a variety of conjugates for immunisation procedures is encouraged to enhance the serum response generated. Selection should as soon as logistically possible be carried out using a competitive assay format to ensure selection of hapten specific clones only. The use of BIAcore at this stage of screening could therefore be used to rank antibodies with respect to specific active antibody concentration and also affinity, allowing the selection and cultivation of the more precious higher affinity clones. Such clones could then be further characterised based on kinetic rate constants for the selection of specific antibodies for particular purposes (i.e. ELISA, biosensor purposes). The dissociation constants determined by the method of Friguet *et al.* (1985) demonstrate the method to be an accurate means of determining equilibrium affinity constants for crude samples when more techniques such as the BIAcore are not available, provided the initial assay prerequisites are fulfilled. Ultimately, the method (solution phase/steady state analysis) of measuring antibody affinity should resemble

the environment for their intended use (i.e. steady state analysis should be used for measuring antibody affinity to surface bound molecules and solution phase assays for situations where the antibody might encounter the antigen in solution).

Chapter 6

Overall Conclusions

6.1. Overall Conclusions:

The purpose of the research work carried out was to develop antibodies to warfarin (i.e. polyclonal and monoclonal) which following characterisation could be used for the development of antibody-based assay systems for the detection of warfarin in biological fluids.

Initial work focused on the production of drug-protein conjugates which were then used for subsequent immunisation, purification and assay purposes. Given that the specificity of the antibodies produced will ultimately be a function of the particular epitopes available the point of attachment is of hapten to carrier protein is therefore of considerable importance. The use of molecular modelling was employed for the generation of 3-dimensional configurations of warfarin and it's major primary metabolites. Molecular modelling techniques, as the experimental observations demonstrate, provide a useful insight as to the 3-dimensional configurations of small atoms that are not always evident from 2-dimensional representations. On the basis of these representations, coupled with the various functional groups available for coupling the nitro group of acenocoumarin was chosen as the point of attachment of hapten to the carrier molecule. A variety of drug-protein conjugates were initially produced, and as the results demonstrate, high specific antibody responses were recorded, with rabbit serum titres exceeding 1/500,000. The high drug-protein coupling ratios recorded underlines the immunogenicity of the conjugates produced. Similar antigen-specific mouse serum titres of antibody were obtained, which demonstrated a > 10 fold increase in specific antibody titre over the course of the immunisation schedule. Somatic cell fusion procedures were carried out at various time intervals throughout the immunisation schedule, and the monoclonal antibodies produced demonstrate a 20-fold increase in antibody affinity during the course of the immunisation schedule, underlining the importance of extended immunisation protocols (i.e. 6 months post initial immunisation clone 48-5 K_D = 2.8 x 10^{-8}, 15 months post initial immunisation clone 3-2-19 K_D = 1.6 x 10^{-9}) for the generation of high affinity clones (Danilova, 1994).

The levels of antibody produced by selected monoclonal antibody preparations were compared using a well-based ELISA affinity-capture assay and also using a biosensor-based assay technique, which showed excellent correlation. The use of the biosensor-based assay procedure described (Karlsson *et al.*, 1993) or a similar variant (Christensen, 1997) is encouraged particularly when screening hybridoma supernatants, because of the wide range of both qualitative (i.e. positive/negative) and quantitative (concentration determinations/affinity analysis/epitope mapping) information which can be recorded automatically in relatively short time periods (i.e. 5 minutes).

The monoclonal antibodies were then characterised in terms of their affinity and specificity to warfarin and structurally-related analogues. A well-based ELISA assay and the use of BIAcore were then compared to measure the affinity of the monoclonal antibodies produced. The results generated using the well-based system generated thermodynamic results of comparable dissociation constants to those determined using BIAcore, highlighting the usefulness of the method of Friguet *et al.* (1985), particularly for crude antibody preparations of unknown antibody concentration. Each of the monoclonal antibodies produced exhibited excellent specificity towards the parent molecule over structurally related analogues. For example, monoclonal antibodies from clone 3-2-19, the highest affinity monoclonal isolated, showed a greater than 500-fold affinity to warfarin (K_D = 1.6 $x10^{-9}$) than to any of the hydroxy metabolites assayed (K_D = 1.2 $x10^{-5}$ - 8.5 $x10^{-7}$)(Table 5.10).

All of the antibodies produced were then used in the development of BIAcore-based inhibition immunoassays for the detection of warfarin in biological fluids. The assay system developed for the detection of warfarin in plasma ultrafiltrate had a working range between 0.5 and 250 ng/ml. These detection limits are only paralleled by those involving the use of GC-MS (Gas Chromatography-Mass Spectrometry) and HPLC with post-column fluorescent techniques that require extensive sample pre-treatment prior to sample analysis and are not particularly well suited to the routine analysis of drug molecules in complex biological matrices. The biosensor-based assay system developed for the detection of warfarin in plasma ultrafiltrate utilised a chip surface with the drug 4'-aminowarfarin covalently coupled. Such surfaces demonstrated exceptional stability and reproducibility (% C.V. < 1%) and were capable of being used for greater than 1,000 assays. In the clinical setting, economics is becoming increasingly more important and the use of such regenerable assay formats offers a very attractive alternative to current high consumable-based alternatives (i.e. ELISA (immunoplates) and HPLC (solvent waste)). The technique developed for the analysis of warfarin could quite easily be reconfigured for the analysis of quite literally any analyte provided that antibodies of the desired specificity are available. Indeed, as the majority of current analytical techniques rely on the inherent physicochemical properties of small molecules for their detection, which are too often limiting factors with regard to assay sensitivity, the use of antibody-based techniques offers very attractive more sensitive, low-cost alternatives which could soon become the mainstay of modern analytical technology. The low degree of sample preparation required and high degree of automation offered by BIACORE-based detection techniques are additional advantages to those outlined compared to traditional techniques such as HPLC and GC-MS which rely on extensive sample pre-treatment. Similarly, as a consequence of the low degree of sample pre-treatment and high degree of automation, the sample throughput of BIACORE assays (run-time

~ 7 mins, ≈500 samples/day) is significantly better than those for most HPLC assays (run time ~ 20 mins, 50-100 samples/day depending on the degree of sample pre-treatment required)

Recent developments in antibody engineering has allowed for the development of antibody fragments with monovalent femtomolar antigen-binding affinity (Boder *et al.*, 2000). These advances allied to the on-going development in the field of transduction technologies, are continually re-defining the boundaries of the clinical, therapeutic and analytical potential of antibodies (and fragments thereof), which ensures that the application of antibody-based techniques will continue to grow at an ever increasing rate as their potential in the clinical/therapeutic and diagnostic/analytical arena are finally fully realised.

Chapter 7

References

Allinger, K. (1989) "Path-integral approaches to the statistical mechanics of quantum systems: Variational methods for influence functionals". *Phys. Rev.*, **39(2)**, 881-96.

Alloza, J.L. (1984) "Updated review of oral anticoagulants. A case report". *Arch. de Farmacol. Y Toxicol.*, **X**:45-57.

Alving, B.M., Strickler, M.P, Knight, R.D., Barr, C.F., Berenberg, J.L. and Peck, C.C. (1985) "Hereditary warfarin resistance". *Arch. Intern. Med.*, **145**, 499-501.

Amirkhosravi, M. and Francis, J.L. (1995) "Coagulation activation by MC28 fibrosarcoma cells facilitates lung tumor formation". *Thromb. Haemost.*, **73(1)**, 59-65.

Andersson, H.S., Koch-Schmidt, A.C., Ohlson, S. and Mosbach, K. (1996) "Study of the nature of recognition in molecularly imprinted polymers". *J. Mol. Recognit.*, **9(5-6)**, 675-82.

Andrews, B.A., Nielson, S. & Asenjo, J.A. (1996) "Partitioning and purification of monoclonal antibodies in aqueous two-phase systems". *Bioseparation*, **6**, 303-13.

Armstrong, D W., Ward, T.J., Armstrong, R.D. & Beesley, T. E. (1986) "Separation of drug stereoisomers by the formation of beta-cyclodextrin inclusion complexes". *Science,* **323**, 1132-5.

Arkel, Y. S. (2000) "Thrombosis and Cancer". *Seminars in Oncology*, **27(3)**, 362-74.

Bach, A.U., Anderson, S.A., Foley, A.L.,Williams, E.C. and Suttie, J.W. (1996) "Assessment of vitamin K status in human subjects administered "minidose" warfarin". *Am. J. Clin. Nutr.*, **64**, 894-902.

Baglin, T. (1998) "Management of warfarin (coumarin) overdose". *Blood Rev.*, **12(2)**, 91-8.

Balon, K., Riebesehl, B.U. and Muller, B.W. (1999) "Drug liposome partitioning as a tool for the prediction of human passive intestinal absorption". *Pharm. Res.*, **16(6)**, 882-8.

Banfield, C. and Rowland, M. (1984) "Stereospecific fluorescence high-performance liquid chromatographic analysis of warfarin and its metabolites in plasma and urine". *J. Pharm. Sci.*, **73(10)**, 1392-6.

Bauer, K.A., Goodman, T,L. and Kass, B.L. (1985) "Elevated factor Xa activity in the blood of asymptomatic patients with congenital antithrombin deficiency". *J. Clin. Invest.*, **76**, 826-36.

Bechtold, H., Lorenz, J., Weilemann, L.S., Meinertz, T., Trenk, D., Andrassy, K. and Jahnchen, E. (1984) "Possible coumarin-like mechanism of action for cephalosporins". *Klin. Wochenschr.*, **62 (18)**, 885-6.

Beckey, N.P. (1999) "Outpatient management of patients on warfarin". *Lippincotts Prim. Care. Pract.*, **3(3)**, 280-9.

Bell, R.G. (1978) "Metabolism of vitamin K and prothrombin synthesis: anticoagulants and the vitamin K–epoxide cycle". *Fed. Proc.*, **37(12)**, 2659-604.

Bell,E.B., Brown, M. and Ritternberg, M.B. (1983) "*In vitro* antibody synthesis in 20 µl hanging drops: initiation of secondary responses and a simple method of cloning hybridomas". *J. Immunol. Meth.*, **62**, 137-145.

Benjamini, E., Sunshine, G. and Leskowitz, S. (1996) *"Immunology: a short course".* 3rd edition, Wiley-Liss, New York, U.S.A.

Bentley, D.P., Backhouse, G., Hutchings, A., Haddon, R.L., Spragg, B. and Routledge, P.A. (1986) "Investigation of patients with abnormal response to warfarin". *Br. J. Clin. Pharmacol.*, **22**, 37-41.

Berkarda, B., Arda, O., Tasyurekli, M. and Derman, U. (1992) "Mitochondria Lytic action of warfarin in lymphocytes". *Int. J. Clin. Pharmacol.*, **30(8)**, 277-9.

Berkner, K.L. (2000) "The vitamin K-dependent carboxylase". *J. Nutr.*, **130(8)**, 1877-80.

Bertucci, C., Canepa, A., Ascoli, G.A., Guimaraes, L.F.L and Felix, G. (1999) "Site I on human albumin: Differences in the binding of (R)- and (S)-warfarin". *Chirality*, **11(9)**, 675-9.

Boder, E.T., Midelfort, K.S. and Wittrup, K.D. (2000) "Directed evolution of antibody fragments with monovalent femtomolar antigen-binding site". *Proc. Natl. Acad. Sci.,(USA)* **97(20)**, 10701-5.

Bonnabry, P., Desmeules, J., Lemman, T., Veuthey, J.-L. and Dayer, P. (1996) "Stereoselective interaction between piroxicam and acenocoumarol". *Br. J. Clin. Pharmacol.*, **41**, 525-30.

Bonwick, G.A., Cresswell, J.E., Tyreman, A.L., Baugh, P.J., Williams, J.J.H., Smith, C.J., Armitage, R. and Davies, D.H. (1996) "Production of murine monoclonal antibodies against sulcofuron and flucofuron by *in vitro* immunisation". *J. Immunol. Meth.*, **196**, 163-73.

Booth, S.L. and Mayer, J. (2000) "Warfarin use and fracture risk". *Nutr. Rev.*, **58(1)**, 20-22.

Borrebaeck, C.A. (1983) "*In vitro* immunization for the production of antigen-specific lymphocyte hybridomas". *Scand. J. Immunol.*, **18(1)**, 9-12.

Borrebaeck, C. (1989) "Strategy for the production of human monoclonal antibodies using *in vitro* activated **B** cells". *J. Immunol. Meth.*, **123,** 157-65.

Borrebaeck, C.A.K. (2000). "Human monoclonal antibodies: The emperor's new clothes?". *Nature Biotechnology*, **17,** 621.

Borrebaeck, C.A.K. (2000). "Antibodies in diagnostics - from immunoassays to protein chips". *Immunol. Today*, **21(8)**, 379-82.

Boulianne, G.L., Hozumi, N. and Shulman, M.J. (1984). "Production of functional chimaeric human/mouse antibody". *Nature (Lond.)*, **312**, 643-6.

Bourinbaiar, A.S., Tan, X. and Nagorny, R. (1993(a)) "Inhibitory effect of coumarins on HIV-1 cell replication and cell-mediated or cell-free viral transmission". *Acta Virol.*, **37**, 241-50.

Bourinbaiar, A.S., Tan, X. and Nagorny, R. (1993(b)) "Effect of the oral anticoagulant, warfarin, on HIV-1 replication and spread". *AIDS*, **7 (1)**, 129-30.

Bowers, W.F., Fulton, S. and Thompson, J. (1984) "Ultrafiltration *vs*. Equilibrium Dialysis for determination of free fraction". *Clin. Pharmacokinetics.*, **9**, 549-60.

Braggio, S., Barnaby, R.J., Grossi, P. and Cugola, M. (1996) "A strategy for validation of bioanalytical methods". *J. Pharm. Biomed. Anal.*, **14**, 375-88.

Breckenbridge, A. and Orme, W. (1973) "Kinetics of warfarin absorption in man". *Clin. Pharmacol. Therapeutics*, **14 (6)**, 955-61.

Breen, D.R. (1987) "Production and characterisation of monoclonal antibodies against human plasma apolipoprotein". **Ph.D. Thesis**, Dublin City University, Dublin, Ireland.

Brigden, M.L., Kay, C., Le, A., Graydon, C. and McLeod, B. (1998) "Audit of the frequency and clinical response to excessive oral anticoagulation in an out-patient population". *Am. J. Hematol.*, **59(1)**, 22-7.

Brodeur, B.R., Tsang, P and Larose, Y. (1984) "Parameters affecting ascites tumour formation in mice and monoclonal antibody production". *J. Immunol. Meth.*, **71**, 265-272.

Brown, J.M. (1973) "A study of the mechanism by which anticoagulation with warfarin inhibits blood-borne metastases". *Cancer Res.* , **33**, 1217-24.

Bruno, J. (1998) "Validation BIACORE Assay". *BIAjournal*, **2**, 9-11.

Buckley, N.A. and Dawson, A.H. (1992) "Drug interactions with warfarin". *Med. J. Aust.*, **157(7),** 479-83.

Bush, E.D., Low. L.K. and Trager, W.F. (1983) "A sensitive and specific stable isotope assay for Warfarin and its metabolites". *Biomed. Mass Spec.*, **10(7)**, 395-8.

Cai, W.M., Hatton, J., Pettigrew, L.C., Dempsey, R.J. and Chandler, M.H.H. (1994) "A simplified high-performance liquid chromatographic method for direct determination of warfarin enantiomers and their protein binding in stroke patients". *Therapeutic Drug Monitoring*, **16**, 509-12.

Caldwell, P.T., Ren, P. and Bell, R.G. (1974) "Warfarin and the metabolism of Vitamin K_1" *Biochem. Pharmacol.*, **23**, 3353-62.

Campbell, H.A., Smith, W.K, Roberts, W.L. and Link, K.P. (1948) "Studies on the haemorrhagic sweet clover disease. II. The bioassay of haemorrhagic concentrates by following the prothrombin level in the plasma of rabbit blood". *J. Biol. Chem.*, **138**, 1-20.

Capitán-Vallvey, L. F., Deheldel, M. K. L. and Avidad, R. (1999) "Determination of warfarin in waters and human plasma by solid-phase room–temperature transmitted phosphorescence". *Archives Environ. Contam. Toxicol.*, **37**, 1-6.

Caraballo, P.J., Gabriel, S.E., Castro, M.R. (1999) "Changes in bone density after exposure to oral anticoagulants". *Osteoporos Int.*, **9**, 441-8.

Carroll, W.E. and Jackson, R.D. (1999) "Modified anticoagulant therapy factor and international normalized ratio in patients in an unstable coagulation state with respect to warfarin therapy". *Res. Commun. Mol. Pathol. Pharmacol.*, **105(3)**, 262-70.

Carroll, K. and O' Kennedy, R. (1988) "The elimination of mycoplasma from infected hybridomas by passaging in Balb/C mice". *J. Immunol. Meth.*, **108**, 189-93.

Carty, P. and O' Kennedy, R. (1988) "Use of high-performance liquid chromatography for the purification of antibodies and antibody conjugates and the study of antibody-antigen interactions". *J.Chrom.*, **442**, 279-88.

Carty, P., O' Kennedy, R., Abad, E.L., Alvarez, J.M.F., Flores, J.R., Smyth, M.R. and Tipton, K. (1990) "Purification of Human glutamate dehydrogenase (GDH) and an adsorptive investigation of the interaction of GDH with rabbit anti-human GDH antibody". *Analyst*, **115**, 617-21.

Catimel, B., Weinstock, J., Nerrie, M., Domagala, T. & Nice, E.C. (2000) "Micropreparative ligand fishing with a cuvette-based optical mirror resonance biosensor". *J. Chrom. A.*, **869**, 261-73.

Chahinian, A.P., Propert, K.J., Ware, J.H., Zimmer, B., Perry, M.C., Hirsh, V., Skerin, A., Kopel, S., Holland, J.F., Comis, R.L. and *et al.* (1998) "A randomized trial of anticoagulation with warfarin and of alternating chemotherapy in extensive small-cell lung cancer by the Cancer and Leukemia Group B". *J. Clin. Oncol.*, **8(7),** 993-1002.

Chaiken, I., Rosé , S., and Karlsson, B. (1992). "Analysis of macromolecular interactions using immobilised ligands." *Anal. Biochem.*, **201**, 197-210.

Chan, K. and Woo, K. (1988) "Determination of warfarin in human plasma by high performance liquid chromatography". *Meth. Find. Exptl. Clin. Pharmacol.*, **10(11)**, 699-703.

Chan, T.K. (1995) "Adverse interactions between warfarin and nonsteroidal antiinflammatory drugs; Mechanisms, clinical significance, and avoidance". *Ann. Pharmacother.*, **29**, 1274-83.

Chan, W.S., Anand, S. and Ginsberg, J.S. (2000) "Anticoagulation of pregnant women with mechanical heart valves: a systematic review of the literature". *Arch. Intern. Med.*, **160(2),** 191-6.

Chan, Y.C., Valenti, D., Mansfield, A.O. and Stanaby, G. (2000) "Warfarin-induced skin necrosis". *Br. J. Surg.*, **87(3)**, 266-72.

Chignell, C.F. (1970) "Optical studies of drug-protein complexes. IV. The interaction of warfarin and dicoumarol with human serum albumin". *Mol. Pharmacol.*, **6**, 1-12.

Chong, B.H. (1996) "Anticoagulation". *Aust. Family Physician*, **25(1)**, 74-9.

Christensen, L.L.H. (1997) "Theoretical analysis of protein concentration determination using biosensor technology under conditions of partial mass transport limitation". *Anal. Biochem.*, **249**, 153-64.

Chu, K.S., Jin, S., Guo, J., Jue, M. and Huang, J.J. (1995) "Studies on affinity constants of hapten-specific monoclonal antibodies using an antibody-immobilized ELISA". *Biotech. Prog.*, **11**, 352-356.

Chu, K., Wu, S.-M.W., Stanley, T., Stafford, D.W. and High, K.A. (1996) "A mutation in the propeptide of factor IX leads to warfarin sensitivity by a novel mechanism". *J. Clin. Invest.*, **98**, 7: 1619-25.

Clark, M. (2000) "Antibody humanisation: a case of the 'Emperor's new clothes'?". *Immunol. Today*, **21(8)**, 397-402..

Clatanoff , D.V., Triggs, P.O. and Meyer, O.O. (1954) "Clinical experience with coumarin anticoagulants warfarin and warfarin sodium". *Arch. Inst. Med.*, **94**, 213.

Clynes, R.A., Towers, T.L., Presta, L.G. and Ravetch, J.V. (2000). "Inhibitory Fc receptors modulate *in vivo* cytotoxicity against tumour targets". *Nature Medicine*, **6(4)**, 443-6.

Cook, C.E., Ballentine, D.E., Seltzman, T.B. and Tallent, C.R. (1979) "Warfarin enantiomer disposition : determination by stereoselective radioimmunoassay". *J. Pharmacol. Exp. Pharm.*, **210**, 391-8.

Corrigan, J.J. and Ulfers, L.L. (1981) "Effect of vitamin E on prothrombin levels in warfarin-induced vitamin K deficiency". *Am. J. Clin. Nutr.*, **34(9)**, 1701-5.

Cosgriff, T.M. and Stuart, W., (1953) "Chronic anticoagulant therapy in recurrent embolism of cardiac origin". *Ann. Intern. Med.* **38**, 278-87.

Crooks, S. R. H., Baxter, G. A., O'Connor, M. and Elliot, C. T. (1998) "Immunobiosensor-an alternative to enzyme immunoassay screening for residues of two sulfonamides in pigs." *Analyst*, **123**, 2755-57.

Currie, L.A. (1999) "Nomenclature in evaluation of analytical methods including detection and quantification capabilities (IUPAC Recommendations 1995)". *Anal. Chim. Acta.*, **391**, 105-126.

Cush, R., Cronin, J.M., Stewart, W.J., Maule, C.H., Molloy, J. and Goddard, N.J.(1993) "The resonant mirror: a novel biosensor for direct sensing of biomolecular interactions Part 1: Principle of operation and associated instrumentation". *Biosensors and Bioelectronic*, **8**, 347-353.

Dam, H. (1929) "Cholesterinstoffweschel in Hühnereirern und hühnchen". *Biochem. Z.*, **215**, 475-92.

Danelian, E., Karlén, A., Karlsson, R., Winiwarter, S., Hansson, A., Löfås, S., Lennernäs, H. and Hämäläinen, M.D. (2000). "SPR Biosensor Studies of the Direct Interaction between 27 Drugs and a Liposome Surface: Correlation with Fraction Absorbed in Humans". *J. Med. Chem.*, **43(11)**, 2084-7.

Danesi, M.A. (1980) "Total resistance to oral anticoagulants (Nicoumalone and warfarin)". *Br. J. Clin. Practice*, **34(2)**, 55-64.

Danilova, N.P. (1994) "ELISA screening of monoclonal antibodies to haptens: influence of the chemical structure of hapten-protein conjugates". *J. Immunol. Meth.*, **117**, 111-7.

Davies, D.R., Chacko, S. and Cohen, G. (1996) "General features of antibody crystal structures". *Immunotechnology*, **2**, 261-314.

Davis, J.M., Pennington, J.E., Kubler, A.M. and Conscience, J.F. (1982) "A simple, single-step technique for selecting and cloning hybridomas for the production of monoclonal antibodies". *J. Immunol. Meth.*, **50**, 161-71.

Davis, P.J. (1988) "Microbial models of mammalian drug metabolism". *Dev. Industrial Microbiol.*, **29**, 197-218.

Davis, P.J. and Rizzo, J.D. (1982) "Microbial transformations of warfarin: Stereoselective reduction by *Nocardia corallina* and *Arthrobacter* species". *Appl. Environ. Microbiol.*, **43(4)**, 884-90.

De Boer, M., Ossendorp, F.A., Van Duijn, G., Ten Voorde, G.H.J. & Tager, J.M. (1989) "Optimal conditions for the generation of monoclonal antibodies using primary immunisation of mouse splenocytes *in vitro* under serum-free conditions". *J. Immunol. Meth.*, **121**, 253-260.

Deckert, F.W. (1974) "Coumarin Anticoagulants: A review of some current research areas". *South. Med. J.*, **67(10)**, 1191-1202.

Deckert, F. and Legay, F. (1999) "Development and Validation of an Immunoreceptor Assay for Simulect Based on Surface Plasmon Resonance". *Anal. Biochem.*, **274**, 81-9.

de Geus, B. and Hendriksen, C.F.M. (1998) "*In vivo* and *In vitro* production of monoclonal antibodies: Current possibilities and Future perspectives". *Res. Immunol.* **149**, 533-34.

Delcros, J.G., Clement, S., Thomas, V., Quemener, V. and Moulinoux, J.P. (1995) "Differential recognition of free and covalently bound polyamines by the monoclonal anti-spermine antibody SPM8-2". *J. Immunol. Meth.*, **185**, 191-8.

Demartis, S., Huber, A., Viti, F., Lozzi, L ., Giovannoni, L.,Neri, P., Winter, G. & Neri, D. (1999) "A strategy for the isolation of catalytic activities from repertoires of enzymes displayed on phage". *J. Mol. Biol.*, **286**, 617-633.

Demirkan, K., Stephens, M.A., Newman, K.P. and Self, T.H. (2000) "Response to warfarin and other oral anticoagulants: Effects of disease states". *South. Med. J.*, **93(5)**, 448-54.

DeNardo, S.J., Kroger, L.A. and DeNardo, G.L. (1999). "A new era for radiolabelled antibodies in cancer ?". *Curr. Opin. Immunol.*, **11**, 558-62.

De Vries, J.X., Harenberg, J., Walter, E., Zimmerman, R. and Simon, M. (1982) "Determination of the anticoagulant phenprocoumon in human plasma and urine by high-performance liquid chromatography". *J. Chrom. Biomed. Appl.*, **231**, 83-92.

De Vries, J. X., Simon, M., Zimmerman, R. and Harenberg, J. (1985) "Identification of phenprocoumon metabolites in human urine by high-performance liquid chromatography and gas chromatography-mass spectrometry". *J. Chrom.*, **338**, 325-34.

De Vries, J.X. and Schmitz-Kummer, E. (1993) "Direct column liquid chromatographic enantiomer separation of the coumarin anticoagulants phenprocoumon, warfarin, acenocoumarol and metabolites on an α-acid glycoprotein chiral stationary phase". *J. Chrom.*, **614**, 315-20.

De Vries, J.X and Volker, U. (1990) "Determination of the plasma protein binding of the coumarin anticoagulants phenprocoumon and it's metabolites, warfarin and acenocoumarol, by ultrafiltration and high performance liquid chromatography". *J. Chrom. Biomed. Appl.*, **529**, 479-85.

de Wildt, RM.T., Mundy, C.R., Gorick, B.D. and Tomlinson, I.M. (2000) " Antibody arrays for high-throughput screening of antibody-antigen interactions." *Nature Biotechnology*, **18**, 989-94.

De Wolff, F. and Cate, J.W.T. (1979) "Transient acquired resistance to the coumarin anticoagulants phenprocoumon and acenocoumarol". *Scand. J. Haematology*, **23**, 437-41.

Diab, F. and Feffer, S. (1994) "Hereditary warfarin resistance". *Southern Med. J.*, **87(3)**, 407-9.

Dockal, M., Carter, D.C. and Ruker, F. (1999) "The three recombinant domains of human serum albumin". *J. Biol. Chem.*, **274(41)**, 29303-310.

Dueñas, M., Malmborg, A.C., Casavilla, R., Ohlin, M. and Borrebaeck, C.A.K. (1996) "Selection of phage displayed antibodies based on kinetic constants". *Mol. Immunol.*, **33(3)**, 279-285.

Ekins, R. P. (1998) "Ligand assay: from electrophoresis to miniaturized microarrays." *Clin. Chem.*, **44 (9)**, 2015-30.

Elgert, K.D. (1996) *"Immunology: understanding the immune system"*. Wiley-Liss Publications, New York.

Erlandson, P., Marle, I., Hannson, L., Isakkson, R., Petterson, C. and Petterson, G. (1990) "Immobilized cellulose (CBH I) as a chiral stationary phase for direct resolution of enantiomers". *J. Amer. Chem. Soc.*, **112**, 4573-4.

Essex, D.W., Wynn, S.S. and Jin, D.K. (1998) "Late-onset warfarin-induced skin-necrosis: case report and review of the literature". *Am. J. Hematol.*, **57(3)**, 233-7.

Evan, S. V. and MacKenzie, R. C. (1999) "Characterization of protein-glycolipid recognition at the membrane bilayer". *J. Mol. Recognit.*, **12**, 155-168.

Fagerstam, L.G. and O' Shannessy, D.J. (1993) "Surface plasmon resonance detection in affinity technologies". Handbook of Affinity Chromatography, **63**, 229-252.

Falkenberg, F.W. (1998(a)) "Monoclonal antibody production: problems and solutions." *Res. Immunol.* **149**, 542-47.

Falkenberg,F, W. (1998(b)) "Production of monoclonal antibodies in the miniPERM(bioreactor comparison with other hybridoma culture methods". *Res. Immunol.* **149**, 560-70.

Fasciglione, G., Marini, S., Bannister, J.V. and Giardina, B. (1996) "Hapten-carrier interactions and their role in the production of monoclonal antibodies against hydrophobic haptens". *Hybridoma,* **15(1)**, 1-9.

Fasco, M.J., Piper, L.J. and Kaminsky, L.S. (1977) "Biochemical applications of a quantitative high-pressure liquid chromatographic assay of warfarin and it's metabolites". *J. Chrom.*, **131**, 365-73.

Ferrer, J. M., Leiton, M. J. & Zaton, A.M. (1998) "The binding of benzopyrones to human serum albumin. A structure-affinity study". *J. Protein Chem.*, **2**, 115-9.

Findlay, J. W. A., Smith, W. C., Lee, J. W., Nordblom, G. D., Das, I., DeSilva, B. S., Khan, M. N., and Bowsher, R.R. (2000) "Validation of immunoassays for bioanalysis: a pharmaceutical industry perspective". *J. Pharm. Biomed. Anal.*, **21**, 1249-73.

Fisher, B. and Fisher, E.R. (1967) "Anticoagulants and tumour cell lodgement". *Cancer Res.*, **27(1)**, 421-5.

Fitzpatrick, J., Fanning, L., Hearty, S., Leonard, P., Manning, B.M., Quinn, J.G. and O'Kennedy, R. (2000). "Applications and recent developments in the use of antibodies for analysis". *Anal. Letters*, **33(13)**, 2563-2609.

Friguet, B., Chaffotte, A.F., Djavadi-Ohaniance, L. and Goldberg, M.E. (1985) "Measurements of the true affinity constant in solution of antigen-antibody complexes by enzyme-linked immunosorbent assay". *J. Immunol. Meth.*, **77**, 305-319.

Freedman, M.D. and Olatidoye, A.G. (1994) "Clinically significant drug intractions with the oral anticoagulants". *Drug Safety*, **10(5)**, 381-94.

Freeman, B.D., Zehnbauer, B.A., McGrath, S., Borecki, I. and Buchman, T.G. (2000) "Cytochrome P450 polymorphisms are associated with reduced warfarin dose". *Surgery*, **128(2)**, 281-5.

Frostell-Karlsson, A., Remaeus, A., Roos H.,Andersson, K., Borg, P., Hamalainen, M.,and Karlsson. (2000) "Biosensor analysis of the interaction between immobilized human serum albumin and drug compounds for prediction of human serum albumin binding levels". *J. Med. Chem.* **43**, 1968-92.

Furie, B.,Diuguid, C.F., Jacoba, M., Diuguid, D.L and Furie, B.C. (1990) "Randomized prospective trial comparing the native prothrombin antigen with the Prothrombin Time for monitoring oral anticoagulant therapy". *Blood*, **75(2)**, 344-49.

Furie, B., Liebman, H.A., Blanchard, R.A., Coleman, M., Kruger, S.F. and Furie, B.C. (1984) "Comparison of the native prothrombin antigen and the prothrombin time for monitoring oral anticoagulant therapy". *Blood*, **64**, 445.

Furuya, H., Fernandez-Salguero, P., Gregory, W., Taber, H., Steward, A., Gonzalez, F.J. and Idle, J.R. (1995) "Genetic polymorphism of CYP2C9 and its effect on warfarin maintenance

dose requirement in patients undergoing anticoagulation therapy". *Pharmacogenetics*, **5**, 389-92.

Gaines Das, R.E. (1999) . "Assessment of Assay Precision: a Case Study of an ELISA for Anti-purtussis Antibody". *Biologicals* , **27**, 125-31.

Ganrot, P.O. and Nilehn, J.E. (1968) "Plasma prothrombin during treatment with Dicoumarol. II. Demonstration of an abnormal prothrombin fraction". *Scand. J. Clin. Lab.*, **22**, 23-8.

Gareil, P., Grammond, J.P. and Guyon, F. (1993) " Separation and determination of warfarin enantiomers in human plasma samples by capillary zone electrophoresis using a methylated β-cyclodextrin containing electrolyte". *J. Chrom.*, **615**, 317-25.

Garrett, L.R., Pascual, D.W., Clem, L.W. and Cuchens, M.A. (1987) "Conformational changes in the DNA of hybridoma cells from pristane-treated mice". *Chem. Biol. Interactions*, **61**, 249-63.

Gartner, B.C., Seifert, C.B., Michalk, D.V. and Roth, B. (1993) " Phenprocoumon therapy during pregnancy: case report and comparison of the teratogenic risk of different coumarin derivatives". *Z. Geburtshilfe. Perinatol.*, **197(6)**, 262-5.

George, S., Parmar, S., Meadway, C. & Braithwaite, R.A. (2000) "Application and validation of a urinary methadone metabolite (EDDP) immunoassay to monitor methadone compliance". *Ann. Clin. Biochem.*, **37**, 350-4.

Ghetie, V. and Ward, E.S. (2000) "FcRn: the MHC class I-related receptor that is more than an IgG transporter". *Immunol. Today*, **18(12)**, 592-598.

Ginsberg, J.S. and Hirsh, J. (1995) "Use of antithrombotic agents during pregnancy". *Chest*, **108(4)**, 305s-11s.

Gitter, M.J., Jaeger, T.M., Petterson, T.M., Gersh, B.J. and Silverstein, M.D. (1995) "Bleeding and thromboembolism during anticoagulant therapy: a population-based study in Rochester, Minnesota". *Mayo Clin. Proc.*, **70(8)**, 725-33.

Glaser, R.W. (1993) "Antigen-antibody binding and mass transport by convection and diffusion to a surface: A two-dimensional computer model of binding and dissociation kinetics". *Anal. Biochem.*, **213**, 152-61.

Glennie, M.J. and Johnson, P.W.M. (2000) "Clinical trials of antibody therapy". *Immunol. Today*, **21(8)**, : 403-410.

Glover, J.J. & Morrill, G.B. (1995) "Conservative treatment of overanticoagulated patients". *Chest*, **108(4)**, 987-90.

Goldenberg, M.M. (1999) "Trastuzumab, a recombinant DNA-derived humanized monoclonal antibody, a novel agent for the treatment of metastatic breast cancer". *Clin. Ther.*, **21**,309-18.

Gorter, A., van de Griend, R.J., van Eendenburg, J.D., Haasnoot, W.H. and Fleuren, G.J. (1993) "Production of bi-specific monoclonal antibodies in a hollow-fibre bioreactor". *J. Immunol. Meth.*, **161(20)**, 145-50.

Green, L.L. (1999) "Antibody engineering via genetic engineering of the mouse: Xenomouse strains are a vehicle for the facile generation of therapeutic human monoclonal antibodies". *J. Immunol. Meth.*, **231**, 11-23.

Griffiths, D.A., Brown, D.E. and Jezequel, S.G. (1992) "Biotransformation of warfarin by the fungus Beauveria bassiana". *Appl. Microbial and Technology*, **37**, 169-75.

Griffiths, D. and Hall, G. (1993) "Biosensors – what real progress is being made?" *TIBTECH*, **11**, 122-30.

Gunneriusson, E., Nord, K., Uhlen, M. and Nygren, P. (1999) "Affinity maturation of a Taq DNA polymerase-specific affibody by helix shuffling". *Protein Eng.*, **12(10),** 873-878.

Gurwitz, J.H., Avonr, J., Ross-Degnan, D., Choodnovskiy, I. & Ansell, J. (1992) "Aging and the anticoagulant response to warfarin therapy". *Ann. Intern. Med.*, **116(11),** 901-4.

Ha, C.-E., Petersen, C.E., Park, D.S., Harohalli, K. and Bhagavan, N.V. (2000) "Investigations into the effects of ethanol on warfarin binding to human serum albumin". *J. Biomed. Sci.*, **7**, 114-21.

Hall, J.G., Pauli, R.M. and Wilson, K.M. (1980) "Maternal and fetal sequelae of anticoagulation during pregnancy". *Am. J. Med.*, **68**, 122-40.

Hallak, H.O., Wedlund, P.J., Modi, M.W., Patel, I.H., Lewis, G.L., Woodruff, B. and Trowbridge, A.A. (1993) "High clearance of (S)-warfarin in a warfarin-resistant subject". *Br. J. Clin. Pharmacol.*, **35**, 327-30.

Hamada, H., Fuchikami, Y., Jansing, R.L. and Kaminsky, L.S. (1993) "Regioselective hydroxylation of warfarin by cell suspensions cultures of *Catharantheus roseus*". *Phytochemistry*, **33(3)**, 599-600.

Hara, K., Akiyama, Y. and Tajima, T. (1994) "Sex differences in the anticoagulant effects of warfarin". *Japanese J. Pharmacol.*, **66**, 387-92.

Harayama, S. (1998) "Artificial evolution by DNA shuffling". *TIBTECH*, **16**, 76-82.

Harder, S. & Thürmann, P. (1996) "Clinically important drug interactions with anticoagulants". *Clin. Pharmacokinet.*, **6**, 416-44.

Harlow, E. and Lane, D. (1988) "Antibodies: A laboratory manual". Cold Spring Harbour Laboratory, USA.

Harris, J.E. "Interaction of dietary factors with oral anticoagulants: Review and applications". *J. Am. Dietetic Assoc.*, **95(5)**, 580-4.

Haupt, K. and Mosbach, K. (1998) "Plastic antibodies: developments and applications". *TIBTECH*, **16**, 468-75.

He, M., Kunze, K.L. and Trager, W.F. (1995) "Inhibition of (S)-Warfarin metabolism by sulfinpyrazone and it's metabolites". *Drug. Metab. Disposition*, **23(6)**, 659-63.

Hemker, H.C., Veltkamp, J.J., Hensen, A., and Loeliger, E.A. (1963) "Nature of prothrombin biosynthesis: preprothrombinemia in vitamin K deficiency". *Nature*, **200**, 589-90.

Hemminki, A., Niemi, S., Hautoniemi, L., Soderlund, H. and Takkiken, K. (1998) "Fine tuning of an anti-testosterone antibody binding site by stepwise optimisation of the CDRs". *Immunotechnology*, **4**, 59-69.

Hendriksen, C.F.M. and Leeuw, W. de. (1998) "Production of monoclonal antibodies by the ascites method in laboratory animals". *Res. Immunol.* **149**, 535-42.

Hensley, P. and Myszka, D. (2000) "Analytical biotechnology -Sorting needles and haystacks". *Curr. Opin. Biotechnol.*, **11**, 9-12.

Hermans, J.J.R. and Thijjsen, H.H.W. (1989) "The *in vitro* ketone reduction of warfarin and analogues. Substrate stereoselectivity, product stereoselectivity, and species differences". *Biochem. Pharmacol.*, **38(19)**, 3365-3370.

Hermans, J.J.R. and Thijjsen, H.H.W. (1993) "Human liver microsomal metabolism of the enantiomers of warfarin and acenocoumarol : P450 isozyme diversity determines the differences in their pharmacokinetics". *Br. J. Pharmacol.*, **110**, 482-90.

Hermanson, G.T. (1996) "*Bioconjugate techniques*". 1st edition, Academic Press, London, England.

Hermanson, G.T., Mallia, A.K. and Smith, P.K. (1992) "*Immobilized Affinity Ligand Techniques*". 1st edition, Academic Press, London.

Hermodson, M.A., Barker, W.M. and Link, K.P. (1971) "Studies on the 4-hydroxycoumarins. Synthesis of the metabolites and some other derivatives of warfarin". *J. Med. Chem.*, **14(2)**, 167-9.

Hetherington, S. (1990) "Solid phase disruption of fluid phase equilibrium in affinity assays with ELISA". *J. Immunol. Meth.*, **131**, 195-202.

Hiatt, A., Cafferkey, R. and Bowdish, K. (1989) "Production of antibodies in transgenic plants". *Nature (Lond.)*, **342**, 76-78.

Hirsh, J. (1982) "Rebound hypercoagulability". *Stroke*, **13**, 527-37.

Hirsh, J., Dalen, J.E. Deykin, D., Poller, L. and Bussey, H. (1995) "Oral Anticoagulants: Mechanism of action, clinical effectiveness, and optimal therapeutic range". *Chest*, **108(4)**, 231-46s.

Holliger, P., Prospero, T. and Winter, G. (1993) " 'Diabodies': small bivalent and bispecific antibody fragments". *Proc. Natl. Acad. Sci. (USA).*, **90**, 6444-8.

Holt, R.J. and Freytes, C.O. (1983) "Familial warfarin resistance". *Drug Intell. Clin. Pharm.*, **17**, 281-3.

Hoogenboom, H.E. and Chames, P. (2000) "Natural and designer binding sites made by phage display technology". *Immunol. Today*, **21(8)**, 371-377.

Hoogenboom, H.E., De Bruine, A.P., Hufton, S.E., Hoet, R.M., Arends, J.-W. and Roovers, R.C. (1998) "Antibody phage display technology and it's applications". *Immunotechnology*, **4**, 1-20.

Høyer-Hansen, G., Hamers, M., Pedersen, A.N., Jørgen Nielsen, H., Brünner, N., Danø, K. and Stephens, R.W. (2000) "Loss of ELISA specificity due to biotinylation of monoclonal antibodies". *J. Immunol. Meth.*, **235**, 91-9.

Huber, A., Demartis, S. and Neri, D. (1999). "The use of biosensor technology for the engineering of antibodies and enzymes". *J. Mol. Recognit.*, **12**, 198-216.

Hubert, P., Chiap, P., Crommen, J., Boulanger, B., Chapuzet, E., Mercier, N., Bervoas-Martin, S., Chevalier, P., Grandjean, D., Lagorce, P., Lallier, M., Laparra, M.C., Laurentie, M. & Nivet, J.C. (1999) "The SFSTP guide on the validation of chromatographic methods for drug bioanalysis: from the Washington Conference to the laboratory". *Anal. Chim. Acta.*, **391**, 135-48.

Hudson, L. and Hay, F.C. (1980), *"Practical Immunology"*. Second Edition, Blackwell Scientific Publications.

Hudson, P.J. (1999) "Recombinant antibody constructs in cancer therapy". *Curr. Opin. Immunol.*, **11**, 558-562.

Hudson, P.J. and Kortt, A.A., (1999). "High Avidity scFv multimers; diabodies and triabodies". *J. Immunol. Meth.*, **231**, 177-189.

Hulse, M.-L. (1996) "Warfarin resistance: diagnosis and therapeutic alternatives". *Pharmacotherapy*, **16(6)**, 1009-17.

Hung, A., Singh, S. and Tait, R.C. (2000) "A prospective randomized study to determine the optimal dose of intravenous vitamin K in reversal of over-warfarinization". *Br. J. Haematol.*, **109**, 537-9.

Hurrell, J.G.R. (1985) "*Monoclonal Hybridoma Antibodies: Techniques and Applications*". CRC Press, Inc. Boca Raton, Florida.

Hutt, A.J., Hadley, M.R. and Tan, S.C. (1994) "Enantiospecific anaylsis: Applications in bioanalysis and metabolism". *Europ. J. Drug Metab. Pharmacokinet.*, **3**, 241-51.

Ikawa, M., Stahmann, M.A., and Link, K.P. (1944) "Studies on 4-hydroxycoumarins. V. The condensation of α, β-unsaturated ketones with 4-hydroxycoumarins". *J. Am. Chem. Soc.*, **66**, 902-6.

Ikeda, M., Conney, A.H. and Burns, J.J. (1968) "Stimulatory effect of phenobarbital and insecticides on warfarin metabolism in the rat". *J. Pharmacol. Exp. Pharm.* **162(2)**, 338-343.

Ikeda, M., Ullrich, V. and Staudinger, H. (1968) "Metabolism *in vitro* of warfarin by enzymic and nonenzymic systems". *Biochem. Pharmacol.*, **17**, 1663-69.

Iliades, P., Kortt, A.A. and Hudson, P.J. (1997) "Triabodies: single chain Fv fragments without a linker form trivalent trimers". *FEBS letters*, **409**, 437-441.

Jaffers, G.J., Fuller, T.C., Cosimi, A.B., Russell, P.S., Winn, H.J. and Colvin, R.B. (1986) "Monoclonal antibody therapy. Anti-idiotypic and non-anti-idiotypic antibodies to OKT3 arising despite intense immunosuppression". *Transplantation,* **41(5)**, 572-8.

James, A.H., Britt, R.P., Raskino, C.L. and Thompson, S.G. (1992) "Factors affecting the maintenance dose of warfarin". *J. Clin. Pathol.*, **45**, 704-6.

Jaspert, R., Geske, T., Teichmann, A., Ka(ner, Y.-M., Kretzschmar, K. and L.'Age-Stehr, J. (1995) "Laboratory scale production of monoclonal antibodies in a tumbling chamber". *J. Immunol. Meth.*, **178**, 77-87.

Jillella, A.P. and Lutcher, C.L. (1996) "Reinstituting warfarin in patients who develop warfarin skin necrosis". *Am. J. Hematol.*, **52(2)**, 117-9.

Jirholt, P., Ohlin, M., Borrebaeck, C.A.K. and Soderlind (1998) "Exploiting sequence space: shuffling *in vivo* formed complentarity determining regions into a master framework". *Gene*, **215**, 471-6.

Jones A. (1996) "HPLC determination of anticoagulant rodenticide residues in animal livers". *Bull. Environ. Contam. Toxicol.*, **56**, 8-15.

Jönsson, U., Fagerstam, L., Ivarsson, B., Lundh, K., Löfas, S., Persson, B., Roos, H., Rönnberg, L., Sjölander, S., Stenberg, E., Stahlberg, R., Urbaniczky,C., Östlin , H. and Malmqvist, M. (1991) "Real-time biospecific interaction analysis using surface plasmon resonance and a sensorchip technology". *BioTechniques,* **11**, 620.

Jortani, S. A., Pinar, A., Johnson, N. A. and Valdes, R. (1999) "Validity of unbound digoxin measurement by immunoassays in presence of antidote (Digibind)". *Clin. Chim. Acta.*, **283**, 159-69.

Joshi, A., Berdon, W.E., Ruzal-Shapiro, C. and Barst, R.J. (2000) "CT detection of tracheobronchial calcification in an 18-year-old on maintenance warfarin sodium therapy: cause and effect?". *Am. J. Roentgenol.*, **175(3),** 921-2.

Josso F., Lavergne, J.M., Gouault, M., Prou-Wartelle, O. and Soulier, J.P. (1968) "Différents états moléculaires du facteur II (prothrombine). Leur étude à l'aide de la staphylocoagulase et d'anticorps anti-facteur II. I. Le facteur II chez les sujets traités par les antagonistes de la vitamine K". *Thromb. Diath. Haemorrh.*, **20**, 88-98.

Kamali, F., Edwards, C., Butler, T.J. and Wynne, H.A. (2000) "The contribution of plasma (R)- and (S)-warfarin and vitamin K concentrations to intra-individual variability in anticoagulation". *Thromb. Haemost.*, **83**, 349-50.

Kampranis, S. C., Gormley, N. A., Tranter, R. Orphanides, G., and Maxwell, A. (1999) "Probing the binding of coumarins and cyclothialidines to DNA gyrase". *Biochemistry*, **38(7),** 1967-76.

Kantor, R., Mayan, H., Puritz, L., Varon, D. and Farfel, Z. (2000) "Acquired haemophilia masked by warfarin". *Am. J. Med. Sci.*, **319(3)**, 197-201.

Kaplan, L.C. (1985) "Congenital Dandy-Walker malformation associated with first trimester warfarin: a case report and literature review". *Teratology,* **32(3)**, 333-7.

Karlsson, R., Fägerstam, L., Nilshans, H. and Persson, B. (1993) "Analysis of active antibody concentration. Separation of affinity and concentration parameters". *J. Immunol. Meth.*, **166**, 75-84.

Karnes, T.H, Shiu, G. & Shah, V.P.(1991). "Validation of Bioanalytical Methods". *Pharm. Res.*, **8(4),** 421-6.

Keating, G. (1998) "Biosensor-based studies on coumarins". **Ph.D. Thesis**, Dublin City University, Dublin, Ireland.

Kelly, J.G. and O' Malley, K. (1979) "Clinical Pharmacokinetics of Oral Anticoagulants". *Clin. Pharmacokinet.*, **4**, 1-15.

Keuh, Y.K., Ee, .K.H. and Teoh, P.C. (1982) "Resistance to oral anticoagulant therapy-case report and a review of literature". *Singapore Med. J.*, **24(2),** 114-5.

Killard, A. (1998) "The production of antibodies to coumarin and its major human metabolites". **Ph.D. Thesis**, Dublin City University, Dublin, Ireland.

Kim, J.M. and White, R.H. (1996) "Effect of vitamin E on the anticoagulant response to warfarin". *Am. J. Cardiol.*, **77(7)**, 545-6.

King, K. (1985) "Uses of heparin and warfarin". *Med. J. Australia,* **142,** 197-201.

King, S-H. P., Joslin, M.A., Raudibaugh, K., Pieniaszek, H.J. Jr. and Benedek, I.H. (1995) "Dose-dependent pharmacokinetics of warfarin in healthy volunteers". *Pharm. Res.*, **12(12),** 1874-77.

Koch-Weser, J. and Sellers, E.M. (1971) "Drug interactions with coumarin anticoagulants". *New Eng. J. Med.*, **285**, 487-98, 547-58.

Kohl, N.E., Emini, E.A., Schleif, W.A., Davis, L.J., Heimbach, J.C., Dixon, R.A., Scolnick, E.M. and Sigal, I.S. (1988) "Active immunodeficiency virus protease is required for viral infectivity". *Proc. Natl. Acad. Sci. (USA),* **85**, 4686-90.

Kohler, G. and Milstein, C. (1975). "Continuous culture of fused cells secreting antibody of predefined specificity". *Nature (Lond)*, **256**, 495-497.

Kontermann, R.E., Martineau, P., Cummings, C.E., Karpas, A., Allen, D., Derbyshire, E. and Winter, G. (1997) "Enzyme immunoassays using bispecific diabodies". *Immunotechnology*, **3**, 137-144.

Krebber, A., Bornhauser, S., Burmester, J., Honegger, A., Willuda, J., Bosshard, H.R. and Pluckthun, A. (1997) "Reliable cloning of functional variable domains from hybridomas and

spleen cell repertoires employing a reengineered phage display system". *J. Immunol. Meth.*, **201**, 35-55.

Kriz-Kozak, K. and Lammle, B. (1999) "46-year-old woman with multiple haematomas and bleeding of the base of the tongue: phenprocoumon poisoning". *Ther. Umsch.*, **56(9)**, 541-3.

Kronick, J., Phelps, N.E., McCallion, D.J. and Hirsh, J. (1974) "Effects of sodium warfarin administered during pregnancy in mice". *Am. J. Obstet Gynaecol.*, **118(6)**, 819-23.

Kruse, J.A. & Carlson, R.W. (1992) "Fatal rodenticide poisoning with brodifacoum". *Ann. Emerg. Med.*, **21 (3)**, 331-6.

Kukanskis, K., Elkind, J., Melendez, J., Murphy, T., Miller, G. and Garner, H. (1999) "Detection of DNA Hybridization Using the TISPR-1 Surface Plasmon Resonance". *Anal. Biochem.*, **274**, 7-17.

Kunze, K.L., Wienkers, W.L., Thummel, K.E. and Trager, W.F. (1996) "Inhibition of the human cytochrome P450-dependent metabolism of warfarin by Fluconazole: *In vitro* studies". *Drug Metab. Disposition*, **24(4)**, 414-21.

Kwaan, H.C. and Keer, H.N. (1990) "Fibrinolysis and cancer". *Semin. Thromb. Hemostasis*, **16(3)**, 230-5.

Lackmann , M., Bucci, T., Mann, R.J., Kravets, L.A.,Viney, E., Smitk, F., Moritz, R.L., Carter, W., Simpson, R.L., Nicola, N.A., Mackwell, K., Nice, E.C., Wilks, A.F. & Boyd, A.W. (1996). "Purification of a ligand for the EPH-like receptor HEK using a biosensor-based affinity detection approach". *Proc. Natl. Acad. Sci. (USA)*, **93(6)**, 2523-7.

Laemmli, U.K. (1970) "Cleavage of structural proteins during the assembly of the head of bacteriopahge T4". *Nature (Lond.)*, **227**, 680-5.

Lancaster, T.R., Singer, D.E., Sheehan, M.A., Oertel, L.B., Maraventano, S.W., Hughes, R.A. and Kistler, J.P. (1991) "The impact of long-term warfarin therapy on quality of life". *Arch. Intern. Med.*, **151**, 1944-9.

Lang, D. and Bocker, R. (1995) "Highly sensitive and specific high-performance liquid chromatographic analysis of 7-hydroxywarfarin, a marker for human cytochrome P-4502C9 activity". *J. Chrom. B.*, **672**, 305-9.

Langseth, W. and Nymoen, U. (1991) "Determination of coumarin anticoagulant rodenticide residues in animal liver by high performance liquid chromatography". *Fresenius. J. Anal. Chem.*, **339**, 249-52.

Larrick, J.W., Yu, L., Chen, J., Jaiswal, S., and Wycoff, K. (1998). "Production of antibodies in transgenic plants". *Res. Immunol.*, **149(6)**, 603-8.

Lee, M. and Schwartz, R.W. (1981) "Warfarin resistance and vitamin K". *Ann. Internal Med.*, **94**, 140.

Lefrere, J.-J., Horellou, M.-H., Conard, J. and Samama, M. (1987) "Proposed classification of resistances to oral anticoagulant therapy". *J. Clin. Pathol.*, **40**, 242.

Lehtonen, O. P., and Eerola, E. (1982). "The effect of different antibody affinities on ELISA absorbance and titer". *J. Immunol. Meth.*, **54,** 233.

Lewis, R.J. and Trager, W.F. (1970) "Warfarin metabolism in man: Identification of metabolites in urine". *J. Clin. Invest.*, **49**, 907-13.

Lewis, R.J., Trager, W.F., Robinson, A.J. and Chan, K. (1973) "Warfarin metabolites: The anticoagulant activity and pharmacology of warfarin alcohols". *J. Lab.Clin. Med.*, **81(6)**, 925-31.

Lietzke, R. and Unsicker, K. (1985) "A statistical approach to determine monoclonality after limiting cell plating of a hybridoma clone". *J. Immunol. Meth.*, **76**, 223-8.

Link, K.P. (1943-44) "The anticoagulant from spoiled sweet clover hay". *Harvey Lecture Series*, **39**, 162-216.

Link, K.P. (1945) "The anticoagulant dicoumarol". *Proc. Inst. Med. Chic.*, 15, 370-89.

Link, K.P. (1948) "Dicoumarol - and the estimation of prothrombin". Transactions of the first conference on blood clotting and allied problems, New York, 126-36.

Link, K.P. (1959) "The discovery of dicoumarol and it's sequels". *Circulation*, **9**, 97-107.

Lipman, N.S. and Jackson, L.R. (1998) "Hollow fibre bioreactors: an alternative to murine ascites for small scale (<1 gram) monoclonal antibody production". *Res. Immunol.* **149**, 571-76.

Lipski, L.A., Witzleb, M.P.,Reddington, G.M. and Reddington, J.J. (1998) "Evaluation of small to moderate scale *in vitro* monoclonal antibody production via the use of the I-Mab gas-permeable bag system". *Res. Immunol.* **149**, 547-52.

Little, M., Kiripanyov, S.M., Le Gall, F. and Moldenhauer, G. (2000) "Of mice and men: hybridoma and recombinant antibodies". *Immunol. Today*, **21(8)**, 364-370.

Littlefield, J.W. (1964) "Selection of hybrids from mating of fibroblasts *in vitro* and their presumed recombinants". *Science*, **145**, 709.

Lodwick, A. (1999). "Warfarin therapy: A review of ther literature since the Fifth American College of Chest Physicians' consensus conference on antithrombotic therapy". *Clin. Appl. Thrombosis/Haemostasis*, **5(4)**, 208-15.

Lui, H., Ong, S., Glunz, L. and Pidgeon, C. (1995). "Predicting drug-membrane interactions by HPLC: structural requirements of chromatographic surfaces". *Anal. Chem.* **67(19)**, 3550-7.

Lutomski, D.M., Bottorff, M. and Sangha, K. (1995) "Pharmacokinetic optimisation of the treatment of embolic disorders". *Clin. Pharmacokinet.*, **28((1)**, 67-92.

Lutomski, D.M., Palascak, J.E. and Bower, R.H. (1987) "Warfarin resistance associated with intravenous lipid administration". *J. Parenteral Enteral Nutr.*, , **11(3)**, 316-318.

Ma, J.K.-C., Hiatt, A., Hein, M., Vine, N.D., Wang, F., Stabila, P., van Dolleweerd, C., Mostov, K. and Lehner, T. (1995) "Generation and assembly of secretory antibodies in plants". *Science*, **268**, 716-719.

MacLaren, R., Wachsman, B.A., Swift, D.K. and Kuhl, D.A. (1997) "Warfarin resistance associated with intravenous lipid administration: discussion of the literature and review of the literature". *Pharmacother.*, **17(6)**, 1331-7.

MacNicoll, A.D. (1995) "A review of the biochemical resistances of warfarin resistances in the house mouse". *Pesticide Science*, **43(1)**, 57-9.

Malhotra, O.P. (1981) "Degradation of normal and dicoumarol-induced prothrombins with thrombin". *Ann. N.Y. Acad. Sci.*, **370**, 438-52.

Malmborg, A. and Borrebaeck, C. (1995) "BIAcore as a tool in antibody engineering". *J. Immunol. Meth.*, **183**, 7-13.

Malmborg, A., Dueñas, M., Ohlin, M., Söderlind, E. and Borrebaeck, C. (1996) "Selection of binding from phage-displayed antibody libraries using the BIAcore biosensor". *J. Immunol. Meth.*, **198,** 51-57.

Marks, J.D.,Hoogenboom, H.R., Griffiths,A.D. & Winter, G. (1992) "Molecular evolution of proteins on filamentous phage. Mimicing the strategy of the immune system". *J. Biol. Chem.*, **267(23)**, 16007-10.

Markgren, P., Hämäläinen, M. and Danielson, H.U.(2000) "Kinetic analysis of the Interaction between HIV-1 protease and inhibitors using optical biosensor technology". *Anal. Biochem.*, **279**, 71-8.

Markgren, P., Hämäläinen, M. and Danielson, H.U. (1998) "Screening of compounds interacting with HIV-1 Proteinase using optical biosensor technology". *Anal. Biochem.*, **265**, 340-50.

Marx, U. (1998). "Membrane-based cell culture technologies: a scientifically and economically satisfactory alternative to malignant ascites production for monoclonal antibodies". *Res. Immunol.* **149**, 557-59.

Matsubara, T., Koike, M., Touchi, A., Tochino, Y. and Sugeno, K. (1976) "Quantitative determination of Cytochrome P-450 in rat liver homogenate". *Anal. Biochem.*, **75**, 596-603.

McBride, J.J., Hanlon, G.W., Hutt, A.J. and Olliff, C.J. (1993) "Stereoselective reduction of warfarin and related compounds by *Nocardia corallina*". *J. Pharm. Pharmacol.*, **45**, suppl 2:1106.

McLaughlin, P., Grillo-Lopez, A.J., Link, B.K., Levy, R., Czuczman, M.S., Williams, M.E., Heyman, M.R., Bence-Bruckler, I., White, C.A., Cabanillas, F., Jain, V., Ho, A.D., Lister, J., Wey, K., Shen, D. & Dallaire, B.K.(1998) "Rituximab chimeric anti-CD20 monoclonal antibody therapy for relapsed indolent lymphoma: half of patients respond to a four-dose treatment program". *J. Clin. Onch.*, **16(8)**, 2825-33.

Mendez, M.J., Green, L.L., Corvalan, J.R., Jia, X.C., Maynard-Currie, C.E., Yang, X.D., Gallo, M.L., Louie, D.M., Lee, D.V., Erickson, K.L., Luna, J., Roy, C.M., Abderrahim, H., Kirschenbaum, F., Noguchi, M., Smith, D.H., Fukushima, A., Hales, J.F., Klapholz, S., Finer, M.H., Davis, C.G., Zsebo, K.M. and Jakobovitis, A. (1997). "Functional transplant of megabase human immunoglobulin loci recapitulates human antibody response in mice". *Nature Genetics*, **15(2)**, 146-56.

Menguy, T., Chenevois, S., Guillain, F., le Maire, M., Falson, P. & Champeil, P. (1998) "Ligand binding to macromolecules or micelles: use of centrifugal ultrafiltration to measure low-affinity binding". *Anal. Biochem.*, **264(2)**, 141-8.

Merlini, P.A., Bauer, K.A., Oltrona, L., Aedissino, D., Cattaneo, M., Belli, C., Mannucci, P.M. and Rosenberg, R.D. (1994) "Persistent activation of coagulation mechanism in unstable angina and myocardial infarction". *Circulation*, **90(1)**, 61-8.

Miller, R.A. (1982) "Treatment of B-cell lymphoma with monoclonal anti-idiotype antibody". *New Engl. J. Med.*, **306**, 17-22.

Miura, Y., Ardenghy, M., Ramasastry, S., Kovach, R. and Hochberg, J. (1996) "Coumadin necrosis of the skin: report of four patients". *Ann. Plast. Surg.*, **37(3)**, 332-7.

Morton, T.A. and Myszka, D.G. (1998) "Kinetic analysis of macromolecular interactions using surface plasmon resonance biosensors". *Methods Enzymol.*, **295**, 71-8.

Muldoon, M.T. and Stanker, L.H. (1997) "Molecularly imprinted solid phase extraction of atrazine from beef liver extracts". *Anal. Chem.*, **69(5),** 803-8

Mungall, D. and Docktor, W. (1983) "Pharmacokinetics: An Introduction". *Applied Clinical Pharmacokinetics,* edited by Dennis Mungall, Raven Press, New York.

Mungall, D. and White, R. (1992) "Aging and warfarin therapy". *Ann. Intern. Med.*, **117**, 878-9.

Mungall, D., Wong, Y.Y., Talbert, R.L., Crawford, M.H., Marshall, J., Hawkins, D.W. and Ludden, T.M. (1984) "Plasma protein binding of warfarin: Methodological considerations". *J. Pharm. Sci.*, **73**, 1000-1.

Myszka, D. G. and Rich, R. L. (2000) "Implementing surface plasmon resonance biosensor in drug discovery". *Pharm. Sci. Technol. Today,* **3(9)**, 310-17.

Nagel, A., Koch, S., Valley, U., Emmrich, F. and Marx, U. (1999) "Membrane-based cell culture systems-an alternative to *in vivo* production of monoclonal antibodies". *Dev. Biol. Stand.,* **101**, 57-64.

Naidong, W. and Lee, J.W. (1993) "Development and validation of a high performance liquid chromatographic method for the quantitation of warfarin enantiomers in human plasma". *J. Pharm. Biomed. Anal.*, **11(9)**, 785-92.

Nakamura, K., Toyohira, H., Kariyazono, H., Ishibashi, M., Saigenji, H., Shimokawa, S. and Taira, A. (1994) "Anticoagulant effects of warfarin and kinetics of K vitamin in faeces and blood". *Artery*, **21(3),** : 148-60.

Navia, M.A., Fitzgerald, P.M.D., McKeever, B.M, Leu, C.-H., Heimbach, J.C., Herber, W.K., Sigal, I.S., Darke, P.L. and Springer, J.P. (1989) "Three-dimensional structure of aspartyl protease from human immunodefeciency virus HIV-1". *Nature(Lond.)*, **337(16)** , 615-20.

Nelsestuen, G.L., Zytkovicz, T.H. and Howard, J.B. (1974) "The mode of action of vitamin K. Identification of γ-carboxyglutamic acid as a component of prothrombin". *J. Biol. Chem.*, **249**, 6347-50.

Nelson, R.W., Krone, J.R. and Jansson, O. (1997(a)) "Surface plasmon resonance biomolecular interaction analysis mass spectrometry. 1 . Chip-based analysis". *Anal. Chem.* **69**, 4363-8.

Nelson, R.W. Krone, J.R. and Jansson, O. (1997(b)). "Surface plasmon resonance biomolecular interaction analysis mass spectromtery. 2. Fiberoptic-based analysis". *Anal. Chem.* **69**, 4369-74.

Newton, D.L., Pollock, D., DiTullio, P., Echelard, Y., Harvey, M., Wilburn, B., Williams, J., Hoogenboom, H.R., Raus, J.C.M., Meade, H.M. and Rybak, S.M. (1999) "Anti-transferrin receptor antibody-Rnase fusion protein expressed in the mammary gland of transgenic mice". *J. Immunol. Meth.*, **231**, 147-57.

Nieba, L., Krebber, A. and Plückthun, A. (1996) "Competition BIAcore for measuring true affinities: large differences from values determined from binding kinetics". *Anal. Biochem.*, **234**, 155-65.

Nieto, A., Gaya, A., Jansa, M., Moreno, C. and Vives, J. (1984). "Direct measurement of antibody affinity distribution by hapten-inhibition enzyme immunoassay." *Immunol.* **21**, 537-43.

Nolin, L., and Courteau, M.,(1999) "Management of IgA nephropathy: Evidence-based recommendations". *Kidney International*, **55(70)**, S56-62.

Nord, K., Gunneriusson, E., Ringdahl, J., Stahl, S., Uhlen, M. and Nygren, P.A. (1997) "Binding proteins selected from combinatorial libraries of an alpha-helical bacterial receptor domain". *Nature Biotechnology*, **15(8)**, 772-7.

Nord, K., Gunneriusson, E., Uhlen, M., Nygren, P.-A. (2000) "Ligands selected from combinatorial libraries of protein A for use in affinity capture of apolipoprotein A-1_M and *Taq* DNA polymerase". *J. Biotech.*, **80,** 45-54.

Oates, A., Jackson, P.R., Austin, C.A. and Channer, K.S. (1998) "A new regimen for starting warfarin therapy in out-patients". *Br. J. Clin. Pharmacol.*, **46(2)**, 157-61.

Oh, S.K.W., Vig, P., Chua, F., Teo, W.K. and Yap, M.G.S. (1993) "Substantial overproduction of antibodies by applying osmotic pressure and sodium butyrate". *Biotechnol. Bioeng.*, **42**, 601-10.

Ohlin, M., Owman, H., Mach, M. and Borrebaeck, C.A.K. (1996) "Light chain shuffling of a high affinity antibody results in a drift in epitope recognition". *Mol. Immunol.*, **33(1)**, 47-56.

Omura, T. and Sato, R. (1964) "The carbon monoxide-binding pigment of liver microsomes". *J. Biol. Chem.*, **239(7)**, 2370-8.

O' Reilly, R.A. (1970) "The second reported kindred with hereditary resistance to oral anticoagulants". *New Eng. J. Med.*, **282**, 1448-51.

O'Reilly, R.A. (1976) "Vitamin K and the oral anticoagulant drugs". *Annu. Rev. Med.*, **27**, 245-61.

O'Reilly, R.A. (1987) "Warfarin metabolism and drug-drug interactions". *Adv. Exp. Med. Biol.*, **214**, 205-12.

O'Reilly, R.A., Aggeler, P.M. and Leong L.S. (1963) "Studies on the coumarin anticoagulant drugs: the pharmacodynamics of warfarin in man". *J. Clin. Invest.*, **42(10)**, 1542-51.

O'Reilly, R.A., Aggeler, P.M., Hoag, M.S., Leong, L.S., Kropatkin, M. (1964) "Hereditary trannsmission of exceptional resistance to coumarin anticoagulant drugs: the first reported kindred". *New Eng. J. Med.*, **271**, 809-15.

Overman, R.S., Stahmann, M.A., Sullivan, W.R., Heubner, C.F., Campbell, H.A. and Link, K.P. (1942) "Studies on the haemorrhagic sweet clover disease. VII. The effect of 3,3'-methylenebis(4-hydroxycoumarin) on the prothrombin time of the plasma of various animals". *J. Biol. Chem.*, **142,** 941-55.

Oyaas,K. Ellingsen,T.E., Dyrset, N. and Levine, D.W. (1994) "Hyperosmotic hybridoma cell cultures: Increased monoclonal antibody production with addition of glycine betaine". *Biotech. Bioeng.*, **44**, 991-8.

Palaretti, G. and Legnani, C. (1996) "Warfarin withdrawal". *Clin. Pharmacokinet.*, **(4)**, 300-13.

Palareti, G., Legnani, C., Guazzaloca, G., Frascaro, M., Grauso, F., De Rosa, F., Fortunato, G. and Coccheri, S. (1994) "Activation or blood coagulation after abrupt or stepwise withdrawal of oral anticoagulants—a prospective study". *Thromb. Haemost.*, **72(2)**, 222-6.

Pancrazio, J. J., Whelan, J.P.,Borkholder, D.A., Ma, W. and Stenger, D.A.(1999) "Development and application of cell-based biosensors". *Ann. Biomed. Eng.* **27(6)**, 697-711.

Pannell, R. and Milstein, C. (1992) "An oscillating bubble chamber for laboratory scale production of monoclonal antibodies as an alternative to ascites tumors". *J. Immunol. Meth.*, **146**, 43-8.

Parikh, H.H., McElwain, K., Balasubramanian, V., Leung, W., Wong, D., Morris, M.E. and Ramanathan, M. (2000) "A rapid spectrofluorimetric technique for determining drug-serum protein binding suitable for high-throughput screening". *Pharm. Res.*, **17(5)**, 632-7.

Park, S.W., Seo, B., Kim, E., Kim, D. and Paeng, K.J. (1996) "Purification and determination procedures of coumarin derivatives". *J. Foren.. Sci.*, **41(4)**, 685-88.

Parslew, R., Pryce, D., Ashworth, J. and Friedmann, P.S. (2000) "Warfarin treatment of chronic idiopathic urticaria and angio-oedema". *Clin. Exp. Allergy.*, **30**, 1161-5.

Passing, H. and Bablok, W.(1983). "A new biometrical procedure for testing the equality of measurements from two different analytical methods". *J. Clin. Chem. Clin. Biochem.*, **21**, 709-20.

Peterson, N, C. (1998) "Considerations for *in vitro* monoclonal antibody production". *Res. Immunol.*, **149**, 553-57.

Piccoli, A., Prandoni, P., Ewenstein, B.M. and Goldhaber, S.Z. (1996) "Cancer and venous thromboembolism". *Am. Heart J.*, **132(4)**, 850-4.

Piehler, J., Brecht, A., Giersch, T., Hock, B. & Gauglitz, G. (1997) "Assessment of affinity constants by rapid solid phase detection of equilibrium binding in a flow system". *J.Immunol. Meth.*, **201**, 189-206.

Pinkerton, T. C., Miller, T. D., and Janis, L. J. (1989). " Effect of protein binding on the high–performance liquid chromatography of phenytoin and imirestat in human serum by direct injection onto internal surface reversed-phase columns". *Anal. Chem.*, **61(10)**, 1171-4.

Pistillo, M.P., Sguerso, V. and Ferrara, G.B.(1992) "High yields of anti-HLA human monoclonal antibodies can be provided by SCID mice". *Hum. Immunol.* , **35**, 256-9.

Pluckthun, A. and Pack, P. (1997) "New protein engineering approaches to multivalent and bispecific antibody fragments". *Immunotechnology,* **3**, 83.

Pohl, L.R., Nelson, S.N., Porter, W.R., Trager, W.F., Fasco, M.J., Baker, F.D. and Fenton, J.W. (1976) "Warfarin – stereochemical aspects of it's metabolism by rat liver microsomes". *Biochem. Pharmacol.*, **25**, 2153-62.

Poller, L. (1987) "Progress in standardisation in anticoagulant control". *Haematol. Rev.*, **1**, 225-41.

Pollock, D.P., Kutzsko, J.P., Birck-Wilson, E., Williams, J.L., Echelard, Y. and Meade, H.M. (1999). "Transgenic milk as a method for the production of recombinant antibodies". *J. Immunol. Meth.*, **231**, 147-57.

Price, C.P. and Newman, D.J. (1997) *"Principles and Practice of enzyme immunoassay"*. 2nd edition, MacMillan Reference Ltd., London, England.

Pullar, T. and Capell, H.A. (1983) "Interactions between oral-anticoagulant drugs and non-steroidal anti-inflammatory agents: A review". *Scott. Med. Journal*, **28(1)**, 42-7.

Quinn, J.G. & O'Kennedy, R. (2001) "Biosensor-based Estimation of Kinetic and Equilibrium Constants". *Anal. Biochem.*, (In press).

Quinn, J., O' Kennedy, R., Smyth, M., Moulds, J. and Frame, T. (1997) "Detection of blood group antigens utilising immobilised antibodies and surface plasmon resonance". *J. Immunol. Meth.*, **206**, 87-96.

Quinn, J., Patel, P., Fitzpatrick, B., Manning, B., Dillon, P., Daly, S., O'Kennedy, R., Alcocer, M., Lee, H., Morgan, M. and Lang, K. (1999) "The use of regenerable, affinity ligand-based surfaces for immunosensor applications". *Biosensors and Bioelectronics*, **14**, 587-95.

Ramstrom, O., Ye, L. and Mosbach, K. (1996) "Chiral recognition in adrenergic receptor binding mimics prepared by molecular imprinting". *J. Mol. Recognit.*, **9(5-6)**, 691-7.

Reedstrom, C.K. and Suttie, J.W. (1995) "Comparative distribution, metabolism, and utilization of phylloquinone and menaquinone-9 in rat liver". *Proc. Soc. Exp. Biol. Med.*, **209(4)**, 403-9.

Rettie, A.E., Eddy, A.C., Heimark, L.D., Gibaldi, M. and Trager, W.F. (1989) "Characteristics of warfarin hydroxylation catalyzed by human liver microsomes". *Drug Metab. Dispos.*, **17(3)**, 265-270.

Rettie, A.E., Korzekwa, K.R., Kunze, K.L., Lawrence, R.F., Eddy, A.C., Aoyama, T., Gelboin, H.V., Gonzalez, F.J. and Trager, W.F. (1992) "Hydroxylation of warfarin by human cDNA-expressed Cytochrome P-450: A role for P-4502C9 in the aetiology of (S)-warfarin–drug interactions". *Chem. Res. Toxicol.*, **5**, 54-9.

Rice, R. L. and Myszka, D.G. (2000) "Advances in surface plasmon resonance biosensor analysis". *Curr. Opin. Biotechnol.*, **11**, 54-61.

Riechmann, L., Clark, M., Waldmann, H. and Winter, G. (1988) "Reshaping human antibodies for therapy". *Nature (Lond.)*, **332**, 323-27.

Rimm, E. B., Stampfer, M.J., Ascherio, A., Giovannucci, E., Colditz, G.A. and Willett, W.C. (1993) "Vitamin E consumption and the risk of coronary heart disease in men". *N. Engl. J. Med.*, **328**, **20**, 1450-6.

Ring, P. R. and Bostick, J. M. (2000) "Validation of a method for the determination of (R)-warfarin and (S)-warfarin in human plasma using LC with UV detection". *J. Pharm. Biomed. Anal.*, **22**, 573-81.

Rizzo, J.D. and Davis, P.J. (1986) "Microbial metabolism of the coumarin anticoagulants warfarin and phenprocoumon". *Pharm. Res.*, **3**, pt 235.

Rizzo, J.D., and Davis, P.J. (1988) "Microbial models of mammalian metabolism: production of novel α-diketone metabolites of warfarin and phenprocoumon using *Aspergillus niger*". *Xenobiotica*, **18(12)**, 1425-37.

Roderick, L.M. (1931) "A problem in the coagulation of the blood, 'sweet clover disease of cattle'". *Am.J. Physiol.*, **96**, 413-25.

Rogers, K. R.(2000). "Principles of Affinity-Based Biosensors". *Mol. Biotechnol.*, **14(2)**, 109-29.

Roos, H., Karlsson, R., Nilshans, H. and Persson, A. (1998) "Thermodynamic analysis of protein interaction with biosensor technology". *J. Mol. Recognit.*, **11**, 204-10.

Rudman, D., Bixler, T.J. and Del Rio, A.E. (1971) "Effects of free fatty acids on binding of drugs by bovine serum albumin, by human serum albumin and by rabbit serum". *J. Pharmacol. Exp. Ther.*, **176**, 261-272.

Ryan, J.J., Ketcham, A.S. and Wexler, H. (1969) "Warfarin therapy as an adjunct to the surgical treatment of malignant tumours in mice". *Cancer Res.*, **29**, 2191-4.

Sallah, S., Abdallah, J.M. and Gagnon, G.A. (1998) "Recurrent warfarin-induced skin necrosis in kindreds with protein S deficiency". *Haemostasis*, **28(1)**, 25-30.

Satoh, H., Hayashi, M. and Satoh, S. (1982) "Anti-warfarin antibody preparation and it's characterization for radioimmunoassay". *J. Pharm. Pharmacol.*, **34**, 429-33.

Sawyer, W.T. (1983) "Warfarin". In: *Applied Clinical Pharmacokinetics*, edited by Dennis Mungall, Raven Press, New York, 1983.

Sblattero, D. and Bradbury, A. (2000) "Exploiting recombination in single bacteria to make large phage antibody libraries". *Nature Biotechnology*, **18(1)**, 75-80.

Scholfield, K.P., Thomson, J.M. and Poller, L. (1987) "Protein C response to induction and withdrawal of oral anticoagulant treatment". *Clin. Lab. Haematol.*, **9(3)**, 225-62.

Sebastien, J.L. and Tresch, D.D. (2000) "Use of oral anticoagulants in older patients". *Drugs Aging*, **16(6),** 409-35.

Segal, D.M, Weiner, G.J. and Weiner, L.M. (1999) "Bispecific antibodies in cancer therapy". *Curr. Opin. Immunol.*, **11**, 563-569.

Sellers, E.M. and Koch-Weser, J. (1975) "Interaction of warfarin stereoisomers with human albumin". *Pharmac. Res. Commun.*, 7, 331-336.

Serlin, M.J., and Breckenbridge, A.M. (1983) "Drug Interactions with warfarin". *Drugs*, **25**, 610-20.

Shah, G.V. and Ritzén, E.M.(1984) "Validation of a bioassay for follitropin in urine samples". *J. Endocrinol Invest.* **7(3)**, 59-66.

Shah, P.V. (1987) "Analytical methods used in bioavailability Studies: A regulatory viewpoint". *Clin. Res. Practices & Drug Reg. Affairs*, **5(1)**, 51-60.

Shah, P.V., Midha, K.K., Dighe, S., McGilveray,I.J,. Skelly, J.P., Yacobi, A., Layloff, T., Viswanathan, C.T., Cook, C.E., McDowall, R.D., Pittman, K.A. and Spector, S. (1991) "Analytical methods validation: Bioavailability, bioequivalence and pharmacokinetic studies". *Eur. J. Drug Metab. Pharmacokinet.*, **16(4)**, 249-255.

Shapiro, S. (1953) "Warfarin sodium derivative (coumadin sodium): Intravenous hypoprothrombinemia-inducing agent". *Angiology,* **4**, 380.

Shaul, W.L. and Hall, J.G. (1977) "Multiple congenital anomalies associated with oral anticoagulants". *Am. J. Obstet. Gynaecol.,* **127(2)**, 191-8.

Shepperd, A.M.M., Hewick, D.S., Moreland, T.A. and Stevenson, I.H. (1977) "Age as a determinant of warfarin sensitivity". *Br. J. Clin. Pharmacol.*, **4**, 315-20.

Shi,Y., Sardonini, C.A. and Goffe, R, A.(1998) "The use of oxygen carriers for increasing the production of monoclonal antibodies from hollow fibre bioreactors". *Res. Immunol.* **149,** 576-87.

Shibukawa, A., Nagoa, M., Kuroda Y., and Nagakawa, T. (1990) "Stereoselective determination of free warfarin concentration in protein binding equilibrium using direct sample injection and an on-line liquid chromatographic system". *Anal. Chem.*, **62**, 712-6.

Shibukawa, A., Nakagawa, T., Miyake, M., Nishimura, N., and Tanaka , H. (1989). "Effect of protein binding on high performance liquid chromatography analysis of drugs with an internal-surface reverse-phase silica column". *Chem. Pharm. Bull*, **37(5)**, 1311-5.

Smith, G.P., Patel, S.U., Windass, J.D., Thornton, J.M., Winter, G. and Griffiths, A.D. (1998) "Small binding proteins selected from a combinatorial repertoire of knottins displayed on phage". *J. Mol. Biol.*, **277(2)**, 317-32.

Smith, R.V. and Rosazza, J.P. (1974) "Microbial models of mammalian metabolism. Aromatic hydroxylation". *Archives Biochem. Biophys.*, **161**, 551-8.

Smith, R.V. and Rosazza, J.P. (1975) "Microbial models of mammalian metabolism". *J. Pharm. Sci.*, **64(11)**, 1737-59.

Sönksen, C. P., Nordhoff, E. Jansson, Ö., Malmqvist, M. and Roepstorff, P. (1998) "Combining MALDI mass spectrometry and biomolecular interaction analysis using a biomolecular interaction analysis instrument". *Anal. Chem.*, **70(13)**, 2731-6.

Spigset, O. (1994) "Reduced effect of warfarin caused by ubidecarone". *Lancet*, **344**, 1372-3.

Stahmann, M.A., Graf, L.H., Heubner, C.F., Roseman, S. and Link, K.P. (1944) "Studies on the 4-hydroxycoumarins. IV. Esters of the 4-hydroxycoumarins". *J. Am. Chem. Soc.*, **66**, 900-2.

Stanley, C. Lew, A.M. and Steward, M.W. (1983) "The measurement of antibody affinity: a comparison of five techniques utilizing a panel of monoclonal anti-DNP antibodies and the effect of high affinity antibody on the measurement of low affinity antibody". *J. Immunol. Meth.*, **64(1-2)**, 119-32.

Stenflo, J. (1970) "Dicoumarol-induced prothrombin in bovine plasma". *Acta Chem. Scand.*, **24**, 3762-3.

Stenflo, J. (1974) "Vitamin K and the biosynthesis of prothrombin. IV. Isolation of peptides containing prosthetic groups from normal prothrombin and the corresponding peptides from dicoumarol-induced prothrombin". *J. Biol. Chem.*, **249**, 5527-35.

Stenflo, J. and Ganrot, P.O. (1972) "Vitamin K and the biosynthesis of prothrombin. I. Identification and purification of a dicoumarol-induced abnormal prothrombin from bovine plasma". *J. Biol. Chem.*, **247**, 8160-6.

Stevens, F.J. (1987) "Modificiation of an ELISA-based procedure for affinity determination: correction necessary for use with bivalent antibody". *Mol. Immunol.*, **24(10)**, 1055-60.

Steward, D.J., Haining, R. L.,Henne, R.K., Davis,G., Rushmore,T.H., Trager, W.F. and Rettie, A.E.(1997). "Genetic association between seneitivity to warfain and expression of CYP2C9*3." *Pharmacogenetics*, **7(5)**, 361-7.

Steward, M.W. (1985) "*Antibodies: Their structure and function*". 1st edition, Chapman and Hall, London, England.

Steyn, J. M., Van Der Merwe, H. M. and De Kock, M. J. (1986) "Reversed-phase high-performance liquid chromatographie method for the determination of warfarin from biological fluids in the low nanogram range". *J. Chrom.*, **378**, 254-60.

Sun, J. and Chang, M.W. (1995) "Initialization of warfarin dosage using computer modeling". *Arch. Phys. Med. Rehabil.*, **76(5)**, 453-6.

Sutcliffe, F.A., MacNicoll, A.D. and Gibson, G.G. (1990) "Hepatic microsomal warfarin metabolism in warfarin-resistant and susceptible mouse strains: influence of pretreatment with cytochrome P-450 inducers". *Chem. Biol. Interactions*, **75**, 171-84.

Suttie, J. W. (1993) "Synthesis of vitamin K-dependent proteins". *FASEB J.*, **7**, 445-52.

Swigar, M.E., Clemow, L.P., Saidi, P. and Kim, H.C. (1990) " 'Superwarfarin' ingestion. A new problem in covert anticoagulant overdose". *Gen. Hosp. Psychiatry*, **12(5)**, 309-12.

Takahashi, H., T Kashima, T., Nomizo, Y., Muramoto, N., Shimizu, T., Nasu, K., Kuboto, Kimura, S., and Echizen, H.(1998) "Metabolism of warfarin enantiomer in Japanese patients with heart disease having different CYP2C9 and CYP2C19 genotypes". *Clin Pharmacol & Ther.*, **63(5)**, 519-28.

Talstad, I. and Gamst, O.N. (1994) "Warfarin resistance due to malabsorption". *J. Internal Med.*, **236**, 465-7.

Taube, J., Halsall, D. and Baglin, T. (2000) "Influence of cytochrome P-450 CYP2C9 polymorphisms on warfarin sensitivity and risk of over anti-coagulation in patients on long term-term treatment". *Blood*, **96(5)**, 1816-1819.

Taylor, C.T., Chester, E.A., Byrd, D.C. and Stephens, M.A. (1999) "Vitamin K to reverse excessive anticoagulation: a review of the literature". *Pharmacotherapy*, **19(12)**, 1415-1425.

Thaisrivongs, S. and Strohbach, J.W. (1999) "Structure-based discovery of Tipranavir disodium (PNU-140690E): a potent, orally bioavailable, nonpeptidic HIV protease inhibitor". *Biopolymers*, **51(1)**, 51-8.

Thaisrivongs, S., Tomich, P.K., Watenpaugh, K.D., Chong, K.-T., Howe, K.D., Yang, C.-P., Strohbach, J.W., Turner, S.R., McGrath, J,P., Bohanon, M.J., Lynn, J.C., Mulichak, A.M., Spinelli, P.A., Hinshaw, R.R., Pagano, P.J., Moon, J.B., Ruwart, M.J., Wilkinson, K.F., Rush,B.D., Zipp, G.L., Dalga, R.J., Schwende, F.J., Howard, G.M., Padbury, G.E., Toth, L.N., Zhao, Z., Koeplinger, K.A., Kakuk, T.J., Cole, S.L., Zaya, R.M., Piper, R.C. and Jeffrey, P. (1994) "Structure-based design of HIV-protease inhibitors: 4-hydroxycoumarins and 4-hydroxy-2-pyrones as non-peptidic inhibitors". *J. Med. Chem.*, **37(20)**, 3200-4.

Thaisrivongs, S., Skulnick, H.I., Turner, S.R., Strohbach, J.W., Tomassi, R.A., Johnson, P.D., Aristoff, P.A., Judge, T.M., Gammill, R.B., Morris, J.K., Romines, K.R., Chrusciel, R.A., Hinshaw, R.R., Chong, K.-T., Tarpley, W.G., Poppe, S.M., Slade, D.E., Lynn, J.C., Horng, M.-M., Tomich, P.K., Seest, E.P., Dolak, L.A., Howe, J.W., Howard, G.M., Schwende, F.J., Toth, L.N., Padbury, G.E., Wilson, G.J., Shiou, L., Zipp, G.L., Wilkinson, K.F., Rush, B.D., Ruwart, M.J., Koeplinger, K.A., Zhao, Z., Cole, S., Zaya, R.M., Kakuk, T.J., Janakiraman, M.N. and Watenpaugh, K.D. (1996) "Structure-based design of HIV-protease inhibitors: Sulfonamide-containing 5,6-dihydro-4-hydroxy-2-pyrones as non-peptidic inhibitors". *J. Med. Chem.*, **39(22)**, 4349-53.

Thompson, A.R. (1996) "Molecular hemostatic variant enhances warfarin toxicity". *J. Clin. Invest.*, **98(7)**, 1508.

Thonnart, N. (1977) "*In vitro* metabolism of a new 4-hydroxycoumarin anticoagulant. Structure of an unusual metabolite". *J. Med. Chem.*, **20(4)**, 604-6.

Tonegawa, S. (1985) "Somatic generation of antibody diversity". *Nature (Lond.)*, **302(14)**, 575-81.

Townsend, M.G., Odam, E.M. and Page, J.M.J. (1975) "Studies of the microsomal drug metabolism system in warfarin-resistant and –susceptible rats". *Biochem. Pharmacol.*, **24**, 729-35.

Trail, P.A. and Bianchi, A.B. (1999) "Monoclonal antibody drug conjugates in the treatment of cancer". *Curr. Opin. Immunol.*, **11**, 584-588.

Trebak, M., Chong, J.M., Herlyn, D. and Speicher, D.W. (1999) "Efficient laboratory-scale production of monoclonal antibodies using membrane-based high-density cell culture technology". *J. Immunol. Meth*, **230**, 59-70.

Truitt, K.E., Larrick, J.W., Raubitschek, A.A., Buck, D.W. and Jacobson, S.W. (1984). "Production of human monoclonal antibody in mouse ascites". *Hybridoma*, **3**, 195-9.

Tsaioun, K.I. (1999) "Vitamin-K dependent proteins in the developing and aging nervous system". *Nutr. Rev.*, **57 (8)**, 231-40.

Tummino, P.J., Ferguson, D. and Hupe, D. (1994) "Competitive inhibitor of HIV-1 protease by warfarin derivatives". *Biochem. Biophys. Res. Commun.*, **201(1)**, 290-4.

Underwood, P.A. (1993) "Problems and pitfalls with measurement of antibody affinity using solid phase binding in the ELISA". *J. Immunol. Meth.*, **164**, 119-130.

Underwood, P.A. and Bean, P.A. (1988) "Hazards of the limiting-dilution method of cloning hybridomas". *J. Immunol. Meth.*, **107**, 119-28.

Valente, M. and Ponte, E. (2000) "Thrombosis and cancer". *Minerva Cardioangiol.*, **48**,117-27.

Van Cleve, R. (1965) "The rebound phenomenon-fact or fancy? Experience with discontinuation of long-term anticoagulation therapy after myocardial infarction". *Circulation*, **32 (6)**, 878-80.

Vanscoy, G.J. and Coax, W.C. (1995) "Oral Anticoagulation: Improving the Risk-Benefit Ratio". *J. Family Practice*, **41 (3)**, 261-9.

Vanscoy, G.J. and McAuley, J.W. (1991) "Exaggerated warfarin sensitivity: a case report" *Vet. Hum. Toxicol.*, **33 (3)**, 270-1.

van Spriel, A.B., van Ojik, H.H. & van de Winkel, J.G.J. (2000) . "Immunotherapeutic perspective for bispecific antibodies". *Immunol. Today*, **21 (8)**, 391-7.

Vaughan, T.J., Osbourn, J.K., and Tempest, P.R. (1998) "Human Antibodies by design". *Nature Biotechnology*, **16**, 535.

Verstraete, M. (1993) "The diagnosis and treatment of deep-vein thrombosis". *New Eng. J. Med.*, **329 (19)**, 51-2.

Viti, F., Tarli, L., Giovannoni, L., Zardi, L. and Neri, D. (1999) "Binding affinity and valence determine the tumour targeting performance of anti-angiogenesis antibodies". *Cancer Res.*, **59**, 347-52.

Vlatakis, G., Andersson, L.I., Muller, R. and Mosbach, K. (1993) "Drug assay using antibody mimics made by molecular imprinting". *Nature (Lond.)*, **361 (6413)**, 645-7.

Wada, H., Ikuma, H., Mori, Y., Shimura, M., Hiyoyama, K., Nakasaki, T., Onoda, K., Yamada, N., Ohta, T., Nishioka, J., Sakuragawa, J. and Shiku, H. (2000) " Increased hemostatic molecular markers in patients undergoing anticoagulant therapy". *Semin. Thromb. Hemost.*, **26 (1)**, 113-8.

Walker, F.B. (1984) "Myocardial infarction after diet-induced warfarin resistance". *Arch. Intern. Med.*, **144**, 2089-90.

Walter-Sack, I. and Klotz, U. (1996) "Influence of diet and nutritional status on drug metabolism". *Clin. Pharmacokinet.*, **1**, 47-64.

Wandell, M. and Wilcox-Thole, W.L. (1983) "Protein Binding and Free Drug Concentrations". In: *Applied Clinical Pharmacokinetics*, edited by Dennis Mungall, Raven Press, New York.

Warrier, I., Brennan, C.A. and Lusher, J.M. (1986) "Familial resistance in a black child". *Am. J. Pediatr. Haematol. Oncol.*, **(4)**, 346-7.

Wedemayer, G.J., Patten, P. A., Wang, L.H., Schultz, P.G. and Stevens, R. C. (1997) "Structural insights into the evolution of an antibody combining site". *Science*, **276**, 1665-9.

Wei, M.C., Hatton, J., Creed Pettigrew, C., Dempsey, R.J and Chandler, M.H.H. (1994) "A simplified high-performance chromatographic method for simple determination of warfarin enantiomers and their protein binding in stroke patients". *Ther. Drug Monitoring*, **16**, 509-12.

Wells, P.S., Holbrook, A.M., Crowther, N.R. and Hirsh, J. (1994) "Interactions of warfarin with drugs and food". *Ann. Internal Med.*, **121(9)**, 676-83.

Wewetzer, K. & Seilheimer, B. (1995) "Establishment of a single-step hybridoma cloning protocol using an automated cell transfer system: comparison with limiting dilution". *J. Immunol. Meth.*, **179**, 71-6.

White, H.D. (1994) "Aspirin or warfarin for non-rheumatic atrial fibrillation?". *The Lancet,* **343**, 683.

Wild, D. *"The immunoassay handbook"*. 1st edition, Stockton Press, New York, U.S.A.

Wilkinson, A.J., Fersht, A.R., Blow, D.M., Carter, P. and Winter, G. (1984) "A large increase in enzyme-substrate affinity by protein engineering". *Nature*, **307**, 187-8.

Williams, C. & Addona, T.A. (2000) "The integration of SPR biosensors with mass spectrometry: possible applications for proteome analysis". *TIBTECH*, **18**:45-8.

Williams, C. (2000) "Biotechnology match making: screening orphan ligands and receptors". *Curr. Opin. Biotechnol.*, **11**: 42-6.

Winter, G. and Milstein, C., (1991) "Man-made antibodies", *Nature (Lond.)*, **349**, 495.

Wojtukiewicz, M.K., Zacharski, L.R., Memoli, V.A., Kisiel, W., Kudryk, B.J., Rousseau, S.M. and Stump, D.C. (1990) "Abnormal regulation of coagulation/fibrinolysis in small cell carcinoma of the lung". *Cancer*, **65**, 481-5.

Wong, Y.W.J. and Davis, P.J. (1987) "Microbial models of mammalian metabolism: multiple pathway modeling of warfarin metabolism with *Cunninghamella elegans*". *Pharm. Res.*, **4**: pt 21.

Wong, Y.W.J. and Davis, P.J. (1989) "Microbial models of mammalian metabolism: Stereoselective metabolism of warfarin in the fungus *Cunninghamella elegans*". *Pharm. Res.*, **6 (11)**, 982-7.

Wong, Y.W.J. and Davis, P.J. (1991) "Microbial models of mammalian metabolism: production of 3'-hydroxywarfarin, a new metabolite of warfarin using *Cunninghamella elegans*". *J. Pharm. Sci.*, **80 (4)**, 305-8.

Wong, R. L. Mytych, D. Jacobs, S. Bordens, R. and Swanson, S. J. (1997) "Validation parameters for a novel biosensor assay which simultaneously measures serum concentrations of a humanized monoclonal antibody and detects induced antibodies". *J. Immunol. Meth.*, **209**, 1-15.

Woo, K. T. (1996) " Recent concepts in the pathogenesis and therapy of IgA nephritis". *Ann. Acad. Med. Singapore*, **25**, 265-9.

Wright, I.S. (1960) "Treatment of thromboembolic disease". *JAMA*, **174**, 1921-4.

Wynne, H., Cope, L., Kelly, P., Whitttingham, T., Edwards, C. and Kamali, F. (1995) "The influence of age, liver size and enantiomer concentrations on liver requirements". *Br. J. Clin. Pharmacol.*, **40**, 203-7.

Yalow, R.S. and Berson, S.A. (1959) "Assay of plasma insulin in human subjects by immunological methods". *Nature (Lond.)*, **184**, 1648-9.

Yanagita, M., Ishii, K., Ozaki, H., Arai, H., Nakano, T., Ohashi, K., Mizuno, K., Kita, T. and Doi, T. (1999) "Mechanism of inhibitory effect of warfarin on mesangial cell proliferation". *J. Am. Soc. Nephrol.*, **10 (12)**, 2503-9.

Zacharski, L.R., Henderson, W.G., Rickles, F.R., Forman, W.B., Cornell, C.J.Jr., Jackson Forcier, R., Edwards, R.L., Headley, E., Kim, S.-H., O'Donnell, J.R., O'Dell, R., Tornyos, K. and Kwaan, H.C. (1981) "Effect of warfarin on survival in small cell carcinoma of the lung. Veterans Administration Study No.75". *JA MA*, **245 (8)**, 831-5.

Zacharski, L.R., Henderson, W.G., Rickles, F.R., Forman, W.B., Cornell, C.J.Jr., Jackson Forcier, R., Edwards, R.L., Headley, E., Kim, S.-H., O'Donnell, J.R., O'Dell, R., Tornyos, K. and Kwaan, H.C. (1984) "Effect of warfarin anticoagulation on survival in carcinoma of the lung, colon, head and neck, and prostate. Final Report of VA Cooperative Study No.75". *Cancer*, **53 (10)**, 2046-52.

Zacharski, L.R., Howell, A.L. and Memoli, V.A. (1992) "The Coagulation biology of cancer". *Fibrinolysis*, suppl 1: 39-42.

Zacharski, L.R., Memoli, V.A., Constantini, V., Wojtukiewicz, M.Z. and Ornstein, D.L. (1990) "Clotting factors in tumour tissue: implications for cancer therapy". *Blood Coagulation and Fibrinolysis*, **1**, 71-8.

Zhang, Z., Fasco, M.J., Huang, Z., Geungerich, P. and Kaminsky, L.S. (1995) "Human Cytochromes P4501A1 and P4501A2: R-warfarin metabolism as a probe". *Drug Metab. Dispos.*, **23 (12)**, 1339-45.

Zilva J.F. and Pannell P.R. (1979) "*Clinical Chemistry in Diagnosis and Treatment*". Lloyd-Duke, third edition, London, England.

Zimbelman, J., Lefkowitz, J., Schaeffer, C., Hays, T., Manco-Johnson, M., Manhalter, M. and Nuss, R. (2000) "Unusual complications of warfarin therapy: Skin necrosis and priapism". *J. Pediatr.*, **137 (2)**, 266-8.

Appendix 1A

Glossary of terms and definitions commonly employed in Bioanalytical Validation procedures:

The terms listed below are commonly referred to in bioanalytical validation procedures and the criteria which they can be defined under have been extensively reviewed (Karnes *et al.*, 1991; Shah *et al.*, 1991; Braggio *et al.*, 1996; Hubert *et al.*, 1999; Currie, 1999; Findlay *et al.*; 2000).

Mean

Describes the average of replicate *(x)* measurements. (i.e. $n_1+n_2+\ldots\ldots n_x/x)$

Accuracy

Is defined as the closeness of agreement of the measured test result with the expected true reference value.

Precision

Is defined as the closeness of agreement, or variance between independent test results of multiple measurements of the same sample obtained under a set of specified analytical test conditions. It is normally expressed in terms of the relative standard deviation (% R.S.D.), or the coefficient of variation (% C.V.) of the determined concentration of a replicate number of assays. The degree of precision assessed between replicates (i.e. % C.V.) performed during a single assay batch, is commonly referred to as the intra-assay variation (also referred to as repeatability). The term inter-assay variation (also referred to as reproducibility) is used to describe the precision between assays when related to multiple batches.

Limit of Detection (L.O.D.)

Defines the lowest analyte concentration that the analytical technique can differentiate from background signals and is usually determined as background noise ± 3 standard deviations.

Upper/ Lower Limit of Quantitation (L.O.Q.):

The lowest/highest analyte concentration that can be measured from the calibration curve with acceptable levels of precision and accuracy, usually the L.O.D. ± 3 standard deviations.

Robustness:

Is a term used to describe the ability of an analytical technique to withstand fluctuations in the described analytical test conditions. For immunoassay procedures the term could be used to describe changes in the ionic strength of the matrix, as well as pH and temperature changes.

Standard Curve:

This describes the relationship between the measured analyte response (i.e. absorbance, response units) and the analyte concentration.

Non-specific binding:

This describes matrix effects which affect the degree of binding of the antibody:antigen interaction, and can occur as a result of increased protein concentration and sample viscosity in the sample matrix (e.g. plasma), and also as result of altered ionic composition (e.g. urine) of the sample matrix. The assay design should therefore be robust enough to be able to withstand such variations in sample composition, and the degree of non-specific binding minimised prior to sample analysis (e.g. use of detergents and/or surface treatment with non-specific protein prior to sample analysis).

Coefficient of Variation (% C.V.)

A quantitative measure of the precision of an analytical measurement expressed as a percent function of the mean value, also referred to as the Relative Standard Deviation (% R.S.D.).

$$\% \text{ C.V.} = [\text{S.D.}/\text{Mean value}] \times 100$$

Bias:

Describes the systematic difference between measured test results and the theoretical true value, and is usually expressed as the relative error (% R.E.).

Batch/Run:

Refers to a single set of samples (standards) analysed together as a single sample set using the same analytical technique.

Residual:

Describes the difference between the value described by the equation model and the true value.

Precision profile:

A quantitative measure of the variation between measurements, usually the coefficient of variation versus the nominal concentration of analyte in the sample.

Normalised Response Values:

The response recorded in response units (RU) at each particular antigen concentration divided by the response recorded in the presence of zero antigen.

i.e.

$$\text{Normalised Response} = \frac{\text{Response measured at particular antigen concentration}}{\text{Response measured at zero antigen concentration}}$$

Normalised Absorbance Values:

The absorbance recorded (AU) at each particular antigen concentration divided by the absorbance recorded in the presence of zero antigen.

i.e.

$$\text{Normalised Absorbance} = \frac{\text{Absorbance measured at particular antigen concentration}}{\text{Absorbance measured at zero antigen concentration}}$$